Emission of Greenhouse Gases from Forest Soils: Measured and Modelled

---

Shirley M. Cade

A thesis submitted for the degree of Doctor of Philosophy at Royal Holloway, University of London

Department of Earth Sciences

Royal Holloway College

University of London

Abstract

Forests and their soils are important for the mitigation of greenhouse gas emissions (GHG) but can become net sources of GHGs following management or environmental change. Their response to multiple changes is best studied by process-based models. This study evaluates the model, LandscapeDNDC for simulating soil CO_2, N_2O and NO fluxes and ecosystem CO_2 fluxes from an oak forest in SE England and a spruce forest in central Scotland. LandscapeDNDC consists of several sub-modules, including two forest physiology options, PnET and PSIM. In the oak forest, where a significant understorey contributes to the ecosystem respiration and productivity, simulations from PnET and PSIM were compared. Statistical evaluation showed that PSIM produced results closer to measurements helped by the fact that it differentiates between competing requirements of understorey and canopy trees. LandscapeDNDC simulated annual N_2O and NO soil emissions at the same order of magnitude as measurements but with less variability. The spruce forest is a relatively young plantation on ploughed heathland with no understorey and therefore only PnET was evaluated. With modifications to parameters and tree shape, LandscapeDNDC simulated measured ecosystem CO_2 fluxes well, but overestimated soil CO_2 and to a lesser extent N_2O.

Soil chamber measurements of CO_2, CH_4, N_2O and NO were made for this study at the oak forest over 16 months to provide data to compare with simulations. This showed seasonal variations and relationships with soil moisture and temperature consistent with previous measurements at the site for CO_2, CH_4 and N_2O. NO had not previously been measured here and only trace quantities were detected. Addition of N fertiliser to plots in the oak forest showed increased N_2O and NO fluxes as pulses of a few days duration and confirmed the technique for NO flux measurement. Soil chambers employed here took part in the international N_2O chamber intercomparison. Peliminary results suggest they perform well compared to other designs.

Acknowledgements

This study was made possible by a combined College Research and Crossland Scholarship from Royal Holloway, together with a University of London travel grant. Work on N_2O chamber comparison was funded by a grant from the Integrated non-CO_2 Greenhouse gas Observing System (InGOS). I would like to thank my supervisors Kevin Clemitshaw, Sirwan Yamulki and David Lowry. Thanks must also go to many other staff at Royal Holloway, Forest Research and the Institute of Meteorology and Climate Research, KIT, particularly to David Ames, for bespoke NO_x data logging software, Jose Valcarcel for help with soil analyses, Jacqui Brunt for GC analysis, Eric Casella for Straits mensuration data and modelling advice, and Steffen Klatt and David Kraus for help with LandscapeDNDC. I would also like to thank my family, particularly my husband, Chris, who continued to support me despite a serious illness, and my daughter, Jennifer, who helped with reproducing the LandscapeDNDC diagram.

Table of Contents

List of Figures

List of Tables

GLOSSARY

Term	Acronym used in this study	Definition
Gross primary production	GPP	Total CO_2 fixed by plants (autotrophs) in an ecosystem by photosynthesis; also known as assimilation.
Total ecosystem respiration	TER	CO_2 emitted in respiration by any living organism in the ecosystem. For modelling soils, autotrophic respiration is separated into above and below ground fractions. The below-ground fraction modelled is purely from roots. The only heterotrophic (non-plant) respiration in the model is from below-ground soil micro-organisms, principally decomposers.
Net ecosystem exchange	NEE	CO_2 fluxes measured by eddy covariance. Technically this includes organic and inorganic fluxes of CO_2, but normally inorganic components can be ignored and NEE is considered numerically equivalent to NEP. A negative NEE indicates a net uptake of CO_2, therefore, NEE = -NEP.0
Net ecosystem production	NEP	The difference between the CO_2 taken up by photosynthesis in an ecosystem and the CO_2 used in total ecosystem respiration over the same time period. NEP is positive when there is a net uptake of CO_2. NEP = GPP – TER
Soil respiration		Below ground respiration derived from plant roots (autotrophic) and soil micro-organisms (heterotrophic)

Chapter 1 Introduction

This study investigates the effect of different forest vegetation on greenhouse gas (GHG) fluxes from forest soils. The 3 most important long-lived GHGs are carbon dioxide (CO_2), methane (CH_4) and nitrous oxide (N_2O) (IPCC, 2014). Forests and their soils can be both important sinks and sources for all of these gases. The pollutant nitric oxide (NO) is a trace gas which is also involved in the N cycle of forest soils and may be emitted or taken up at the soil surface. Change can tip the balance in these ecosystems between source and sink; changes such as land use change, climate change, forest management practices and pollution, which in the UK is principally nitrogen (N) deposition. Currently 13% of UK land area is forested (Forestry Statistics 2015), a lower proportion than most of Europe, where forest area estimates range from 27 to 33% for the whole of the EU 27 countries (Seebach et al., 2011). Read et al. (2009) have called for the UK forested area to increase to 16% which could deliver emissions abatement equivalent to 10% of UK GHG emissions by the 2050s provided new and existing stocks are managed sustainably. Trees that are grown for timber can store carbon (C) in timber products for many years after felling and replanting, so commercial plantations are effective forms of emissions abatement.

Atmospheric CO_2 concentration continues to increase despite efforts to reduce emissions. Global emissions from fossil fuel combustion and cement production were 54% higher in 2011 than in 1990. 2002-2011 showed a higher decadal rate of increase, at 2.0 ±0.1 ppm y^{-1}, than any decade since direct measurements began in 1958 (IPCC 2013). CH_4 concentrations have returned to an increasing trend since 2007 following a stable period that began in the 1990s, although the reasons are not fully understood. N_2O concentration has increased steadily at a rate of 0.73 ±0.03 ppb y^{-1} over the last 3 decades (IPCC, 2013). Emissions of N_2O to the atmosphere are mostly caused by nitrification and denitrification reactions in soils and oceans (IPCC, 2013). Anthropogenic N_2O emissions derive from application of nitrogenous fertilisers in agriculture, from fossil fuel use, industrial processes and biomass burning. These lead to further emissions from land as the reactive N is deposited from the atmosphere on soils and vegetation, triggering increased growth and soil reactions.

The potential impact of climate change on forest growth has been much studied but mostly as single factors (reviewed in Hyvonen et al., 2006). The increased concentration of CO_2 is known to increase photosynthetic rate but the resulting increased biomass also increases respiration. Increased temperature increases length of growing season, and an increase in N deposition causes a higher leaf area. More leaves per unit area increases shade but also increases the litter input to the soil and hence increases soil organic matter (SOM). N deposition tends to slow

decomposition of this SOM, but increased temperature increases the rate of decomposition. An increased growth in the forest increases demand for N. Thus, there are clearly many processes involving tree growth, environmental conditions and soil biochemical reactions that interact following any environmental change. Forest management practices, such as thinning and fertiliser application, add to the variables that influence the balance. The easiest way to understand how these conflicting factors and processes interact is to employ a process-based model.

This study uses the model LandscapeDNDC (Haas et al, 2013) which is a deterministic, process-based biogeochemical model of C, N and water cycling that combines vegetation cover, a litter layer and multiple soil layers to simulate gas fluxes. It can be employed at a single site level or combined with other sites to allow regional modelling via a GIS. As three vegetation types are available, forest, grassland and arable, with their own sub-modules, land use change can also be simulated. The model has potential for use with national GHG inventory reporting, required by all signatories to the Kyoto agreement. It has been tested with data from various countries in Europe and elsewhere, e.g. Haas et al. (2013), Cameron et al. (2013), Molina-Herrera et al. (2015) but not with UK data. It is currently not able to model CH_4 for any vegetation other than rice, for which a methanogenesis sub-module was recently developed (Kraus et al., 2015). This study therefore concentrates on CO_2, N_2O and NO fluxes.

The aim of the study is principally to evaluate the use of LandscapeDNDC for simulating GHG fluxes from forest soils in the UK. The UK has approximately equal areas forested with conifers and broadleaved trees, 1.6m ha conifers and 1.54m ha broadleaved (Forestry Statistics 2015). Therefore, one broadleaved forest and one coniferous forest have been chosen, both of which are long-standing monitoring sites and both are plantations managed by the Forestry Commission. The broadleaved forest is an oak plantation in Hampshire, known as the Straits Inclosure, and the coniferous forest is a Sitka spruce plantation in Perthshire, Griffin Forest. These represent the most common forest species in England and Scotland respectively (Forestry Statistics, 2013). The oak forest, as is typical of many natural and planted forests, has a significant understorey, in this case of hazel, hawthorn, ash and holly in addition to a ground vegetation of shrubs and herbs. This introduces additional complexities of competition for light and nutrients which are also investigated by comparing two vegetation sub-modules.

Model evaluation requires data. Therefore this study has also involved measurements of soil CO_2, CH_4, N_2O and NO fluxes using soil chambers at the Straits Inclosure oak forest site. They took place over a 16-month period at a frequency of approximately 2 weeks, which is more frequent than previous measurements at the site. The chambers used for these measurements

were taken to an international inter-comparison campaign organised and funded by InGOS (Integrated non-CO2 Greenhouse gas Observing System) in Hyytiala, Finland. Only preliminary results are currently available from this campaign, which are discussed in Chapter 7 (Critical evaluation) together with other aspects of measurement and modelling error, uncertainty and bias.

N deposition is an important factor in climate change resulting from increased emissions of reactive N (particularly N_2O, NO_x, NH_3 and NO_3^-). Therefore an experiment was carried out to investigate the effects of N addition to soil plots within the Straits Inclosure and the resulting soil gas fluxes were measured with soil chambers. These results were also compared to simulations with LandscapeDNDC.

Thesis overview

Chapter 2 describes the methodology used for field measurements of fluxes, sample analyses and ancillary data, and for a laboratory-based soil chamber inter-comparison study. The model LandscapeDNDC and its components are explained here.

Chapter 3 is a paper in preparation for submission to Biogeosciences in which the model LandscapeDNDC is evaluated for its ability to simulate greenhouse gas fluxes from an oak plantation in Hampshire (Straits Inclosure). Simulations are compared with field measurements of soil gas fluxes made with soil chambers for this project over a 16-month period, with soil gas flux measurements made by Forest Research (2007-2012) and eddy covariance flux data from Forest Research. The importance of the forest understorey is investigated by comparing two different sub-modules and considering the effect of management thinning of part of the forest.

Chapter 4 is a paper in preparation for submission to Biogeosciences in which LandscapeDNDC is evaluated for simulating GHG fluxes from a Sitka spruce plantation in Perthshire (Griffin Forest). In this case, the field measurements were supplied by Forest Research and the eddy covariance data by University of Edinburgh.

Chapter 5 is a paper in preparation for submission to Biogeosciences describing an experiment in which 3 levels of nitrogen fertiliser were added to soil plots in the Straits Inclosure oak plantation and resulting soil gas fluxes were measured for the following 2 months. The fertiliser application was also modelled with LandscapeDNDC.

Chapter 6 is an extended abstract submitted to the Finnish National Centre of Excellence Annual Meeting October 2014 as part of the inter-comparison work on N_2O soil chambers.

Chapter 7 is a critical evaluation and discussion of work carried out and methods used as described in the previous chapters. It includes further preliminary results from the international inter-comparison of N_2O soil chambers funded by InGOS at Hyytiala, Finland in which the author participated (in addition to those in Chapter 6).

Chapter 8 contains concluding comments.

Chapter 2 Methodology

2.1 Soil chamber measurements

The basic principle of the chamber measurement involves covering a known area of soil with a closed chamber that allows gas exchange between the soil and the chamber headspace. The change in gas concentration in the headspace over time is measured and converted to a flux rate. The simplest method, as just described is known as 'non-steady state non-flow-through' since the increase in concentration changes the state inside the chamber (Livingston and Hutchinson, 1995). Samples are extracted at intervals to measure the concentration as it changes over time. This method is used here for CO_2, CH_4 and N_2O flux measurements. An alternative method is known as 'steady state flow through', where a steady flow of air is maintained through the chamber sampled and the concentration in the inflow and the outflow are measured. The difference between the concentrations, together with the flow rate are used to calculate the flux. This method was used for NO flux measurements.

Before commencing measurements, frames to hold the chambers were placed in the soil to a depth of approximately 6 cm (Figure 2.1a). As few roots as possible were cut or disturbed during this process. A period of at least a week is recommended after frame insertion before measurements are made. The frames remained in place until the end of the measurement period.

N_2O, CO_2, and CH_4 soil fluxes were measured at the same time by collecting samples using a non-steady state non-flow through chamber method. As NO is short-lived and quickly oxidises to NO_2 by photolysis, it requires the use of an on-site analyser and a flow-through method to deliver the sample to the analyser. Measurements made as part of this study in 2013 and 2014 involved carrying out non-flow through gas sampling first, in the morning, followed by flow through NO measurements in the early afternoon. As water was used as a seal in the first method, it was siphoned off and frames dried in between the 2 methods.

2.1.1 N_2O, CO_2 and CH_4 soil flux measurements (non-steady state non-flow-through chamber)

The chamber used for sampling N_2O, CH_4 and CO_2 fluxes was a Forest Research design made of white opaque PVC, rectangular in cross section with exterior dimensions 40 x 40 x 25 cm, also used in Yamulki et al. (2013) (Figure 2.1b) and follows a method described in Ryden and Rolston (1983). The chamber fits into a trough on the frame into which water is added to form a seal.

No fans or vent tubes are present in the chamber. One of the chambers is fitted with a circular vent in the upper surface of the chamber.

For the initial measurements at the Straits Inclosure 6 chambers were placed at random around the Tower Site. Each chamber was closed for 60 minutes and 3 samples were collected in 20ml vials at 0, 20, 40 and 60 minutes from each chamber, giving a total of 12 sample vials per chamber. Sampling was carried out in sequence with an interval of 3 minutes between chambers. This allowed 6 chambers to be closed and sampled before returning to the first chamber for the next sampling time.

The procedure for taking a sample from the chamber is as follows:

- Add water to the frame, avoiding any spillage on the soil, to about half the available height
- Ensure the valve on top of chamber is open
- Carefully place chamber into the trough in the frame, ensuring no water is spilled
- Record time, start stop watch and attach 60 ml syringe to the chamber valve
- Slowly fill the syringe with chamber headspace air and then push back into chamber
- Repeat 2 more times to mix air in the chamber headspace
- Fill the syringe for a 4^{th} time to a volume of 40ml
- Close valve on the chamber lid
- Remove syringe and attach a needle to the syringe, then insert the needle into the septum of an evacuated vial (20ml volume). The gas moves into the vial as the pressure is equalised and then insert a second needle into the vial septum (open to the atmosphere). Push the remaining gas from the syringe in to the vial.
- Remove the syringe and its needle from the septum. Wait 3 seconds to ensure atmospheric pressure is reached, and then remove the second needle.
- Repeat with second and third vials. A total of 120 ml headspace gas has been removed and 3 samples of 20ml have been collected. (No headspace mixing is required for second and third samples.)
- Place filled vials in a labelled, sealable plastic bag. Move to next chamber.

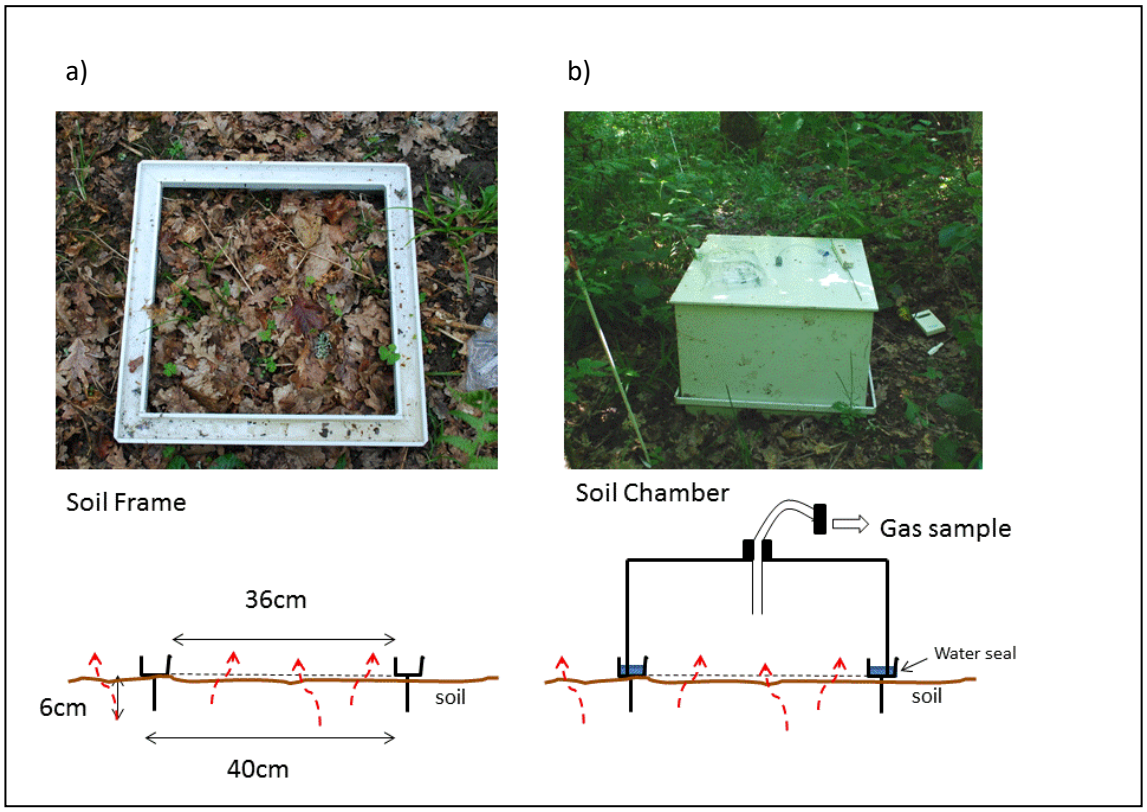

Figure 2.1: Soil chamber design for steady state non-flow-through method showing a) frame in soil with trough to hold water and b) chamber placed on frame.

Once sampling was completed, the soil chambers were removed from the frames and placed on their sides nearby. Samples were taken immediately to the nearby Forest Research laboratory at Alice Holt and stored in an air-conditioned room prior to analysis. Each vial was analysed for CO_2, CH_4 and N_2O by gas chromatography equipped with ECD (Electron Capture Detector) and FID (Flame Ionisation Detector) at Forest Research.

Fluxes (F) for each of the 3 gases are calculated from the change in concentration over time, using the formula:

$$F = \frac{dC}{dt} \times \frac{V}{A} \times \frac{P}{GT} \times m \qquad (1)$$

Where, $\frac{dC}{dt}$ = change in concentration over time (in ppm min^{-1})

V = volume of chamber (0.04m^3)

A = surface area of soil covered by chamber (0.14m^2)

P = atmospheric pressure (assumed to be 1atm)

G = volume of 1 mole of gas at STP = 22.4 L

T = temperature conversion factor, derived from air temperature in Kelvin (K)

m = molecular mass (e.g. CO_2 = 44, C = 12).

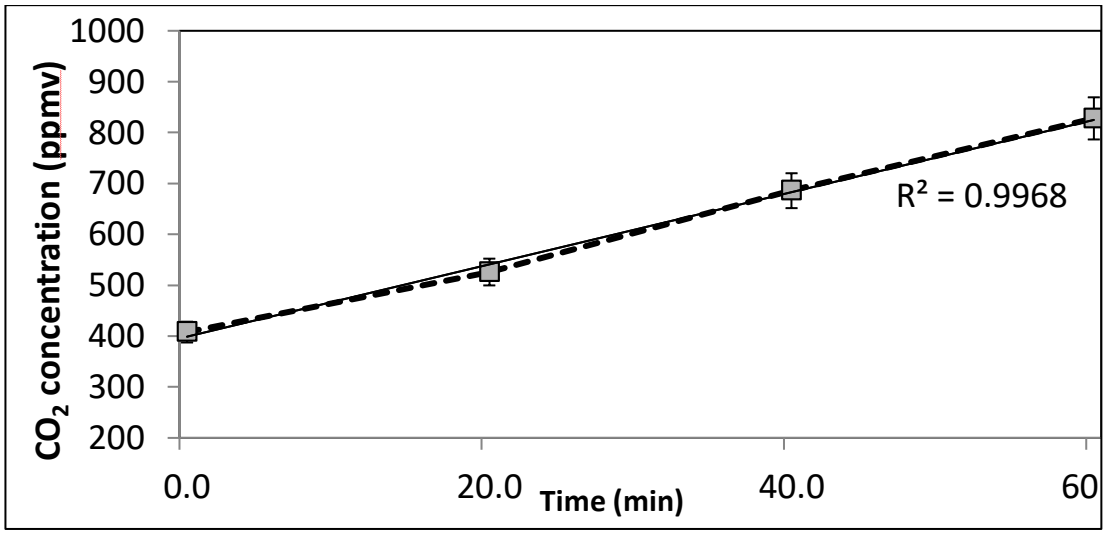

Figure 2.2: CO_2 concentration of samples collected at 20 min intervals from one soil chamber at the Straits Inclosure. Error bars show 1 SD from 3 samples. Air temperature during sampling = 11°C.

For example, the CO_2 flux from Figure 2.2 is calculated below:

F = ((800 – 400)/60 x (0.04 / 0.14) x (12/22.4) x (273/(273 + 11)) mg CO_2-C m^{-2} min^{-1}

= 61.74 mg CO_2-C m^{-2} h^{-1}

The length of measurement time (60 min) was chosen to match the chamber dimension such that the response of the concentration change over time is linear. The linearity of the response was checked for each chamber. Atmospheric CO_2 concentration is an order of magnitude greater than N_2O and CH_4 concentrations, therefore it was used to check the validity of the samples. Any samples where CO_2 flux was not consistent and linear were rejected for all gases (see Section 2.1.3).

Gas chromatography calibration from the equipment at Alice Holt is shown in Table 2.1

Table 2.1: Results from gas chromatography validation tests

	CH_4 (ppm)	**CO_2 (ppm)**	**N_2O (ppm)**
Limit of detection	0.096	1.211	0.033
Limit of quantification	0.321	4.038	0.100
Ambient concentration (mean of 10 samples)	1.962	395.981	0.315
SD on 10 repeated ambient concentrations	0.027	2.637	0.004

2.1.2 NO soil flux measurements (steady state flow through)

The NO flux measurement method followed that used by Yamulki et al. (1995) and Pilegaard et al. (1999). Two chambers as described in Section 2.1.1 were adapted for use as flow-through chambers by adding inlet and outlet ports and a vent and lining with polytetrafluoroethylene (PTFE) (Figure 2.3a). All connectors and tubing were made from PTFE. A customised rubber seal on the base of the chambers was fitted into the troughs on the soil frames to provide an air-tight seal without using water, to prevent NO_x absorption by water. A mass flow controller (Clemitshaw own design) provided a uniform flow of air into the chamber, driven by an external pump. This took ambient air and passed it through Sofnofil (Al/KMnO4) to remove NO_x and activated carbon to remove O_3 resulting in a 'zero' air inflow to the chamber (Figure 2.3b). The use of zero air is to prevent fluctuations in NO_x concentration in the inflow caused by reactions between O_3 and NO. The flow rate was set at 3 L min^{-1} as a compromise between ensuring a complete turnover of air in the 40 L chamber and not allowing too long for NO_x to settle or react with the soil surface. One chamber acted as the control, attached to a frame sealed at the base for measuring NO_x concentration in the 'zero' inlet flow alone. The second chamber was attached to each of the sample frames in turn for a fixed time of 20-25minutes, while the concentration of the outlet flow was analysed by a Thermo Electron Corporation 42C NO- NO_2 - NO_x Analyser, (trace level). Custom data logging software (by D Ames) logged NO and NO_2 every 10s and controlled a two-way valve which switched input flow to the analyser between the outflow from the two chambers. The NO_x analyser has a detection limit of 50 ppt.

If a positive flux is present, the difference between the concentration in the inflow (zero air, measured in control chamber) and outflow of the sample chamber can be used to calculate the flux (F). A negative flux cannot be detected due to the use of zero air inflow.

$$\boldsymbol{F = (C_o - C_i) \times \frac{Q}{A} \times \frac{P}{GT}\, m} \qquad (2)$$

Where C_o= NO concentration at outlet

C_i = NO concentration at inlet = concentration from control chamber

Q = flow rate of air

A = surface area enclosed by chamber (e.g. 0.14 m^2 for chamber with trough)

P = atmospheric pressure

G = volume of 1 mole of gas at STP = 22.4 L

T = temperature conversion factor (K)

m = molecular mass (N = 14).

a)

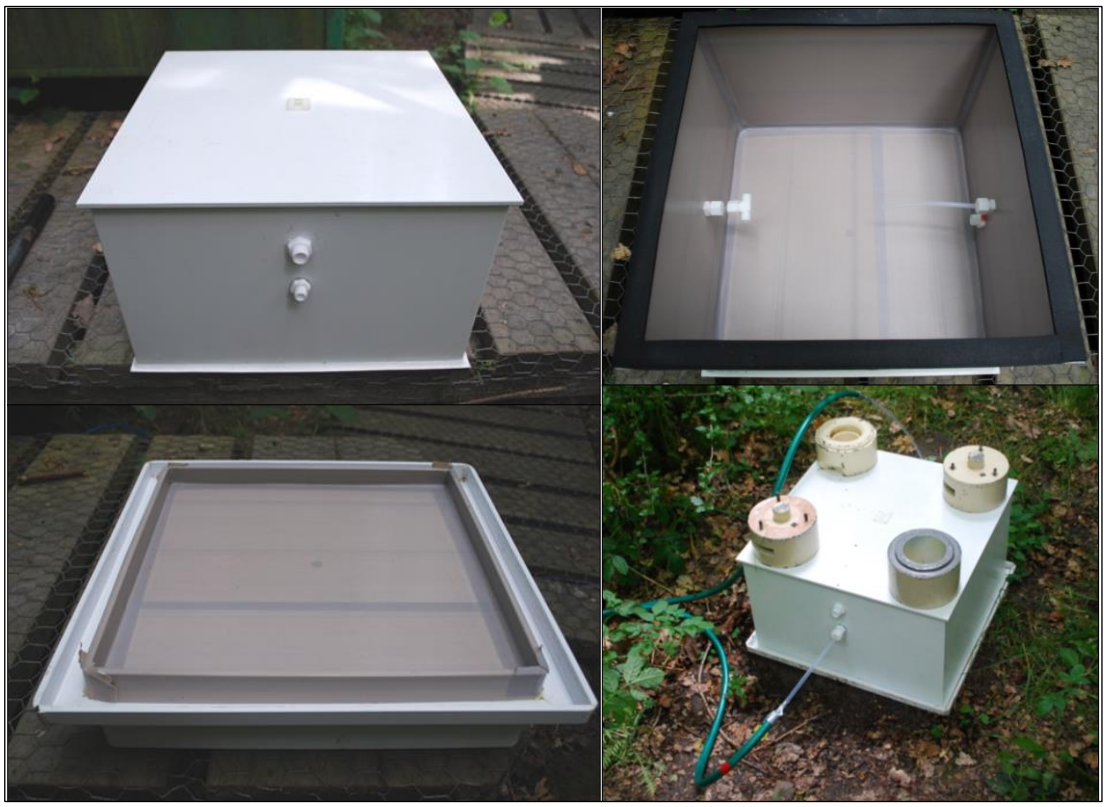

b)

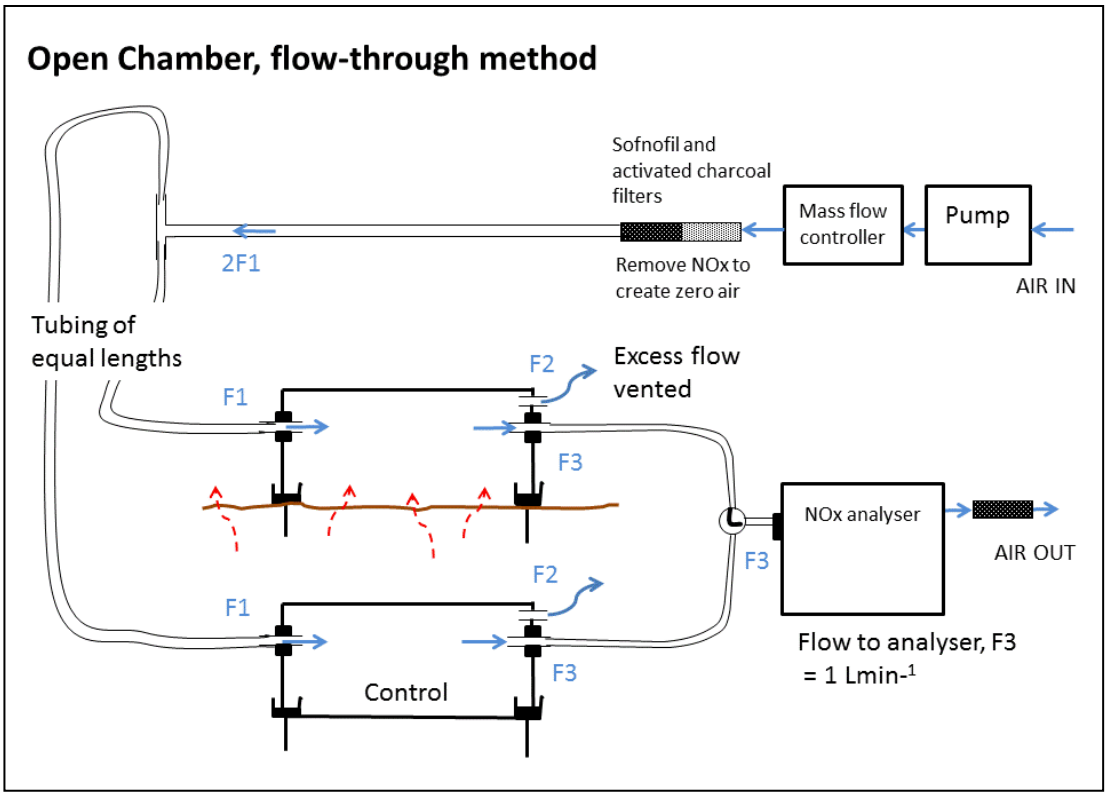

Figure 2.3: Soil chamber design for steady state flow-through method, a) photographs illustrate PTFE interior lining and rubber foam seal on base of chamber; top right photo shows split inflow on the left to promote mixing and extended tubing for outflow to sample away from vent; bottom right photo shows weights used to optimise foam rubber seal; b) schematic diagram of NO_x measurement system.

Figure 2.4 illustrates a measurement from the control chamber followed by a sample chamber, from which the following calculation of flux was made:

$F = (0.777 – 0.147) \times (0.003 / 0.14) \times 14/22.4 \times 273 / (273+17.7)$ µg NO-N m^{-2} min^{-1}

(where air temperature = 17.7 °C and flow rate = 0.003 m^3 min^{-1})

Changing units, this becomes,

$F = 0.48$ µg NO-N m^{-2} h^{-1}

The sample chamber was moved between soil frames while air was analysed in the control chamber. Ambient air therefore entered the sample chamber and a period of time is required for this to return to zero after a seal is made with the new frame. There is also a short piece of tubing between the switching device and NO_x analyser which is used by both sample and control chambers, explaining the raised concentration at the start of recording from the control chamber (Fig. 2.4).

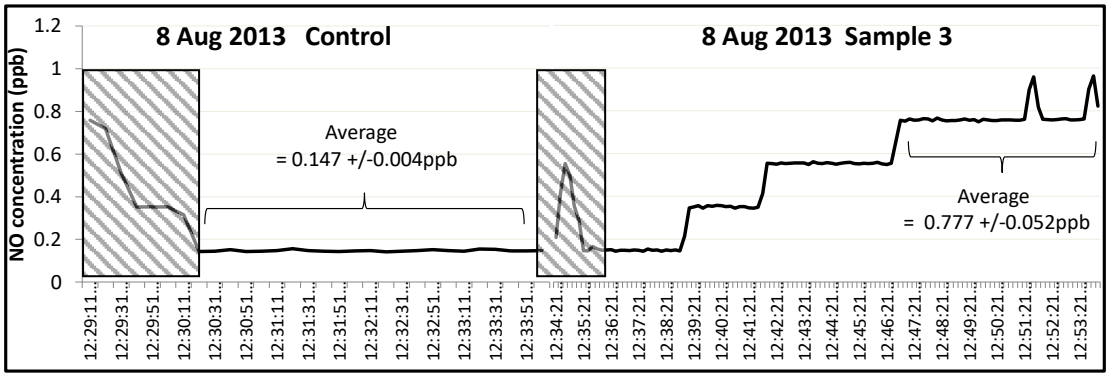

Figure 2.4: NO concentration in control chamber, left, and sample chamber, right. Shaded areas represent elevated concentrations in tubing resulting from moving chambers and switching input to the analyser.

2.2 Gas Chromatography

Gas Chromatography (GC) separates different chemicals within a gas sample using a flow-through method. The sample is carried in an inert carrier gas through a narrow tube (the column) containing a chemical (the stationary phase) which provides a high surface area over which to react with the sample gas. The time taken to pass through this column will vary depending on the physical properties and chemical reactions between the stationary phase and analyte components. Thus, components are separated and exit the column after a time specific to their chemistry (retention time) and the operating conditions. They then pass through a detector

which identifies and quantifies them electronically, with reference to standard gas samples analysed at intervals during the sample batch.

Concentrations of CO_2, CH_4 and N_2O in the gas sample vials were determined within one week of collection at Forest Research, Alice Holt, using a headspace-sampler and gas chromatograph with the following specifications:

Gas chromatograph:	Clarus 500, Perkin Elmer
Column type:	Elite PLOT Q 30 m x 30mm internal diameter megabore capillary Porous Layer Open Tubular column
Operating temperature of column:	35 °C
Carrier gas:	N_2
Detectors:	• Electron Capture Detector (ECD) for N_2O • Flame Ionisation Detector (FID) for CH_4 With methanizer to reduce CO_2 in the sample to CH_4 before analysis by the FID detector
Operating temperature of the detectors	350 °C
Automated headspace sampler:	Turbo Matrix HS-1100
Standard gas mixtures used for calibration:	• 0.2 – 5 ppm N_2O • 1.2 – 30 ppm CH_4 • 300 -7500 ppm CO_2
Peak area calculation software:	PerkinElmer Integrator
Precision of the GC gas analysis:	Assessed as 3 × standard deviation of 20 repeated measurements of standard gas concentrations at ambient levels: • 13 ppb for N_2O • 69 ppb for CH_4 • 8 ppm for CO_2

2.2.1 Gas sample quality control

Fluxes were calculated from the linear increase of gas concentrations inside the chamber with time (Section 2.1.1, Figure 2.2). Data quality of the gas sample concentrations were assessed and samples were rejected in the following circumstances:

- Sample vial septum damaged (12 out of 2097 vials),
- Known problem during sampling (7 out of 2097 vials),
- Any sample for which the CO_2 concentration was 'anomalous' (31 out of 2097 vials).

A sample was defined as 'anomalous' when a plot of the CO_2 concentration (from 12 vials) against sample time gave a linear regression correlation coefficient (R^2) < 0.80 and the removal of one vial's data (the anomalous one) can improve this to R^2 >= 0.80. This is because the CO_2

concentration increase with time is usually well above the precision of the GC detection analysis and therefore any single sample deviating significantly from a linear trend defined by 11 other samples is assumed to have a problem. Results for all gases were rejected for the anomalous sample.

a)

b)

c)

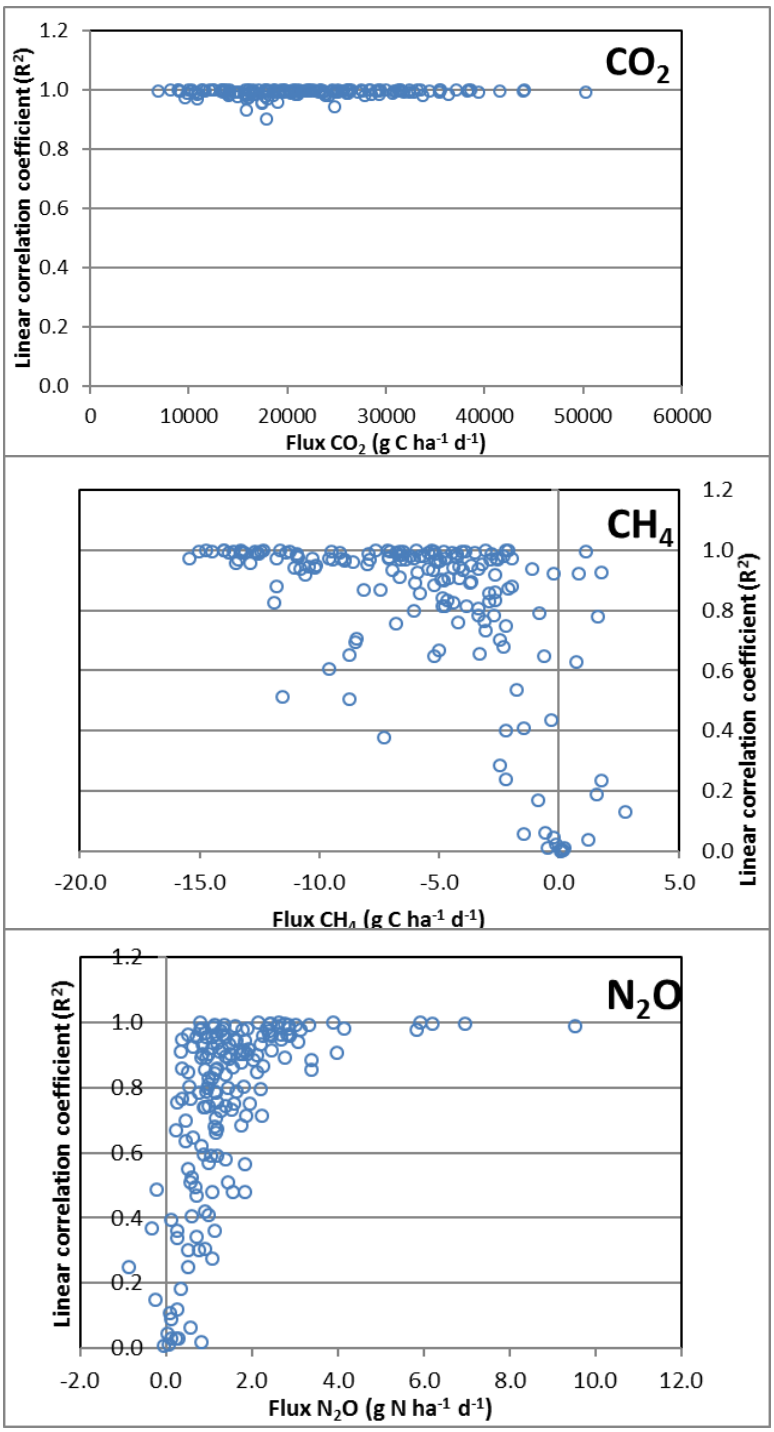

Figure 2.5: Data quality: soil gas flux vs correlation coefficient (R^2) for concentration increase over time; a) CO_2, b) CH_4 and c) N_2O measured at the Straits Inclosure. Each circle represents the measured flux from a single chamber on one day, normally derived from 12 sample vials.

Figure 2.5(a) illustrates the resulting CO_2 data, after removal of anomalous results. Figure 2.5(b) and (c) show decreasing R^2 values as the flux value decreases to zero, illustrating that low flux levels normally have a poor correlation coefficient.

2.3 Soil analyses

A soil sample was collected on each day of gas sampling at the Straits Inclosure from the soil surface near each soil frame and aggregated. Loose litter and large roots were removed and the sample mixed to ensure subsamples were representative. The samples were stored in a fridge until analysed for soil moisture content, loss on ignition, NH_4 and NO_3.

2.3.1 Soil moisture and LOI

From each day's aggregated soil sample five subsamples of approx. 10g were weighed in small beakers, dried overnight (>12hrs) in an oven at 105°C and reweighed. The difference is the soil water content (SWC), expressed as a weight percent of the dried sample. The dried sample was then placed in a furnace for 4 hours at 550°C to measure the Loss on Ignition (LOI). Material lost by burning is mainly organic matter, which has been shown to be approx. 58% carbon (e.g. De Leenheer et al., 1957; Bhatti and Bauer, 2002). This provides a guide as to the soil organic carbon (SOC) content of the soil. It is less accurate for clay-rich soils, such as are found at Straits, because clay and sesquioxides lose structural water at this temperature (Rowell, 1994). An equation derived by de Vos et al. (2005) can been used to account for the clay content:

SOC = -0.1046 * CLAY + 0.5936 * LOI (% wt) (here CLAY = 52%, in top 10cm soil).

2.3.2 NO_3 and NH_4,

Soil nitrate (NO_3) and ammonium (NH_4) content were determined using 10g of fresh soil sample, replicated 5 times, in 1M potassium chloride solution (100ml total volume). The mixtures were shaken for 30min and then allowed to settle for a further 30min before the supernatant was filtered into Skalar vials. Automated analysis for both NO_3 and NH_4 was performed simultaneously by photo-colorimetry by Skalar SAN+ with continuous segmented flow analysis. Within the Skalar analyser nitrate is first reduced to nitrite by hydrazine sulphate and the resultant nitrite (plus any original nitrite) is quantified by diazotizing with α-naphthyl-ethylenediamine dihydrochloride to form a highly coloured (red) dye which is measured at 540nm. The hydrazine reduction method is described in Kempers and Luft (1988). The ammonium in the sample is chlorinated to monochloramine which reacts with salicylate to 5-

aminosalicylate. A green dye complex is formed by oxidation and oxidative coupling, which can be measured photometrically at 600nm. The procedure, known as a modified Bertholot reaction, is described in Searle (1984). Resultant concentrations are given for the dry weight of sample, using SWC values calculated earlier.

2.4 InGOS N_2O chamber inter-comparison

Comparison of chambers used for N_2O flux measurements was carried out at an indoor facility at Hyytiala Forestry Field Station, Finland. The calibration system followed similar comparisons carried out for CO_2 flux measurement described by Pumpanen et al. (2004) and for CH_4 flux measurements described by Pihlatie et al. (2013). The system comprised a large gas reservoir (stainless-steel cylindrical tank, diameter 1.6m, height 1.0m, volume 2.6 m^3) covered with a perforated lid on which a layer of quartz sand (particle size 0.2-0.6 mm) was set to act as a porous medium (Figure 2.6). Chamber measurements were conducted on top of the sand bed and these chamber fluxes were compared to simultaneously measured reference fluxes from the tank.

Three laser absorption spectrometry gas analysers were available. One of these, an LGR N_2O/CO Analyser (Model N_2O/CO-23d, Los Gatos Research, LGR, Mountain View, CA, USA) was constantly measuring N_2O concentration within the reference cylinder and used to derive the reference flux as this decreased with time. The remaining two analysers, both Quantum Cascade Lasers (QCL, Model CW-QC-TILDAS-76-CS, Aerodyne, Research Inc., Billerica, MA, USA), were available to either record from the headspaces of two chambers being tested simultaneously or from one chamber and from within the sand layer.

At the start of the measurements, a high concentration of N_2O (1000 ppb) was injected into the tank, and the system was allowed to stabilize for 20 minutes to reach a steady-state. After the stabilization, chamber N_2O fluxes from the sand bed were measured together with measurements of the tank N_2O concentration (reference fluxes). These reference fluxes derived from measurements within the tank ranged between 20 and 120 µg N_2O-N m^{-2} h^{-1}.

In total 22 chambers of different sizes, shapes and attributes (fan, vent-tube, sampling, seals) from different research groups were tested against the known reference fluxes. Tests were defined as either ‘campaign protocol’ tests involving all chambers or ‘extra tests’ for specific chambers. At the start of each test N_2O was injected into the reference cylinder to obtain a concentration of approximately 1000 ppb N_2O. Each campaign ‘protocol’ test lasted 10 minutes and was replicated 3 times, with a pause of 20 minutes between each test, during which the chamber (but not the frame) was removed to prevent gas build up in the headspace.

Campaign 'Protocol' tests in which the Forest Research chambers were involved included the following variables:

- Sand depth - 10 cm and 20cm
- Wind speed - with external fans (approx. 1.5 m s^{-1} wind) and without fans.

All chambers were subjected to leak tests. These were carried out by placing chambers on their frames (if appropriate) in a pool of water approximately 4 cm deep. N_2O was injected into the headspace of each chamber and manipulated until a concentration of approximately 1000 ppb was obtained. The concentration within the chamber was then recorded over the following hour.

The reference flux from the calibration tank was calculated as follows:

$$C_f(t_i) = C_0 \exp(-\alpha t_i)$$

Where,

$C_f(t_i)$ = fitted CO_2 concentration inside the tank at time t_i

C_0 = the measured concentration in the tank at the beginning of the testing period

t = time

α = a parameter.

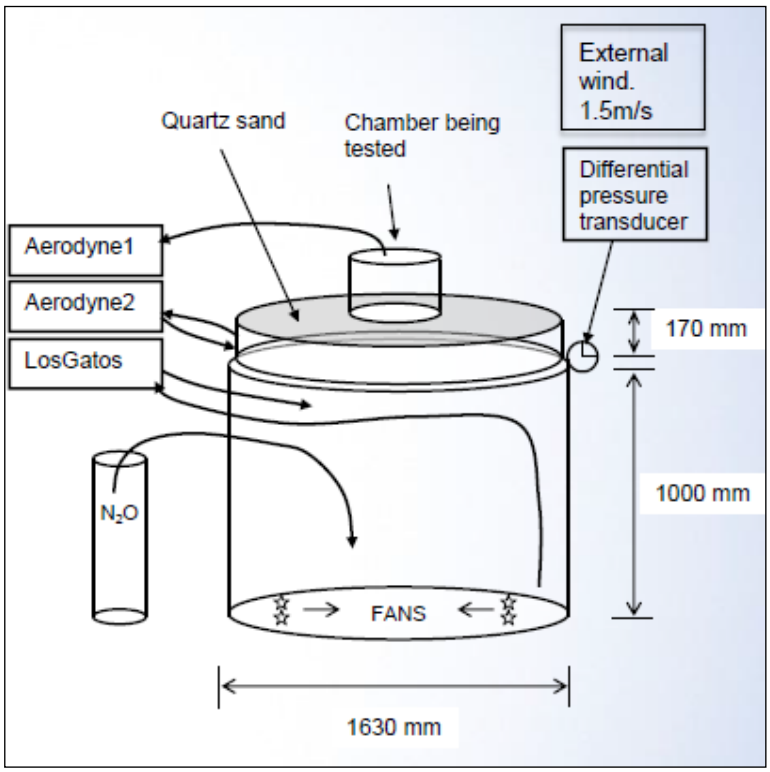

Figure 2.6: Calibration tank used for comparing N_2O flux chambers at Hyytiala Forestry Research Station. Project funded by InGOS.

The 2 chambers studied from Forest Research differed in the seal used between chamber and frame and these differences were investigated using the calibration system. One chamber used a water seal, as described for measurements at the Straits Inclosure and the other used a foam rubber seal, as used for fertiliser experiments. The different configuration results in slightly different dimensions as illustrated in Figure 2.7.

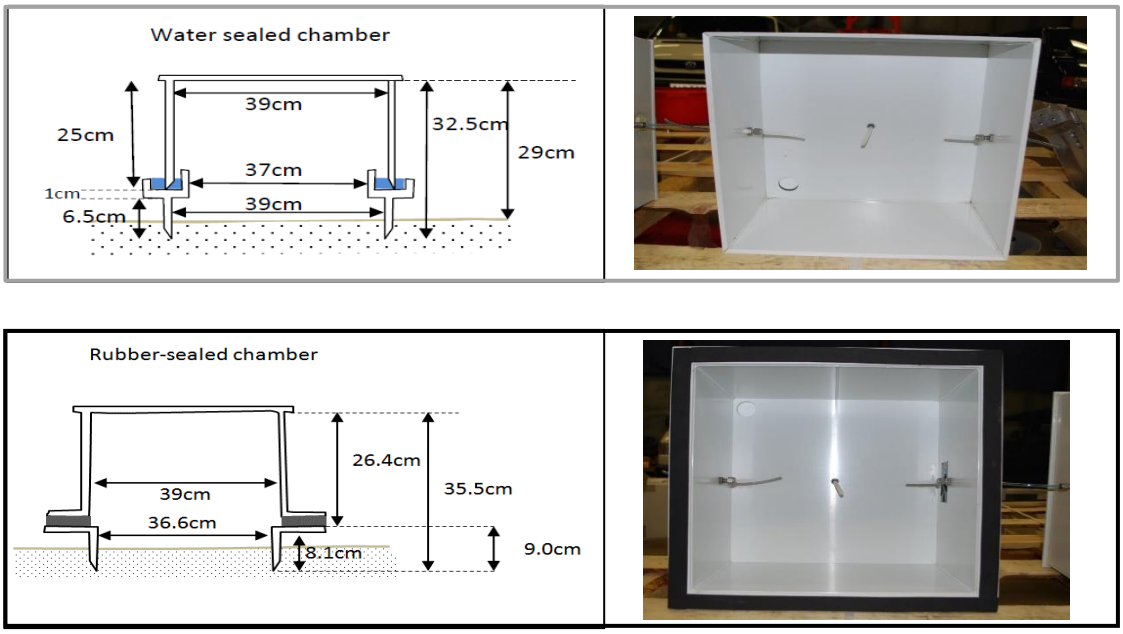

Figure 2.7: Water sealed chamber, above, and rubber-sealed chamber, below, illustrating differences in dimensions resulting from design differences.

The 2 chambers were placed on the calibration tank at the same time and gas vial sampling was carried out over 60 minutes and compared to the reference flux calculated from inside the tank.

2.5 Eddy covariance

CO_2 eddy covariance flux data has been used in this study. For the Straits Inclosure it was supplied by Forest Research and for Griffin Forest it was supplied by University of Edinburgh.

The eddy covariance technique requires a relatively flat surface, such that vertical flow and density fluctuations can both be considered negligible. It measures high frequency data, sampling every 5 s and logging the average every half hour. Each parcel of air has a gas concentration, pressure, temperature, humidity and wind speed. Three-dimensional wind and gas concentrations are decomposed into mean and fluctuating components. The covariance is calculated between the fluctuating component of the vertical wind and the fluctuating component of the gas concentration. The measured flux is proportional to the covariance (Baldocchi et al. 1988, Burba and Anderson, 2010). The area from which the detected eddies originate is described probabilistically and called a 'flux footprint'. The area of the flux footprint

is dynamic in size and shape, changing with wind direction, thermal stability and measurement height, and has a gradual border.

The CO_2 covariance flux measurement is of net ecosystem exchange (NEE) from which total ecosystem respiration (TER) is derived using the night time flux measurements and day time air temperatures (Lloyd and Taylor, 1994; Swanson and Flanagan, 2001). NEE is conventionally, but not exclusively, given a negative sign when there is a net uptake of CO_2. For ecosystem modelling purposes the term net ecosystem production (NEP) is used to describe the difference between gross primary production (GPP) and total ecosystem respiration (TER). NEP is conventionally positive when there is a net uptake of CO_2. For this study, NEP = -NEE, when conventional signs are used. Using eddy covariance data, GPP is calculated from the sum of TER and positive NEE (i.e. NEP).

2.6 LandscapeDNDC model description

LandscapeDNDC is a recent addition to a suite of models based on DNDC (DeNitrification-DeComposition) (Li et al., 1992), a process-based numerical biogeochemical model that was designed to simulate biosphere-atmosphere-hydrosphere exchanges within and above the soil, and has been used to estimate greenhouse gas exchanges in a range of terrestrial environments.

The original DNDC model was developed to better understand and quantify N_2O, CO_2 and N_2 evolution from agricultural soils (Li et al., 1992). The aim was to predict emissions of N_2O from different agricultural crops and management practices and improve large scale assessments of N_2O from agro-systems in the USA and globally. The model used parameters that were average values for US soils and modelled crops commonly grown in the USA. In 2000, this DNDC model was combined with the forest growth model PnET (Photosynthesis - EvapoTranspiration) (Aber and Federer, 1992), together with some further enhancements to model greenhouse gas emissions from forest soils (Li et al, 2000; Stange et al., 2000). This combined model was known as PnET-N-DNDC, and was designed to describe C, N and both N-trace gases (N_2O and NO) in forest ecosystems. Sensitivity testing was carried out with data from 7 forest sites in the USA and Europe, including 2 sites in the Höglwald Forest, S Germany. The data from Höglwald was measured and provided by Butterbach-Bahl and colleagues from the Fraunhofer Institute for Atmospheric Environment Research (IFU), based in Garmisch-Partenkirchen, Germany, which started their involvement with the model.

Giltrap et al. (2010) describe various modifications undertaken to make the DNDC model work for other specific environments. These include changing soil parameters to match local conditions, but also adding algorithms to simulate additional or alternative processes. For

example, Kiese et al. (2005) enabled forest growth to continue all year and included very heavy rainfall to model tropical rainforest soils in Australia; Zhang et al. (2002) included water table dynamics and resultant methane emissions from wetland environments. Thus, many variants have been developed over the years, resulting in a Wetland-DNDC (Zhang et al., 2002), Forest-DNDC (Li et al., 2000), NZ-DNDC (for dairy pastures, Saggar et al., 2004), UK-DNDC (for UK crops, Brown et al., 2002) and more, each with its own special parameters, processes and environments in which they are valid.

LandscapeDNDC (Haas et al., 2013) has been developed recently at the Institute of Meteorology and Climate Research – Atmospheric Environmental Research (IMK-IFU), Garmisch-Partenkirchen, Germany (previously the Fraunhofer Institute for Atmospheric Environment Research). It uses concepts and algorithms from the original PnET-N-DNDC but not the original software code. It has been re-written with a new structure and data input/output and can be run as a single site or in multi-site, regional mode. Different vegetation sub-modules can be called to model different land use types (currently agriculture, grassland and forest) and parameters specific to the vegetation or environment can be entered as part of the simulation set up. The re-coding of the model is to improve speed when run in regional mode and, as each site is run synchronously, some exchange of materials can take place such as fertiliser runoff from an arable ecosystem into a forest or grassland (Haas et al., 2013). Thus, in regional mode, lateral movement of water, nutrient transport and feedbacks can be simulated, which has not been possible before. C and N pools within the soil accumulated under one land use can also be carried over to a subsequent land use.

LandscapeDNDC has been used in this study in site mode only which comprises 6 sub-modules, as listed in Table 2.2 and illustrated in Figure 2.8. Data required at input is listed in Table 2.3. The duration of the simulation is set as an input variable and is ideally at least 10 years when modelling forests. Daily climate data is required for every day of that duration. The timestep chosen is normally daily, but reverts to hourly while rain is falling. Output is given for 130 variables for each day of the simulation in 5 files as well as aggregated annual data. Each sub-module is summarised below.

Table 2.2: LandscapeDNDC sub-modules used when vegetation = forest

Sub-module function	Sub-module used to model forest vegetation	Reference
Microclimate	ECM	Grote, 2007
Vegetation structure	Treedyn	Bossel, 1996
Vegetation growth	PnET or	Aber and Federer, 1992; Aber et al., 1995
	PSIM	Grote, 2007; Grote et al., 2011
Decomposition (or mineralisation)	DNDC	Li et al. 1992
Denitrification	DNDC	Li et al. 1992
Nitrification	DNDC	Li et al. 1992

Table 2.3: LandscapeDNDC input files required for simulations (X = project name)

Data type	File name	Example data
System	X.xml	Sources for remaining project data input files, location for output files, Start date and duration of simulation, with timestep
Site location	X_setup.xml	Latitude, longitude, time zone, slope, aspect Defines sub-modules to be used and output filenames
Climate	X_climate.txt	Repeats latitude and longitude, plus elevation. Annual average precipitation, temperature, temperature amplitude and wind speed, rainfall intensity, cloudiness. Daily figures for precipitation, average maximum and minimum temperature. Also (if available) daily wind speed, vapour pressure deficit, solar radiation.
Air chemistry	X_airchem.txt	Annual NH_4 and NO_3 deposition. CO_2 concentration
Events	X_mana.xml	Start event: define species type, size and number per unit area or biomass Subsequent management events, eg. fertiliser application, thinning, felling
Soil type and characteristics	X_site.xml	Bulk density, Organic C and N content, clay content, water holding capacity, wilting point, pH, for each layer having the same characteristics. Thickness must also be given (minimum thickness = 2 cm)
Vegetation species parameters	X_parameters-species.xml	Parameters set here overrule default values in a system file

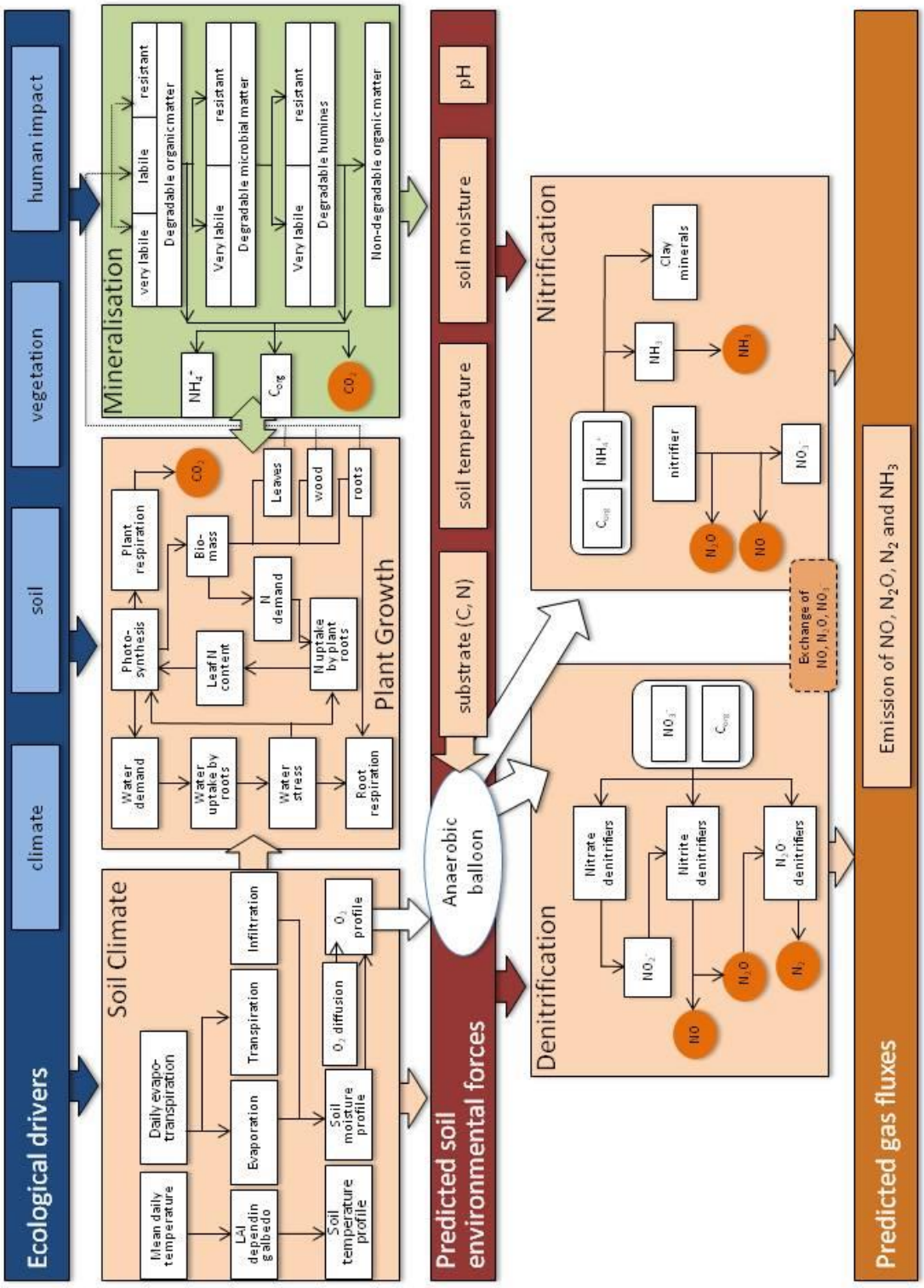

Figure 2.8 Diagram illustrating LandscapeDNDC model with sub-modules and processes (after Butterbach-bahl et al., 2001 and Haas et al., 2012).

2.6.1 Micro-climate

The microclimate is calculated at 2 levels: canopy and soil. These are in two separate sub-modules, Canopy ECM and soil microclimate.

Canopy ECM

This module adjusts daily temperature input values and provides a temperature for each above ground layer in the system. When sub-daily data is required, a distribution of temperature throughout the day is calculated, based on latitude, daylength, and daily average, minimum and maximum temperatures. Both temperature and radiation are calculated throughout the canopy. Temperature is scaled using an empirically derived interpolation function that links temperature above the canopy with upper soil temperature (Grote et al., 2009a). The tree structure and leaf area index (LAI) are used to calculate degree of shading at each canopy layer and hence amount of reduction in temperature required. Calculations are also made of the effect of the canopy on rainfall and evapo-transpiration, such that appropriate water content can be passed to the DNDC modules for soil moisture content.

Soil micro-climate

Values for surface soil temperature and moisture are passed from CanopyECM every timestep. From these, soil temperature and moisture profiles are calculated using soil physical properties, soil water status, thermal/ hydraulic impact of plants and soil respiration to give a value for each layer defined in the soil together with an oxygen diffusion profile (Li et al., 2000).

2.6.2 Vegetation structure: Treedyn

As implemented in LandscapeDNDC, Treedyn (Bossel, 1995) models the structure of an average tree as it grows. It therefore determines the stem diameter and height, number and distribution of branches and crown size. Species specific parameters define the ratio of diameter to height and of crown to height and diameter, in other words the shape of the tree. This then determines the distribution of leaves throughout the canopy.

2.6.3 Vegetation growth: PnET

The PnET (Photosynthesis – Evapotranspiration) model (Aber and Federer, 1992; Aber et al., 1996) is based on photosynthesis at the leaf level and was developed using data from Field and Mooney (1986) and Reich et al. (1995) who found a linear relationship between leaf N

concentration and maximum photosynthetic rate, also known as assimilation, (A_{max}) which was different for broadleaves and needle shaped leaves. The equation is:

$A_{max} = A_{max}A + (A_{max}B * foliar\_N)$

Where AmaxA and AmaxB are constants defining the intercept and slope of the linear relationship. The actual, realised photosynthesis on any particular day is reduced in response to radiation intensity, temperature and vapour pressure deficit at the top of the canopy (see Appendix A.1). The layered canopy simulated has reduced radiation intensity and specific leaf weight which decrease with canopy depth. A fraction of the Amax is allocated to basal respiration at 20°C (set in the parameter BASEFOLRESPFRAC). From this, actual respiration is calculated separately for average daytime and night time temperatures, using a Q10 value (defined in the parameter RESPQ10). Net C gained is allocated to wood, leaves and roots in ratios determined by parameters, which allow growth of the trees. Each year, new leaves are produced and the timing is defined by a concept of growing degree days (GDDs), used widely in agriculture (summarised in McMaster and Wilhelm, 1997). In PnET, GDDs are calculated as the accumulated mean temperature above 0°C from 1st January. Two parameters, GDDFOLSTART and GDDFOLEND, set for the vegetation species being modelled, define the GDD required at the start of budburst and when leaves finish opening, reaching maximum area. Thus, budburst can vary from year to year, dependent on temperatures. Further details and equations are given in Appendix A.

2.6.4 Vegetation growth: PSIM

The PSIM (Physiological Simulation Model) vegetation model (Grote, 2007, Grote et al., 2011) was designed for use with several vegetation cohorts in parallel. The environmental conditions that a cohort experiences are defined by the canopy and soil layer properties that it occupies according to its height, start of crown height and rooting depth. Leaves and roots are equally distributed in layers shared between vegetation cohorts, but competition is created by different resource use (principally N and water) and shading. Above ground competition is dominated by shading from cohorts with higher canopies, while below ground competition depends on the presence of fine roots in a certain soil layer and the species-specific uptake capacity of water and N.

For each vegetation type, C uptake is calculated from functions of light, temperature and enzyme activity based on Farquhar et al. (1980) and the water constraint according to Ball et al. (1987). Thus, the C gained is determined by iteratively adjusting the stomatal conductivity (rate of passage of CO_2 entering or water leaving through the stomata of a leaf) and hence

transpiration demand which is limited by water availability. The potential maximum rate of carboxylation at 25°C (parameter VCMAX25) is reduced by suboptimal levels of foliar N and when the seasonal physiological status is below 1. For deciduous trees this status is 1, when budburst is completed and before senescence starts. For evergreen trees, it is calculated using an S-model proposed by Mäkelä et al. (2004). C is split into leaf, wood and root fractions determined by parameters, as with PnET.

Budburst is defined by a parameter, GDDFOLSTART, as in PnET but the end of budburst is not temperature dependent. The number of days taken to open leaves fully is set in the species-specific parameter, NDFLUSH. This may aid differentiation between vegetation cohorts within the same ecosystem but reduces the degree of temperature dependence of the phenology.

2.6.5 Mineralisation: DNDC

Mineralisation is the process by which organic C and N are transformed to inorganic C and N. This sub-module, originally called 'decomposition' by Li et al. (2000), tracks concentrations of substrates within the soil, principally dissolved organic C, NO_3^- and NH_4^+. Inputs are from litter fallen from trees (with a known C/N ratio), dead microbes (also with a known C/N ratio) and N pollution (wet and dry). Initial values for organic C and organic N are defined for each soil stratum as part of the setup process, the top stratum being the litter layer. Three organic matter pools are defined: degradable organic matter (mainly from plant litter), degradable microbial matter and degradable humins, within each of which there is a split into very labile and resistant components. Rates of decomposition are mainly determined by first order kinetics (dependant principally on temperature and Eh), and equations are given in Appendix B. The outputs from this sub-module are quantities of dissolved organic C and N available for other soil processes and for tree growth and a contribution to soil respiration.

2.6.6 Denitrification: DNDC

The denitrification sub-module simulates the anaerobic process of denitrification. It can take place at the same time as the aerobic process of nitrification when rainwater locally fills soil pore spaces to produce anaerobic micro-sites. The sub-module allows for two soil fractions, anaerobic and aerobic, with a variable partial pressure of oxygen (pO_2). Li et al. (2000) describe the dynamic process by which the model changes the volume of the anaerobic fraction as an "anaerobic balloon" driven by a simple kinetic scheme. pO_2 in each soil layer is determined by rates of diffusion and consumption of O_2. Oxygen within the soil is consumed by microbial and root respiration (data provided by the mineralisation and tree growth sub-modules). Oxygen diffusion rates vary according to the soil texture and structure and the water content. Rainfall

events in the model saturate each layer completely before moving down to the next. They are assumed to have constant intensity but variable duration. The oxygen diffusion rate is reduced to 1/10,000th of the diffusion rate in air when a layer is filled with rainwater. Thus, the volumetric fraction of the anaerobic balloon increases using a linear correlation as the partial pressure of oxygen for a soil layer decreases.

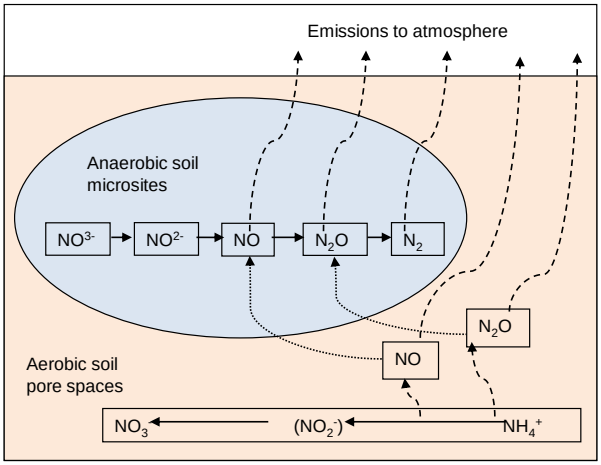

Figure 2.9: Diagram to illustrate the anaerobic balloon concept which separates anaerobic and aerobic micro-sites within the same soil matrix (after Li et al., 2000)

Substrates, including dissolved organic carbon (DOC), NH_4^+, NO_3^-, NO and N_2O, are divided between the anaerobic and aerobic fractions proportionately. As the anaerobic balloon increases, more substrates are allocated to it, removing them from the aerobic fraction. After calculating diffusion rates, a portion of the gases is emitted into the air and the remainder is reallocated to reactions for the next time-step. When the diffusion rates are low, a smaller fraction of the gas products of denitrification (NO and N_2O) will be emitted at the soil surface, increasing the likelihood of further denitrification within the anaerobic micro-sites. Thus, the volumes of NO and N_2O emitted are the result of a competition between consumption, production and diffusion within the anaerobic balloon (Figure 2.9). Equations are given in Appendix C.

2.6.7 Nitrification: DNDC

Nitrification only takes place outside the "anaerobic balloon" described above. The rate of nitrification is controlled by temperature, pH and substrate concentrations and to a lesser extent soil moisture. The initial soil nitrifier population is set at 10 % of the total soil microbial biomass, based on observations at Höglwald Forest site in Germany (Li et al., 2000). The exact mechanism by which NO and N_2O are produced by nitrification is not clear and therefore the model defines NO and N_2O production as fractions of the predicted nitrification rates. Baumgartner and Conrad

(1992) report NO production as 0.1 – 4 % of nitrification from laboratory experiments on a range of soil types. Li et al. (2000) set an arbitrary maximum rate of NO production at 0.25 % of nitrification. The maximum fraction for N_2O production from nitrification was set at 0.06 %, based on laboratory experiments by Ingwersen et al. (1999) on soil core samples. Equations are given in Appendix D.1.

Chemo-denitrification is the purely chemical process by which nitrite breaks down to NO. It takes place in acidic soils and does not involve micro-organisms (e.g. Yamulki et al., 1997). It is included in the nitrification sub-module as a function of nitrification rate, soil temperature and soil pH. Equations are given in Appendix D.2.

NO and N_2O produced from nitrification, denitrification and chemo-nitrification are combined into a common gas pool. A proportion of the gases are emitted to the atmosphere, following a diffusion calculation and the remainder is reallocated for new reactions in the next time-step.

2.6.8 Vegetation species parameters

Standard parameters which define relevant tree species characteristics in PnET and PSIM tree growth submodules are listed in Tables 2.4 and 2.5. In many cases, these standard values have not been previously tested for these species and do not necessarily represent an ideal generic value for that parameter. Hence the need to evaluate and adjust the parameters for specific sites. As an example, Figure 2.10 shows the results of simulations using the standard species parameters for pedunculate oak (Q. robur, QURO) compared with EC data from the Straits Inclosure.

Table 2.4: Principal standard PnET parameters for trees studied; QURO = Quercus robur; FREX = Fraxinus excelsior; PISI = Picea Sitchensis.

Parameter	Description	Units	PnET QURO	PnET FREX	PnET PISI
CO_2 exchange parameters					
AMAXA	Intercept value for linear relationship of photosynthesis and foliar N	$nmolCO_2\ g^{-1}\ s^{-1}$	5.73	5.73	5.3
AMAXB	Maximal photosynthetic rate per unit of foliar N	$nmolCO_2\ g^{-1}\ s^{-1}$ / %N	50.5	18.1	21.5
BASEFOLRESPFRAC	Night respiration as fraction of photosynthesis	0-1	0.1	0.1	0.1
GRESPFRAC	Fraction of C allocation used in growth respiration	0-1	0.25	0.25	0.25
RESPQ10	Temperature dependency of leaf respiration	-	1.84	2	2
ROOTMRESPFRAC	Ratio of fine root maintenance respiration to biomass production	-	1.0	1.0	1.0
WOODMRESPA	Wood maintenance respiration as a fraction of gross photosynthesis		0.07	0.07	0.07
Phenology related parameters					
GDDFOLSTART	Daily temperature sum for start of foliage budburst	°days	400	0	550
GDDFOLEND	Daily temperature sum for end of foliage growth (maximum leaf area)	°days	900	900	1500
GDDWODSTART	Daily temperature sum for start of C storage as wood (set at GDDFOLSTART + 100)	°days	500	100	650
GDDWODEND	Daily temperature sum for end of C storage as wood	°days	900	900	1500
MFOLOPT	Foliage biomass under optimal, closed canopy conditions	kg DW m^{-2}	0.24	0.36	2
SENESCSTART	Day of year after which leaf death can occur	day of year	246	270	270
Resource acquisition parameters					
NCFOLOPT	Optimum nitrogen concentration of foliage	g N gDW^{-1}	0.026	0.032	0.018
SLAMIN	Specific leaf area under full light	m2 kg-1	5.9	8.5	3.6
EXPL_NH4	Relative exploitation rate of NH_4	%	0.245	0.01	0.306
EXPL_NO3	Relative exploitation rate of NO_3	%	0.301	0.01	0.189
EXT	Light extinction (attenuation) coefficient	0-1	0.54	0.65	0.5
WUECMAX	Maximum water use efficiency constant	$gCO_2\ gH_2O^{-1}$	9.6	7.8	10.9

Table 2.5: Principal standard PSIM parameters for trees studied; QURO = Quercus robur; FREX = Fraxinus excelsior (proxy for multiple understorey species); PISI = Picea Sitchensis.

Parameter	Description	Units	PSIM QURO	PSIM FREX	PSIM PISI
CO_2 exchange parameters					
RESPQ10	Temperature dependency of leaf respiration	-	1.84	2	
VCMAX25	Maximum RubP saturated rate of carboxylation at 25°C for leaves in full sun	µmol m^{-2} s^{-1}	90.5	84.6	27.8
KM20	Respiration maintenance coefficient at reference temperature	0-1	0.1	0.1	0.1
Phenology related parameters					
GDDFOLSTART	Daily temperature sum for start of foliage budburst	°days	400	0	550
MFOLOPT	Foliage biomass under optimal, closed canopy conditions	kg DW m^{-2}	0.24	0.36	2
NDFLUSH	No of days required to complete growth of new foliage	days	41	40	90
NDMORTA	No of days required to complete leaf fall	days	41	40	1625
DLEAFSHED	Day by which leaf fall is complete	day of year	287	310	2010
Resource acquisition parameters					
NCFOLOPT	Optimum nitrogen concentration of foliage	g N gDW^{-1}	0.026	0.024	0.018
US_NH4	Maximum rate of NH_4-N uptake	$kgNH_4$-N kg^{-1} fine root dry weight day^{-1}	0.00033	0.012	0.012
US_NO3	Maximum rate of NO_3-N uptake	$kgNO_3$-N kg^{-1} fine root dry weight day^{-1}	0.00033	0.006	0.006

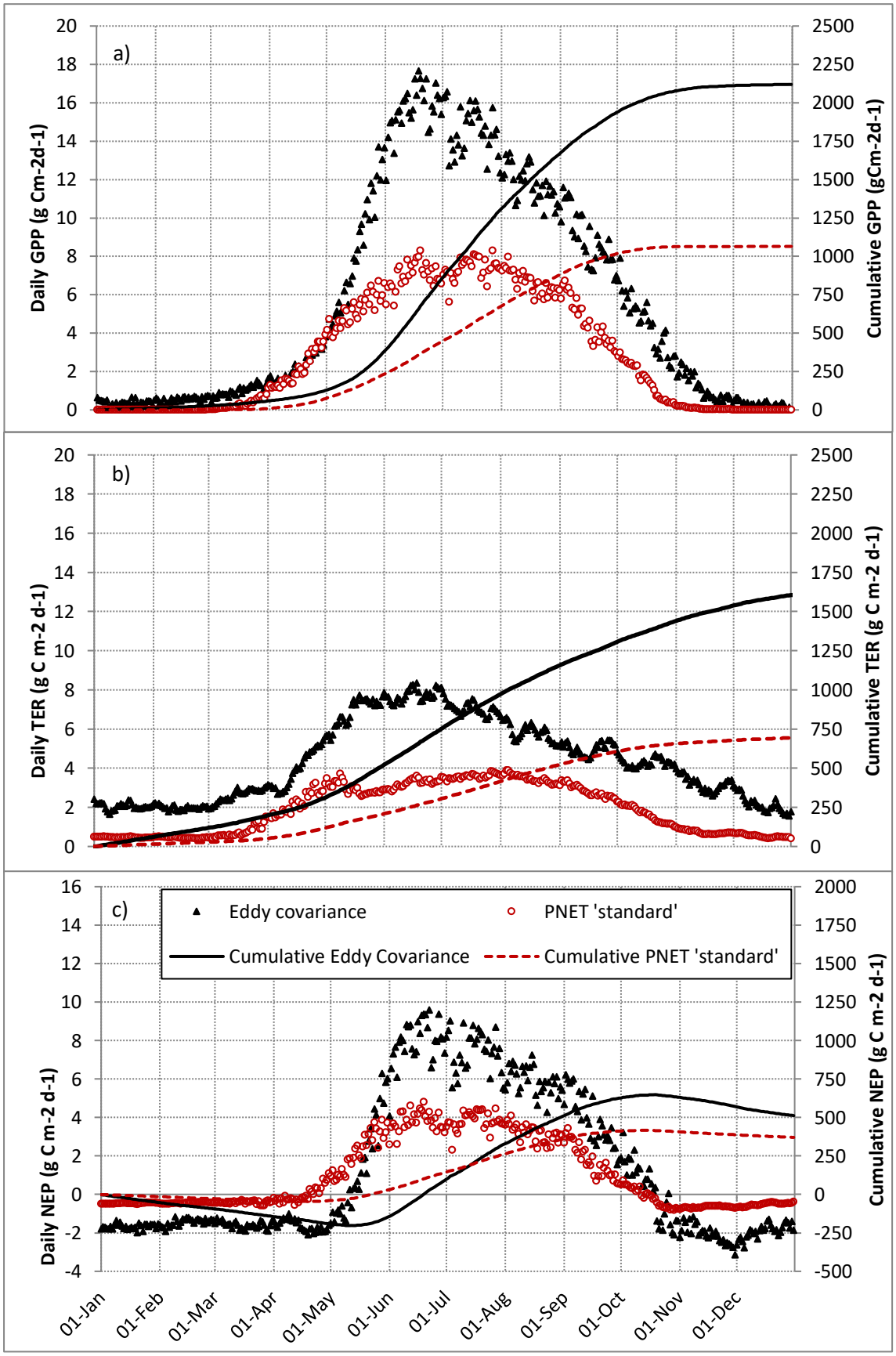

Figure 2.10: Ecosystem CO_2 flux data derived from eddy covariance compared to PnET simulated data using standard parameters; a) GPP, b) TER, c) NEP. Each plot shows average daily and cumulative values for 1997-2007 for the Straits Inclosure, Hampshire.

2.7 Statistical analysis

Statistical analysis to quantify the comparison of simulated values with measurements has followed the principles laid out in Smith et al. (1997) who in turn refer to Loague and Green (1991). These principles are shown in the flow diagram in Fig. 2.11, taken from Smith et al. (1997). All the statistical calculations are available within ModEval v2, an Excel add-on developed by Smith et al. and used to perform the calculations for this study. A brief explanation of the three main statistics referred to here is given below, as explained by Smith et al. (1997).

In all equations below the following abbreviations are used:

P= predicted or simulated value
O = observed or measured value
$\bar{O}$ = mean of observed values
n = number of observations

2.7.1 Root Mean Squared Error

Root Mean Squared Error (RMSE), is the square root of the variance of residuals. It indicates the absolute fit of a model to measured data. It can be presented in the same units as the observed variable, but here has been converted to a percentage of the observed mean. Loague and Green (1991) describe it as the total difference between the simulated and measured values. The equation is:

$$RMSE = \left[\sum_{i=1}^{n} \frac{(P_i - O_i)^2}{n}\right]^{0.5} * \frac{100}{\bar{O}}$$

The lowest value is zero, which indicates there was no difference between observed and predicted values. Therefore, the closer to zero the RMSE value is the smaller the error and the better the fit of simulations to measurements. The value may be more than 100% when calculated relative to the mean of the observed values.

When standard errors of the measurements were available ($S_e(i)$), or estimated, the statistical significance of RMSE has been assessed by comparing the result with the value obtained from an error corresponding to the 95% confidence interval of the measurements, as below:

$$RMSE_{95\%} = \frac{100}{\bar{O}} \sqrt{\sum_{i=1} \left(t_{(n-2)95\%} * S_e(i)\right)^2 / n}$$

where $t_{(n-2)95\%}$ = Student's t distribution with n-2 degrees of freedom and a 2-tailed P-value of 0.05.

An RMSE value less than $RMSE_{95\%}$ indicates that the simulated values fit within the 95% confidence interval of measurements.

2.7.2 Modelling Efficiency

The modelling efficiency (ME) is useful when no estimates are available for standard errors on measurements. ME compares the efficiency of the model to the efficiency of describing the data as the mean of the observations, as below:

$$\boldsymbol{ME} = \left(\sum_{\boldsymbol{i=1}}^{\boldsymbol{n}}(\boldsymbol{O_i} - \boldsymbol{\bar{O}})^{\boldsymbol{2}} - \sum_{\boldsymbol{i=1}}^{\boldsymbol{n}}(\boldsymbol{P_i} - \boldsymbol{O_i})^{\boldsymbol{2}}\right) / \sum_{\boldsymbol{i=1}}^{\boldsymbol{n}}(\boldsymbol{O_i} - \boldsymbol{\bar{O}})^{\boldsymbol{2}}$$

ME can be negative or positive with a maximum value of +1.0. A positive value shows the simulated values describe the variation in the measured data better than the mean of the observations. The perfect fit would have an ME = 1.0. If ME = 0, then the predicted data are as accurate as the mean of the measurements. A negative value shows that the simulated values describe the data less well than the mean of the observations. ME can be < -1.

2.7.4 Coefficient of determination

The coefficient of determination (CD) is a measure of the proportion of total variance in the observed data that is explained by the predicted data. The equation is:

$$\boldsymbol{CD} = \sum_{\boldsymbol{i=1}}^{\boldsymbol{n}}(O_i - \bar{O})^2 / \sum_{\boldsymbol{i=1}}^{\boldsymbol{n}}(P_i - \bar{O})^2$$

The lowest value is zero. If CD = 1.0 or CD > 1.0, it shows that the deviation of the predictions from the mean of the measured values is less than that observed in the measurements. Therefore, the model describes the measured data better than the mean of the measurements and it is a good fit. If CD < 1.0, it indicates that the deviation of the predictions from the mean of the measured data is greater than that observed in the measurements. Therefore, the mean of the measurements describes the data better than the model, which does not show a good fit.

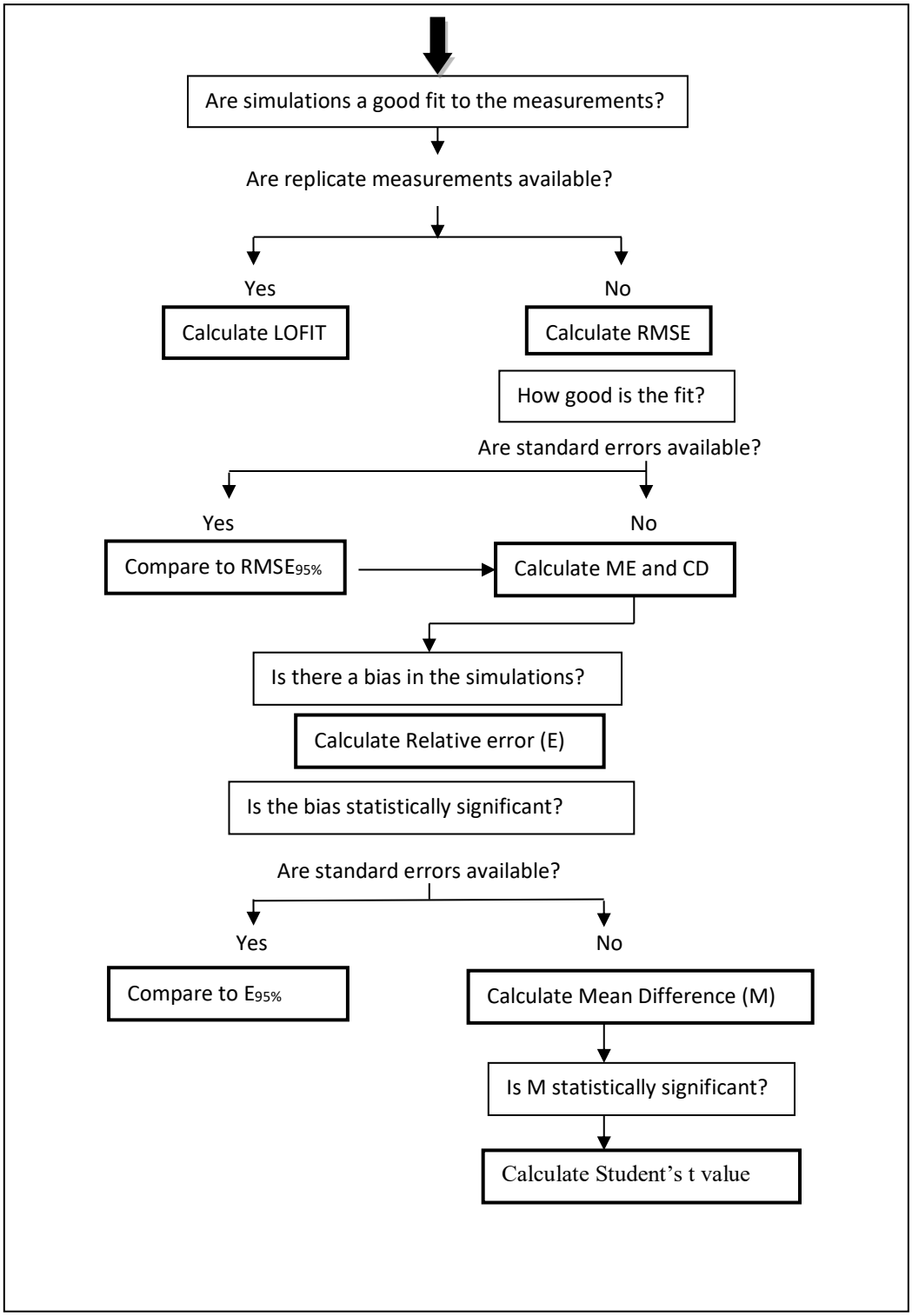

Figure 2.11: Flow chart for statistical methods, after Smith et al. (1997)

Chapter 3

Measured and modelled gas fluxes of CO_2, CH_4, N_2O and NO from a forest soil under an oak plantation in south east England

Shirley M. Cade[1], Saúl Molina-Herrera[2], Edwin Haas[2], Rüdiger Grote[2], James I. L. Morison[3], Kevin C. Clemitshaw[1], David Lowry[1], Matthew Wilkinson[3], and Sirwan Yamulki[3]

Paper in preparation for submission to Biogeosciences

(Number of manuscript pages: 48)

My Contribution to this work:

- Carried out soil flux measurements of CO_2, CH_4, N_2O and NO and soil analyses (April 2013 – Aug 2014)
- Analysed soil flux and soil analysis data
- Collated and formatted meteorological and eddy covariance flux data for LandscapeDNDC model simulations
- Carried out all modelling work with LandscapeDNDC
- Performed all statistical analyses using ModEval
- Wrote first draft of manuscript
- Produced all figures

Measured and modelled fluxes of CO_2, CH_4, N_2O and NO from a forest soil under an oak plantation in SE England.

Shirley M. Cade[1], Saúl Molina-Herrera[2], Rüdiger Grote[2], Edwin Haas[2], James I. L. Morison[3], Kevin C. Clemitshaw[1], David Lowry[1], Matthew Wilkinson[3] and Sirwan Yamulki[3]

[1]{Department of Earth Sciences, Royal Holloway, University of London, Egham, TW20 0EX, UK}
[2]{Karlsruhe Institute of Technology, Institute of Meteorology and Climate Research, Atmospheric Environmental Research, Kreuzeckbahnstraße 19, 82467 Garmisch-Partenkirchen, Germany}
[3]{Forest Research, Alice Holt Lodge, Farnham, GU10 4LH, UK}

Correspondence to: S. M. Cade (Shirley.Cade.2008@live.rhul.ac.uk)

Abstract

Forests and their soils affect greenhouse gas (GHG) emissions as they are typically net sinks for carbon but may become sources of GHGs CO_2, CH_4 and N_2O and of NO, following management disturbance or climatic change. Process-based biogeochemical models are valuable tools to better understand GHG fluxes and to evaluate impacts of environmental changes or management scenarios. Here, we evaluate LandscapeDNDC, a model developed to simulate processes of C, N and water cycling in grassland, arable and forest ecosystems at ecosystem and regional scales, against eddy covariance and soil chamber measurements of GHG fluxes in an 80-year-old deciduous oak plantation in SE England over several years. This plantation has a substantial understorey which is likely to contribute considerably to GHG exchange processes but is generally not explicitly considered in biosphere models. Therefore, we compared two process-based vegetation modules within the LandscapeDNDC framework where one (PSIM, Physiological Simulation Model) considers the understorey explicitly, while the other (PnET, Photosynthesis-Evapotranspiration model) does not. Species parameters for both modules were adjusted to match local measurements. LandscapeDNDC was able to reproduce daily microclimatic conditions which serve as input for the vegetation modules (although soil moisture had a restricted range) and both modules reproduced the seasonal patterns and cumulative annual fluxes of gross primary production (GPP) and total ecosystem respiration (TER) to within 15 %. Inter-annual variation in CO_2 fluxes was not reproduced, especially with the PSIM module (max. standard deviation values: 60, 261, 175 g C m^{-2} yr^{-1}, for PSIM, PnET and EC data respectively), possibly due to lack of a processes to vary peak LAI annually. Using the PSIM module, the understorey contributed substantial GPP, TER and soil CO_2 fluxes (17, 21 and

21 %, respectively) to the simulated results. Simulated annual soil fluxes of CO_2, N_2O and NO compared less well (up to 49% different) to measurements, reflecting increased variability and uncertainty in the measurements. Nevertheless, simulations of soil CO_2 emissions using PSIM as a vegetation module correlate much better with aggregated monthly measurements during the period 2008–2012 than simulations with PnET. Sensitivity analysis showed soil N_2O and NO fluxes simulated by LandscapeDNDC were most sensitive to initialisation of organic C content, bulk density and field capacity. Ecosystem level CO_2 fluxes were consistently insensitive to changes in input. A model experiment to assess the effect of a selective thinning showed that both modules gave different GPP and TER responses, and neither reproduced well the observed changes in ecosystem CO_2 flux components. Overall, this study demonstrates the need to further assess model processes to improve inter-annual variability and understorey contributions, particularly if models are to be used to predict GHG balances following climatic or management changes at this site.

1 Introduction

The three long-lived GHGs that contribute most to global warming are carbon dioxide (CO_2), methane (CH_4) and nitrous oxide (N_2O) (IPCC 2013). Forests are sinks and sources for CO_2 and are estimated to store 861 ± 66 Pg C globally, of which 44 % is in the soil, to 1 m depth (Pan et al., 2011). Temperate forests occupy an area of 767 Mha and contribute 0.8 ± 0.1 Pg C yr^{-1} to the global C sinks (Pan et al., 2011). In European forests, C density is higher than in other continents, possibly as a result of management with low harvest rates (Thurner et al., 2014). Forest soils can be sources or sinks for CH_4, N_2O and NO, which is a precursor of the tropospheric air pollutant NO_2.

Soil microbiological processes that result in fluxes of GHGs and NO are reasonably well understood. CO_2 is produced by autotrophic respiration of roots and heterotrophic respiration of soil-dwelling macro- and micro-organisms that decompose soil organic material. Denitrification under anaerobic conditions and nitrification in aerobic conditions are the main soil processes responsible for N_2O and NO production; chemo-denitrification is the main path responsible for soil NO production under acidic soil conditions (Yamulki et al., 1997; Medinets et al., 2015). CH_4 oxidation takes place when available N is low, and the addition of N, particularly as NO_3^-, has been shown to reduce CH_4 uptake (e.g. Reay and Nedwell, 2004; Gunderson et al., 2012). Many laboratory studies have contributed to the understanding and quantification of

these soil processes (e.g. Anderson & Levine, 1986; Blagodatsky et al., 1998; Ingwersen et al., 1999; Schindlbacher et al., 2004), and field measurements have helped to understand spatial and temporal variability, and differences between forest types (e.g. Pilegaard et al., 2006; Luo et al., 2012). Soil environmental conditions (temperature and moisture) and nutrient levels are the primary controls of micro-biological processes that lead to GHG fluxes, and are influenced directly and indirectly by secondary factors such as tree shading and density.

Process-based biogeochemical models such as LandscapeDNDC (Haas et al, 2013) have been developed to study how soil processes and their controlling factors interact to influence the C and N cycles and related soil gas fluxes at local and regional scales, and to consider the effect of future climate scenarios. LandscapeDNDC links a choice of vegetation modules with microclimate and soil process modules in a framework that behaves functionally as a single model. In the case of forest vegetation, two sub-modules are available, namely PnET (Photosynthesis–Evapotranspiration, Aber and Federer, 1992; Aber et al, 1995) and PSIM (Physiological Simulation Model, Grote, 2007; Grote et al., 2011). PnET has been used in numerous studies, including many in which it was combined with the soil process model DNDC (DeNitrification-DeComposition, Li et al. 1992; Li et al., 2005; Werner et al., 2007), but it is limited in only being able to describe a single species-type for a given site.

There is a silvicultural trend away from forest monocultures, and in Europe 70 % of forests are now dominated by two or more tree species (Forest Europe, 2015), partly due to a move away from a management focus on yield, towards conservation, biodiversity and recreation (Porté and Bartelink, 2002). Many forests naturally develop an understorey of smaller trees (including canopy offspring) and/or shrubs. Modelling these intermixed and understorey species, together with local environmental factors requires compromises in choice of parameter values originally designed to model a single canopy species (Groenendijk, 2011). Molina-Herrera et al. (2015) compared statistically derived site-specific and general parameter sets for three tree species, beech, spruce and pine (typically having no understorey), in continental Europe, and conclude that site-specific parameters consistently simulate measured CO_2 fluxes better than generic parameters, but the latter can reproduce C uptake reasonably accurately when averaged monthly over several years. The current PnET parameters defined for oak species are mainly derived from oak in North America (Harvard Forest) or continental Europe (Matra Mountains, Hungary) (Pilegaard et al., 2006) and the milder, maritime UK climate warrants evaluating GHG models for these conditions. The PSIM module can be substituted for PnET within the

LandscapeDNDC framework. The advantage of PSIM is that it enables modelling of separate vegetation types within an ecosystem and can therefore simulate the main canopy trees separately from understorey trees. It can simulate different responses in canopy and understorey trees following changes, whether in climate or management, and compensatory mechanisms that can be triggered when the canopy is disturbed and the two vegetation types 'compete' for light, water and nutrients.

Data to evaluate biogeochemical models can come from eddy covariance (EC) estimates of CO_2 fluxes calculated from continuous measurements at field and ecosystem scale. In Europe, there are relatively few forest data sets longer than 10 years, most of which are from spruce (e.g. Hoeglwald, Germany; Norunda, Sweden), pine (e.g. Hyytiala, Finland; Loobos, Netherlands) or beech forests (e.g. Hoeglwald, Germany; Hesse, France), set up as part of the EUROFLUX project (Moncrieff et al., 1997; Aubinet et al., 2000). In the UK, the oak plantation in the Straits Inclosure in south east England, is the only deciduous forest-based EC measurement site with more than 10 years of data.

This study evaluates the LandscapeDNDC model with measured GHG flux data from eddy covariance and soil chambers in the Straits Inclosure where N deposition is relatively low (12.3 kg N ha^{-1} yr^{-1}). Some parameter changes were necessary and sensitivity analyses were carried out to identify which parameters and input values most influenced the resulting modelled GHG fluxes. The aims of this study were: i) to determine the suitability of process-based ecosystem models to represent gas exchange fluxes of an oak stand with a substantial understorey; ii) to evaluate the sensitivity of the modelled stand to natural and management imposed influences; iii) to use the evaluated models to determine C balances over a period of 16 years including thinning, and to discuss uncertainties and model requirements for assessing climate change impacts.

2 Materials and methods

2.1 Site description

The Straits Inclosure GHG flux measurement site, with its eddy covariance tower, is in a managed oak plantation of approx. 90 ha in the SE of England (51° 09' N, 0° 51' W), with an elevation of 80 m AMSL. The Inclosure is a flat area with an annual precipitation of 877 mm and temperature of 10.3 °C averaged over the period simulated, 1995–2014 and was replanted in the 1930s. The

Inclosure is located at the SW corner of the larger, mainly coniferous, Alice Holt Forest (850 ha), and is surrounded on three sides by agricultural land (both arable and sheep pasture). The forest is a site for the UK Environmental Change Network (www.ecn.ac.uk) and has a long-term forest health observation plot within the European 'Level II' Network (ICP Forests, www.ipc-forests.net); further details are given in Wilkinson et al. (2012), and site characteristics used for model input are shown in Table 1.

The tree species in the Straits Inclosure are mainly pedunculate oak (*Quercus robur*) with about 10 % other species including ash (*Fraxinus excelsior*), sessile oak (*Q. petraea*) and Turkey oak (*Q. cerris*). There is a small area of mixed conifers (*Pinus nigra* and *P. sylvestris*) on the NW edge of the plantation. The understorey is substantial, dominated by hazel (*Corylus avellana*) and hawthorn (*Crataegus monogyna*). There are also climbers and a ground flora including grasses, sedges and herbs (Pitman & Broadmeadow, 2001).

The forest soil is a surface water stagno-gley (Pyatt, 1982), classified by the FAO as a eutric vertisol, silty clay in texture, 80 cm in depth, and developed on a bedrock of Cretaceous Gault Clay. Table 2 summarises site soil information used in the modelling. With prevailing winds from the SW, N deposition (wet and dry) of 12.3 kg N ha^{-1} yr^{-1} averaged over 1995-2002 (Benham et al., 2012) is relatively low for northern Europe.

2.2 LandscapeDNDC model

LandscapeDNDC is a process-oriented bio-geochemical model of C, N and water cycling in grassland, arable and forest ecosystems at site and regional scales (Haas et al., 2013). Each site is considered as a one-dimensional, vertically structured grid cell that comprises vegetation, humus horizons and mineral soil, each of which can have multiple layers as appropriate. LandscapeDNDC combines 6 principle modules: air chemistry, vegetation physiology, vegetation structure (for forests only), soil microclimate, water cycle and soil biogeochemistry. Each of these modules is a pre-existing model which has been re-written to fit within the LandscapeDNDC framework. Modules can be selected according to the land use and conditions being simulated.

This study used LandscapeDNDC version 36.1 (win64), run in 'site mode' for a forest. The modules used were canopy ECM for air chemistry (Grote, 2007), Treedyn for vegetation structure (Bossel, 1996) and either PnET (Aber & Federer, 1992, Li et al., 2000) or PSIM (Grote

et al., 2011) for vegetation physiology (incorporating tree growth). The remaining three modules (soil microclimate, water cycle and soil biogeochemistry) were derived from the original DNDC (Li et al., 1992). Each module requires initial inputs to define characteristics of the soil, vegetation and location. The progress of the simulation is defined by the climate file containing daily climate data and the management file which provides dates and details of events of forest management.

The model time-step chosen was daily, while evapotranspiration, photosynthesis and respiration processes are calculated hourly. Each module runs once in sequence each time-step for an input-defined duration, in this case 20 years. Grote et al. (2009) and Kiese et al. (2011) describe the calculations of microclimate within the canopy and soil water availability within the soil profile. The distribution of radiation, relative humidity and temperature depends on leaf area distribution (in up to 40 layers) while soil water availability depends on canopy (leaf area for rainfall interception), root distribution, as well as soil properties (initialized in 2 cm thick layers). Leaf area and root distribution are updated each time step in the vegetation structure module (Treedyn).

This study focused on an evaluation of two different tree growth modules, PnET and PSIM, to estimate soil gas fluxes**.** PnET calculates C uptake, or gross primary production, from a function of maximum photosynthetic rate (AMAXB) and leaf N concentration (Field and Mooney, 1986) as defined in Kattge et al. (2009) and determines respiration from the actual photosynthetic rate, temperature and biomass of roots, wood and leaves. PSIM uses the Farquhar, von Caemmerer & Berry model (Farquhar et al., 1980; Buckley et al., 2003) for photosynthesis with the potential carboxylation rate at 25 °C as a key parameter (VCMAX25), and the Thornley and Cannell (2000) approach which determines respiration rate from temperature and nitrogen content controlled by a Michaelis-Menton co-efficient parameter (KM20). The Farquhar et al. model has more detail on leaf physiology including explicit consideration of stomatal limitation of photosynthetic uptake. The ability of PSIM to simulate more than one vegetation cohort enables it to separate different phenologies of understorey and canopy trees. To allow for component pools to stabilise, model simulations were run from January 1995 to December 2014, with the first 4 years' results discarded from further analysis.

A minimum set of parameter changes were made (Table 3) for each of the two vegetation modules, PnET and PSIM, selecting site-specific information for those parameters where data were available (LAI, Q10, light extinction factor, and those relating to phenology) and modifying

others incrementally (relating to photosynthesis and respiration) in order to produce best agreement of all modelled annual CO_2 fluxes with the measured EC values averaged for 1999-2007. In the case of PSIM, emphasis was placed on optimising parameters for canopy trees; further parameter optimisation could be carried out for the understorey vegetation, but no data were available to justify changes. Ash species parameters were used to represent this understorey in the absence of an existing set of parameters for other species present. Simulated soil fluxes of CO_2, N_2O and NO are compared with a series of monthly soil chamber measurements, from which monthly and annual totals were estimated.

Daily climate input data for 1995-1998 (comprising mean, maximum and minimum air temperature, precipitation, global radiation and wind speed) were taken from a UK Meteorological Office affiliated climatology station, situated in an open area 1.8 km from the Straits Inclosure site. Since 1999, climate data were recorded at the Straits EC Tower site itself and provided model input, as listed above, with additional vapour pressure deficit and air pressure (for 1999–2011). Soil temperature and soil moisture, used for comparison with modelled output, were also recorded continuously near the tower at depths of 10 cm and 30 cm. Local soil moisture data was absent or unreliable from 2004–2008.

Model output is provided as daily and annual values for 133 entities in 5 categories: microclimate, physiology, soil chemistry, vegetation structure and water cycle. Values for gross primary production (GPP), and total ecosystem respiration (TER) were calculated as daily and cumulative annual values. GPP is recorded directly by the models as C uptake for each day; TER is calculated by summing model output for soil heterotrophic respiration and respiration from plants' growth and 'maintenance' (including roots). NEP is calculated as the difference between GPP and TER, which is positive if there is a net uptake of CO_2. Eddy covariance conventionally records net ecosystem exchange (NEE) as negative when there is a net uptake of CO_2. Although NEE may include other sinks and sources of carbon, we assume them to be negligible in the short term so that modelled NEP equates to measured -NEE.

The eastern half of the forest was thinned in summer 2007, which reduced the tree density by about 30 %. Although the prevailing wind is from the SW and the EC tower is in the centre of the Inclosure, nearly 30 % of the CO_2 flux data recorded was from the eastern, thinned part of the forest (Wilkinson et al., 2016). Therefore, to reduce uncertainties, the period prior to thinning, 1999–2007, was used to optimise the model parameters. The results were then evaluated using measured GHG soil fluxes and EC data recorded between 2008 and 2014.

2.3 Model evaluation

Statistical analysis using ModEval v2.0, with methods outlined in Smith et al. (1997), were applied to quantify differences between simulated and measured daily-averaged and annual ecosystem GPP, TER and NEP, and monthly and annual soil fluxes of CO_2 and N_2O. There were insufficient measured NO data for statistical analysis. Model outputs produced with optimised parameters are not independent if the same measurements are used to optimise and test models but F and t tests can be used to examine if there are significant differences (Smith et al., 1997). Initial optimising of parameters was carried out using only EC data from 1999–2007 and soil flux measurements from 2008–2012. Standard errors were calculated for soil flux measurements made subsequently during 2013–14 with 6 replicate chambers, which were used to put 95 % confidence limits on Root Mean Squared Error (RMSE) values to assess the significance of the errors to this soil flux data. As described by Smith et al. (1997), modelling efficiency (ME) was calculated to compare the efficiency of the model with the efficiency of describing the data by the mean of the observations, with a positive value indicating the simulated values describe the trend in the measurements better than the mean of the measurements (maximum = 1.0). The coefficient of determination (CD, the proportion of total variance in observed data explained by simulated data) and mean difference were also calculated.

In the case of GPP, TER and NEP from EC data, no replicate measurements were made and therefore, no statistical significance could be derived for differences between measurements and simulated values, but a total RMSE could be calculated. However, Oren et al. (2006) have estimated that most EC data have an error of 10–15 %, when measurement and gap-filling errors and spatial variability are taken into account. An error of 15 % was therefore used to estimate the statistical significance of RMSE (a calculation which requires a positive value for n-2, and hence n=3 was used).

A sensitivity analysis was carried out to identify those input variables which had the largest influence on simulated GHG fluxes. The method for so-called simple models, as described by Smith et al. (2012) was used in which each set of input variables that describe soil characteristics, N deposition or climate, were changed individually by ± 10 %. Input variables that produced differences of more than ± 10 % in annual total GHG fluxes averaged over 1999–2007 using PnET and PSIM, were considered to be sensitive. The same method was used to quantify the contributions of selected parameters.

2.4 Thinning

Impacts of forest management were assessed by modelling the effect of thinning on the micro-environment in tree canopy and understorey. In late summer 2007, the eastern half of the Straits Inclosure was selectively thinned by removing approximately 30 % of the main stem timber volume, whereby commercially viable wood was removed but foliage and branches were left. For modelling, the effects of a 0 %, 15 % and 30 % thinning on GHG fluxes were simulated and were compared with measured EC (2007–2012) and soil GHG flux data (2007–2012). In the case of the PSIM module, this also included thinning the understorey by 0 %, 15 % and 60 %, as more understorey trees than canopy trees were felled to allow access by heavy machinery. In contrast to upper canopy trees, all the understorey biomass was left on site. No such distinction can be made in PnET. The simulated 30 % thin output was compared with EC data from the eastern sector, the 0 % thin was compared with western sector EC data, and the 15 % thin output compared with data from both sectors. In both models, C and N pools of tree components, soil and litter layers were affected instantly by the thinning event, which was simulated for 19 September 2007.

2.5 Soil gas flux measurements

Soil chamber measurements of CO_2, CH_4 and N_2O fluxes were made where the EC tower is located ("Tower site"). Measurements using 6 soil chambers placed temporarily on fixed frames, inserted 5cm into soil, were made from April 2013 to Aug 2014 at intervals of approximately 2 weeks, except in December and January when measurements were made monthly. Prior to this, fluxes were measured monthly using 4 replicated flux chambers positioned at several sites within the Straits Inclosure, including the Tower Site, from Sept 2007–Aug 2012 (Yamulki and Morison, in press). CO_2, CH_4 and N_2O fluxes were measured with a non-steady state, non-flow-through chamber method and analysed, as described by Yamulki et al. (2013). The chambers (40 x 40 x 25cm, made from opaque PVC) were closed and 3 air samples were taken at 0, 20, 40 and 60 minutes for subsequent analysis by gas chromatography. The rate of change of mixing ratio was calculated using linear regression to determine the flux. Individual samples in which the CO_2 mixing ratio was judged to be anomalous (resulting in $R^2 < 0.8$ for linear regression over the whole chamber closure time) were rejected for all gases.

NO fluxes were measured using the same type of chamber, but lined with Teflon, on the same frames, starting on 25 July 2013. The method used was the steady-state, flow-through method,

using the principle described by Pilegaard et al. (1999). Ambient air, passed through Sofnofil and activated charcoal to remove NO_x and O_3, was pumped through the chamber at a constant flow of 3 L min^{-1} for 20–25 min and NO_x mixing ratios in the outflow measured using a Thermo Electron Corporation 42C NO-NO_2-NO_x analyser calibrated using independently certified standard cylinders of 152 ppb NO in N_2 and 155 ppb NO_2 in air. NOx measurements were also made from an identical control chamber, sealed at the base, in parallel with the soil flux sampling chamber. NO fluxes were calculated as the product of the air flow rate through the soil flux chamber and the difference in NO mixing ratios from the control and sample chamber. The detection limit of the analyser was 50 ppt NO.

During flux measurements, soil temperature was measured with a probe (Hanna model Checktemp 1) at 0.5, 10 and 15 cm depths around all 4 chamber sides and averaged for each depth. Volumetric soil moisture was measured using a probe (Theta probe ML3 attached to HH2 moisture meter, Delta-T Devices Ltd, with default mineral soil settings) at a depth of 6 cm as above. Replicated soil samples were collected from 0-10cm depth near the 6 chamber frames, aggregated, and 5 sub-samples analysed for soil water content by weight to produce a daily average. The soil moisture calculated by weight was converted to %vol using the soil bulk density at the appropriate depth. In addition, wet and dry bulb air temperature (model DTS-5, ELE International, Loveland, USA) and soil temperature at 10 cm depth (2K Thermistor, Delta-T Devices) were recorded at 10 second intervals, and averaged half-hourly using dataloggers (DT 500, DataTaker, Thermo Fisher Scientific, Australia).

2.6 CO_2 flux data from eddy covariance

Net CO_2 flux data acquired by EC were used to validate the C balance within the LandscapeDNDC model at the level of the whole ecosystem. The EC tower is part of FLUXNET, with the identifier "UK-HAM" and started recording data in 1998. It is located in the centre of the Straits Inclosure, with a fetch over the woodland between 350 m to the south and 700 m to the east. The system is described in full in Wilkinson et al. (2012), and uses procedures, including data quality checking, that follow those standardised in the CarboEurope project (Aubinet et al., 2000). TER was derived using night-time flux measurements and temperatures, adjusted according to day-time air temperatures (Lloyd and Taylor, 1994; Wilkinson et al., 2012), and GPP was calculated as the sum of TER and -NEE.

3 Results

3.1 Model validation

3.1.1 Environmental conditions

Using daily air temperature as climate inputs, the simulated daily mean soil temperature data at 10 cm depth from January 2007 to December 2012 matched available measurements well (Fig. 1a, linear regression: $y = 0.8x + 2.1$, $R^2 = 0.90$), although the simulated data do not show the same degree of variation and have a 5–6 °C lower amplitude range in some years. The 30 cm simulated data are in closer agreement with measurements (Fig. 1b, linear regression: $y = 0.9 x -0.6$, $R^2 = 0.97$). Residual values from PnET data (Fig. 1c) illustrate that the largest differences are at 10 cm, mainly in the winter months, when simulated soil temperatures are mostly 1–5 °C higher than measured. At 30 cm depth, simulated temperatures are mostly 1–2 °C lower than measured). Simulated soil temperature is not an independent variable (because it is derived from local air temperature measurements) and therefore no statistical analysis has been carried out on these data, but inaccuracies here could account for inaccuracies in simulated GHG flux results.

For 2013 and 2014, there is good agreement between manual soil temperature measurements taken near the soil chambers during flux measurements and the automatic measurements, and a good match between both temperature measurements and simulated temperatures (Fig. 1d, linear regression: $y = 1.08x – 1.1$, $R^2 = 0.90$). Simulated daily mean soil moisture data at 10 cm depth for January 1999 to December 2008 show some agreement with available measurements from 1999–2003 (Fig. 2), including during the late summer heatwave and drought of 2003 (linear regression: $y = 0.5x + 23.7$, $R^2 = 0.59$). However, simulated values are consistently 2–5 % higher in summer and 2–3 % lower in winter. Data simulated with PSIM is almost exactly the same as PnET, except during the summer of 2003. Spikes of high simulated soil moisture (60–65 %) from both models indicate occasions when heavy rainfall has caused surface water to accumulate within the model. These events are not observed in the measurements.

For 2013–14, simulated soil moisture compared with manual probe measurements during gas flux sampling and measurements from soil samples indicate that the model does not reproduce the wide range of values measured. The model simulated a minimum soil moisture of 40 % vol in the summer of 2013, compared to 21 %vol from measured soil samples and 16 % vol from

manual probe measurements. The first half of 2014 was very wet with soil moisture being consistently between 38.5 and 50.4 (average 44.0) % vol in soil samples and 47-67 (average 57.5) % vol from soil probes, whereas the model values remained steady at 51 ± 0.6 % vol from 7 January to 11 July 2014 (data not shown). The reason for the discrepancies between measurements in the different time periods is unknown but may result from the heterogeneity of the soil or from a bias in the instrumentation.

3.1.2 Ecosystem CO_2 fluxes

Annual totals of GPP, TER and NEP for 1999–2007 derived from EC are compared to simulated results using either PnET or PSIM modules in Table 4 (after model parameter optimisation). The differences between mean measured annual values and those simulated by PnET are less than 15 % (-8.5 %, -6.7 % and -14.1 %, for GPP, TER and NEP, respectively). Even closer agreements were obtained with PSIM, with differences between mean measured and simulated values of less than 1 % for each CO_2 flux component. However, standard deviations for these PSIM values of 35 to 60 g C m^{-2} yr^{-1} are much smaller than those for the measured EC values (101–175 g C m^{-2} yr^{-1}) and PnET values (111–261 g C m^{-2} yr^{-1}), which indicates limited sensitivity to inter-annual environmental variation in PSIM simulations.

Statistical analysis of annual GPP, TER and NEP totals for 1999–2007 using ModEval (Smith et al., 1997) shows lower (and therefore better) RMSE values when using the PSIM module (7.7, 10.5 and 19.3 % for GPP, TER and NEP respectively) than when using PnET (14.8, 10.8 and 38.1 %) (Table 5a). However, none are significant total errors (RMSE at 95 % confidence = 191–193 %). Both modules have a negative modelling efficiency (ME) value and a coefficient of determination (CD) < 1 which indicates that the simulated annual totals describe the data less well than the mean of the observations. In other words, confirming that inter-annual variation is not well simulated.

The seasonal pattern of the daily GPP averaged over 1999–2007 is quite well simulated by both PnET and PSIM (Fig. 3a), as expected, since parameters were chosen to optimise this match. The cumulative values highlight the small mean annual differences between the simulations. By the end of the averaged year, PSIM cumulative total GPP (2119 g C m^{-2} yr^{-1}) is indistinguishable from the EC value (2120 g C m^{-2} yr^{-1}), whereas the value for PnET is lower, at 1938 g C m^{-2} yr^{-1}. Understorey plants produce leaves earlier than canopy trees and PSIM is able to model the 2 plant cohorts separately. However, the averaged data from EC suggests that PSIM is

overestimating this contribution by a factor of approx. 2 during March, although the overestimation is small in comparison to total annual GPP. For TER (Fig. 3b), averaged values from the PnET module are closest to measurements in spring and early summer when respiration increases rapidly during canopy growth (April–July), while averaged PSIM values are closest in late autumn and winter (November–March). For both models, differences balance out over the year to produce a close match with the average annual total TER, but the PSIM value is closer to EC measurements than the PnET value (Table 4). Simulated NEP, being the difference between GPP and TER, combines the differences of the other two values (Fig 3c). Averaged PSIM NEP values show the largest difference from EC NEP values during May due to a poorer TER match, but a better TER match during winter months, results in PSIM having the better averaged annual total NEP values. These net values are arguably the most important as they determine whether the ecosystem is a net sink or source of CO_2 for the year.

The residuals for daily GPP, TER and NEP (measured – modelled) were calculated using PnET and PSIM modules for 1999–2007 (Fig. 4). For each component (GPP, TER and NEP) residuals are mostly between ± 5 g C m^{-2} d^{-1} for both PnET and PSIM methods, but the summer residuals are larger in many years, with a maximum absolute GPP residual of -13 g C m^{-2} d^{-1} in 2006. Residual TER values show the clearest distinction between PnET and PSIM, mainly due to the absence of above ground winter respiration in PnET simulations, and in particular, 2004 and 2006 show the largest summer residuals for TER from both models.

Simulated monthly totals for GPP, TER and NEP show a better fit to measured equivalents than annual data (Fig. 5, high positive ME and CD >1, Table 5b). Monthly GPP is particularly well simulated with an ME of 0.94 using PSIM and 0.92 using PnET. While PnET estimated a reduced GPP and TER in 2003, which was a drought year (annual rainfall 700 mm, annual average 877 mm) with high summer temperatures (maximum 33.8 °C), the EC measurements suggest there was not sufficient reduction in soil water availability to reduce CO_2 uptake possibly due to the heavy clay soil, and the wet previous year (annual rainfall 1094 mm) so that higher than average GPP and TER were measured. PSIM simulations showed no change in GPP for 2003 over the previous year.

The PnET and PSIM model parameters were modified to optimise the fit of model output with mean annual EC data for GPP, TER and NEP averaged over 1999–2007. The large inter-annual variations observed (Table 4) were less well simulated, and were complicated after this period by the thinning event of 2007 and infestations of defoliating moth caterpillars in 2009 and 2010,

which reduced the GPP, TER and to a lesser extent, NEP especially in the second year of infestation (Wilkinson et al., 2012). EC measurements also showed a significant long term (1999 to 2010) decrease in annual GPP (-46.1 g C m^{-2} yr^{-1}, $p < 0.01$) and annual TER (-44.7 g C m^{-2} yr^{-1}, $p < 0.001$) with no resultant trend for NEP (Wilkinson et al, 2012). These decreasing trends in annual GPP and TER are also shown in simulated data (and evident in Fig. 5), although with larger declines when using PnET, -86.4 g C m^{-2} yr^{-1} for GPP and -48.4 g C m^{-2} yr^{-1} for TER, and smaller when using PSIM, -26.0 g C m^{-2} yr^{-1} and -21.7 g C m^{-2} yr^{-1}, respectively.

The annual biomass increment for Straits Inclosure has been estimated as 347 g C m^{-2} yr^{-1} from measurements in 2005 and 2009 (Wilkinson et al., 2012), although this may be conservative due to thinning in 2007 and caterpillar infestations in 2009 (Pitman et al. 2010). Simulated biomass (from end of year C pools of wood and coarse roots, after loss of leaves and fine roots) with no thinning gave an annual increment of 501 g C m^{-2} yr^{-1}, using PnET and 432 g C m^{-2} yr^{-1}, using PSIM, nearly 1.5 times the estimated value. However, PnET and PSIM modelling of a 15 % thinning event in Sept 2007 to represent 30 % thinning of half of the Inclosure, produced a total biomass by 2014 that was consistent with that estimated.

3.1.3 Soil CO_2 fluxes

Measured soil CO_2 fluxes show large spatial variability between chambers on some days (indicated by the error bars, Fig. 6a), which were not simulated. The PnET module underestimates mean daily soil CO_2 fluxes measured during 2008–2012 but more closely matches measurements in 2013–14. In contrast, the PSIM module simulated soil CO_2 flux data more closely for 2008–12 than 2013–14 (statistics in Table 5c). The proportion of simulated annual soil CO_2 emissions contributed by autotrophic respiration when using PSIM was 27.5% compared to 32.3% for PnET simulations.

Annual total soil CO_2 fluxes simulated from 1999–2007 (before thinning) with PnET average 619 g C m^{-2} yr^{-1} (range 546–745 g C m^{-2} yr^{-1}) and with PSIM average 1042 g C m^{-2} yr^{-1} (range 979–1081 g C m^{-2} yr^{-1}). For 2008–2014, averages of 575 g C m^{-2} yr^{-1} are obtained using PnET and 1018 g C m^{-2} yr^{-1} using PSIM, compared to a measured value of 818 g C m^{-2} yr^{-1}. The ModEval statistical analysis of monthly simulated and measured soil CO_2 fluxes (Table 5c) shows a better fit of PSIM simulations for 2008–12 (ME =0.38, CD =1.60) than PnET simulations for 2013–14 (ME = 0.08, CD = 1.09).

3.1.4 Soil gaseous N fluxes

Daily soil N_2O fluxes simulated with PnET and PSIM both produced similar seasonal patterns of N_2O fluxes ranging from near 0 to 300 μg N m^{-2} d^{-1} and spikes of 700–900 μg N m^{-2} d^{-1}, comparable, but mainly lower than measured peak fluxes of 500–1700 μg N m^{-2} d^{-1} (Fig. 6b). Measured values show much greater variation and no obvious seasonal pattern, particularly from 2008–2012. On occasions, negative N_2O fluxes were recorded but LandscapeDNDC cannot currently simulate N_2O uptake. Under wet soil conditions, both PnET and PSIM simulated short-lived spikes in N_2O fluxes, which do not necessarily coincide with each other in time or size, or with measurement dates, such as in early January 2014 when N_2O fluxes of 600 μg N m^{-2} d^{-1} were simulated by PnET (and 300 μg N m^{-2} d^{-1} by PSIM). PnET N_2O simulations showed a positive correlation with temperature, ($r = 0.53$, $p < 0.01$) resulting in annual highs (excluding rain-related spikes) in the summer, whereas PSIM N_2O simulations showed no correlation with temperature ($r = 0.04$) and timing of annual highs (excluding rain-related spikes) varied from year to year. Measured N_2O fluxes showed no correlation with temperature (Yamulki and Morison, in press). Annual N_2O fluxes estimated from measurements ranged from 15.4 to 174.6 mg N m^{-2} yr^{-1} during 2008–12 (Yamulki and Morison, in press, adjusted to calendar year), whereas simulated values with PnET and PSIM were smaller, 38.9–55.5 mg N m^{-2} yr^{-1} and 36.9–60.3 mg N m^{-2} yr^{-1}, respectively (Table 6) and closer to the estimated total for 2013 of 57.4 mg N m^{-2} yr^{-1}.

Monthly measured N_2O flux totals were compared with those simulated using PnET and PSIM modules with data from 2008–12 analysed separately from 2013–14 data (Table 5c). For PnET, RMSE total error was not significant for 2008–12 but was for 2013–14, whereas for PSIM, the RMSE total error was not significant for either set of measurements. However, ME was negative and $CD < 1$ for all simulated N_2O flux results, suggesting that the measured data are better described by the mean of measurements. Given the high degree of variability in soil N_2O fluxes, annual totals are most appropriate for comparative purposes, although, with relatively infrequent measurements of 2–4 weeks, there is considerable uncertainty in the annual total.

Soil NO fluxes were measured from July 2013 to August 2014 (Fig. 6c) and showed a daily average of 5 μg N m^{-2} d^{-1} and peak values of 14 μg N m^{-2} d^{-1} although measured NO concentrations were close to the limit of detection of the NO-NOx analyser. Measurement of NO uptake was not possible because zero air was used as input to the chambers. Simulated NO fluxes using PnET and PSIM were mostly 10–30 μg N m^{-2} d^{-1} and therefore 5–25 μg N m^{-2} d^{-1} higher than measurements, but both had peak simulated values of approximately 100–400 μg

N m^{-2} d^{-1}, an order of magnitude higher than measured values. There is no correlation with temperature but simulated flux peaks (from both PnET and PSIM) follow heavy rainfall events, although this was not observed in measurements. NO soil fluxes simulated with PnET and PSIM are approximately 10 % of simulated N_2O fluxes. The PnET and PSIM modules over-estimate NO fluxes, but there are insufficient measured data for meaningful statistical analysis. The annual total soil NO flux was estimated as 1.1 mg N m^{-2} yr^{-1} from measurements, 6.4 mg N m^{-2} yr^{-1} from PnET and 8.1 mg N m^{-2} yr^{-1} from PSIM (simulated data averaged over 2008–14).

3.2 Model sensitivity analysis

Table 7a illustrates the effect of changes by ± 10 % to key input values on annual totals of GPP, TER, NEP and soil CO_2, N_2O and NO fluxes simulated using PnET and averaged over 1999–2007. The largest proportional effect was on the soil NO fluxes: changing the pH by 1 unit to below 5.0 permitted chemo-denitrification to produce NO, and led to a 6-fold increase in annual soil NO fluxes compared with a minor decrease in soil N_2O fluxes. Increasing the pH by 1 unit reduced both NO and N_2O soil fluxes by 2.7 and 5.3 %, respectively.

Changing the soil organic C content, bulk density and field capacity input values also produced disproportionate changes of >10 %. These are linked as bulk density controls the initial organic C (and N) stock in the soil as well as soil porosity. A higher bulk density (BD, given in gcm^{-3}) results in higher organic C content (input as a fraction of BD) and lower porosity (input as % of BD), which provides more nutrients for microbes and anaerobic conditions during wetting. An increase in field capacity potentially increases the amount of water held in the soil and thus the proportion of anaerobic conditions. There was some uncertainty regarding the hydraulic conductivity of the soil, as it was not determined. Although the soil is clay-rich, tree roots promote conduits for water percolation. Values of 10 and 100 times higher than the selected value of 0.00006 cm min^{-1} were shown to reduce the simulated gas fluxes by less than 5 %.

Changing the daily climate variables of temperature (min, max and mean) or precipitation by ± 10 % produced changes to gas fluxes of <10 % except for NO where the decreased temperature produced a 15.0 % increase in the total flux, with a shift from litter layer to mineral soil nitrification due to reduced microbial activity in the litter layer. Changes in N deposition of ± 10 % changed soil N_2O and NO fluxes by less than 4 %. Increasing N deposition by 100 % to 2.46 g N m^{-2} yr^{-1}, which is similar to values of 2.0–3.5 g N m^{-2} yr^{-1} recorded for a broadleaved forest at Hoeglwald in central Europe (Butterbach-Bahl et al., 1997), produced significant simulated

increases in NO fluxes of 24.8 % and in N_2O fluxes of 17.7 %. This analysis therefore showed the model was particularly sensitive to initial organic C content and factors that control soil moisture and hence anaerobic conditions, namely bulk density and field capacity as well as a pH change below 5. It also showed that stand-scale CO_2 fluxes were relatively insensitive to changes in input values, which is relevant for inter-annual variation.

Model sensitivity to selected PnET parameters is shown in Table 7b. Changes of ±10 % to GDDFOLEND (daily temperature sum for end of foliage growth, see Table 3) produced >10 % change in all simulated soil fluxes, and increasing SENESCSTART (leaf death timing) by 10 % decreased simulated TER, soil CO_2 and soil NO fluxes by > 10 %, which indicates the importance of defining the start and end of the growing season to simulated respiration and soil processes, although these effects were cumulative and only apparent after several years. However, SENESCSTART defines a day of year and therefore is not readily compared to % change in outputs and changing GDDFOLEND affects the leaf N uptake and therefore soil emission intensity, rather than timing. Table 7c shows model sensitivity to PSIM parameters. No single parameter had a disproportionate effect on the simulated results. Comparing using the PSIM module with and without an understorey (included as defined in Table 1) showed that the understorey contributed 20 %, 17 % and 20 % of simulated TER, GPP, and soil CO_2 emissions, respectively and 14 % of simulated soil N_2O emissions. The understorey vegetation characteristics vary substantially across the Inclosure, and there are few measurements of understorey parameters on which to base the selection, and no measurements to evaluate its proportional contribution to fluxes.

3.3 Thinning

With 30 % thinning, GPP was simulated to decline after the thin in both modules, and then recover over several years (Fig. 7a). In the case of PSIM, the biggest difference from unthinned simulations was in 2009 (17 % less) and simulated GPP recovered to be equal to unthinned data by 2013. For PnET, the biggest difference from unthinned data was in 2008 (20 % reduction) and, although this difference reduced by 2010, it maintained a similar difference (4–11 % lower) for the duration of the simulations. TER (Fig. 7b) was also simulated to decline in PSIM following the thin (maximum difference 15 % in 2009) and recover gradually but not completely by the end of the study (6 % difference in 2014). For PnET, simulated TER increased slightly (by 5 %) in 2007 and 2008, before declining and the difference in simulated values continued to increase over

the study period (12 % by 2014). The initial small change in GPP after thinning in the PSIM module more closely fits the observed change than the PnET output, which had a larger initial decline. For PSIM, the maximum change in NEP was small (28 %) compared to PnET, which showed a maximum reduction in NEP of 131 %, resulting in negative NEP in 2008 (Fig. 7c). PnET produced a 47 % increase in soil CO_2 flux in 2008, but PSIM simulated a 12 % decrease in the same year, increasing to 15 % in the two following years (Fig. 7d). Both modules also showed an increase in simulated N_2O emissions after the thin, although relatively small in absolute values, the proportional increase was greater in PnET (39 %) than for PSIM (17 %) (Fig. 7e). The differences simulated by the 15 % thin follow the same trends as those produced by the 30 % thin but rarely had exactly half the values of the larger thin. For PSIM simulations, the 15 % thin closely matches whole stand EC measurements immediately after the thin, 2007–2009 (Figs. 7a–c). The significant decrease in both measured GPP and TER in 2010 has been attributed to a defoliating caterpillar infestation which would explain a poor model fit for 2010 and possibly subsequent years.

Wilkinson et al. (2016) have reported changes in measured stand CO_2 fluxes after the thinning event in September 2007; while fluxes in 2008 were little changed, there were markedly lowered NEP and increased TER rates in 2009 from the eastern, thinned area. In 2010–12, NEP measured when the fluxes were from the east were lower than from the west while TER showed little difference.

Figure 8 compares monthly TER data partitioned into eastern (thinned) and western (unthinned) sectors from Wilkinson et al. (2016) in 2009 and 2012 with 0 % and 30 % thinning simulated using PnET and PSIM. In 2009, 2 years after thinning, measured TER was predominantly higher throughout the year during easterly winds. PnET-simulated monthly TER was almost identical for 0 % and 30 % thinning and was in better agreement with measured data from the west (unthinned) than the east. In contrast, PSIM-simulated TER showed a clear difference from March to November 2009 between the 0 % and 30 % thinning results, with TER values higher for 0 % thinning conditions. TER simulations by PSIM were mostly between the values measured from east and west sectors. In 2012, 5 years after the thinning, measured TER values were very similar in the western and eastern sectors, except that the summer peak in the eastern (thinned) sector lagged behind that of the western sector by about a month, possibly due to temperature differences. PnET-simulated TER values were lower than measured values throughout the year and unlike in 2009, simulated TER under thinned conditions were slightly lower than those in

the unthinned case between May and October 2012. PSIM-simulated TER after 30 % thinning increased between 2009 and 2012 in the growing season, which can be attributed to increased growth in the remaining understorey, although TER values were still lower than for simulated unthinned conditions.

Statistical evaluation (ModEval by Smith et al., 1997) of simulated monthly TER for 2009 and 2012 compared to equivalent results from EC separated into western and eastern sectors are shown in Table 8. All these results are considered to be good as ME values were > 0 and CD values > 1, but this mainly assesses the ability of the models to simulate seasonal variation within a year. PSIM produces better simulated monthly results, giving slightly higher ME and CD values and slightly lower RMSE and total errors, than PnET. However, for both years, the unthinned data gave a better match to the western sector data than the thinned data did to the eastern sector data. Because of the high variability in the soil gas fluxes and the low frequency of the measurements, the models' ability to simulate the effect of thinning on these fluxes could not be assessed statistically.

4 Discussion

4.1 Environmental conditions

As soil temperature and soil moisture are major controls on GHG fluxes from soils, accurate simulation of these values is important, especially in the uppermost soil layers (0–30 cm) where most biological activity takes place (e.g. Taylor et al. 2002; Fierer et al., 2003). Soil temperature measurement errors here are small (relative standard error on 2013–14 manual measurements typically < 1 %, and closely match fixed probe data), therefore any mismatch with simulated temperature data suggests inconsistencies in the model rather than measurements. The mismatch here is a reduced annual amplitude in simulated data for years 2007–8 and 2011–12, which suggests that some improvement of fit to measured data could be made by adjusting soil inputs or the empirical function involving air temperature. However, 2013, the only year studied when simulated temperature amplitude exceeded measured amplitude, had an anomalously dry summer (68 mm, average summer rainfall = 167 mm) and cold Jan-March (average temperature 3.3 °C, equivalent for 1995–2013 = 5.8 °C) suggesting a link with climatic conditions. DNDC calculates soil temperature from soil properties including thermal conductivity derived from a combination of solid and water phases, depending on moisture content (Li et al, 2000).

It seems that when the moisture content is high, the simulation of soil temperature is less accurate. The small difference of < 1 °C in extreme values of PSIM and PnET soil temperatures is probably generated in the ECM module, due to differences in canopy structure (causing shading) and evapotranspiration, before soil surface temperature is calculated in the DNDC soil microclimate module.

Soil moisture measurements at the Straits Inclosure Tower Site have been unreliable at times, especially following dry conditions in the clay-rich soils when cracks reduce the probe accuracy, and spatial variation from proximity to vegetation is expected (relative standard error on soil moisture from samples was 1–6 %). As with soil temperature, simulated soil moisture generally shows a reduced seasonal range, with the exception of peaks (often one day long) following heavy rainfall events. The original aim of DNDC was to predict seasonal or annual N_2O emissions (Li et al., 1992) and therefore the timing of rain events was not important; they start at midnight and continue at the same pre-defined intensity until the daily rainfall has finished (Kiese et al. 2011). The vegetation model takes account of canopy interception and evapotranspiration, and then rainwater saturates the soil, layer by layer, at a rate determined by each layer's soil hydraulic conductivity (K). Altering K, changes soil moisture during and after rainfall events, but changing K from 0.00006 to 0.006 cm min^{-1}, only changed soil moisture by 1–2 % on most days. This is still 2–3 % away from the measured values and does not affect the simulated soil temperature. However, the effect of simulating rainfall in this way in a clay-rich soil, is to create more occasions when surface water accumulates and hence more times when anaerobic conditions are simulated for denitrification. This simplification therefore probably contributed to the overestimation of N_2O peak emissions at this site. Many of the studies using combined PnET and DNDC models have involved forests on loams and sandy loams, e.g. Li et al. (2000) for which simplified rainfall and drainage models produce good results. Saggar et al. (2004) and Li et al. (2006) studying clay-rich agricultural soils with DNDC, modified soil moisture processes to obtain appropriate results.

4.2 Vegetation species parameters and CO_2 fluxes

Simulations using the standard species parameters for pedunculate oak (Q. robur) resulted in annual GPP values approximately half those estimated by EC, indicating that customisation was required. However, if the model is to be applicable at more than one site, the number of parameters altered should be minimal. For PnET, the principle control on a species' C uptake is

the parameter AMAXB (optimal photosynthetic rate), together with MFOLOPT (optimal foliage biomass) which determines LAI. These two parameters directly control the simulated GPP values and were changed incrementally to match EC GPP. Simulated autotrophic respiration is summed from maintenance and growth of three C pools (leaves, wood and roots) and four parameters define the fractions of photosynthesis and biomass used to calculate respiration, together with a Q10 and three C allocation parameters. There is no parameter control of heterotrophic soil respiration. Therefore, matching TER from EC data is less straightforward and requires balancing with resultant NEP values derived from GPP and TER. Although suboptimal GPP values may be necessary to ensure both TER and NEP are optimised, it is most likely that there will be a better fit for GPP than both TER and NEP when modelling with PnET. For PSIM, there are also two key parameters controlling photosynthesis (VCMAX25 and MCFOLOPT) but only one key parameter controlling respiration (KM20), which simplifies the optimisation process, but gives less control.

These gas exchange parameter values were selected to match averaged annual values for GPP, TER and NEP. Changing phenology-related parameters helped match seasonal variation but not inter-annual variation, particularly in PSIM data. PnET uses daily temperature, through GDD, to control the start and end of leaf unfolding, whereas PSIM only uses GDD at the start and a parameter defines the number of days to complete the process. Similarly, the timing and length of leaf fall is fixed by parameter for each year in PSIM, but in PnET these can vary according to conditions. Thus, PnET simulated a greater range of growing season length (51 days) compared to PSIM (38 days). This must contribute to the difference in amount of inter-annnual variation between the modules. Both PnET and PSIM show a positive correlation between growing season length (GSL) and simulated annual GPP (PSIM $r = 0.78$, $p < 0.01$; PnET $r = 0.52$, $p < 0.05$), which has been reported by Goulden et al. (1996) as a control on annual GPP in a deciduous forest in New England. However, Wilkinson et al. (2012) did not find any such correlation between actual GSL and EC GPP. The strongest correlation they found to explain inter-annual variation was between peak LAI and GPP in the Straits data from 1999–2010. Conversely, simulated LAI shows very little annual variation in peak values (PnET range: 4.85–5.79; PSIM QURO range: 5.47–5.86, understorey: 3.16–3.92, total: 8.64–9.69) and no correlation with simulated GPP or TER. Thus, it seems the inability to vary peak LAI appropriately in both models may be the cause for the poor match in inter-annual variability. However, the exfoliating caterpillar infestations of 2009–2010 were known external factors affecting the forest LAI and therefore GPP, and there may have been others (e.g. disease, storm damage) which are not simulated, accounting for some of the mismatch. No correlation was found between annual rainfall and GPP in either PnET or PSIM,

but drought stress affected PnET more than PSIM in 2003, although EC measurements showed the Straits Inclosure was not adversely affected. It would be beneficial to continue the comparison beyond the period with known external factors to assess.

4.3 Soil gas fluxes and measurement uncertainty

Soil chamber measurements are known to be subject to errors and both spatial and temporal variability are expected (Pumpanen et al., 2004; Levy et al., 2011). Furthermore, since measurements were made only every 2–4 weeks, an estimated annual flux has compounded errors. The difference in scale of summer soil CO_2 measurements between 2008–12 (June-Aug mean: 3.9 ± 1.6 g C m^{-2} d^{-1}) and 2013–14 (June-Aug mean: 2.6 ± 0.5 g C m^{-2} d^{-1}), suggests a change in method or in field/environmental conditions. The growth of ground vegetation in the earlier period will have contributed to higher CO_2 fluxes from plant dark respiration, but has not been quantified. Heinemeyer et al. (2012) measured soil CO_2 fluxes at the Straits Inclosure using smaller automated chambers to record fluxes hourly and estimated an average summer soil CO_2 flux of 3.1 g C m^{-2} d^{-1} for 2007–2010 without ground vegetation. Although thinning took place in the inclosure between measurement periods, it did not take place at the Tower Site. One diseased tree was felled within the site in May 2013 and storm damage removed significant branches in October 2013, but in each case only 1 or 2 of 6 chambers were affected. The most likely cause (in addition to ground vegetation) for this difference in summer soil CO_2 emissions is root cutting during frame insertion, which can reduce respiration from roots by 15–50% (Heinemayer et al., 2011). This suggests that PSIM-simulated soil CO_2 emissions match measurements more closely than those simulated by PnET. PSIM gives a mean ratio of soil CO_2: TER of 0.67 for 2008–2011 (with and without thinning) which closely matches the mean ratio from measurements of Yamulki and Morison (in press), 0.61 and Heinemeyer et al. (2012), 0.60. The PnET equivalent ratio is 0.47 for 2013–14. PSIM simulates a greater total root mass (annual maximum PSIM: 0.9 kg DW m^{-2}, PnET: 0.25 kg DW m^{-2}) due to addition of understorey trees, but the difference in total CO_2 is largely due to simulation of root exudates that takes place in PSIM to generate extra nutrients for heterotrophic respiration. This process is not modelled in PnET.

Chamber measurement of soil N_2O and NO fluxes are subject to similar measurement errors as soil CO_2 fluxes (Rochette et al., 2008; Venterea et al., 2009), but the depth of insertion of chambers used here is not thought to have had a long-term effect on these fluxes. Increased activity at the measurement site prior to frame insertion in 2013, may have resulted in soil

compaction and hence reduced gas diffusivity through the soil. The overestimation of N_2O peak fluxes has been discussed above as an effect of the simplification of rainfall simulation and resulting moisture content. The presence of the understorey affects the intensity of simulated fluxes, rather than seasonal pattern, and is linked to simulated N uptake. A constant N deposition has been simulated but Vanguelova et al. (2010) report decreases in NH_4-N throughfall at Alice Holt from 1995 to 2006 of approximately 0.7 NH_4-N eq ha^{-1} y^{-1}, which would result in a decrease in N_2O fluxes if continued. This may also be a contributory cause of GPP decline, 46.1 g C m^{-2} yr^{-1}, observed by Wilkinson et al. (2012).

CH_4 oxidation has been measured at the Tower Site giving an annual uptake 192–326 mg C m^{-2} yr^{-1} (Yamulki and Morison, in press), but is not modelled in this version of LandsacpeDNDC. This, together with the lack of modelled uptake of N gases, is a further simplification that can contribute to poor fits with measured data.

4.4 Thinning / response to management change

Representing the thinning event was complicated by the fact that thinning took place over only half of the plantation and there was only one EC tower to measure the change. Furthermore, there is a heterogeneity across the site, particularly in the understorey, which has not been quantified. Differences in weather conditions coming from the western and the eastern sectors contribute to different GPP and TER measurements in addition to the thinning status and as the dominant wind is from the SW, the unpartitioned, ecosystem scale EC data has a higher proportion of the warmer westerly conditions. However, the PnET-simulated negative NEP was probably caused by simulated GPP being too low, rather than TER being too high. Partitioned EC data from 2009 showed that TER was higher in the thinned sector (Fig. 8a). PnET also simulated an increase in TER after thinning (Fig. 7b), principally as a result of increased soil respiration (Fig. 7d), but this started in 2007 and by 2009 it had returned to unthinned values. In contrast, PSIM simulated a decrease in TER from the 1997. The main difference between the modules was the simulated soil respiration, which increased with PnET due to increased litter input, causing higher heterotrophic respiration from increased mineralisation, but decreased in PSIM because mineralization remained unchanged and root respiration decreased (Fig. 7d). Both modules simulated an increase in N_2O fluxes following the thin, but there are no measurements currently available from the thinned sector with which to compare the results.

A further advantage of PSIM over PnET is that it allows input atmospheric CO_2 concentration and N deposition to vary during a simulation run. Although not used in this study to allow a fair comparison this would be an advantage in simulating future climate scenarios.

5 Conclusions

LandscapeDNDC with the PnET and PSIM tree growth sub-modules was evaluated for application in an oak forest in southern England by modifying a limited set of species parameters that define tree physiology.

The PnET module simulated annual GPP, TER and NEP averaged over 1999–2007 to within 8.5 %, 6.7 % and 14.1 % respectively, of values derived from EC measurements, which is within the estimated uncertainty of the EC method (10–15 %) suggested by Oren et al. (2006). The PSIM module simulated the same annual data to within < 1%. For both modules, the inter-annual variability of GPP, TER and NEP was not well represented, and yielded negative ME values. However, when monthly CO_2 fluxes are compared, the model efficiency for PnET and PSIM improved to high positive values, PSIM giving an ME of 0.94 for GPP, 0.67 for TER and 0.83 for NEP.

Annual soil CO_2 fluxes were consistently underestimated by PnET by 32 % compared with average soil chamber measurements, 807 g C m^{-2} yr^{-1} (range 689–1016 g C m^{-2} yr^{-1}), but were overestimated by PSIM (by 26 %). Measured soil N_2O fluxes exhibited considerable inter-annual variation of 15.4–174.6 mg N m^{-2} yr^{-1} (SD = 65.1 mg N m^{-2} yr^{-1}), which was not reproduced by PnET or PSIM but in both cases simulated annual totals were of the same order of magnitude as measurements (PnET: 38.9–55.2 mg N m^{-2} yr^{-1} and PSIM: 36.9–60.3 mg N m^{-2} yr^{-1}). NO emissions of 5.4–8.0 mg N m^{-2} yr^{-1} (PnET) and 5.8–11.5 mg N m^{-2} yr^{-1} (PSIM) were much larger than measured values of approximately 1 mg N m^{-2} yr^{-1}. Comparison between monthly simulated and measured N_2O soil flux data showed poor fits for both models, with negative ME values, and mixed results for soil CO_2 fluxes. PSIM produced the best results when compared with measurements from 2008–2012, ME = 0.38.

For soil N_2O and NO fluxes, LandscapeDNDC was most sensitive to organic carbon content as input values (given as a fraction of bulk density), or resulting from bulk density input, and to field capacity input. Decreasing soil pH below 5.0 significantly increased simulated NO emissions. Of the climate variables, decreasing the temperature by 10 % had a greater effect on both NO and

N_2O emissions than increasing temperature or changing precipitation by 10 %. The PnET parameter to which simulated soil N_2O, NO and CO_2 fluxes were most sensitive was GDDFOLEND, defining the cumulative temperature required to reach maximum leaf area. There was no single PSIM parameter to which the simulated fluxes were particularly sensitive, but the inclusion of the understorey contributed 14–22% to all simulated flux outputs.

Simulation of forest thinning showed that PSIM produced a better match to measured GPP and NEP data than PnET but PnET simulated a more appropriate response for TER, through increased soil respiration. Both modules reproduced monthly variation well statistically for two separate years following thinning (PnET ME = 0.44 and 0.43; PSIM ME = 0.45 and 0.74) but neither module was good in detail or in variability. The simulated increases in N_2O gas emissions could not be assessed.

This study showed that the LandscapeDNDC model can simulate monthly and averaged annual ecosystem CO_2 fluxes measured at the Straits Inclosure well. PSIM performed better than PnET partly due to its ability to simulate the significant understorey component present at the site. Further studies would be helpful following quantification of the understorey. While soil CO_2 fluxes have been shown to be well simulated by PSIM in normal conditions, N_2O and NO fluxes and their variability are not. Improvements to the inter-annual variability would be necessary before using either module to predict effects of change, whether related to climate or management, at this site.

Author Contribution

Shirley Cade performed soil chamber measurements (2013–14), carried out simulations, analysed results and produced the manuscript. Sirwan Yamulki advised on methodology and soil flux measurements, supervised the work and reviewed the manuscript. Kevin Clemitshaw and David Lowry supervised the work and reviewed the manuscript and Kevin Clemitshaw helped with NO_x analysis. Saúl Molina-Herrera and Rüdiger Grote advised on LandscapeDNDC and parameter selection and provided text about model description and performance analysis. Matthew Wilkinson advised on and provided the EC and climate data and Edwin Haas developed the model software.

The authors declare that they have no conflict of interest.

Acknowledgements

This study was made possible by a combined College Research and Crossland Scholarship from Royal Holloway, together with a University of London travel grant. Thanks must also go to many staff at Royal Holloway, Forest Research and the Institute of Meteorology and Climate Research, KIT, particularly to David Ames, for bespoke NO_x data logging software, Jose Valcarcel for help with soil analyses, Jacqui Brunt for GC analysis, Eric Casella for Straits mensuration data and modelling advice, and Steffen Klatt and David Kraus for help with LandscapeDNDC and Ralf Kiese for enabling use of the model.

References

Aber, J.D. and Federer, C.A.: A generalized, lumped-parameter model of photosynthesis, evapotranspiration and net primary production in temperate and boreal forest ecosystems, Oecologia, 92, 463-474, 1992.

Aber, J. D., Ollinger, S. V., Federer, C. A., Reich, P. B., Goulden, M. L., Kicklighter, D. W., Melillo, J. and Lathrop Jr, R. G.: Predicting the effects of climate change on water yield and forest production in the northeastern United States, Climate Res., 5, 207-222, 1995.

Anderson, I. C. and Levine, J. S.: Relative rates of nitric oxide and nitrous oxide production by nitrifiers, denitrifiers, and nitrate respirers, Appl. Environ. Microbiol., 51, 938-945, 1986.

Aubinet, M., Grelle, A., Ibrom, A., Rannik, Ü., Moncrieff, J., Foken, T., Kowalski, A., Martin, P., Berbigier, P. and Bernhofer, C.: Estimates of the annual net carbon and water exchange of forests: the EUROFLUX methodology., 2000.

Benham, S., Vanguelova, E. and Pitman, R.: Short and long term changes in carbon, nitrogen and acidity in the forest soils under oak at the Alice Holt Environmental Change Network site, Sci. Total Environ., 421, 82-93, 2012.

Blagodatsky, S., Yevdokimov, I., Larionova, A. and Richter, J.: Microbial growth in soil and nitrogen turnover: model calibration with laboratory data, Soil Biol. Biochem., 30, 1757-1764, 1998.

Bossel, H.: TREEDYN3 forest simulation model, Ecol. Model., 90, 187-227, 1996.

Broadmeadow, M., Pitman, R., Jackson, S., Randle, T., Durrant, D. and Lodge, A. H.: Upgrading the Level II Protocol for Physiological Modelling of Cause-effect Relationships: A Pilot Study, Forestry Commission, Edinburgh, 2000.

Buckley, T., Mott, K. and Farquhar, G.: A hydromechanical and biochemical model of stomatal conductance, Plant, Cell Environ., 26, 1767-1785, 2003.

Butterbach-Bahl, K., Gasche, R., Breuer, L. and Papen, H.: Fluxes of NO and N_2O from temperate forest soils: impact of forest type, N deposition and of liming on the NO and N_2O emissions, Nutr. Cycling Agroecosyst., 48, 79-90, 1997.

Crown 2008, Climate Change Act 2008. UK: The Stationary Office Limited. Chapter 27. http://www.opsi.gov.uk/acts/acts2008/pdf/ukpga20080027en.pdf, Environ., 421, 82-93, 2012.

Farquhar, G., von Caemmerer, S. v. and Berry, J.: A biochemical model of photosynthetic CO_2 assimilation in leaves of C3 species, Planta, 149, 78-90, 1980.

Field, C. and Mooney, H.: Photosynthesis--nitrogen relationship in wild plants, in: On the Economy of Plant Form and Function: Proceedings of the Sixth Maria Moors Cabot Symposium, Evolutionary Constraints on Primary Productivity, Adaptive Patterns of Energy Capture in Plants, Harvard Forest, August 1983, 1986.

Fierer, N., Schimel, J. P. and Holden, P. A.: Variations in microbial community composition through two soil depth profiles, Soil Biol. Biochem., 35, 167-176, 2003.

Forest Europe and FAO.: State of Europe's Forests 2015, Status and trends in sustainable forest management in Europe, 2015. Ministerial Conference on the Protection of Forests in Europe. FOREST EUROPE Liaison Unit, Madrid.314pp

Groenendijk, M., Dolman, A., Van der Molen, M., Leuning, R., Arneth, A., Delpierre, N., Gash, J., Lindroth, A., Richardson, A. and Verbeeck, H.: Assessing parameter variability in a photosynthesis model within and between plant functional types using global Fluxnet eddy covariance data, Agric. For. Meteorol., 151, 22-38, 2011.

Grote, R.: Sensitivity of volatile monoterpene emission to changes in canopy structure: A model-based exercise with a process-based emission model, New Phytol., 173, 550-561, 2007.

Grote, R., Kiese, R., Grünwald, T., Ourcival, J. and Granier, A.: Modelling forest carbon balances considering tree mortality and removal, Agric. For. Meteorol., 151, 179-190, 2011.

Grote, R., Lehmann, E., Brümmer, C., Brüggemann, N., Szarzynski, J. and Kunstmann, H.: Modelling and observation of biosphere–atmosphere interactions in natural savannah in Burkina Faso, West Africa, Phys. Chem. Earth, Parts A/B/C, 34, 251-260, 2009.

Gundersen, P., Christiansen, J. R., Alberti, G., Brüggemann, N., Castaldi, S., Gasche, R., Kitzler, B., Klemedtsson, L., Lobo-do-Vale, R. and Moldan, F.: The response of methane and nitrous oxide fluxes to forest change in Europe, Biogeosciences, 9, 3999-4012, 2012.

Haas, E., Klatt, S., Fröhlich, A., Kraft, P., Werner, C., Kiese, R., Grote, R., Breuer, L. and Butterbach-Bahl, K.: LandscapeDNDC: a process model for simulation of biosphere–atmosphere–hydrosphere exchange processes at site and regional scale, Landscape Ecol., 28, 615-636, 2013.

Heinemeyer, A., Wilkinson, M., Vargas, R., Subke, J., Casella, E., Morison, J. I. and Ineson, P.: Exploring the "overflow tap" theory: linking forest soil CO_2 fluxes and individual mycorrhizosphere components to photosynthesis, Biogeosciences, 9, 79-95, 2012.

Ingwersen, J., Butterbach-Bahl, K., Gasche, R., Papen, H. and Richter, O.: Barometric process separation: new method for quantifying nitrification, denitrification, and nitrous oxide sources in soils, Soil Sci. Soc. Am. J., 63, 117-128, 1999.

IPCC: Climate Change 2013: The Physical Science Basis. Contribution of Working Group I to the Fifth Assessment Report of the Intergovernmental Panel on Climate Change [Stocker, T.F., D. Qin, G.-K. Plattner, M. Tignor, S.K. Allen, J. Boschung, A. Nauels, Y. Xia, V. Bex and P.M. Midgley (eds.)]. Cambridge University Press, Cambridge, United Kingdom and New York, NY, US, 2013.

Kattge, J., Knorr, W., Raddatz, T. and Wirth, C.: Quantifying photosynthetic capacity and its relationship to leaf nitrogen content for global ‐ scale terrestrial biosphere models, Global Change Biol., 15, 976-991, 2009.Kiese, R., Heinzeller, C., Werner, C., Wochele, S., Grote, R. and Butterbach-Bahl, K.: Quantification of nitrate leaching from German forest ecosystems by use of a process oriented biogeochemical model, Environmental Pollution, 159, 3204-3214, 2011.

Li, C., Frolking, S. and Frolking, T. A.: A model of nitrous oxide evolution from soil driven by rainfall events: 1. Model structure and sensitivity, J.Geophys.Res, 97, 9759-9776, 1992.

Li, C., Trettin, C., Sun, G., McNulty, S. and Butterbach-Bahl, K.: Modeling carbon and nitrogen biogeochemistry in forest ecosystems, 2005.

Li, C., Aber, J., Stange, F., Papen, H. and Butterbach-Bahl, K.: A process-oriented model of N_2O and NO emissions from forest soils: 1. Model development, J. Geophys. Res.-Atmospheres, 105, 4369-4384, 2000.

Lloyd, J. and Taylor, J.: On the temperature dependence of soil respiration, Funct. Ecol., 315-323, 1994.

Luo, G., Brüggemann, N., Wolf, B., Gasche, R., Grote, R. and Butterbach-Bahl, K.: Decadal variability of soil CO_2, NO, N_2O, and CH_4 fluxes at the Höglwald Forest, Germany, Biogeosciences, 9, 1741-1763, 2012.

Medinets, S., Skiba, U., Rennenberg, H. and Butterbach-Bahl, K.: A review of soil NO transformation: associated processes and possible physiological significance on organisms, Soil Biol. Biochem., 80, 92-117, 2015.

Molina-Herrera, S., Grote, R., Santabárbara-Ruiz, I., Kraus, D., Klatt, S., Haas, E., Kiese, R. and Butterbach-Bahl, K.: Simulation of CO_2 Fluxes in European Forest Ecosystems with the Coupled Soil-Vegetation Process Model "LandscapeDNDC", Forests, 6, 1779-1809, 2015.

Moncrieff, J. B., Massheder, J., De Bruin, H., Elbers, J., Friborg, T., Heusinkveld, B., Kabat, P., Scott, S., Søgaard, H. and Verhoef, A.: A system to measure surface fluxes of momentum, sensible heat, water vapour and carbon dioxide, J. Hydrol., 188, 589-611, 1997.

Oren, R., Hsieh, C., Stoy, P., Albertson, J., Mccarthy, H. R., Harrell, P. and Katul, G. G.: Estimating the uncertainty in annual net ecosystem carbon exchange: Spatial variation in turbulent fluxes and sampling errors in eddy-covariance measurements, Global Change Biol., 12, 883-896, 2006.

Pan, Y., Birdsey, R. A., Fang, J., Houghton, R., Kauppi, P. E., Kurz, W. A., Phillips, O. L., Shvidenko, A., Lewis, S. L., Canadell, J. G., Ciais, P., Jackson, R. B., Pacala, S. W., McGuire, A. D., Piao, S., Rautiainen, A., Sitch, S. and Hayes, D.: A large and persistent carbon sink in the world's forests, Science, 333, 988-993, 2011.

Pilegaard, K., Hummelshøj, P. and Jensen, N.: Nitric oxide emission from a Norway spruce forest floor, J. Geophys.Res.: Atmospheres, 104, 3433-3445, 1999.

Pilegaard, K., Skiba, U., Ambus, P., Beier, C., Brüggemann, N., Butterbach-Bahl, K., Dick, J., Dorsey, J., Duyzer, J. and Gallagher, M.: Factors controlling regional differences in forest soil emission of nitrogen oxides (NO and N_2O), Biogeosciences, 3, 651-661, 2006.

Pitman, R. and Broadmeadow, M.: Leaf area, biomass and physiological parameterisation of ground vegetation of lowland oak woodland, Forestry Commission, Edinburgh, 2001.

Pitman, R., Vanguelova, E. and Benham, S.: The effects of phytophagous insects on water and soil nutrient concentrations and fluxes through forest stands of the Level II monitoring network in the UK, Sci. Total Environ., 409, 169-181, 2010.

Porté, A. and Bartelink, H.: Modelling mixed forest growth: a review of models for forest management, Ecol. Model., 150, 141-188, 2002.

Pyatt, D.: Soil classification [UK]., Research Information Note-Forestry Commission (UK). no.68., 1982.

Reay, D. S. and Nedwell, D. B.: Methane oxidation in temperate soils: effects of inorganic N, Soil Biol. Biochem., 36, 2059-2065, 2004.

Schindlbacher, A., Zechmeister-Boltenstern, S. and Butterbach-Bahl, K.: Effects of soil moisture and temperature on NO, NO_2, and N_2O emissions from European forest soils, J. Geophys. Res.: Atmospheres, 109, 2004.

Smith, P., Smith, J., Powlson, D., McGill, W., Arah, J., Chertov, O., Coleman, K., Franko, U., Frolking, S. and Jenkinson, D.: A comparison of the performance of nine soil organic matter models using datasets from seven long-term experiments, Geoderma, 81, 153-225, 1997.

Smith, P., Albanito, F., Bell, M., Bellarby, J., Blagodatskiy, S., Datta, A., Dondini, M., Fitton, N., Flynn, H., Hastings, A., Hillier, J., Jones, E. O., Kuhnert, M., Nayak, D. R., Pogson, M., Richards, M., Sozanska-Stanton, G., Wang, S., Yeluripati, J. B., Bottoms, E., Brown, C., Farmer, J., Feliciano, D., Hao, C., Robertson, A., Vetter, S.,

Wong, H. M. and Smith, J.: Systems approaches in global change and biogeochemistry research, Philos. Trans. R. Soc. Lond. B. Biol. Sci., 367, 311-321, 2012.

Taylor, J., Wilson, B., Mills, M. S. and Burns, R. G.: Comparison of microbial numbers and enzymatic activities in surface soils and subsoils using various techniques, Soil Biol. Biochem., 34, 387-401, 2002.

Thornley, J.H.M., Cannell, M.G.R.: Modelling the components of plant respiration: Representation and realism. Ann. Bot. 85, 55-67, 2000.

Thurner, M., Beer, C., Santoro, M., Carvalhais, N., Wutzler, T., Schepaschenko, D., Shvidenko, A., Kompter, E., Ahrens, B. and Levick, S. R.: Carbon stock and density of northern boreal and temperate forests, Global Ecol. Biogeogr., 23, 297-310, 2014.

Valentini, R., Matteucci, G., Dolman, A., Schulze, E., Rebmann, C., Moors, E., Granier, A., Gross, P., Jensen, N. and Pilegaard, K.: Respiration as the main determinant of carbon balance in European forests, Nature, 404, 861-865, 2000.

Valentini, R.: Fluxes of carbon, water and energy of European forests, Springer Science & Business Media, 2003.

Vanguelova, E., Benham, S., Pitman, R., Moffat, A., Broadmeadow, M., Nisbet, T., Durrant, D., Barsoum, N., Wilkinson, M. and Bochereau, F.: Chemical fluxes in time through forest ecosystems in the UK–Soil response to pollution recovery, Environ. Pollut., 158, 1857-1869, 2010.

Werner, C., Butterbach-Bahl, K., Haas, E., Hickler, T. and Kiese, R.: A global inventory of N_2O emissions from tropical rainforest soils using a detailed biogeochemical model, Global Biogeochem. Cy., 21, 2007.

Wilkinson, M., Eaton, E., Broadmeadow, M. and Morison, J.: Inter-annual variation of carbon uptake by a plantation oak woodland in south-eastern England, Biogeosciences, 9, 5373-5389, 2012.

Wilkinson, M., Crow, P., Eaton, E.L. and Morison, J.I.L: Effects of management thinning on CO_2 exchange by a plantation oak woodland in south-eastern England. Biogeosciences, 13, 2367–2378, 2016.

Yamulki, S. and Morison, J. I. L.: Annual greenhouse gas fluxes from a temperate deciduous oak forest floor. Forestry, in press.

Yamulki, S., Anderson, R., Peace, A. and Morison, J.: Soil CO_2 CH_4 and N_2O fluxes from an afforested lowland raised peatbog in Scotland: implications for drainage and restoration, Biogeosciences, 10, 1051-1065, 2013.

Yamulki, S., Harrison, R. M., Goulding, K. and Webster, C.: N_2O, NO and NO_2 fluxes from a grassland: Effect of soil pH, Soil Biol. Biochem., 29, 1199-1208, 1997.

Table 1: Site and vegetation properties in 1995 with average climate and air chemistry input (1995-2014) for the LandscapeDNDC model specific for the Straits Inclosure, Alice Holt Forest.

Property	Value
Latitude	51° 09'N
Longitude	0° 51'W
Average annual rainfall	877 mm
Average annual temperature	10.3 °C
Annual N deposition as NH_4	0.89 g m^{-3}
Annual N deposition as NO_3	0.51 g m^{-3}
Total annual N deposition	1.4 g m^{-3}
Slope	0°
Altitude	80.0 m a.s.l.
Upper storey trees: main species	*Pedunculate oak (Q. robur)*
Number of trees per hectare	442
Height	16.5 m
Diameter at breast height	0.233 m
Understorey trees: species (aggregated, for PSIM only)	European Ash (F. excelsior) (representing hazel, hawthorn, ash and holly)
Number of trees per hectare	8000
Height	3.0 m
Diameter at breast height	0.03 m
Modelling start date	1/1/1995
Thinning event (eastern half of Inclosure)	20/9/2007
Proportion of stemwood removed by thinning	0.3

Table 2: Soil property initialization for the Straits Inclosure for use with the LandscapeDNDC model.

Soil texture: silty clay; Humus type: mull; Hydraulic conductivity (in horizons A-C): 0.00006 cm min^{-1};

Water table: 1.1m; no stones

Horizon	Thickness	Organic C	Organic N	pH	Bulk density	Field capacity	Wilting point	Clay fraction
	mm	(proportion)			g cm^{-3}	mm m^{-3}	mm m^{-3}	
O	20	0.2162	0.0114	5.08	0.0670	-	-	0.035
A	80	0.0560	0.0038	5.4	0.7043	530	240	0.52
E	80	0.0287	0.0023	5.2	0.9682	530	240	0.516
B	200	0.0159	0.0010	5.4	1.1334	480	240	0.51
BC	380	0.0108	0.0003	6.2	0.9350	530	240	0.601
C	260	0.0146	0.0005	5.4	1.0123	520	240	0.578

Table 3: LandscapeDNDC vegetation sub-model species parameters adjusted to simulate GHG fluxes for pedunculate oak at the Straits Inclosure.

Parameter	Description	Units	PnET	PSIM
CO_2 exchange parameters				
BASEFOLRESPFRAC	Dark respiration as fraction of photosynthesis	0-1	0.15	na
AMAXB	Maximal net photosynthetic rate	$nmolCO_2\ g^{-1}\ s^{-1}$ / %N	55.0	na
RESPQ10[2]	Temperature dependency of leaf respiration	-	2.0	na
ROOTMRESPFRAC	Ratio of fine root maintenance respiration to biomass production	-	2.0	na
VCMAX25	Maximum RubP saturated rate of carboxylation at 25°C for leaves in full sun	µmol $m^{-2}\ s^{-1}$	na	90
KM20	Respiration maintenance coefficient at reference temperature	0-1	na	0.3
Phenology related parameters				
GDDFOLSTART[3]	Daily temperature sum for start of foliage budburst	°days	500	500
GDDFOLEND[3]	Daily temperature sum for end of foliage growth (maximum leaf area)	°days	1100	na
GDDWODSTART[3]	Daily temperature sum for start of C storage as wood (set at GDDFOLSTART + 100)	°days	600	na
GDDWODEND[3]	Daily temperature sum for end of C storage as wood	°days	1100	na
MFOLOPT[1]	Foliage biomass under optimal, closed canopy conditions	kg DW m^{-2}	0.47	0.47
NDFLUSH[3]	Time required to complete growth of new foliage	days	na	45
NDMORTA[4]	Time required to complete leaf fall	days	na	100
DLEAFSHED[4]	Day by which leaf fall is complete	day of year	na	330
SENESCSTART[4]	Day of year after which leaf death can occur	day of year	300	na
Resource acquisition parameters				
NCFOLOPT	Optimum nitrogen concentration of foliage	g N gDW^{-1}	0.024	0.024
EXPL_NH4	Relative exploitation rate of NH_4	%	0.3	na
EXPL_NO3	Relative exploitation rate of NO_3	%	0.16	na
EXT[5]	Light extinction (attenuation) coefficient	0-1	0.4	0.4

1. Average LAI = 5.92 $m^2\ m^{-2}$ between 1999-2010 (Wilkinson et al., 2012)
2. Q10 for TER calculated as 2.26-4.72, mean 3.0 (SD =0.78) (Wilkinson et al., 2012)
3. Average start of growing season (1999-2007) = doy 132 (Wilkinson et al., 2012)
4. Average end of growing season (1999-2007) = doy 298 (Wilkinson et al., 2012)
5. Light extinction factor = 0.4 (Broadmeadow et al., 2000)

Table 4: Annual CO_2 fluxes for 1999-2007 at the Straits Inclosure measured by eddy covariance and simulated by PnET and PSIM. '%Difference' is the percentage difference between the mean annual simulated and measured values.

Year	GPP (g C m^{-2} yr^{-1})			TER (g C m^{-2} yr^{-1})			NEP (g C m^{-2} yr^{-1})		
	EC	PnET	PSIM	EC	PnET	PSIM	EC	PnET	PSIM
1999	1983	2440	2204	1625	1805	1638	357	635	566
2000	2346	2127	2046	1940	1641	1588	406	486	458
2001	2227	2089	2037	1670	1600	1576	557	489	461
2002	2180	2062	2171	1767	1545	1650	412	517	521
2003	2223	1666	2173	1606	1360	1542	617	306	631
2004	2172	1856	2102	1573	1423	1599	600	433	503
2005	1992	1697	2109	1441	1348	1601	551	349	508
2006	1862	1671	2077	1374	1385	1635	488	286	442
2007	2094	1839	2122	1466	1410	1577	629	429	545
Mean	2120	1939	2119	1607	1502	1602	513	437	515
SD	151	261	58	175	156	35	101	111	60
% Difference		-8.5	-0.04		-6.7	-0.12		-14.1	0.19

Table 5: Statistical analysis using ModEval v 2.0 (Smith et al., 1997) for comparison of CO_2 fluxes simulated by PnET and PSIM with a) annual (n = 9) and b) monthly (n = 108) eddy covariance measurements of GPP, TER and NEP c) monthly soil chamber measurements of CO_2 and N_2O fluxes. 'Average total error' is (RMSE% * Measured mean/100).

a) Statistic	Annual GPP 1999-2007		Annual TER 1999-2007		Annual NEP 1999-2007	
	PnET	PSIM	PnET	PSIM	PnET	PSIM
RMSE (%)	14.8+	7.8+	10.8+	10.5+	38.2+	19.3+
Average total error (uy)	314.2	164.4	173.5	169.1	195.7	98.8
ME	-3.89	-0.34	-0.11	-3.89	-3.21	-0.07
CD	0.20	0.75	0.90	0.20	0.24	0.93
Relative Error (E; %)	8.55*	0.20*	6.53*	0.39*	14.86*	-0.41*
Mean Difference (M; uy)	181.3	4.22	105.0	6.22	76.22	-2.11
Student's t of M (t)	2.0*	0.07*	2.15*	0.10*	1.20*	-0.06*
Correlation coefficient (r)	0.21	-0.24	0.61	-0.04	-0.63	0.23
F	0.34	0.44	4.2	0.01	4.56	0.40

b) Statistic	Monthly GPP 1999-2007		Monthly TER 1999-2007		Monthly NEP 1999-2007	
	PnET	PSIM	PnET	PSIM	PnET	PSIM
RMSE (%)	59.4+	55.9+	36.6+	28.7+	170.6+	124.6+
Average total error (um)	104.9	98.7	49.0	38.4	72.9	53.3
ME	0.92	0.94	0.46	0.67	0.82	0.83
CD	12.21	17.54	1.85	3.01	5.49	6.03
Relative Error (E; %)	8.48*	0.33*	6.71*	0.55*	14.05*	-0.37*
Mean Difference (M; um)	14.99	0.58	8.98	0.73	6.08	0.02
Student's t of M (t)	1.49*	0.06*	1.93*	0.20*	0.86*	0.003*
Correlation coefficient (r)	0.96	0.97	0.88	0.84	0.95	0.91
F	1338**	1785**	373.6**	256.6**	959.9**	536.1**

c) Statistic	Monthly Soil CO_2				Monthly N_2O			
	2008-2012		2013-14		2008-2012		2013-14	
Model	PnET	PSIM	PnET	PSIM	PnET	PSIM	PnET	PSIM
RMSE (%)	60.8+	72.8+	28.9	68.1	149.0+	142.0+	61.5	41.4+
Average total error (um)	46.5	55.7	18.8	44.4	14.5	13.8	2.8	1.9
ME	-0.14	0.38	0.08	-4.11	-0.23	-0.12	-2.22	-0.46
CD	0.88	1.60	1.09	0.20	0.81	0.89	0.31	0.69
Relative Error (E; %)	41.9*	-11.3*	12.7*	-48.9	55.2*	52.1*	0.6*	18.5*
Mean Difference (M; um)	32.0	-8.6	8.25	-31.88	5.94	5.61	0.03	0.83
Student's t of M (t)	7.3	-1.98*	1.89*	-3.99*	3.34	3.30	0.04*	1.95*
Correlation coefficient (r)	0.64	0.68	0.76	0.68	-0.02	0.37	-0.47	0.38
F	41.3**	50.55**	18.73**	12.24**	0.03	8.41**	3.98	2.31
No. of values	60	60	16	16	56	56	16	16

+No significant total error, *No significant bias, **Significant association at P=0.05

uy = g CO_2-C m^{-2} yr^{-1}

um = g CO_2-C m^{-2} $month^{-1}$ or g N_2O-N m^{-2} $month^{-1}$

Table 6: Annual soil gas fluxes for 2008-2014 at the Tower Site of the Straits Inclosure comparing measured soil chamber (SC) data with data simulated using PnET and PSIM. Results from a simulated 30% thin are also given. Mean values given averaged over years after thin, 2008-14.

Year	Soil CO_2 (g C m^{-2} yr^{-1})					Soil N_2O (mg Nm^{-2} yr^{-1})					Soil NO (mg Nm^{-2} yr^{-1})				
	SC	PnET	PnET	PSIM	PSIM	SC	PnET	PnET	PSIM	PSIM	SC	PnET	PnET	PSIM	PSIM
Thinning:		0%	30%	0%	30%		0%	30%	0%	30%		0%	30%	0%	30%
2006	Na	571	571	1081	1081	Na	49.1	49.1	57.3	57.3	Na	6.8	6.8	10.7	10.7
2007	Na	561	629	1059	1026	Na	47.0	41.7	55.2	52.7	Na	7.0	5.9	10.9	10.6
2008	1015.5	514	758	1033	904	174.6	52.6	56.5	60.3	61.1	Na	8.0	8.7	11.5	12.6
2009	697.0	543	682	1046	888	155.7	43.8	61.1	52.3	61.3	Na	6.1	9.1	9.2	11.5
2010	797.3	496	547	934	793	33.8	38.9	51.8	40.7	37.6	Na	5.4	8.4	7.2	7.5
2011	835.8	598	586	1078	926	15.4	41.4	51.6	43.9	37.1	Na	5.7	8.2	7.5	7.7
2012	816.6[1]	514	488	1007	884	83.5[1]	48.2	50.5	44.7	36.4	Na	7.0	8.6	7.6	7.6
2013	689.3[2]	523	473	941	871	57.4[2]	41.7	43.3	36.9	32.7	1.1[3]	5.6	6.9	5.8	6.0
2014	Na	638	554	1087	998	Na	55.2	52.1	51.5	46.1	Na	7.1	7.7	7.8	8.2
Mean	807	575	584	1018	895	87.4	46.0	52.4	43.3	44.6	-	6.4	8.2	8.1	8.7
SD	118.7	54.5	102.8	61.2	61.6	65.2	6.2	5.5	8.0	12.0	-	1.0	0.7	1.8	2.4
Difference	-	-32%	-28%	26%	11%	-	-47%	-40%	-46%	-49%	-	-	-	-	-

1= Jan-Aug 2012 only (not included in mean),
2=April 2013-April 2014, (Aug 2013-Aug 2014: CO_2 = 775.8 g C m^{-2} yr^{-1}, N2O = 52.4 mg N m^{-2} yr^{-1})
3=July 2013-Aug 2014 (adjusted to 365 days)
Na = Not available

Table 7: Sensitivity tests showing % change in simulated annual total GHG fluxes averaged over 1999-2007 for a) input variable changes simulated with PNET (see Table 1 for initial input values), b) parameter value changes simulated with PNET and c) parameter value changes simulated with PSIM. Parameter value units are given in Table 3.

(a)

Input variable	GPP % change		TER % change		NEP % change		Soil CO_2 % change		N_2O % change		NO % change	
	+10%	-10%	+10%	-10%	+10%	-10%	+10%	-10%	+10%	-10%	+10%	-10%
Soil pH (±1 pH unit)	-1.13	0.77	-0.80	0.60	-2.29	1.14	-0.32	0.64	-5.32	-0.95	-2.66	661.24
Clay (±10%)	-0.41	0.00	-0.40	0.20	-0.46	-0.69	-0.16	0.48	-1.20	-0.63	1.06	1.60
Organic C (±10%)	2.06	-2.84	2.20	-2.80	1.60	-2.97	2.57	-3.05	6.43	-8.67	21.62	-22.04
Organic N (±10%)	-1.19	0.72	-1.20	0.93	-1.37	0.00	-0.96	1.28	-3.06	1.25	-5.57	4.47
Bulk density (±10%)	1.50	-0.31	1.66	-0.40	0.92	-0.23	1.93	-0.48	12.43	-6.69	39.30	-22.58
Field capacity (±10%)	-1.34	0.93	-1.80	1.66	0.00	-1.60	-1.93	2.09	5.90	-4.47	16.19	-8.53
Wilting point (±10%)	-0.05	0.05	0.27	-0.07	-1.14	0.46	0.32	0.16	0.41	-0.30	1.52	-1.19
Hydraulic conductivity /10	-0.57		-0.60		-0.46		-0.64		1.39		1.52	
Hydraulic conductivity x10	-0.15		-0.07		-0.46		0.00		-3.17		-0.11	
Hydraulic conductivity x100	-0.21		0.00		-0.92		-0.16		-4.79		-0.53	
N deposition (±10%)	0.10	-1.34	0.00	-1.07	0.46	-2.06	-0.16	-0.96	0.39	-3.84	1.88	-2.85
N deposition (+100, -50%)	7.01	-5.31	5.66	4.53	11.67	-8.24	4.65	-3.85	17.67	-14.13	24.83	-15.40
Temperature* (±10%)	3.2	-1.5	2.8	0.3	4.8	-7.8	-3.9	6.9	-1.9	8.0	-6.3	15.0
Precipitation (±10%)	-1.5	-0.8	-3.3	-2.1	4.6	3.4	-6.7	-5.8	-3.7	-5.6	-3.1	-4.2

'*' = min., max and mean

(b)

PnET Parameter	GPP % change		TER % change		NEP % change		Soil CO_2 % change		N_2O % change		NO % change	
	+10%	-10%	+10%	-10%	+10%	-10%	+10%	-10%	+10%	-10%	+10%	-10%
BASEFOLRESPFRAC (0.165, 0.135)	3.51	-3.97	5.13	-5.53	-1.83	1.37	0.16	-0.64	5.11	-6.07	1.04	-3.59
MFOLOPT (0.517, 0.423)	7.58	-7.79	9.05	-8.85	2.29	-4.12	6.74	-6.10	4.37	-0.75	5.65	-6.78
RESPQ10 (2.2, 1.8)	-2.42	2.99	-3.60	4.73	1.60	-2.97	1.12	-0.48	-6.52	5.22	-3.56	2.38
ROOTMRESPFRAC (2.2, 1.8)	0.72	-0.98	1.46	-1.40	-1.60	0.46	2.89	-2.25	3.62	-3.19	0.32	-1.43
EXT (0.44, 0.36)	0.36	-1.44	2.00	-2.73	-5.26	2.97	0.64	-0.96	7.56	-8.73	3.50	-5.64
NCFOLOPT (0.0264, 0.0216)	0.41	-2.42	0.47	-1.93	0.23	-4.35	0.32	-1.12	-4.47	3.30	-3.03	0.62
EXPL_NH4 (0.33, 0.270	-0.57	-0.46	-0.53	-0.33	-0.46	-0.92	-0.48	-0.32	-0.21	2.13	-2.20	0.18
EXPL_NO3 (0.176, 0.144)	-0.15	-0.46	-0.13	-0.27	-0.23	-1.37	0.00	0.00	-2.02	3.41	-3.50	1.20
SENESCSTART (330, 270)[1]	-12.58	-4.85	-14.91	-5.26	-4.81	-3.43	-11.40	-2.73	0.43	-3.19	-13.51	-3.70
GDDFOLSTART (550, 450)	-2.94	2.48	-3.93	3.66	0.23	-1.37	-5.94	5.94	-4.15	1.60	-2.78	2.34
GDDFOLEND (1210, 990)	5.83	-6.03	9.92	-8.85	-8.01	3.66	17.01	-13.16	19.28	-14.91	11.78	-11.48

1 = SENESCSTART ± 30 days

(c)

PSIM parameter	GPP % change		TER % change		NEP % change		Soil CO_2 % change		N_2O % change		NO % change	
	+10%	-10%	+10%	-10%	+10%	-10%	+10%	-10%	+10%	-10%	+10%	-10%
MFOLOPT (0.517, 0.423)	1.94	-0.85	2.75	-1.50	0.78	1.17	3.17	-1.25	3.91	-4.75	1.14	-4.73
NCFOLOPT (0.0264, 0.0216)	0.00	-0.09	0.19	-0.25	-0.58	0.39	-0.19	0.38	-1.70	-0.93	-2.61	-2.61
GDDFOLSTART (550, 450)	-1.79	1.46	-0.81	0.69	-4.85	3.88	-0.10	0.19	-1.65	0.48	-2.86	0.95
NDFLUSH (49.5, 40.5)	-1.18	1.46	-0.62	0.75	-2.91	3.69	-0.19	0.29	-0.88	0.63	-1.97	1.08
DLEAFSHED (340, 320)[1]	1.89	-1.98	1.44	-1.31	3.30	-4.08	1.06	-0.67	2.53	-2.93	5.03	-4.73
DLEAFSHED (350, 300)[2]	3.73	-4.53	3.00	-2.25	6.02	-11.65	2.21	0.38	5.11	-8.87	9.55	-12.79
NDMORTA (110, 90)	-0.71	0.66	-0.50	0.56	-1.17	1.17	-0.38	0.48	-1.75	5.81	-2.42	1.92
VCMAX25 (99, 81)	3.78	-4.16	2.12	-2.37	8.93	-9.90	1.25	-1.35	-1.78	1.72	-2.89	2.26
KM20 (0.33, 0.27)	0.05	-0.05	0.75	-0.81	-2.14	2.14	0.29	-0.29	0.47	-0.97	0.71	-1.48
EXT (0.44, 0.26)	-2.36	2.83	-2.37	2.93	-2.52	2.52	-2.60	3.46	2.28	-1.98	2.48	-3.25
FREX VCMAX (93.5, 76.5)	0.19	-0.33	0.12	-0.25	0.39	-0.39	0.19	-0.29	-0.74	0.60	-0.77	0.78
No understorey	-17.38		-20.72		-6.99		-21.73		-13.80		-4.38	

1=DLEAFSHED ± 10 days 2 = DLEAFSHED ± 20 days

Table 8: Results from ModEval statistical analysis (Smith et al., 1997) of monthly TER data for 2009 and 2012 simulated with PnET and PSIM and compared with eddy covariance measurements at the Straits Inclosure. Results from modelling with 0% thin are compared with measurements from the western, unthinned sector and those from modelling with 30% thin are compared with the eastern thinned sector. (EC data from Wilkinson et al., 2016).

	PnET		**PSIM**	
Level of thinning:	0%	30%	0%	30%
2009				
RMSE (%)	28.6+	39.9+	33.7+	39.3+
Average total error	31.4	59.0	37.1	58.1
Modelling efficiency	0.73	0.44	0.62	0.45
Coefficient of determination	3.70	1.78	2.66	1.83
Correlation coefficient, r	0.93	0.86	0.89	0.82
No. of values	12	12	12	12
2012				
RMSE (%)	38.1+	45.1+	28.1+	27.0+
Average total error	52.2	64.5	39.3	38.6
Modelling efficiency	0.54	0.43	0.75	0.74
Coefficient of determination	2.17	1.76	3.98	3.85
Correlation coefficient, r	0.91	0.91	0.88	0.95
No. of values	12	12	12	12

+No significant total error

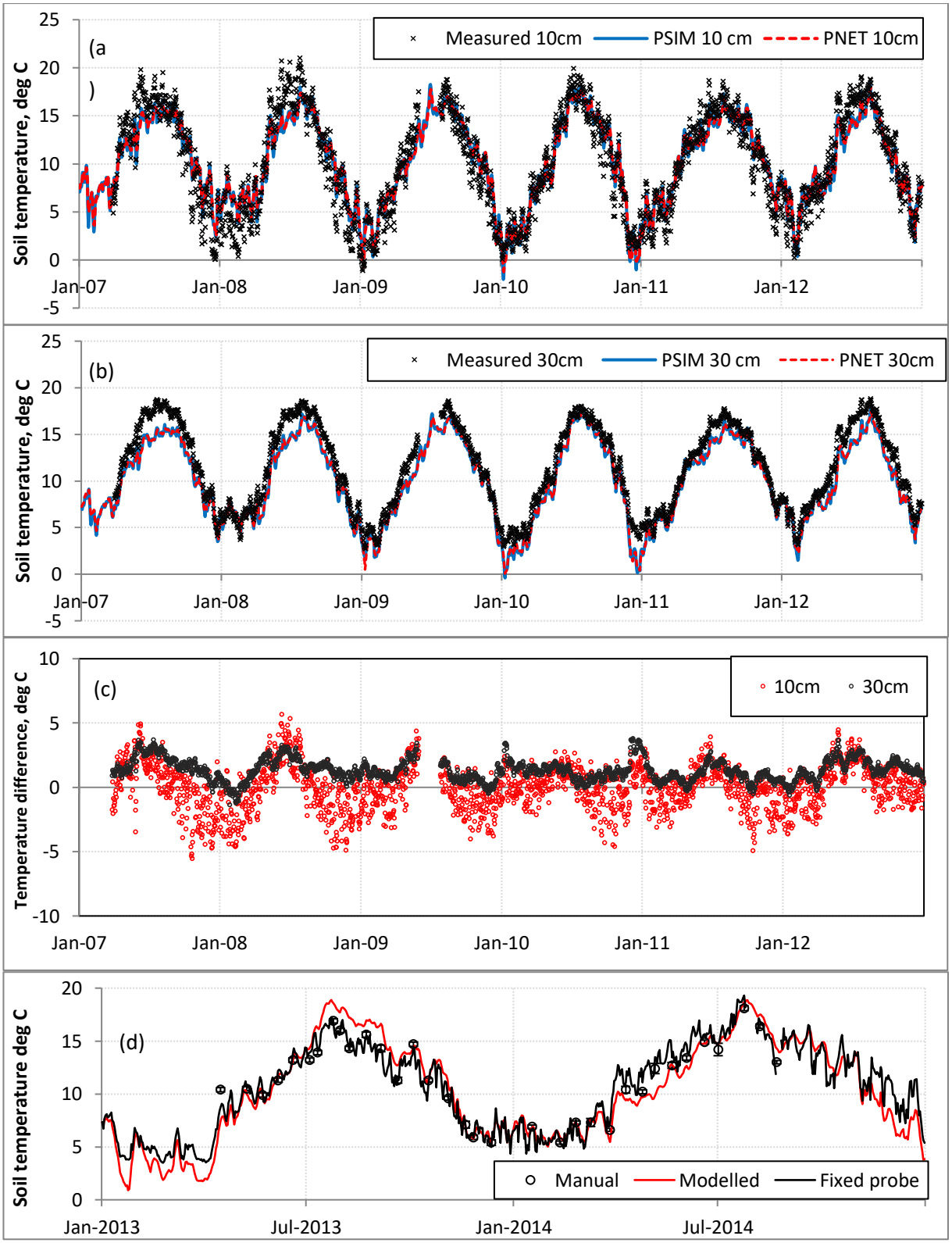

Figure 1: Daily mean measured and simulated soil temperature for years 2007-2013 at the Straits Inclosure, Alice Holt Forest. Measured data are from a fixed automatic probe at the Tower Site. Simulated data from LandscapeDNDC with PnET and PSIM, a) temperatures at 10 cm soil depth, b) temperatures at 30 cm soil depth, c) residuals (measured – simulated with PnET) at 10 cm and 30 cm, d) temperatures at 10 cm recorded manually and from fixed probe during 2013-2014 soil gas sampling. Error bars on manual measurements are 1 SD from 24 daily measurements

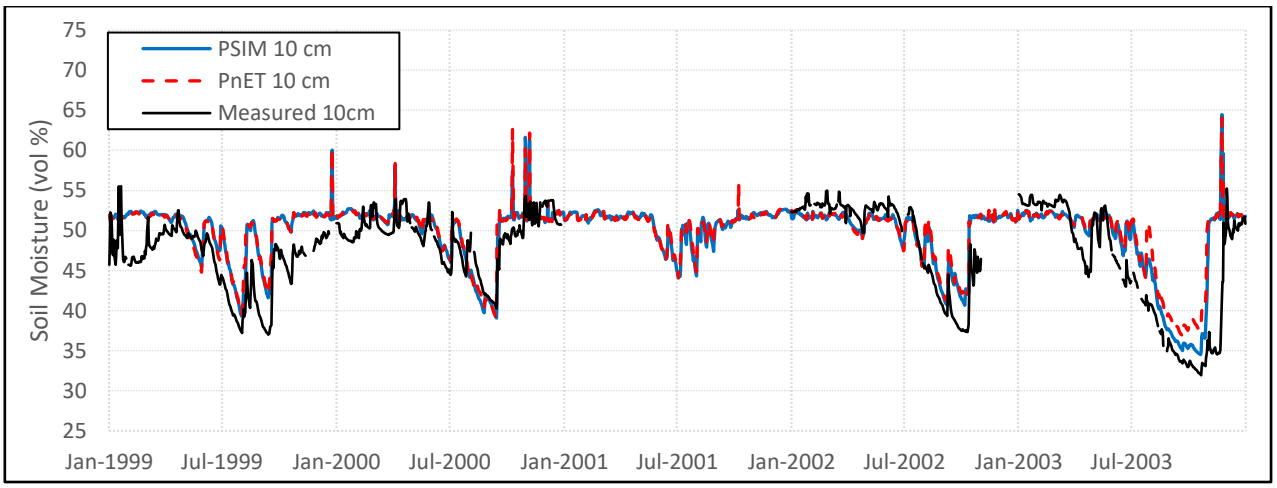

Figure 2: Daily soil moisture measured at the Tower Site, Straits Inclosure during 1999–2003 and simulated by LandscapeDNDC (with PnET and PSIM as the vegetation modules). Measured data are from a fixed probe at the Tower site.

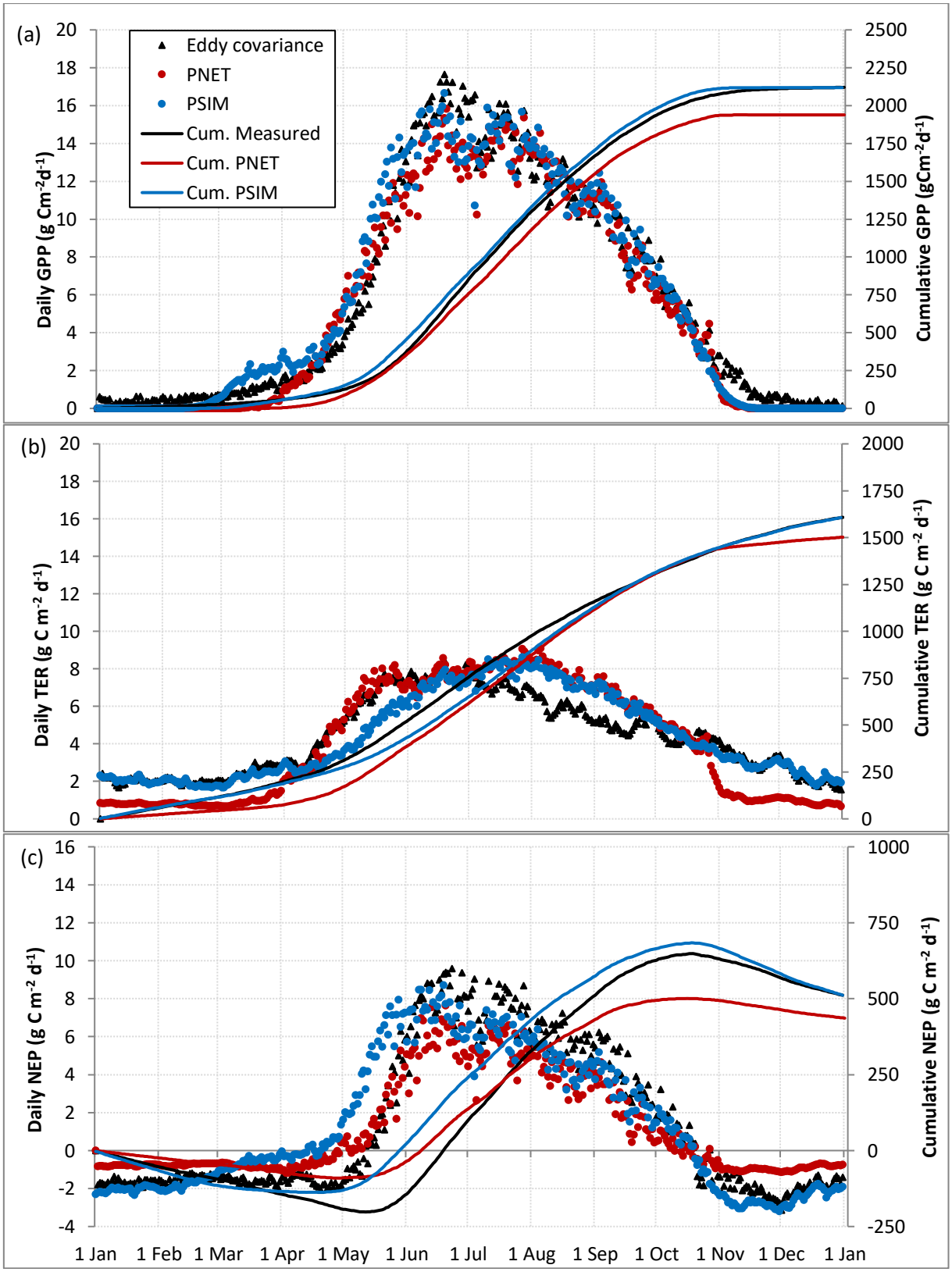

Figure 3: Average seasonal time course of ecosystem CO_2 flux components for the Straits Inclosure for 1999-2007 a) GPP, b) TER, c) NEP. Each plot shows average daily and cumulative values of measured eddy covariance fluxes with simulated PnET and PSIM data.

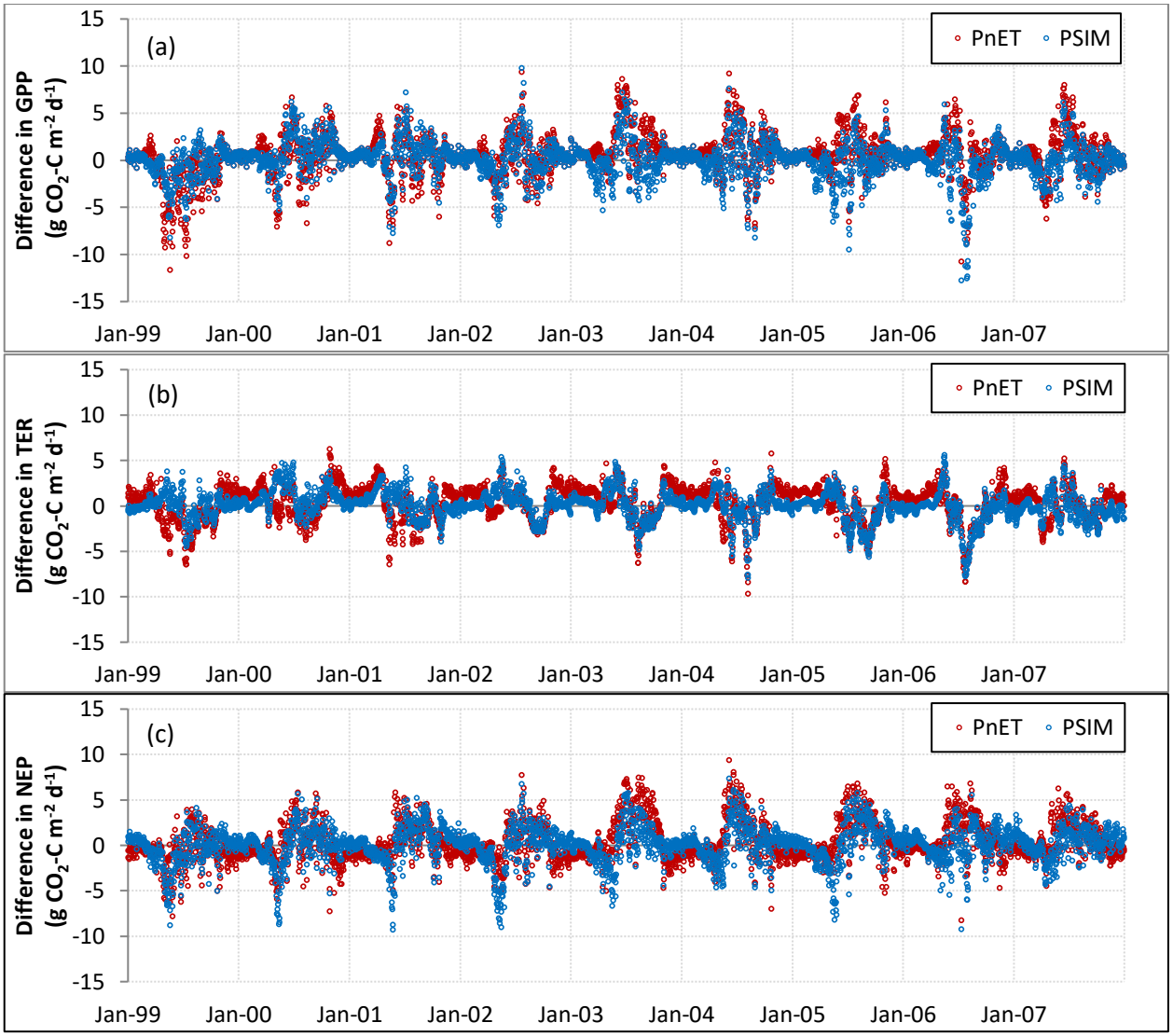

Figure 4: Daily residual values (measured – simulated) for a) GPP, b) TER and c) NEP at the Straits Inclosure, modelled with PnET (red circles) and PSIM (blue circles) modules 1999-2007.

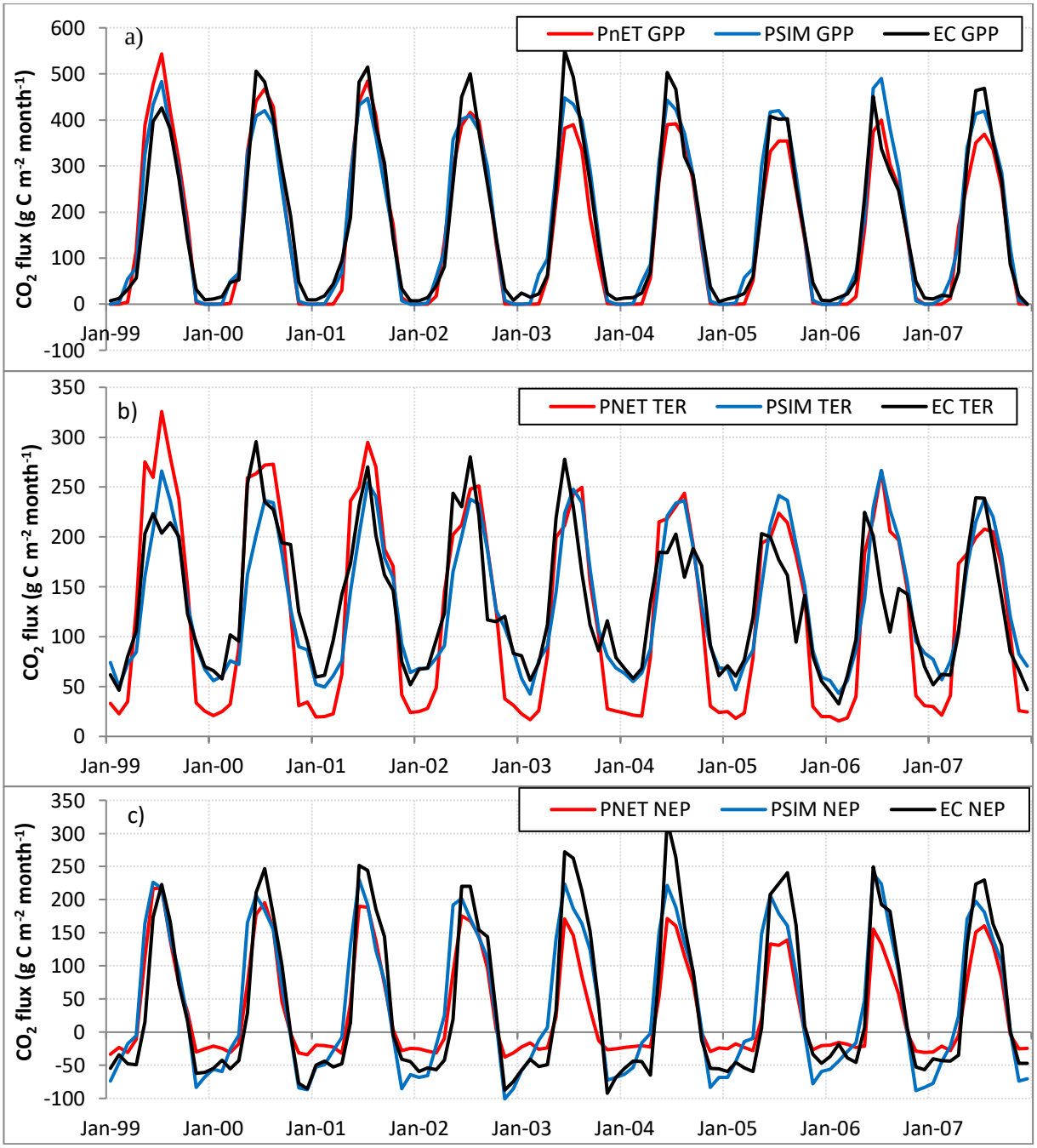

Figure 5: Monthly CO2 exchange at the Straits Inclosure simulated by PSIM and PnET and measured by eddy covariance (EC); a) GPP, b) TER, c) NEP.

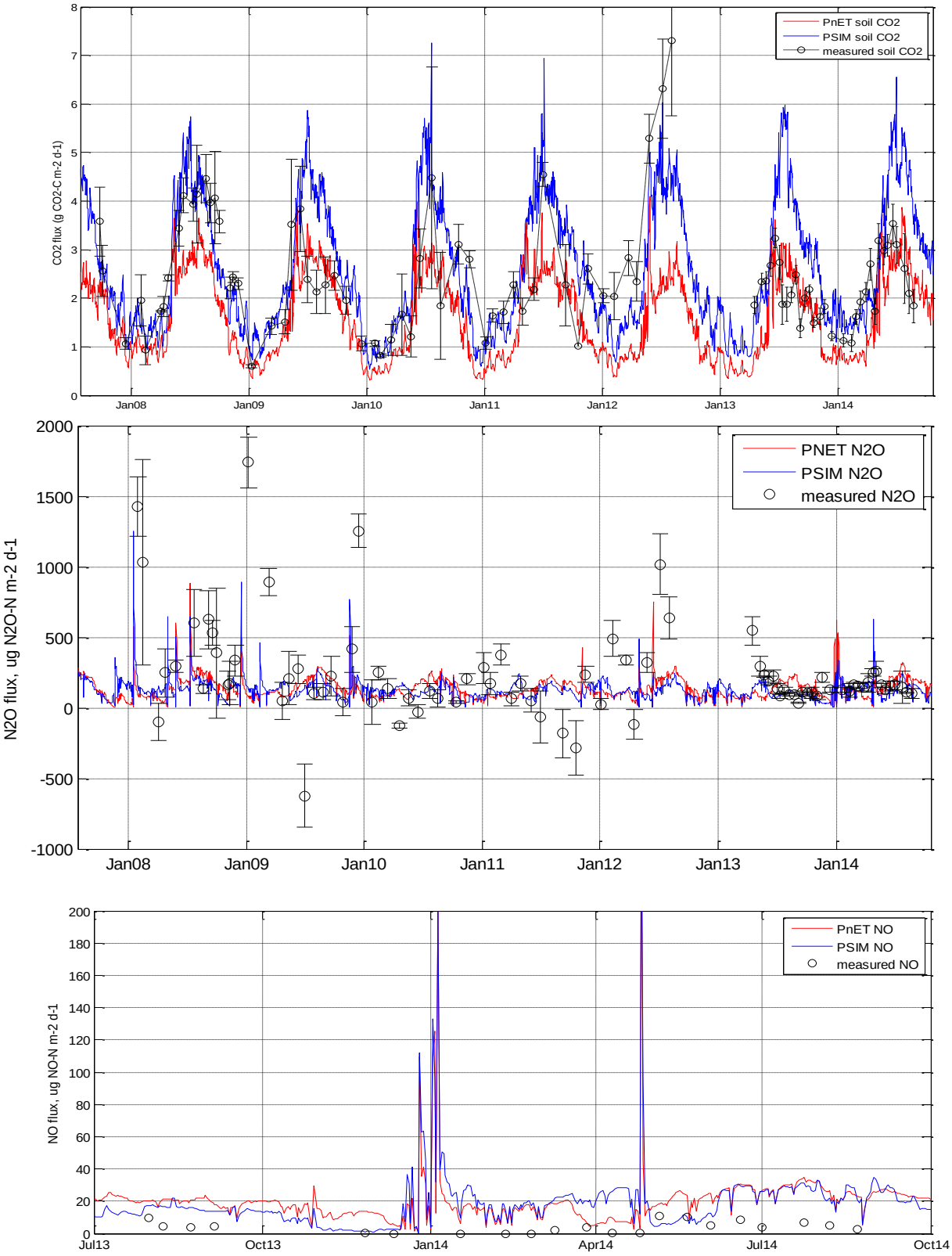

Figure 6: Soil emissions simulated by LandscapeDNDC with PnET (red) and with PSIM (blue) and measured from chambers (black) at the Straits Inclosure; a) CO_2, b) N_2O and c) NO. Standard error bars shown on CO_2 and N_2O measurements; not shown for NO for clarity.

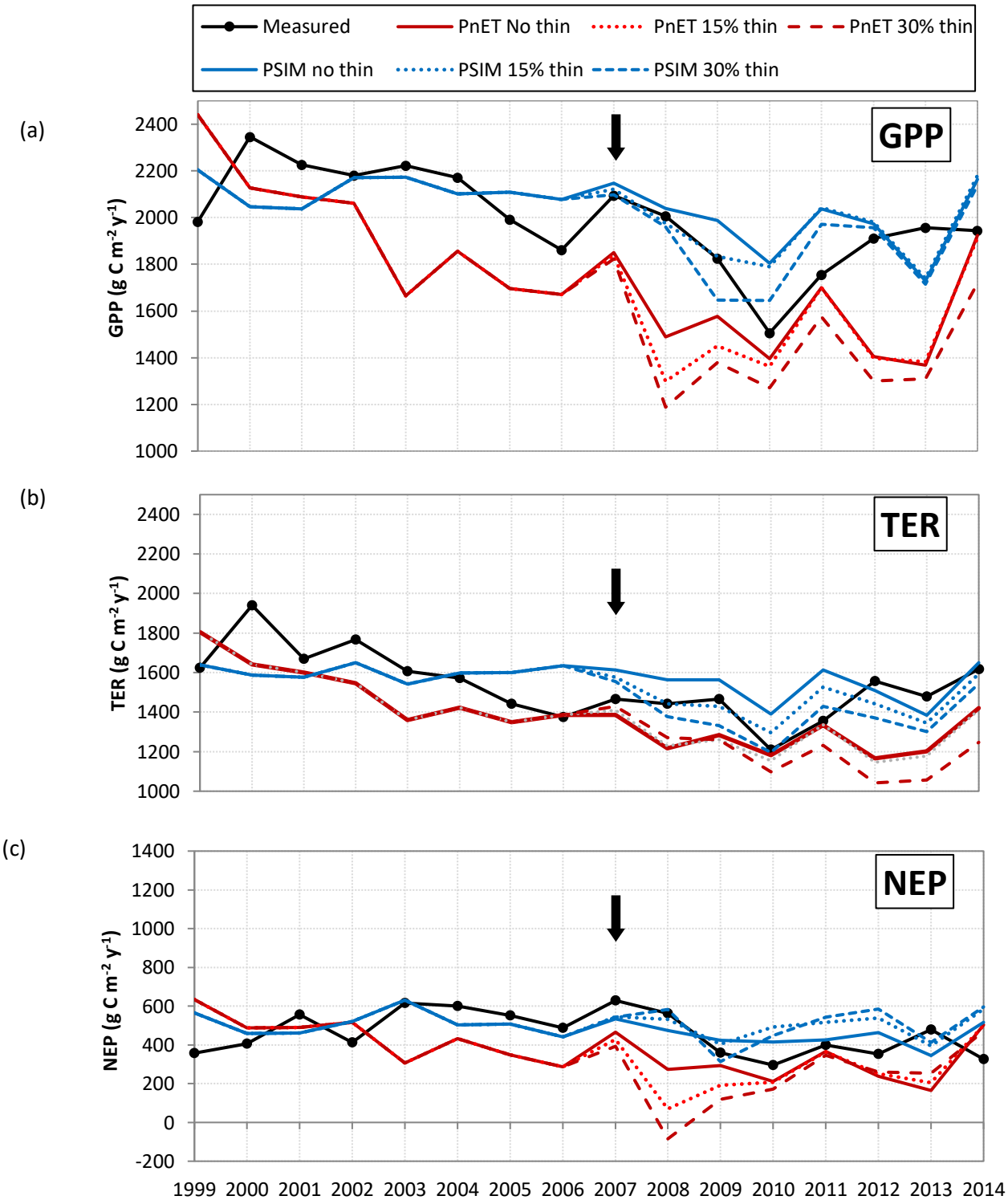

Figure 7: Annual eddy covariance CO_2 and soil gas flux measurements at the Straits Inclosure Tower Site for a) GPP, b) TER, c) NEP, d) soil CO_2 and e) soil N_2O compared with simulated values from PnET, and PSIM with a 0%, 15% and 30% thinning event in September 2007 (marked with black arrow).

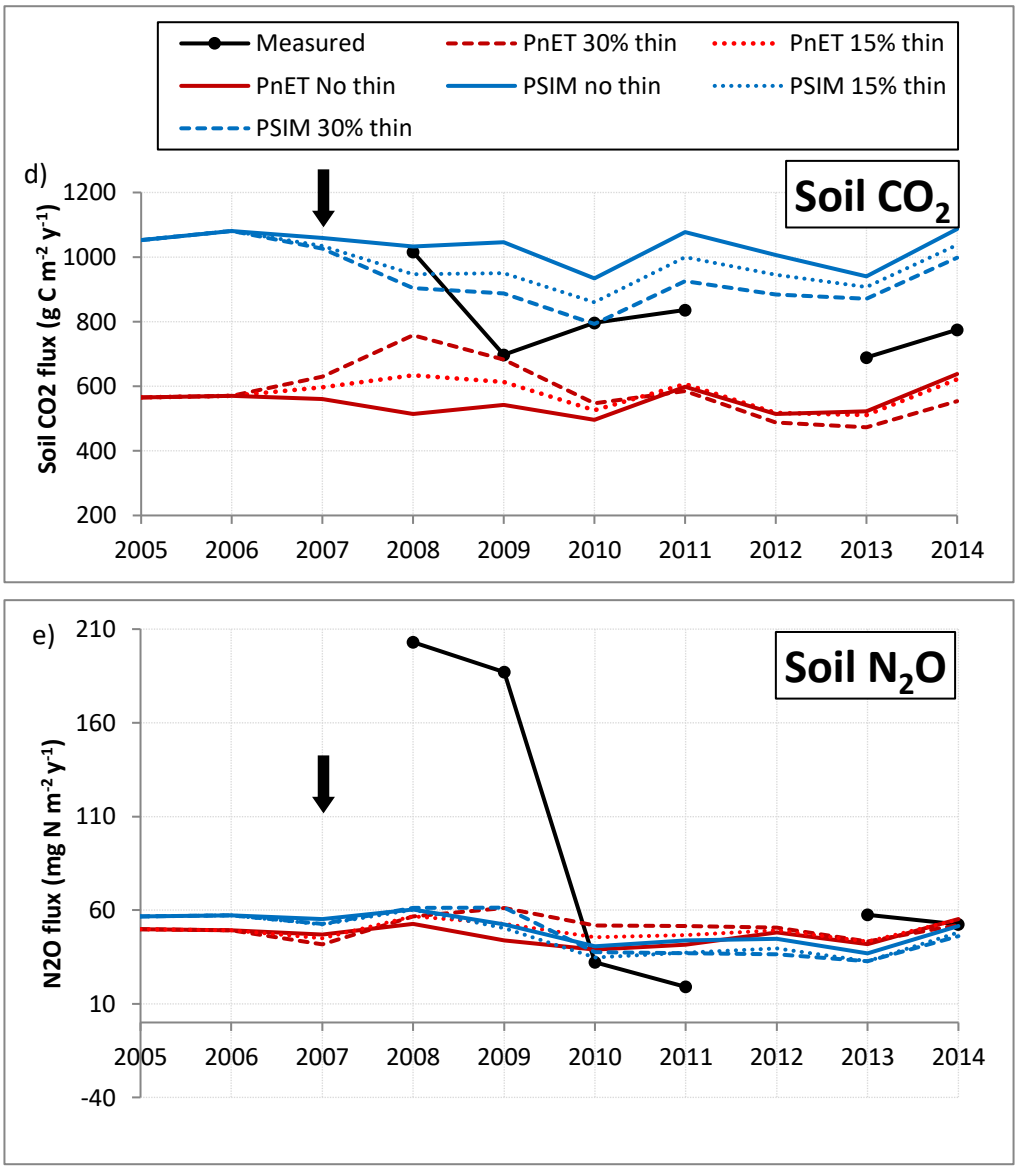
Measured
PnET 30% thin
PnET 15% thin
PnET No thin
PSIM no thin
PSIM 15% thin
PSIM 30% thin
d)
Soil CO_2
Soil CO2 flux (g C m-2 y-1)
1200
1000
800
600
400
200
2005
2006
2007
2008
2009
2010
2011
2012
2013
2014
e)
Soil N_2O
N2O flux (mg N m-2 y-1)
210
160
110
60
10
-40

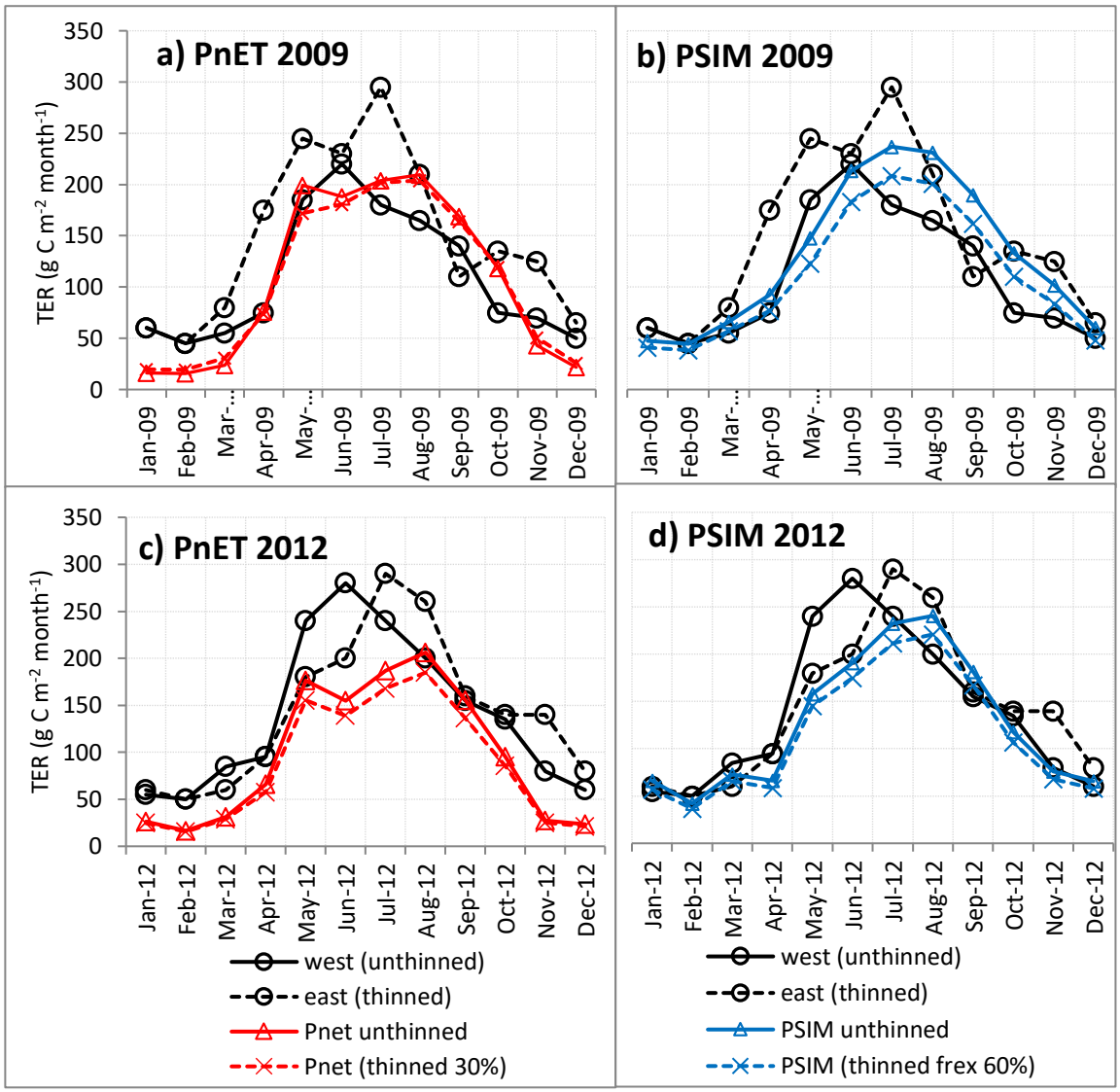

Figure 8: Monthly TER at the Straits Inclosure for 2009 (a and b) and 2012 (c and d). Measured EC TER data is separated into data originating from the eastern (thinned) sector and western (unthinned) sector (Wilkinson et al., 2016). Equivalent simulated TER data is shown for PnET (a and c) and PSIM (b and d) with 0% and 30% thinning

Chapter 4

Carbon dioxide, nitrous oxide and nitric oxide fluxes from a forest soil under a spruce plantation in Perthshire, Scotland: Simulations by LandscapeDNDC

Shirley M. Cade[1], Saúl Molina-Herrera[2], Edwin Haas[2], Rüdiger Grote[2], Robert Clement[4], Kevin C. Clemitshaw[1], David Lowry[1], Matthew Wilkinson[3], and Sirwan Yamulki[3]

Paper in preparation for submission to Biogeosciences

(Number of manuscript pages: 31)

My Contribution to this work:

- Collated and formatted meteorological, eddy covariance flux and all other input data for LandscapeDNDC model simulations
- Carried out all modelling work with LandscapeDNDC
- Performed all statistical analyses using ModEval
- Wrote first draft of manuscript
- Produced all figures

Carbon dioxide, nitrous oxide and nitric oxide fluxes from a forest soil under a spruce plantation in Perthshire, Scotland: Simulations by LandscapeDNDC

Shirley M. Cade[1], Saúl Molina-Herrera[2], Edwin Haas[2], Rüdiger Grote[2], Kevin C. Clemitshaw[1], David Lowry[1], Robert Clement[4] and Sirwan Yamulki[3]

[1]{Department of Earth Sciences, Royal Holloway, University of London, Egham, TW20 0EX, UK}
[2]{Karlsruhe Institute of Technology, Institute of Meteorology and Climate Research Atmospheric Environmental Research, Kreuzeckbahnstraße 19, 82467 Garmisch-Partenkirchen, Germany}
[3]{Forest Research, Alice Holt Lodge, Farnham, GU10 4LH, UK}
[4] School of Geosciences, University of Edinburgh, West Mains Rd, Edinburgh, EH9 3JN, UK}

Correspondence to: S. M. Cade (Shirley.Cade.2008@live.rhul.ac.uk)

Abstract

Intensely managed forests on drained heathland can sequester large amounts of CO_2, helping to mitigate against climate change, but the soil disturbance necessary to establish these plantations can result in increased emissions of CO_2, N_2O and NO from the soil. Modelling is the best way to understand the long-term balance of these gases in forest ecosystems and facilitate planning for future environmental change. In this study, the process-based model LandscapeDNDC was evaluated to simulate soil and ecosystem fluxes of CO_2 and soil fluxes of N_2O and NO from a Sitka spruce plantation and to assess the suitability of the model by comparing the simulated results with results obtained from eddy covariance and soil chamber flux measurements at this site. The ecosystem level simulations comprising net ecosystem production (NEP), gross primary production (GPP) and total ecosystem respiration (TER) averaged over the period between 1997 and 2000 were 716, 2259 and 1544 g CO_2-C m^{-2} y^{-1} respectively and produced results within 1 % of the average annual eddy covariance fluxes measured. The simulation results showed no significant errors on monthly fluxes, with positive model efficiency values for monthly TER (0.93) and GPP (0.59), although negative for NEP (-0.21), indicating that these fluxes were modelled adequately at a monthly level. The average soil N_2O, NO and CO_2 fluxes simulated by the LandscapeDNDC model over the study period were 33.5 ± 9.9 mg N_2O-N m^{-2} y^{-1}, 130.0 ± 27.3 mg NO-N m^{-2} y^{-1} and 695 ± 50 g CO_2-C m^{-2} y^{-1} respectively. The simulated average soil CO_2 efflux was nearly twice measured values

reported for this site, representing 45 % of the measured and modelled TER. Although chamber measurements are known to be subject to inherent errors, causing underestimation of fluxes, overestimation of soil effluxes by the model may also contribute to the discrepancy due to uncertainties in input data. Further investigation with contemporary climate data for the model would be required to understand the cause of the large difference for soil CO_2 effluxes.

1 Introduction

Forests have an important role in the mitigation of greenhouse gas (GHG) emissions through their uptake and storage of CO_2, and therefore afforestation and sustainable forest management have been promoted as contributions to the UK efforts to combat climate change (Read et al., 2009). Soils store more carbon under forests than any other vegetation (Read et al., 2009) and in Britain, forest soils are estimated to store 664 M t C in the top 1 m of soil (Vanguelova et al., 2013). Forest soils can also be sources for CO_2, from aerobic processes, CH_4 from anaerobic microbial processes and N_2O and NO produced principally by nitrification and denitrification of soil organic matter.

Sitka spruce accounts for approximately half of coniferous forests in Britain, both by volume and by forested area and is the dominant conifer species in Scotland (National Forest Inventory, 2013) following major afforestation in the 1950s to 1980s. Sitka spruce was imported from the W coast of N America in the 20th century because it is well adapted to the mild maritime climate and is highly productive, even on marginal upland soils. It was also widely planted in Ireland at the same time, where it has proved highly productive (Carbonnier, 1991). Goodale et al. (1998) used the model PnET to show that site-specific conditions and management practices have a greater impact on Sitka spruce forest productivity in Ireland than potential climate change scenarios involving changes in temperature, precipitation and ambient CO_2 concentrations.

Griffin Forest, the Sitka spruce plantation in Perthshire studied here, has been the subject of several previous studies since the eddy covariance Tower was established in 1997 (Clement, 2004). Valentini et al. (2000) compared eddy covariance data collected between 1996 and 1998 from 15 European forests, including Griffin, and established a correlation between net ecosystem production (NEP) and latitude, and by inference, annual temperature, such that lower latitudes have a greater net CO_2 uptake than higher latitudes. There was no significant

correlation with gross CO_2 uptake and the conclusion was that total ecosystem respiration (TER) was the primary control on NEP. The 2 years of data from Griffin, however, did not fit this trend, which was attributed to a combination of the maritime climate, young, fast-growing species and intense management. In a subsequent study of eddy covariance data from 18 European forests, including Griffin, Janssens et al. (2001) identified a correlation between annual TER (and soil respiration) and GPP in undisturbed forests. The explanation was that an increase in productivity results in greater autotrophic respiration and provides more litter for heterotrophic respiration, whereas in forests with disturbed soils, such as Griffin, soil heterotrophic respiration was a higher proportion of TER driven more by mineralisation of older soil organic material and the correlation with GPP was poor. TER for 1997 and 1998 at Griffin (1320 and 1350 g C m^{-2} y^{-1}) was higher than the average for the 18 forests (1100 g C $m^{-}2$ y^{-1}), which was assumed to be due to enhanced decomposition within the soil following site ploughing, draining and fertilising prior to afforestation (Janssens et al., 2001).

Medlyn et al. (2005) modelled Griffin C balance with the forest canopy model MAESTRA and compared Griffin, which had the highest net ecosystem production (NEP) and lowest respiration, with 2 other coniferous forests from different climates (in France and Sweden). The conclusion was that respiration, particularly in the soil, was key to control NEP and that models which incorporate soil processes were required. Ibrom et al. (2006) used MAESTRA to compare the CO_2 uptake of Griffin Forest with an older German Norway spruce forest which had 25 % lower CO_2 uptake and concluded that this difference was partly due to the Griffin Sitka spruce canopy being more evenly distributed and therefore making more efficient use of light. Kurbatova et al. (2008) showed that lowering the water table could change a Russian spruce forest from a net sink to a net source of CO_2 following modelling work using ForestDNDC after species parameters were validated with data from Griffin and 3 other forests. Clement et al. (2012) reanalysed eddy covariance data from Griffin for the years 1997–2000 and developed a site-specific correction for advective flux losses to include topographic effects. This resulted in higher NEP values for 1997 and 1998 than those used by Valentini et al. (2000), Janssens et al. (2001) and Medlyn et al. (2005) by 20–50 g C m^{-2} y^{-1} with even larger changes in TER and GPP (200–300 g C m^{-2} y^{-1}).

As trees typically have lifespans of several decades, process-based models can help understand their complex interactions with the soil, environmental conditions and how they

might react to change. In this study the model LandscapeDNDC (Haas et al., 2013) has been evaluated for use with Griffin Forest in central Scotland. It combines sub-modules for tree growth (PnET, Photosynthesis-Evapotranspiration, Aber et al., 1995) and soil biogeochemical processes (DNDC, Denitrification-Decomposition, Li et al., 1992) and simulates gas exchanges between soil and atmosphere.

The many studies that have considered the C balance of Griffin Forest have found it to be different from the majority of other coniferous forests studied in Europe. The aims of this study were to consider N_2O and NO together with CO_2, in evaluating LandscapeDNDC to simulate GHG fluxes for the Griffin Forest.

2 Materials and Methods

2.1 Site Description

The Griffin Forest is in the Tay River Valley, near Aberfeldy in central Scotland with a complex terrain, and an average altitude of 350 m (Fig. 1). The area was originally heather moorland but about 3800 ha was planted in 1980–81 mainly with Sitka spruce (81 %) but also Douglas fir, larch and Scots pine. The area within the fetch of the EC tower has a higher proportion of spruce trees (97 %) whose dense foliage, extending to a low level, prevents understorey development and the only localised ground cover is heather from the original moorland. Prior to planting, the heather was burnt and the ground ploughed, producing a ridge and furrow soil surface with about 2m between ridges, and furrows about 40 cm deep (Clement et al., 2012). Ploughing was in the direction of slope to promote drainage and trees were planted on the ridge tops to improve root aeration. In 1997 the site was fertilized at a rate of 350 kg ha^{-1} with urea (43 % N) to reduce the effects of competition from heather. Further details of the site used for input to the model are given in Table 1. The soil is a stagno-gley, approximately 80 cm thick overlying glacial till. Four distinct soil types have been identified according to their location on the ridge and furrow transect (Clement, 2004), but for modelling purposes the ridge soil type is used to initialise the model simulations, details of which are in Table 2.

2.2 LandscapeDNDC model

The LandscapeDNDC model (Haas et al., 2013) has been used to simulate ecosystem and soil flux gases together with the tree growth sub-module PnET (Aber and Federer, 1992; Aber et al., 1995) in combination with Treedyn (Bossel, 1996), the tree structure submodule which defines how the tree shape changes as it grows, as described in Chapter 2.6. The model used is version 36.1 of LandscapeDNDC. The tree species *Picea sitchensis*, referred to as PISI within the model, can be treated as a monoculture for modelling purposes.

The model is initialised with site data, annual average climate data, vegetation information and relevant management events and timings (Table 1) together with details of soil layers (Table 2). The simulation process is then controlled by daily values input for air temperature (mean, maximum and minimum) and rainfall. In the absence of data measurements of photosynthetically active radiation, this is generated internally. Daily climate data, comprising rainfall, atmospheric and soil temperatures were provided by Robert Clement, University of Edinburgh, from measurements made at the EC tower within the Griffin site from January 1997 to December 2000 together with the EC data. In order to provide a longer time period for the model to achieve balance, the daily climate data was replicated to allow a simulation start date of 1/1/1989. Only results from 1997–2000 were compared with measurements, matching the available climate data. Further replication of climate data was made to extend the simulation period to 2014. Soil temperature and EC data from 1997 - 2000 were used for comparison with simulation results and not used as input.

The PnET sub-model calculates daily CO_2 uptake from photosynthesis, based on leaf area cover per unit area, N content of the leaves and photosynthetically active radiation (which reduces with depth of canopy layer). This CO_2 uptake, is known as the gross primary production (GPP), and a proportion (defined in species-specific parameter, BASEFOLFRESPFRAC) is directly allocated to leaf maintenance respiration, together with a Q10 function. Additional autotrophic respiration for growth and maintenance of wood, and for root and leaf growth are defined by fractions of biomass or C allocation. Heterotrophic soil respiration is calculated from a combination of microbial biomass, soil nutrient mass, temperature and moisture. Summing autotrophic and heterotrophic respiration gives the total ecosystem respiration (TER). The difference between the simulated GPP and simulated TER gives the net ecosystem production (NEP) which is normally positive when GPP exceeds TER.

2.3 Model evaluation

As LandscapeDNDC had not previously been run with a maritime Sitka spruce, some modifications were required to species parameters in PnET and Treedyn. The shape of the Griffin Sitka spruce trees was unusual in having branches almost to the ground and, when measured, the lowest branches had the highest leaf area density (Ibrom et al., 2006). This was attributed to the young stand age at the time, canopy closure being achieved between 1997 and 1999 (Ibrom et al., 2006). Values from Ibrom et al. were used to modify Treedyn submodel parameters, to ensure that leaves throughout the height of the tree were actively contributing to photosynthesis in order to obtain the appropriate annual GPP values for the density of trees planted. Selected PnET parameters were changed incrementally (Table 3) to optimise the fit of annual GPP, TER, NEP and soil CO_2, averaged over 1997-2000. Measured values from Clement (2004) and Clement et al. (2012) for leaf area index (LAI), tree growth, timing of canopy closure and biomass increments were also used to check fit. Once these checks were completed, simulated monthly data for GPP, TER, NEP were compared with equivalent values derived from EC measurements for 1997–2000 using the ModEval statistical package (Smith et al., 1997). An error on EC measurements and subsequent processing of 15 % was assumed for the purpose of statistical analysis (based on Oren et al., 2006). Soil CO_2 and N_2O flux data from chamber measurements made in 2013–2015 were also available, however, detailed meteorological data from that period was not available to generate appropriate contemporaneous simulations. Therefore, climate data have been repeated to continue the simulations forwards to 2014 and hence allow longer term trends in simulated fluxes to be compared in very broad terms with more recent soil measurements.

2.4 Eddy covariance CO_2 flux measurements

In order to evaluate the LandscapeDNDC model the ecosystem CO_2 simulated fluxes were compared with results obtained from EC measurements at this site (Clement et al, 2012). The EC tower was established at Griffin in 1997 and is part of the EUROFLUX network, with the identifier 'Aberfeldy', which uses standard methodology as described by Aubinet et al. (2000). The tower site is in a well defined catchment area of about 150 ha within a much larger spruce plantation, with a minimum fetch of 750 m to the NE and SW and 1000 m in the direction defined by the catchment (SE and NW), which are therefore predominant wind directions (Fig. 1). Approximately 97 % of the trees within the fetch of the EC tower are Sitka

spruce. Clement et al. (2012) explain the methods for data capture (following Moncrieff et al. 1997 and 2000), data processing and data correction. The largest correction component was for frequency response losses and advection-related losses, relating to the complex topography.

The EC technique measures net ecosystem exchange (NEE) which is the net result of photosynthetic CO_2 uptake and CO_2 emissions from TER. A calculation is normally made of daytime TER using a model involving night time NEE (assumed to be only respiration) and temperature in conjunction with daytime temperature and a Q10 function (Lloyd and Taylor, 1994). Clement et al. (2012) experimented with different models to calculate TER and concluded that a model incorporating soil moisture as well as temperature can better explain variation than temperature alone. In this study, NEP is positive when CO_2 uptake exceeds emissions and therefore simulated NEP has the opposite sign to conventional NEE.

2.5 Soil Chamber measurements

The soil gas fluxes simulated by the LandscapeDNDC model were compared with soil CO_2 and N_2O efflux measurements at this site (Sirwan Yamulki, Foreset Research, unpublished data). Soil CO_2 and N_2O fluxes were measured on 16 occasions between September 2013 and April 2015 at 2 sites in the Griffin Forest (Site 1 is the EC tower site and site 2 is known as the Profile Tower site, Fig. 1). CO_2 and N_2O fluxes were measured using a water-sealed closed chamber method, syringe sampling and GC analysis (Yamulki et al., 2013, see detail described in Chapter 2.1.1). Nine chambers were employed at each of the 2 sites and mean fluxes for each site were used for comparison with simulations.

3 Results

3.1 Environmental conditions

Soil moisture and temperature are important factors controlling fluxes (eg Slemr and Seiler, 19991; Li and Aber 2000; Pilegaard et al. 2006). Measured soil temperature from the Griffin site showed close agreement with simulated values for the duration of the study period except that summer simulated peak values were often higher than measurements (Fig. 2a). The resulting residuals were ± 3.5 °C, but mostly less than ± 2 °C and predominantly negative (mean difference over 4 years is -0.7 °C, Fig. 2b). These higher simulated soil temperatures

may give rise to higher simulated gas fluxes, particularly in the summer. However, simulations with reduced initial input temperatures did not consistently reduce simulated soil respiration (data not shown) and therefore it is difficult to quantify the possible effect. Measurements of soil moisture were not available for comparison, but simulations of the period 1997-2000 suggest relatively constant soil moisture content of between 40 and 45 % apart from late summer in 1997 and 1999, when simulated soil moisture was reduced to 32 % (Fig. 2c) due to lower than average rainfall (no rainfall was recorded between 15 July and 5 September 1999). Wetter periods were also frequent in the simulated data but short lived, probably due to the forest being on a slope (6 ^{o}) which allows for run-off of excess water.

3.2 Ecosystem CO_2 fluxes

Averaged annual totals for GPP, TER and NEP estimated from measurements were reproduced by simulations within 0.2, 0.0 and 0.6 %, respectively over the 4-year study period (Table 4), However, there were larger seasonal differences over an averaged year (Fig. 3). Simulated GPP is underestimated in the winter by a small amount, 1-2 g C m^{-2} d^{-1}, although representing 50–60 % of the measurement, and overestimated in summer, by up to 6 g C m^{-2} d^{-1}, representing approximately 20 % of the measurement, whilst simulated TER values were very close to those estimated by EC (±1 g C m^{-2} d^{-1}) over the whole year, (although this represents up to 50 % in the winter and spring, it is less than 10 % of the measurements for most of the summer). Simulated NEP, derived from GPP and TER, shows similar differences to those of simulated GPP. Furthermore, annual data show a steady decline in all simulated values, but particularly GPP and NEP, over the 4 years following the stimulation from fertiliser application in 1997 (Table 4), which is not observed in the EC data. Projecting the simulation to 2014, this decline ceases by about 2001 and remains reasonably stable for the remaining simulated years (Fig. 4)

Statistical analysis of 1997–2000 monthly data using ModEval (Smith et al., 1997) showed no significant errors from root mean squared error (RMSE) data indicating a good match in simulated monthly ecosystem fluxes with measurements. Monthly TER simulations had the lowest RMSE, 14.6 %, the GPP value was 37.4 % and monthly NEP had the highest RMSE, 115.2 % (Table 5), all three were within 95 % confidence limits of natural variation within the measurements (assuming a 15 % error on EC data). The modelling efficiency (ME) values, 0.59 and 0.93 for monthly GPP and TER respectively, were good, but were poor for NEP, -

0.21. A negative ME indicates the data is better explained by the mean of the observed values than by the simulations. Similarly, coefficient of determination (CD) values were positive and therefore good for monthly GPP (2.42) and better for monthly TER (14.29), but poor for monthly NEP (0.83). The poorer statistics for monthly NEP values reflect the decrease in simulated annual values following fertiliser stimulation in 1997, which are a greater proportion of NEP than the much larger GPP values (Fig. 4).

3.3 Soil CO_2 fluxes

Annual soil CO_2 effluxes estimated from measurements in 2014 were 372 g C m^{-2} y^{-1} at site 1 and 419 g C m^{-2} y^{-1} at site 2 (Table 6). In contrast, simulated values ranged from 628 to 732 g C m^{-2} y^{-1}, which is approaching twice the measured values. Monthly soil CO_2 effluxes simulated for the period 1997–2000 showed a regular seasonal pattern, with higher effluxes in the warmer summer months (Fig. 5a), reaching a maximum of 111 g C m^{-2} mth^{-1} in July 1999, when maximum air temperature was higher (22.1 °C) than the 1981–2010 average for July, 19.2 °C. Winter CO_2 fluxes ranged from 28 to 44 g C m^{-2} mth^{-1}. Heterotrophic respiration was simulated to account for about 93 % of the soil respiration annually, and no below ground autotrophic respiration was simulated between October and April each year. CO_2 effluxes from soil chamber measurements made in September and October 2013 were equal to minimum values for those months in the whole extended simulation period (1997-2014), but all other measurements were 20 % or more below the equivalent minimum simulated values (Fig. 5b). No statistical analysis has been performed on these data because of the different years in which they took place.

Simulated annual soil CO_2 fluxes increased during the extended study period, reaching a constant value of approximately 800 g C m^{-2} y^{-1} by 2010, from a starting value of 328 g C m^{-2} y^{-1} in 1989-90 (Fig. 6), following an inverse exponential or logarithmic curve. The addition of fertiliser in 1997 had a minor effect, with a slightly higher increase in soil CO_2 that year than a curve fit would suggest. Simulated soil CO_2 fluxes averaged 15 % of simulated GPP in 1989 – 1992 and 35 % of simulated TER but as the simulated values increased, these proportions increased to 46 % and 54 % respectively, for years 2002–2014.

3.4 Soil N_2O and NO fluxes

Simulated annual N_2O fluxes averaged 28 mg N_2O-N m^{-2} y^{-1} between 1990 and 1997 (initial 1989 value can be ignored because the model needs time to establish a balance), and show an increase after fertiliser application to an average of 42 mg N_2O-N m^{-2} y^{-1} from 1999–2014 (Fig.6). A similar pattern was simulated in the NO fluxes, but there was a sharp decline in the years prior to fertiliser application. NO fluxes were consistently 3–4 times higher than N_2O fluxes (annual average after 1997: 140 mg NO-N m^{-2} y^{-1}). Fluxes of N_2 were also simulated to increase sharply (about two-fold) after fertilisation and remain high, with an average of 204 mg N_2-N m^{-2} y^{-1}, from 1998 to 2014. Chamber measurements of N_2O made in 2013–2015 averaged 15.1 mg N_2O-N m^{-2} y^{-1} which is less than half the simulated values.

4 Discussion

LandscapeDNDC has simulated the ecosystem level CO_2 fluxes reasonably well (monthly TER and GPP have positive ME values and CD values > 1, although NEP values are not so good, with ME= -0.2, CD = 0.8, all show RMSE values lower than 95 % confidence limits) but appears to have overestimated soil CO_2 effluxes. The higher simulated soil temperatures may have contributed to this difference (Section 3.1) but the link between temperature and soil respiration is complex (Davidson et al. 1998) and closely linked to soil moisture, as confirmed in the latest estimation of TER from EC data (Clement et al., 2012). PnET species parameters modified to optimise the fit at ecosystem level included AMAXB, the principal photosynthesis parameter, BASEFOLRESPFRAC, the fraction of photosynthetic C assigned to leaf respiration and ROOTMRESPFRAC, the fraction of root biomass production assigned to root respiration (Table 3). Since soil CO_2 efflux is an integral part of TER, any changes to species parameter values that improve simulation of soil CO_2 effluxes (by reducing soil respiration), would be detrimental to the overall fit of ecosystem level fluxes. Using the parameter values implemented (Table 3), root respiration only contributed 7 % to the annual soil CO_2 efflux. Therefore, to optimise the model fit for soil CO_2, changes to controls on heterotrophic respiration would be necessary. Sensitivity tests were undertaken to establish which input variables and parameters have the most direct effect. Chapter 3 (section 3.2) identified three inputs, soil bulk density, soil organic C and soil field capacity, and the species phenology-related parameter, GDDFOLEND, which had the greatest effect on simulation of soil N_2O and NO fluxes from an oak forest site, although soil inputs had less effect on soil CO_2 fluxes.

Results of these sensitivity tests for Griffin (Table 7) confirmed that N_2O and NO fluxes are most influenced by organic C content, bulk density and field capacity and are less sensitive to organic N in the initial soil setup.

For CO_2, the sensitivity tests suggested that soil effluxes could be better simulated by reducing initial organic C and field capacity and increasing bulk density, therefore reducing the overall CO_2 efflux and improving the simulation fit. However, when these were each changed by 20 % the combined effect was only a 12 % reduction in soil CO_2 effluxes (Table 7). Such changes could be justified on the grounds that the low quality, woody tissue from heather is not available organic C and should therefore be excluded from the initial soil setup, but changes greater than 20 % in the input values would be needed to produce nearly 50 % reduction in soil CO_2 effluxes.

Sensitivity of the model to the parameter GDDFOLEND (related to cumulative temperature when new leaves are fully open each year) was tested independently and showed that a reduction from 1500 to 800 produced a reduction in annual soil CO_2 efflux averaged for 1997–2000 of 31.8 % (Table7). The default value used in this study for Sitka spruce, 1500, was that used by Goodale et al. (1998) following observations of Sitka spruce phenology in Moffat Forest, Scotland by Ford et al. (1987) as no data for Griffin were available. When GDDFOLEND = 1500, budburst at Griffin in 1997–2000 would have been completed each year in the first half of August, compared to a June completion if GDDFOLEND = 800. A study of Sitka spruce phenology in British Columbia suggests there is variation within the species and a strong genetic control over budburst timing (Alfaro et al., 2000) and it may be that the strain planted at Griffin has a different phenology from that studied by Ford et al. (1987). However, without specific information it was not appropriate to change this parameter.

Thus, there are ways to improve the model fit by changing species parameters and certain soil input variables, but it could be that there are conditions at the site which account for the low soil CO_2 effluxes which are not being simulated. For example, it has been suggested that addition of N to forests, whether from fertiliser or atmospheric pollution, can reduce forest soil respiration in some circumstances (Fog, 1988; Treseder, 2008; Janssens et al, 2010). Although the area of Griffin Forest within the footprint of the EC tower has only received one fertiliser application since planting and the N deposition levels are low, it is possible it has had a long-term negative effect on soil respiration due to the low quality of litter. It is also possible that additional N has been received in run-off from fertiliser applied to areas

immediately uphill from the site. Clement (2004) noted that some areas received repeated doses with total applications up to 1400 kg N ha^{-1} between 1990 and 1999, some of which are upslope from the study site.

In 2014, the year with the lowest soil CO_2 flux measurements, rainfall was particularly high in the UK and east Scotland had the second wettest winter and the third wettest year since Met Office records began in 1910. Although mean annual temperature was the highest since 1910, an excess of rain water is likely to have reduced the availability of oxygen within the soil and therefore respiration, resulting in low CO_2 flux measurements from chambers that year, but higher N_2O fluxes might be expected. Soil flux measurements with static chambers and manual gas sampling as used in this study can underestimate soil CO_2 effluxes by as much as 35 % due to a combination of systematic errors in the method and calculations (Pumpanen et al., 2004, Heinemayer et al, 2011), which, together with the wet conditions, could account for the difference (Table 6). However, Medlyn et al. (2005) quoted a soil CO_2 flux of 449 g C m^{-2} y^{-1} from 24 measurements at the Griffin site between Aug 2000 and June 2001 using a portable CO_2 analyser. Errors on this non-steady state through-flow system tested by Pumpanen et al. (2004) varied according to the nature of the collar used but in most cases resulted in overestimations, which were higher in dry conditions. Although there is no information on collar use by Medlyn et al., the clay-rich, often-wet soil, suggests a small overestimation (about 5 %) is possible. Therefore, the two sets of measurements at Griffin are consistent and, after accounting for errors, suggest soil CO_2 fluxes in the range 420–530 g C m^{-2} y^{-1} with no obvious change between the measurement periods. Long term simulations, using repeated climate input data, also suggest very little increase between 2001 and 2014 (Fig 6), although simulated values are close to 800 g C m^{-2} y^{-1} over this period.

The ratio of TER:GPP in this study was 0.68, for both simulated and EC data and was similar to the 0.66 ratio calculated for this site by Medlyn et al. (2005). However, if the model is to match measured soil respiration in 2000–2001 and NEP from EC data (1997-2000) and maintain this ratio of TER:GPP, then GPP needs to be reduced as well. Although this is possible, it does not help understand the reason for the low soil respiration compared to simulated values and therefore requires further investigation. The intense management of the Griffin site, including down-slope ditches which maintain drainage, would suggest that high soil CO_2 fluxes would be expected, as discussed by Janssens et al. (2001), with soil respiration more than the European average of 69 % of TER and 55 % of GPP. Chamber

measurements suggest soil CO_2 fluxes of 25–30 % of TER and 18 – 20 % of GPP, although these proportions are higher (37 % and 25 % respectively) if EC values from Medlyn et al. (2005) are used. The mismatch of soil CO_2 fluxes from chamber measurements made in 2014 with simulated data could be a result of a combination of errors inherent in the method, the unusually wet conditions that year and lack of matching climate data for the simulations.

Simulated annual N_2O fluxes in the range of 0.20 – 0.42 g N ha^{-1} y^{-1} were higher than measured values of 0.13–0.17 g N ha^{-1} y^{-1} but within the range of those recorded elsewhere in European spruce forests (e.g. 0.16 g N ha^{-1} y^{-1}, Ambus and Christensen, 1995; 0.16 g N ha^{-1} y^{-1} Papen and Butterbach-Bahl, 1999; 0.39–2.05 g N ha^{-1} y^{-1}, Pilegaard et al., 2006). Although simulations were made with inaccurate climate data, and there are no measurements from the period 1997-2001 for comparison, the N_2O flux measurements were subject to the same inherent errors as soil CO_2 flux measurements, suggesting an underestimation is likely. There were no measurements of NO fluxes at the site, but the simulated annual values were comparable to those measured elsewhere in Europe. For example, Pilegaard et al. (2006) reported NO fluxes higher in coniferous forests than deciduous forests because of lower spring soil moisture content and a thick, well aerated litter layer which favours nitrification and therefore NO production. From ten years of measurements at the Norway spruce forest of Hoeglwald, in Germany, Luo et al. (2012) showed that annual NO fluxes were up to 4 times more than N_2O fluxes and annual NO fluxes ranged from 0.64–1.14 g N m^{-2} y^{-1} in an area of particularly high N deposition with very acidic soil (2.9–3.2 in the litter layer and 3.6-4.0 in the upper mineral soil layers). Soil pH values below 5.0 can also promote NO production from chemo-denitrification (Yamulki et al., 1997). Similarly, LandscapeDNDC model simulations in this study showed a ratio of NO:N_2O fluxes higher than the oak forest (Chapter 3), where NO fluxes were about 10 % of N_2O fluxes. This is because litter under broadleaved trees decomposes quickly and does not build up into thick dry layers, as found under coniferous forests. Even when partially decomposed, the shape of deciduous leaves helps to maintain moisture in the soil and hence promote denitrification and thus lower NO to N_2O ratio (Pilegaard et al. 2006).

5 Conclusions

LandscapeDNDC with the PnET sub-module reproduced annual ecosystem CO_2 fluxes from EC data averaged over 1997–2000 to less than 1 %. The model showed a decreasing annual

trend in GPP and NEP following a growth boost from fertiliser application in 1997 that was not observed in the measurements. Statistical analysis of comparisons between simulated and measured monthly ecosystem CO_2 fluxes showed errors were not significant, and the RMSE value for TER (14.6 %) was particularly good. Larger RMSE values for GPP (37.4 %) and NEP (115.2 %) reflected the decreasing trends shown in annual figures. Although monthly NEP showed a negative ME (-0.21) and low CD (0.83), monthly TER and GPP showed high positive ME values (0.93 and 0.59, respectively) and CD values greater than one (14.3 and 2.42) giving confidence in the model simulation at the ecosystem level.

Simulated soil CO_2 effluxes were higher than chamber measurements made in 2001 and 2014 by a factor of nearly 2, but wet conditions during 2014 measurement (not represented in climate input data), inherent errors in the chamber measurement method and the lack of specific phenology data for the Sitka spruce variety at Griffin will have contributed to the difference in CO_2 flux values.

Simulated N_2O fluxes could not be directly compared with soil chamber measurements, since there were no measurements made during 1997–2001, but appear to be overestimated, also by a factor of about 2. Simulated NO fluxes were 3–4 times higher than simulated N_2O fluxes. Although there were no measurements of NO fluxes at Griffin for comparison the NO:N_2O ratio simulated was typical for those measured from other coniferous forests with an acid topsoil.

More information about the soil at Griffin, such as pH, field capacity and water table depth, will be required to improve the modelling of this productive forest site. Further soil chamber measurements of CO_2, N_2O and NO soil fluxes would also be beneficial to determine if the soil processes have been appropriately modelled. Matching years of climate and eddy covariance data with soil measurements would allow a better evaluation of the simulated soil fluxes.

Acknowledgements

This study was made possible by a combined College Research and Crossland Scholarship from Royal Holloway. Thank you to Robert Clement, University of Edinburgh, and Sirwan Yamulki, Forest Research for providing data and to Steffen Klatt and David Kraus from the Institute of Meteorology and Climate Research, KIT, for help with LandscapeDNDC and Ralf Kiese for enabling use of the model.

References

Aber, J.D. & Federer, C.A.: A generalized, lumped-parameter model of photosynthesis, evapotranspiration and net primary production in temperate and boreal forest ecosystems, Oecologia, 92, 463-474, 1992.

Aber, J. D., Ollinger, S. V., Fédérer, C. A., Reich, P. B., Goulden, M. L., Kicklighter, D. W., Melillo, J. M. and Lathrop, R.: Predicting the effects of climate change on water yield and forest production in the northeastern United States, Climate Research, 5, 1995.

Alfaro, R. I., Lewis, K. G., King, J. N., El-Kassaby, Y. A., Brown, G. and Smith, L. D.: Budburst phenology of sitka spruce and its relationship to white pine weevil attack, For. Ecol. Manage., 127, 19-29, 2000.

Ambus, P. and Christensen, S.: Spatial and seasonal nitrous oxide and methane fluxes in Danish forest-, grassland-, and agroecosystems, J. Environ. Qual., 24, 993-1001, 1995.

Aubinet, M., Grelle, A., Ibrom, A., Rannik, Ü., Moncrieff, J., Foken, T., Kowalski, A., Martin, P., Berbigier, P. and Bernhofer, C.: Estimates of the annual net carbon and water exchange of forests: The EUROFLUX methodology, Adv. Ecol. Res., 30, 113-175, 2000.

Bossel, H.: TREEDYN3 forest simulation model, Ecol. Model., 90, 187-227, 1996.

Carbonnier, L.: Ireland - Forestry: The potential, in: The right trees in the right places: The proceedings of a conference on forestry and the environment, Mollan, R. and Maloney, M. (Eds.), Royal Dublin Society, Dublin, 48-55, 1991.

Clement, R. J.: Mass and Energy Exchange of a Plantation Forest in Scotland Using Micrometeorological Methods, PhD thesis/masters, University of Edinburgh, http://www.geos.ed.ac.uk/homes/rclement/PHD/, 2004.

Clement, R. J., Jarvis, P. G. and Moncrieff, J. B.: Carbon dioxide exchange of a Sitka spruce plantation in Scotland over five years, Agric. For. Meteorol., 153, 106-123, 2012.

Davidson, E., Belk, E. and Boone, R. D.: Soil water content and temperature as independent or confounded factors controlling soil respiration in a temperate mixed hardwood forest, Global Change Biol., 4, 217-227, 1998.

Fog, K.: The effect of added nitrogen on the rate of decomposition of organic matter, Biol. Revs., 63, 433-462, 1988.

Ford, E., Deans, J. and Milne, R.: Shoot extension in Picea sitchensis I. Seasonal variation within a forest canopy, Annals of Botany, 60, 531-542, 1987.

Goodale, C. L., Abet, J. and Farrell, E. P.: Predicting the relative sensitivity of forest production in Ireland to site quality and climate change, Climate Research, 10, 51-67, 1998.

Haas, E., Klatt, S., Fröhlich, A., Kraft, P., Werner, C., Kiese, R., Grote, R., Breuer, L. and Butterbach-Bahl, K.: LandscapeDNDC: a process model for simulation of biosphere–atmosphere–hydrosphere exchange processes at site and regional scale, Landscape Ecol., 28, 615-636, 2013.

Heinemeyer, A., Di Bene, C., Lloyd, A., Tortorella, D., Baxter, R., Huntley, B., Gelsomino, A. and Ineson, P.: Soil respiration: implications of the plant-soil continuum and respiration chamber collar-insertion depth on measurement and modelling of soil CO2 efflux rates in three ecosystems, Eur. J. Soil Sci., 62, 82-94, 2011.

Ibrom, A., Jarvis, P. G., Clement, R., Morgenstern, K., Oltchev, A., Medlyn, B. E., Wang, Y. P., Wingate, L., Moncrieff, J. B. and Gravenhorst, G.: A comparative analysis of simulated and observed photosynthetic CO_2 uptake in two coniferous forest canopies, Tree Physiol., 26, 845-864, 2006.

Janssens, I., Lankreijer, H., Matteucci, G., Kowalski, A., Buchmann, N., Epron, D., Pilegaard, K., Kutsch, W., Longdoz, B. and Grünwald, T.: Productivity overshadows temperature in determining soil and ecosystem respiration across European forests, Global Change Biol., 7, 269-278, 2001.

Janssens, I., Dieleman, W., Luyssaert, S., Subke, J., Reichstein, M., Ceulemans, R., Ciais, P., Dolman, A. J., Grace, J. and Matteucci, G.: Reduction of forest soil respiration in response to nitrogen deposition, Nature Geoscience, 3, 315-322, 2010.

Kurbatova, J., Li, C., Varlagin, A., Xiao, X. and Vygodskaya, N.: Modeling carbon dynamics in two adjacent spruce forests with different soil conditions in Russia, Biogeosciences, 5, 969-980, 2008.

Li, C., Frolking, S. and Frolking, T. A.: A model of nitrous oxide evolution from soil driven by rainfall events: 1. Model structure and sensitivity, J.Geophys.Res, 97, 9759-9776, 1992.

Li, C. and Aber, J.: A process-oriented model of N_2O and NO, J. Geophys. Res., 105, 4369-4384, 2000.

Lloyd, J. and Taylor, J.: On the temperature dependence of soil respiration, Funct. Ecol., 315-323, 1994.

Luo, G., Brüggemann, N., Wolf, B., Gasche, R., Grote, R. and Butterbach-Bahl, K.: Decadal variability of soil CO_2, NO, N_2O, and CH_4 fluxes at the Höglwald Forest, Germany, Biogeosciences, 9, 1741-1763, 2012.

Medlyn, B. E., Berbigier, P., Clement, R., Grelle, A., Loustau, D., Linder, S., Wingate, L., Jarvis, P. G., Sigurdsson, B. D. and McMurtrie, R. E.: Carbon balance of coniferous forests growing in contrasting climates: Model-based analysis, Agric. For. Meteorol., 131, 97-124, 2005.

Moncrieff, J. B., Jarvis, P. G. and Valentini, R.: Canopy Fluxes, in: Methods in Ecosystem Science, Odum, E. P., Sala, O. E., Jackson, R. B., Mooney, H. A. and Howarth, R. (Eds.), Springer Science & Business Media, New York, 161-180, 2013.

Moncrieff, J. B., Massheder, J., De Bruin, H., Elbers, J., Friborg, T., Heusinkveld, B., Kabat, P., Scott, S., Søgaard, H. and Verhoef, A.: A system to measure surface fluxes of momentum, sensible heat, water vapour and carbon dioxide, J. Hydrol., 188, 589-611, 1997.

Moore, J.: Wood properties and uses of Sitka spruce in Britain, Forestry Commission, Edinburgh, 2011.

Morison, J., Matthews, R., Miller, G., Perks, M., Randle, T., Vanguelova, E., White, M. and Yamulki, S.: Understanding the carbon and greenhouse gas balance of forests in Britain, Forestry Commission Research Report, 18, 149, 2012.

National Forestry Inventory Report: Standing timber volume for coniferous trees in Britain. Forestry Commission, Edinburgh, 2013.

Oren, R., HSIEH, C., Stoy, P., Albertson, J., Mccarthy, H. R., Harrell, P. and Katul, G. G.: Estimating the uncertainty in annual net ecosystem carbon exchange: Spatial variation in turbulent fluxes and sampling errors in eddy-covariance measurements, Global Change Biol., 12, 883-896, 2006.

Papen, H. and Butterbach-Bahl, K.: A 3-year continuous record of nitrogen trace gas fluxes from untreated and limed soil of a N-saturated spruce and beech forest ecosystem in Germany. 1- N2O emissions, Journal of Geophysical Research, 104, 18487-18503, 1999.

Pilegaard, K., Skiba, U., Ambus, P., Beier, C., Brüggemann, N., Butterbach-Bahl, K., Dick, J., Dorsey, J., Duyzer, J. and Gallagher, M.: Factors controlling regional differences in forest soil emission of nitrogen oxides (NO and N_2O), Biogeosciences, 3, 651-661, 2006.

Pumpanen, J., Kolari, P., Ilvesniemi, H., Minkkinen, K., Vesala, T., Niinistö, S., Lohila, A., Larmola, T., Morero, M. and Pihlatie, M.: Comparison of different chamber techniques for measuring soil CO_2 efflux, Agric. For. Meteorol., 123, 159-176, 2004.

Read, D. J., Freer-Smith, P., Morison, J., Hanley, N., West, C. and Snowdon, P.: Combating climate change: A role for UK forests. An assessment of the potential of the UK's trees and woodlands to mitigate and adapt to climate change. The Stationery Office Limited, 2009.

Slemr, F. and Seiler, W.: Field study of environmental variables controlling the NO emissions from soil and the NO compensation point, J. Geophys. Res.: Atmospheres, 96, 13017-13031, 1991.

Smith, P., Smith, J., Powlson, D., McGill, W., Arah, J., Chertov, O., Coleman, K., Franko, U., Frolking, S. and Jenkinson, D.: A comparison of the performance of nine soil organic matter models using datasets from seven long-term experiments, Geoderma, 81, 153-225, 1997.

Treseder, K. K.: Nitrogen additions and microbial biomass: A meta-analysis of ecosystem studies, Ecol. Lett., 11, 1111-1120, 2008.

Vanguelova, E., Nisbet, T., Moffat, A., Broadmeadow, S., Sanders, T. and Morison, J.: A new evaluation of carbon stocks in British forest soils, Soil Use Manage., 29, 169-181, 2013.

Valentini, R., Matteucci, G., Dolman, A., Schulze, E., Rebmann, C., Moors, E., Granier, A., Gross, P., Jensen, N. and Pilegaard, K.: Respiration as the main determinant of carbon balance in European forests, Nature, 404, 861-865, 2000.

Yamulki, S., Anderson, R., Peace, A. and Morison, J.: Soil CO_2 CH_4 and N_2O fluxes from an afforested lowland raised peatbog in Scotland: Implications for drainage and restoration, Biogeosciences, 10, 1051-1065, 2013.

Yamulki, S., Harrison, R. M., Goulding, K. and Webster, C.: N2O, NO and NO2 fluxes from a grassland: Effect of soil pH, Soil Biol. Biochem., 29, 1199-1208, 1997.

Table 1: Griffin site details used as model input. (Data from Clement et al., 2012).

Property	Value
Latitude	56° 36.4'N
Longitude	3° 47.8'W
Average annual rainfall (1997-2001)	1126 mm
Average annual temperature (1997-2001)	6.6 °C
Slope	6°
Altitude	340 m AMSL
Main Species (planted 1981)	Picea sitchensis
No. of trees per hectare in 1997	2215
Max height in 1997	6.7 m
Diameter at breast height (DBH), 1995	0.09 m
Modelling start date	1/1/1989
Fertiliser event (urea, 43 %N, 35g m^{-2}))	1/9/1997
Annual N deposition as NH_4	0.4 g m^{-3}
Annual N deposition as NO_3	0.6g m^{-3}
Total annual N deposition	1.0 g m^{-3}
Soil type	Stagno-humic gley

Table 2: LandscapeDNDC soil input data for Griffin Forest. pH values use standard pH scale. (Clement, 2004 and pers. comm.)

Horizon	depth	Organic C	Organic N	pH[1]	Bulk density	Field capacity[2]	Wilting point	Clay fraction
	mm	(proportion)			g cm^{-3}	mm m^{-3}	mm m^{-3}	
LF	0-4	0.3394	0.0110	3.8	0.12	403.8	280	0.02
O_1	4-6	0.0461	0.0024	5	1.30	388.1	280	0.49
O_1	6-8	0.0340	0.0021	5	1.21	388.1	280	0.49
O_1	8-10	0.0411	0.0026	5	1.09	388.1	280	0.5
O_1	10-12	0.0458	0.0032	5	0.99	388.1	280	0.5
O_1	12-14	0.0493	0.0034	5	0.91	388.1	280	0.5
O_1	14-16	0.0533	0.0037	5	0.81	305.0	280	0.5
O_1	16-18	0.0609	0.0039	5	0.82	305.0	280	0.5
O_1	18-20	0.0393	0.0028	5	0.88	305.0	280	0.5
O_2	20-24	0.03	0.0020	5	1.0	305.0	280	0.4
Bg_1	24-34	0.005	0.0003	5	1.3	305.0	280	0.25
Bg_2	34-48	0.005	0.0003	5	1.5	305.0	280	0.2

1 = All pH values generated by LandscapeDNDC.

2 = Field capacity values modified by LandscapeDNDC (initial input = 440 mm m^{-3})

Table 3: Modified PnET and Treedyn species parameters for Griffin Sitka spruce forest.

Parameter	Description	Units	Griffin value	previous value
PnET CO_2 exchange parameters				
AMAXB	Maximal net photosynthetic rate	$nmolCO_2\ g^{-1}\ s^{-1}\ leaf\_N^{-1}$	49	21.5
BASEFOLRESPFRAC	dark respiration as fraction of Amax	0-1	0.054	0.1
ROOTMRESPFRAC	ratio of fine root maintenance respiration to biomass production	0-1	0.01	1.0
QWODFOLMIN	minimum ratio of carbon allocation to wood and foliage	0-1	0.011	1.25
Treedyn parameters				
CDR_P1	} Crown to stem diameter ratio at three points		-1.4	-2.0
CDR_P2	}		1.0	1.0
CDR_P3	}		0.0	0.0
HDMAX	Ratio of height to diameter at breast height for mature trees in dense stands		66.0	70
UGWDF	Underground wood fraction (= coarse root biomass in relation to total wood biomass)	$kgDW\ kgDW^{-1}$	0.65	0.23

Key unmodified PnET parameter values:

RESPQ10 =2.0, AMAXA = 5.3, SLAMIN = 3.6

Table 4: Annual CO_2 flux data for Griffin Forest: eddy covariance data from Clement et al. (2012) is compared with simulated data. Difference was calculated on the 4 year averages

Year	GPP		TER		NEP	
	g C m^{-2} y^{-1}		g C m^{-2} y^{-1}		g C m^{-2} y^{-1}	
	EC	simulated	EC	simulated	EC	simulated
1997	2236	2634	1546	1606	693	1028
1998	2168	2443	1530	1608	641	834
1999	2389	2016	1587	1514	802	502
2000	2258	1943	1514	1446	745	498
Average	2263	2259	1544	1544	720	716
SD	92	330	31	80	69	26
Difference		0.2 %		0 %		0.6 %

Valentini et al. (2000) and Janssens et al. (2001)

1997 TER: 1320, NEE: 670

1998 TER: 1350, NEE: 570

Medlyn et al. (2005)

1998 TER: 1213, NEE: 618

Table 5: Results from statistical analysis with ModEval (Smith et al., 1997), comparing simulated and measured monthly ecosystem CO_2 fluxes at Griffin Forest. N = 48.
Average total error = RMSE (%) * measured mean /100.

Statistic	Monthly GPP	Monthly TER	Monthly NEP
RMSE (%)	37.4^{+}	14.6^{+}	115.2^{+}
Average total error	71.42	19.2	69.08
Modelling Efficiency (ME)	0.59	0.93	-0.21
Coefficient of determination (CD)	2.42	14.29	0.83
Relative error (E)	1.39*	1.76*	0.57*
Mean difference (M)	2.64	2.30	0.34
Students t of M (t)	0.25*	0.83*	0.03*
Correlation coefficient (r)	0.93	0.97	0.77
F	318.6**	643.3**	69.07**

+No significant total error, *No significant bias (at 95 % confidence), **Significant association at P=0.05

Table 6: Annual soil gas flux data at Griffin Forest simulated for 1997-2000 and measured at 2 sites in 2014 (unpublished data). Average and SD calculated from 1997-2000.

Year	Soil CO_2		N_2O		NO
	g C m^{-2} y^{-1}		mg N m^{-2} y^{-1}		mg N m^{-2} y^{-1}
	Simulated	Measured	Simulated	Measured	Simulated
1997	628	na	20.5	na	91.5
1998	696	na	30.9	na	130.7
1999	724	na	40.9	na	153.7
2000	732	449*	41.6	na	144.0
Average	695		33.5		130.0
SD	50		9.9		27.3
2014 site 1		372		13.0	
2014 site 2		419		17.2	

'*' Data from Medlyn et al. (2005), measured with portable CO_2 analyser equipped with a soil chamber; from 24 measurements between Aug 2000 and June 2001.

Table 7: Results from sensitivity analysis on Griffin Forest data. The amount changed for each input value and the parameter GDDFOLEND is shown on the left. The results are percentage change from simulated annual average results for 1997-2000 (given in Tables 4 and 6).

Change	GPP	TER	NEP	Soil CO_2	N_2O	NO
1) Bulk density – 10 %	-0.62	-0.65	-0.70	+0.29	-12.84	-8.08
2) Bulk density – 20 %	-1.20	-1.30	-1.12	+0.14	-19.70	-16.85
3) Bulk density + 20 %	-0.18	-2.33	+4.47	-4.75	+53.13	+23.77
4) Organic C – 10 %	-1.73	-2.72	+0.28	-2.30	-9.25	-14.62
5) Organic C – 20 %	-2.43	-4.40	+1.54	-4.32	-17.31	-28.92
6) Organic C + 20 %	+3.98	+3.17	+5.45	+2.88	+29.55	+33.46
7) Organic N – 10 %	+0.75	+0.97	+0.14	+1.15	+5.07	+7.38
8) Organic N – 20 %	+1.73	+2.46	0.00	+2.59	+13.73	+18.15
9) Organic N + 20 %	-1.06	-1.68	+0.14	-1.58	-7.76	-10.31
10) Field capacity -10 %	-3.05	-4.66	+0.28	-5.90	+3.08	-13.43
11) Combined 3,5 & 10	-6.64	-9.26	-1.12	-12.23	-9.69	+4.18
12) GDDFOLEND = 1000	-2.35	-6.41	+6.28	-14.96	-17.01	-7.54
13) GDDFOLEND = 800	+0.89	-14.77	+34.50	-31.80	-20.3	-0.38

Figure 1: Map of Griffin Forest location in Perthshire, Scotland (black square) and satellite image of the forest with Site 1, EC tower location (1) and Site 2, profile tower location (2) indicated. Streams flow in a NW direction parallel to the principal roads visible.

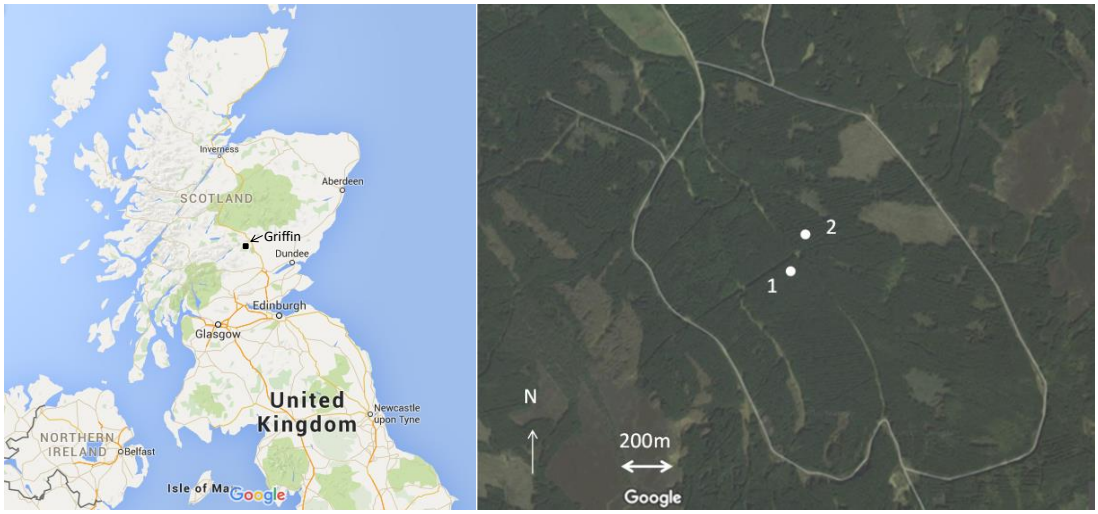

Figure 2: Environmental conditions at Griffin Forest, Perthshire: a) measured and simulated soil temperature; b) residuals (measured – simulated temperature), dashed line shows 4-year average; c) simulated soil water content at 10cm.

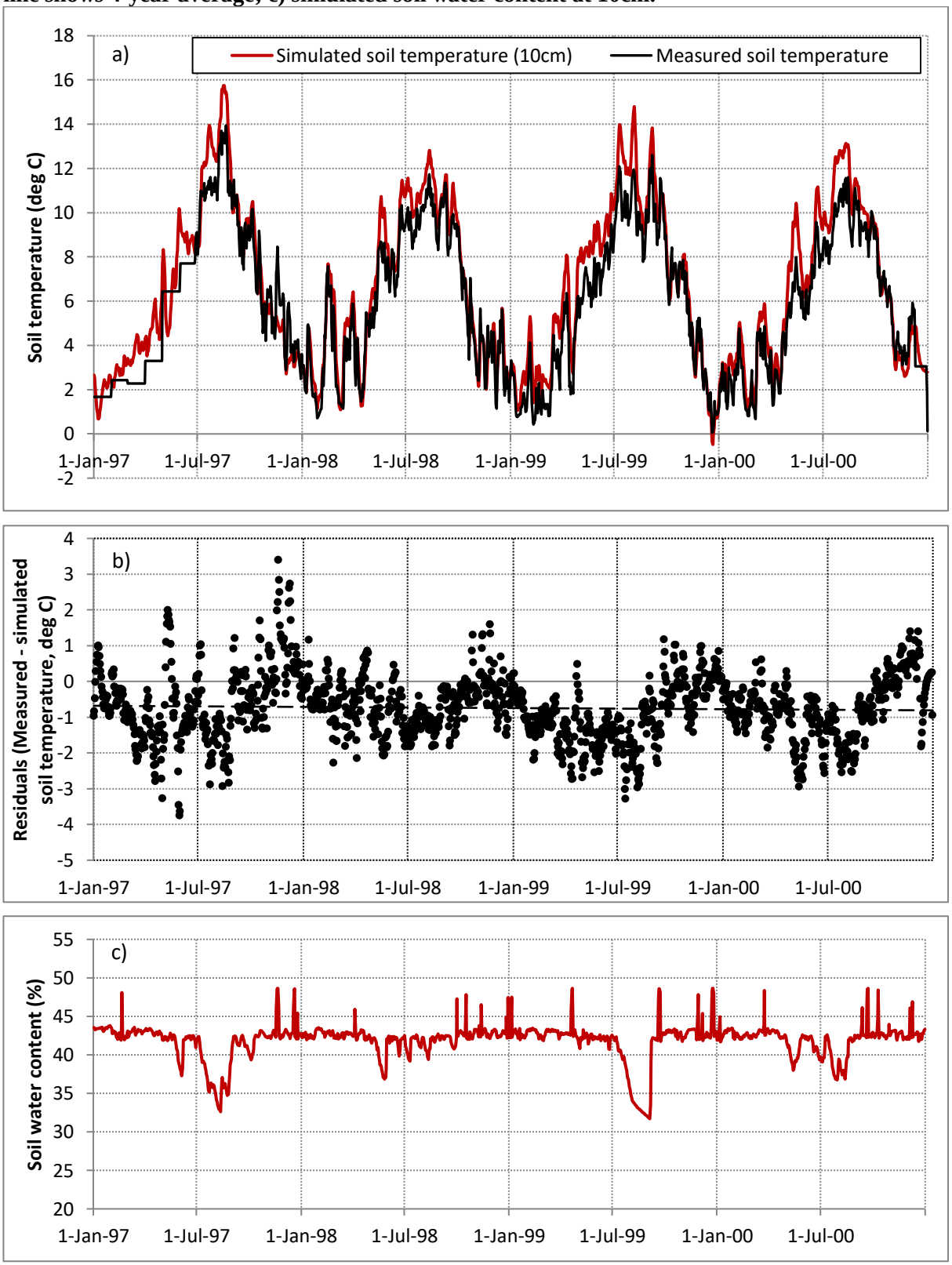

Figure 3: Daily ecosystem CO_2 flux data from EC at Griffin Forest compared with simulations averaged over 1997-2000: a) GPP; b) TER; c) NEP.

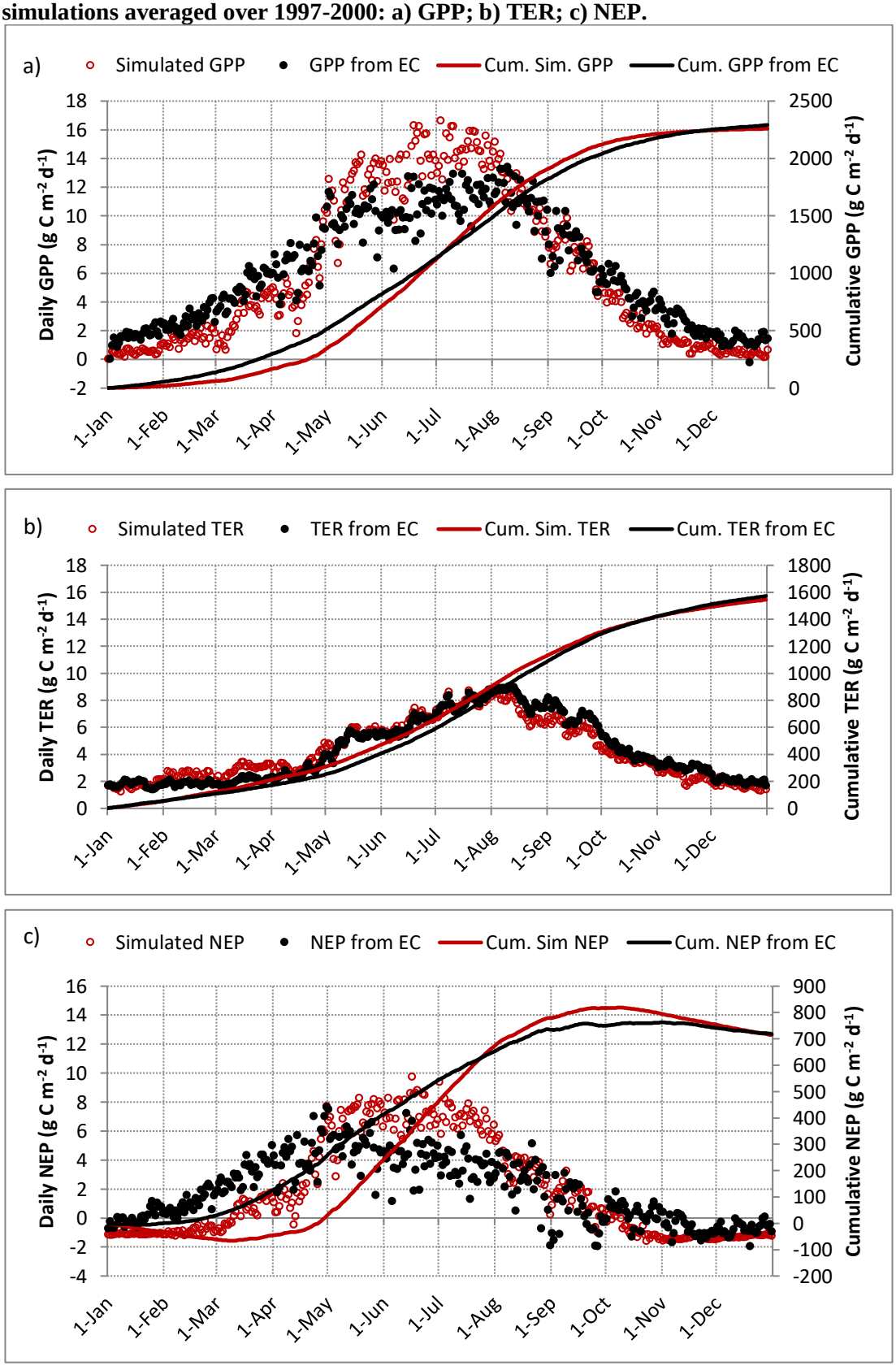

Figure 4: Simulated annual GPP, TER and NEP for Griffin Forest 1989–2014. Arrow indicates fertiliser application in 1997.

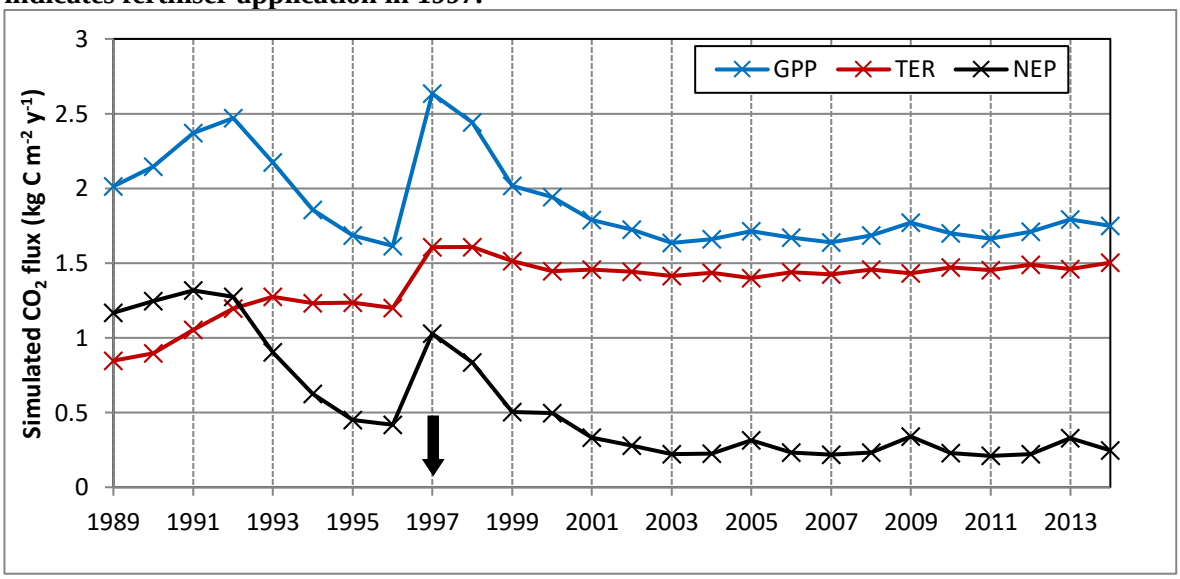

Figure 5: Monthly soil CO_2 fluxes at Griffin Forest; a) simulated from 1997-2000 (stacked graph), b) soil chamber measurements averaged from 2 sites, Sept 2013 – April 2015, shown with monthly soil CO_2 flux data averaged over 1997 – 2014, together with minimum and maximum monthly values over this period and 20 % error bounds for the simulations. Chamber error bars show 1 standard deviation

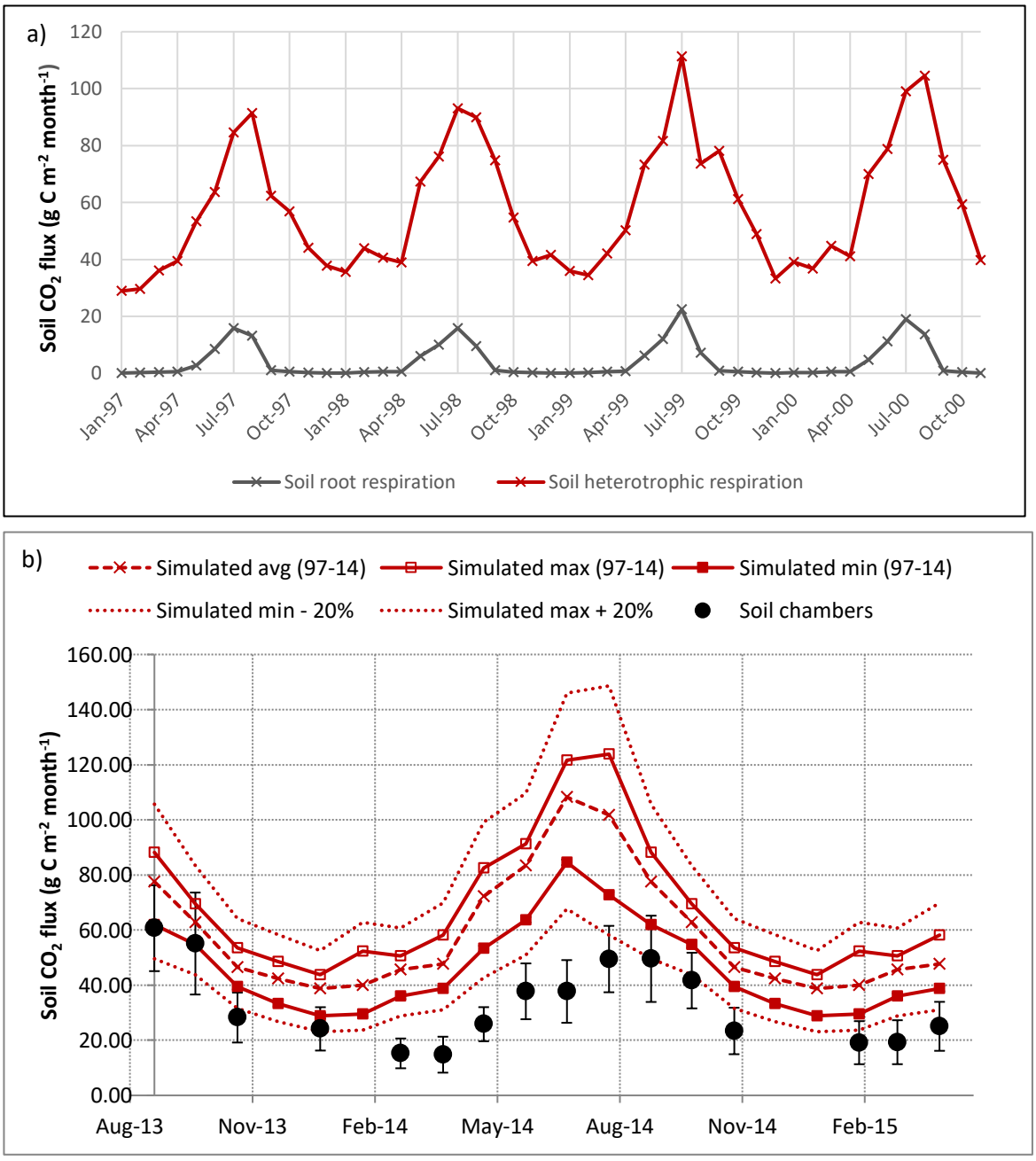

Figure 6: Simulated annual soil CO_2, NO, N_2O and N_2 fluxes for Griffin Forest from 1989 – 2014. Arrow indicates fertiliser application in 1997.

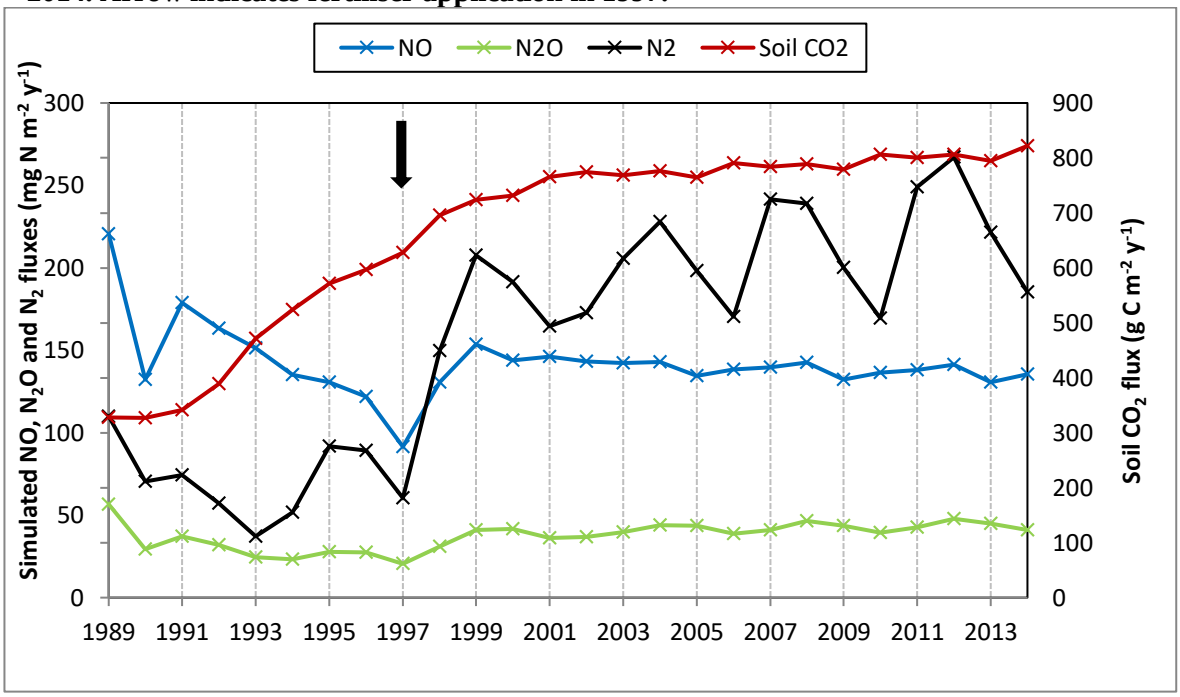

Chapter 5

Soil gas fluxes following addition of N fertilizer to a forest under an oak plantation in south east England

Shirley M. Cade[1], Kevin C. Clemitshaw[1], Jacqui Brunt[2] and Sirwan Yamulki[2]

Paper in preparation for submission to Biogeosciences

(Number of manuscript pages: 19)

My Contribution to this work:

- Carried out soil flux measurements of CO_2, CH_4, N_2O and NO and soil analyses
- Analysed soil flux and soil analysis data
- Collated and formatted meteorological, eddy covariance flux and all other input data for LandscapeDNDC model simulations
- Carried out all modelling work with LandscapeDNDC
- Performed all statistical analyses using ModEval
- Wrote first draft of manuscript
- Produced all figures

Soil gas fluxes following addition of N fertiliser to a forest soil under an oak plantation in south east England

Shirley M. Cade[1], Kevin C. Clemitshaw[1], Jacqui Brunt[2] and Sirwan Yamulki[2]

[1]{Department of Earth Sciences, Royal Holloway, University of London, Egham, TW20 0EX, UK}
[2]{Forest Research, Alice Holt Lodge, Farnham, GU10 4LH, UK}

Correspondence to: S. M. Cade (Shirley.Cade.2008@live.rhul.ac.uk)

Abstract

The addition of N fertiliser can detrimentally affect greenhouse gas fluxes from a forest soil as well as potentially increasing forest productivity. In this study three levels of ammonium nitrate fertiliser were each applied to three plots within the Straits Inclosure oak plantation in SE England. Fluxes of N_2O, NO, CO_2 and CH_4 were measured using soil chambers on 12 occasions during the following 50 days. Three measurements from each of the 9 plots made before the fertiliser treatment were treated as control data. Fertiliser doses (FD) used were equivalent to 16 kg N ha^{-1} (FD1), 150 kg N ha^{-1} (FD2) and 400 kg N ha^{-1} (FD3). LandscapeDNDC with the PSIM tree growth submodule was used to simulate the fluxes following fertiliser application and results were compared with measurements. Measured CO_2 fluxes showed an average increase after fertiliser application (5 - 42 %) but the size of the increase related to the size of the flux before treatment, rather than the concentration of fertiliser applied. LandscapeDNDC simulated very little change in CO_2 fluxes after treatment (-7 to 8 %). All measured CH_4 fluxes were negative and could not be simulated in LandscapeDNDC. Measurements showed that there was a reduced uptake following treatment and the highest dose (FD3) showed the greatest reduction in CH_4 uptake (24 % on average compared to 12 % for FD1 and 15 % for FD3). N_2O and NO fluxes were both simulated to increase in proportion to the fertiliser dose, with simulated N_2O fluxes on average 1.5, 4.7 and 11.4 times the before-treatment simulations, following application of FD1, FD2 and FD3, respectively. Equivalent numbers for simulated NO fluxes are 1.3, 5.7 and 9.2. Measurements for these fluxes did not follow the same relationship. NO fluxes decreased by approximately 80 % following FD1, and increased following FD2 (67 %) and FD3 (3.9 times). N_2O fluxes from FD1 plots were the same as before treatment and the highest fluxes (2.4 times the pre-treatment flux) were measured from plots with a medium dose (FD2) which had the highest fluxes prior to treatment, suggesting antecedent soil conditions rather than fertiliser dose controlled the N_2O flux size at this site.

1 Introduction

Managed forests are often subjected to N fertiliser as part of the management process to encourage growth (Albaugh et al., 2007; Shrestha et al., 2015). Relatively few studies have addressed the specific effect of N fertiliser on greenhouse gas fluxes from forest soils and there is a requirement for more long term and larger scale studies on this subject (Shrestha et al., 2015). Agricultural fertiliser use together with an increase in demand for fossil fuel burning and increased legume cultivation has resulted in N deposition which has continued to increase globally over the last three decades (IPCC 2013) and several studies predict a continued increase, principally as a result of increasing demand for N fertilisers over the coming century (FAO, 2000; Tilman et al., 2001; Tubiello & Fischer, 2007; Erisman et al., 2008). In N-limited natural ecosystems, the deposition of additional N causes increased growth (de Vries et al., 2009; Tipping et al., 2012), loss of biodiversity (Sala et al., 2000) and an imbalance of N which can affect the soil microbial population and hence soil gas fluxes. In forest soils, N deposition is known to increase NO and N_2O emissions (e.g. Butterbach-Bahl et al., 1997; Kesik et al., 2006) and in some circumstances, may inhibit CH_4 oxidation (Reay and Nedwell, 2004; Smith et al., 2000; Gunderson et al., 2012) and reduce soil CO_2 respiration as a result of a reduction in soil biomass (Fog, 1988; Treseder etal., 2008; Janssens et al., 2010). Process-based models can offer a means of investigation on a larger scale and a longer term than chamber flux measurements allow. Therefore, the aim of this study was i) to assess the short-term effect on soil gas fluxes of different levels of N addition to an oak forest soil in SE England and ii) to evaluate the biogeochemical model LandscapeDNDC (discussed in detail in Chapter 3) for GHG and NO simulation after N addition. At a later stage, it is intended to apply the model to simulate the longer-term effect of N addition on the GHG balance at this forest.

2 Methods

2.1 Site location

The experiment site is within the Straits Inclosure, an oak plantation at the SW corner of Alice Holt Forest in Hampshire, south east England, described in more detail in Chapter 3 and in Wilkinson et al. (2012). The site is referred to as the Deer Seat Site (DS, Fig. 1) located some 100m WNW of a long-term monitoring eddy covariance flux tower referred to as the Tower Site (T, Fig. 1) where soil flux measurements were also made monthly over 5 years (Yamulki et al. in prep; Chapter 3). The DS Site was open to public access and located between the main central ride and a smaller footpath. No interference was detected at any of the soil chamber frames between measurements. The soil is a surface water stagno-gley overlying Gault Clay.

Climate data were recorded continuously at the eddy covariance tower and logged every half hour. Soil temperature and soil moisture were also recorded manually at the DS Site on each sampling day from the soil surface and 10 cm depth (see Chapter 3 for more details on the Straits Inclosure). At this oak site, the N deposition is low (ca. 11 kg N ha^{-1} yr^{-1}).

2.2 Soil flux measurements

Soil fluxes of CO_2, CH_4 and N_2O were measured from 9 PVC soil chambers using the manual closed chamber method and design described in Chapter 2 (after Yamulki et al., 2013). The chambers had a foam rubber seal to enable a gas-tight fit with frames that were inserted 5 cm into the soil. In order to measure fluxes, gas samples within the headspace of the chambers were collected at time 0, 20, 40 and 60 min after chamber closure. In this experiment, ambient air gas concentrations of 6 replicated samples were taken from outside the chambers as a surrogate for T0 (sampling inside the chamber immediately after closure) to enable measurement from all chamber replications in a shorter time period. This should not result in any consistent bias in the calculated fluxes (Chadwick et al., 2014). Fluxes were calculated from the linear concentration increase with time after chamber closure. Soil NO emissions were measured using the manual open chamber method (steady state flow-through principle described by Pilegaard et al., 1999) and design described in Chapter 2. The NO chamber design was such that it fits on the same soil frames used for the GHG fluxes and therefore NO fluxes were measured from the same treatment plots and replications as those used for N_2O, CH_4 and CO_2 fluxes. Flux measurements at this site started on 29 September 2014 and continued until 25 November 2014. Three days of sampling (30 Sept, 3 Oct and 6 Oct) took place before fertiliser was applied on 6 October to measure the background fluxes. After fertiliser application (day 0) fluxes were measured on 6 occasions in the following 2 weeks, 2 occasions in week 3, once in each of weeks 4 to 6; the final measurement was on day 49, 8 weeks after fertiliser application, giving a total of 12 days of sampling after treatment.

The chamber frames were placed in the ground one week prior to the start of the experiment to reduce the effect of disturbance. All chamber frames were located within 20m of a cabin in which the NO_x analyser and ancillary equipment were placed.

2.3 Fertiliser application

Soil chamber frames were placed in a semi-randomised experimental design providing 9 plots (labelled 1-9) for three replicates of three NH_4NO_3 fertiliser doses exhibiting an exponential increase in N concentration (see Table 1). Fertiliser dose 1 (FD1) represents the maximum expected N deposition at this site (16 Kg N ha^{-1} yr^{-1}) and was applied to plots 1, 2 and 5; fertiliser

dose 2 (FD2) is a recommended forest fertiliser dose for upland Britain (150 kg N ha^{-1} yr^{-1}) (McIntosh (1983) and was applied to plots 2, 4 and 7; and an extreme fertiliser dose (FD3), greater than expected in normal forestry practice (400 kg N ha^{-1} yr^{-1}), was applied to plots 6, 8 and 9. There were no additional replicated control treatments without fertiliser application in order to reduce the number of flux chambers to sample in one day. However, soil flux measurements were made on 3 occasions prior to the fertiliser application to measure the pre-treatment fluxes.

The fertiliser used was ammonium nitrate with a total N content of 34.5 % containing equal amounts of ammonium and nitrate concentrations. The three fertiliser doses, FD1, FD2 and FD3 (Table 1), were prepared to cover an area equivalent to the area enclosed by a soil chamber (0.134 m^2). Dry fertiliser granules were weighed into 9 separate sealed containers in advance of application. Before the application on 6 October 2014 the dry granules were mixed with 1 litre of de-ionised water and sprayed from a watering can, with an extension designed for fertiliser application, on to each of the 9 plots. The dimensions of this extension matched the size of the soil frames (Fig. 2) to ensure even spread of the fertiliser within each soil frame. Three frames were selected at random to receive each of the three doses of fertiliser. The lowest concentration was mixed and applied first and the highest concentration last in order to prevent contamination between doses.

2.4 Modelling

The biogeochemical model LandscapeDNDC (Haas et al, 2013), together with the PSIM tree growth sub-module, with parameters selected for the Straits Inclosure from previous work (described in Chapter 3), was used to simulate soil gas fluxes. The application of NH_4NO_3 fertiliser at three different doses was modelled as an event with the appropriate date, 6 October 2014, in three separate model runs. The results analysed covered the time period from 10 days before fertiliser application to 50 days after application. The model is known to overestimate NO soil fluxes and not represent the full range of peak N_2O soil fluxes when run with Straits data (Chapter 3) and there are limited data points for comparing measured data with simulated values. Therefore, the data has been normalised, using an average daily value for all measurements before day 0 (n = 27) and for simulated fluxes from the same time period (n = 10). An average daily value (measured fluxes: n = 36 simulated fluxes: n=50) from all fluxes after day 0 for each of the fertiliser doses was then compared as a ratio of the before day 0 value. No comparative statistics are attempted for this preliminary study. This model does not simulate CH_4 fluxes and therefore it was only CO_2, N_2O and NO fluxes that were compared with simulations.

3 Results

The fertiliser application coincided with a change in weather conditions (Fig. 3). On 6 October, the ambient temperature dropped 5°C and several days of heavy rainfall started, following a warm dry period lasting throughout September to 5 October. On the final day of sampling (25 Nov) a temperature inversion caused a high concentration of ambient NO_x and therefore no meaningful NO fluxes could be recorded on that day. Mean fluxes measured over three sampling days before application of fertiliser were 2080 ± 309 mg CO_2-C m^{-2} d^{-1} for CO_2, 1.78 ± 0.32 mg CH_4-C m^{-2} d^{-1} for CH_4, 144.4 ± 55.4 µg N_2O-N m^{-2} d^{-1} for N_2O and 8.41 ± 7.40 µg NO-N m^{-2} d^{-1} for NO (Table 2). A comparison of these fluxes with measurements made from the nearby Tower Site during the previous year (late September- early October, see Chapter 3) indicated similar soil gas fluxes at the 2 sites (Table 2). This confirms that the LandscapeDNDC model parameterised to simulate conditions at the Tower Site is likely to be suitable to simulate conditions at the DS Site. The coefficient of variation (CV) was low (< 15 %) for both CO_2 and CH_4 fluxes at both sites, whereas for N_2O fluxes CV was higher (35 % at the Tower Site and 38 % at the DS Site). The highest CV observed was for NO fluxes at both sites with 88 % and 62 % respectively), indicating the greater spatial and temporal variation of N_2O and NO compared with CO_2 and CH_4. There was some consistency in the relative size of soil gas fluxes between plots at the DS Site. For example, the highest values for N_2O, CO_2 and NO emissions and greatest CH_4 uptake were measured from plot 2 on at least 2 of the 3 initial sampling days and it had the highest average values over the 3 days for all fluxes measured before fertiliser application. In contrast, measurements from plot 1 and plot 6 consistently showed the lowest fluxes. This may suggest uneven distribution of microbial activities within the soil, reflecting local environmental conditions and nutrient availability.

Figure 4 illustrates soil N_2O, NO, CO_2 and CH_4 fluxes from the three fertiliser doses, each of which is an average from three sample plots. After fertiliser application, FD1 showed no significant change in N_2O or NO fluxes compared to before day 0 and mean fluxes were 144.1 ± 46.8 µg N_2O-N m^{-2} d^{-1}, mean ± SD, (before treatment 124.7 ± 78.1) for N_2O and 0.99 ± 1.47 µg NO-N m^{-2} d^{-1} (before treatment 4.7 ± 6.3) for NO, variations showed no correlation with higher N fertiliser doses, suggesting that this level of additional N was not sufficient to alter existing processes. Plots receiving FD2 and FD3 all showed an increase in both N_2O and NO fluxes after treatment. The main peak in N_2O flux was observed on day 17 and for NO fluxes there were 2 peaks on days 2 and 21. NO fluxes, from the plots receiving the higher dose produced the highest average NO fluxes (67.7 and 75.4 µg NO-N m^{-2} d^{-1}, on days 2 and 21 respectively) as expected and plots

receiving a medium dose (FD2) had applicably lower peak average NO flux values (20.9 and 23.4 μg NO-N m^{-2} d^{-1}). However, the highest N_2O fluxes were recorded from plots which received the medium dose of fertiliser (FD2) with an average over the three replicates measured on day 17 of 877.1 μg N_2O-N m^{-2} d^{-1}, which includes the highest flux recorded during the study (1664.6 μg N_2O-N m^{-2} d^{-1}) from plot 2. The average peak N_2O flux measured from FD3 plots on day 17 was 594.4 μg N_2O-N m^{-2} d^{-1}.

Soil CO_2 effluxes from all the plots follow a similar pattern with peaks on days 4, 11 and 24, and fluxes increased during the measurement period from all doses to a maximum of 3,843 mg C m^{-2} d^{-1} measured from FD2 (Fig. 4c). The magnitude of mean fluxes after day 0 appears to correlate with the magnitude of the flux before fertiliser application rather than the dose of fertiliser received. Maximum CO_2 fluxes did not coincide with maximum N_2O or NO fluxes. There was a weak correlation (R^2 = 0.26) between surface temperature and the soil CO_2 effluxes after day 0 (data not shown).

All plots showed a consistent uptake of CH_4 throughout the study period, ranging from -1.24 to -2.21 mg CH_4-C m^{-2} d^{-1}, on the first sampling day and maintained a very similar range on most subsequent sampling days (Fig. 4d). Reduced uptakes were recorded on days 2, 9 and 36 in some plots, with the greatest change shown in plots with FD3 (peak on day 9 was -0.23 mg CH_4-C m^{-2} d^{-1} in plot 9). This suggests the additional N may have had an inhibitory effect on CH_4 oxidation (Reay and Nedwell, 2004; Gunderson et al., 2012).

Fluxes simulated by LandscapeDNDC before fertiliser application were similar to measurements. Average daily flux values were simulated to be 99.9 ± 8.1 μg N_2O-N m^{-2} d^{-1} for N_2O, 14.5 ± 0.6 μg NO-N m^{-2} d^{-1} for NO and 3039.5 ± 122.9 mg CO_2-C m^{-2} d^{-1} for CO_2. Results from simulations are illustrated in Fig. 5 showing changes in daily average N_2O, NO and CO_2 fluxes after day 0 with the three different fertiliser doses compared to normalised daily average fluxes before day 0. For both N_2O and NO fluxes the model simulated an increase in average flux magnitude from all plots compared to the normalised pre-day 0 value and the increase was proportional to the fertiliser dose (Fig. 5a and 5b), demonstrating an exponential increase with increasing dose (R^2 = 0.97 for N_2O; R^2 = 0.93 for NO). In contrast, the measurements did not show a consistent increase in flux magnitude with increasing fertiliser dose and did not match the increases simulated. On 6 of the 12 measurement days after day 0, NO fluxes from FD1 plots were recorded as zero, resulting in an average daily flux much less than before day 0. Measured N_2O fluxes from FD1 plots were the same as the average of all plots before treatment (within 0.2 %). Measurements showed higher average N_2O fluxes from FD2 than FD3 plots but the simulations showed higher N_2O fluxes from the higher dose, FD3 plots. For CO_2, the simulated average fluxes reduced after day 0, with the greatest reduction from FD1 but fluxes were similar for FD2 and

FD3 (Fig. 5d). Measurements showed an increase in daily average CO_2 fluxes for all fertiliser doses after day 0.

Table 3 lists ratios of NO:N_2O fluxes measured at the DS Site for each sampling day, shown as percentages. Before day 0, NO:N_2O ratio varied from 0 %-29 %, depending on the measurement day. After day 0, there were clear differences in this ratio between the fertiliser doses with average values of 0.7 % for FD1, 4.4 % for FD2 and 11.7 % for FD3 plots. Days with peak NO fluxes (day 2 and 21) produced a larger NO:N_2O ratio, reaching 42 % on day 2. In contrast, the model simulated less variation in NO or N_2O fluxes from before day 0, with average NO:N_2O ratio of 14.5 ± 0.9 %, but after day 0 the average simulated ratio reduces slightly on average in FD1 (11.6 ± 4.4 %) and FD3 (11.7 ± 7.1 %) plots and increased slightly in FD2 (18.3 ± 4.6 %) plots.

4 Discussion

There was a limit to the number of soil chambers that could be sampled in a day, particularly as the day length decreased towards the end of the experiment. Therefore, a compromise was required between reducing the effects of environmental variables (by measuring all plots on the same day), reducing the number of treatments and reducing treatment replications. This resulted in no control plots (without fertiliser) in the experiment, but measurements before fertiliser application were used as an indication of background variation in the fluxes. In addition, the FD1 plots only received fertiliser equivalent to N deposition at the study site and therefore can be indicative of plots with no fertiliser.

Soil gas fluxes generally vary according to environmental conditions, and the principal controls at a local level are soil moisture, temperature and nutrient levels (Pilegaard et al., 2006). LandscapeDNDC encapsulates the major soil processes relating to C and N cycling of nitrification, denitrification and decomposition and their environmental controls. These predict that an addition of N fertiliser will increase emissions of N_2O and NO for all doses in proportion to those doses. The model predicts effectively no change in soil CO_2 emissions for all fertiliser doses, with a small reduction for FD1 and small increases in FD2 and FD3. The experiment shows the effect of increasing fertiliser doses on CO_2, CH_4, N_2O and NO measured fluxes, are not all consistent with the model simulations.

The heavy rain that occurred on day 0 followed by more than a week of further rain, is likely to have affected the concentrations of fertiliser applied and may have caused leaching of fertiliser nitrate in run off. Although each plot in theory was subject to the same levels of wetness and therefore relative concentrations should remain constant, the level of protection from surrounding trees may not have been equal.

However, fluxes measured from FD1 plots after day 0 do not appear to differ significantly from fluxes measured before day 0, except that average NO fluxes decreased slightly and CO_2 fluxes increase slightly. These small changes probably relate to the changes in environmental conditions. Standard deviation in these small magnitude fluxes is high, as a result of local variation in environmental conditions. FD1 was designed to be equivalent to or slightly above the levels of N deposition recorded at the Straits during a year, most of which is normally received over about 2 months during late spring time. These results suggest that this level of additional N was either washed away in the rain or taken up by tree roots and not made available for microbial processes. It also suggests that this ecosystem is N limited which means addition of N will affect the growth and productivity of the forest.

Measured fluxes from FD2 and FD3 plots after day 0, show increases in NO, N_2O and CO_2 effluxes and a decrease in the CH_4 uptake. NO and CH_4 fluxes varied according to the fertiliser dose received, showing a higher NO flux and decreased CH_4 uptake with FD3 than FD2, as expected. However, CO_2 fluxes appeared to show a greater correlation with flux values before day 0 than with amount of fertiliser dose received and N_2O fluxes from FD2 plots exceeded those from FD3 plots. This suggests that plots with higher fluxes before fertiliser application (such as those measured from plot 2, Fig. 4a) might have had a higher nutrient content within the soil micro-sites and therefore lower microbial competition in the smaller doses of fertiliser producing larger fluxes compared with plots with initially low fluxes (such as plot 1 and 6). The uneven distribution of nutrients between the plots may relate to proximity to tree and understorey vegetation, tree shading and the quality of litterfall or may be due to animals marking territory repeatedly in the same place.

A longer measurement period together with additional measurements of soil factors such as nutrient levels would be required to better understand the factors controlling responses to additional N in this forest site. However, the main aim of this experiment was to see how the LandscapeDNDC model can simulate the effect of different fertiliser application rates on GHG and NO fluxes. The model simulations show that there are limitations in modelled soil processes which do not permit the capture of variation in nutrient status of all plots and its implications. This could be addressed by giving multiple input variables following e.g. Monte Carlo simulation of C, N and bulk density components of soil input data.

The very small difference in both simulation and measurements between FD1 and pre-treatment fluxes suggest that the annual N deposition rates would need to increase above the current annual maximum of 16 kg N ha^{-1} yr^{-1} before annual N_2O and NO emissions in this forest are affected by it.

5 Conclusions

Changes in the soil gas fluxes were detected following fertiliser application at the Deer Seat Site in the Straits Inclosure when fertiliser was applied at rates equivalent to 150 and 400 kg N ha^{-1} despite suboptimal weather conditions and decreasing temperatures of mid-autumn.

There was no linear increase in measured N_2O fluxes with fertiliser application dose and the results suggest that when N addition is higher than maximum N deposition rate at this study site the flux increase is more likely to respond to the antecedent soil conditions rather than the fertiliser dose.

LandscapeDNDC simulations of soil gas fluxes showed an exponential increase in the NO and N_2O fluxes with increasing fertiliser dose and a decrease in CO_2 fluxes but this was not consistent with the measurements. The model has previously overestimated NO and not reproduced the variability of N_2O fluxes well from the Straits Inclosure and it may be that not all critical processes are represented although measurements are also subject to error. Inclusion of spatial variations in soil nutrients could be achieved by multiple runs with a range of soil input values.

References

Albaugh, T. J., Allen, H. L. and Fox, T. R.: Historical patterns of forest fertilization in the southeastern United States from 1969 to 2004, South. J. Appl. For., 31, 129-137, 2007.

Bowden, R. D., Davidson, E., Savage, K., Arabia, C. and Steudler, P.: Chronic nitrogen additions reduce total soil respiration and microbial respiration in temperate forest soils at the Harvard Forest, For. Ecol. Manage., 196, 43-56, 2004.

Brown, J. R., Blankinship, J. C., Niboyet, A., van Groenigen, K. J., Dijkstra, P., Le Roux, X., Leadley, P. W. and Hungate, B. A.: Effects of multiple global change treatments on soil N2O fluxes, Biogeochemistry, 109, 85-100, 2012.

Butterbach-Bahl, K., Gasche, R., Breuer, L. and Papen, H.: Fluxes of NO and N_2O from temperate forest soils: impact of forest type, N deposition and of liming on the NO and N_2O emissions, Nutr. Cycling Agroecosyst., 48, 79-90, 1997.

Chadwick, D., Cardenas, L., Misselbrook, T., Smith, K., Rees, R., Watson, C., McGeough, K., Williams, J., Cloy, J. and Thorman, R.: Optimizing chamber methods for measuring nitrous oxide emissions from plot-based agricultural experiments, Eur. J. Soil Sci., 65, 295-307, 2014.

de Vries, W., Solberg, S., Dobbertin, M., Sterba, H., Laubhann, D., Van Oijen, M., Evans, C., Gundersen, P., Kros, J. and Wamelink, G.: The impact of nitrogen deposition on carbon sequestration by European forests and heathlands, For. Ecol. Manage., 258, 1814-1823, 2009.

Erisman, J. W., Sutton, M. A., Galloway, J., Klimont, Z. and Winiwarter, W.: How a century of ammonia synthesis changed the world, Nature Geoscience, 1, 636-639, 2008.

FAO: Global Forest Resources Assessment 2010 Main report, FAO Forestry paper 163, Food and Agriculture Organisation of the United Nations, Rome, 2010.

Fog, K.: The effect of added nitrogen on the rate of decomposition of organic matter, Biological Reviews, 63, 433-462, 1988.

Gundersen, P., Christiansen, J. R., Alberti, G., Brüggemann, N., Castaldi, S., Gasche, R., Kitzler, B., Klemedtsson, L., Lobo-do-Vale, R. and Moldan, F.: The response of methane and nitrous oxide fluxes to forest change in Europe, Biogeosciences, 9, 3999-4012, 2012.

Haas, E., Klatt, S., Fröhlich, A., Kraft, P., Werner, C., Kiese, R., Grote, R., Breuer, L. and Butterbach-Bahl, K.: LandscapeDNDC: a process model for simulation of biosphere–atmosphere–hydrosphere exchange processes at site and regional scale, Landscape Ecol., 28, 615-636, 2013.

IPCC: Climate Change 2013: The Physical Science Basis. Contribution of Working Group I to the Fifth Assessment Report of the Intergovernmental Panel on Climate Change [Stocker, T.F., D. Qin, G.-K. Plattner, M. Tignor, S.K. Allen, J. Boschung, A. Nauels, Y. Xia, V. Bex and P.M. Midgley (eds.)]. Cambridge University Press, Cambridge, United Kingdom and New York, NY, US, 2013.

Janssens, I., Dieleman, W., Luyssaert, S., Subke, J., Reichstein, M., Ceulemans, R., Ciais, P., Dolman, A. J., Grace, J. and Matteucci, G.: Reduction of forest soil respiration in response to nitrogen deposition, Nature Geoscience, 3, 315-322, 2010.

Kesik, M., Brüggemann, N., Forkel, R., Kiese, R., Knoche, R., Li, C., Seufert, G., Simpson, D. and Butterbach-Bahl, K.: Future scenarios of N_2O and NO emissions from European forest soils, Journal of Geophysical Research: Biogeosciences (2005–2012), 111, 2006.

Pilegaard, K., Hummelshøj, P. and Jensen, N.: Nitric oxide emission from a Norway spruce forest floor, Journal of Geophysical Research: Atmospheres, 104, 3433-3445, 1999.

Pilegaard, K., Skiba, U., Ambus, P., Beier, C., Brüggemann, N., Butterbach-Bahl, K., Dick, J., Dorsey, J., Duyzer, J. and Gallagher, M.: Factors controlling regional differences in forest soil emission of nitrogen oxides (NO and N_2O), Biogeosciences, 3, 651-661, 2006.

Reay, D. S. and Nedwell, D. B.: Methane oxidation in temperate soils: effects of inorganic N, Soil Biol. Biochem., 36, 2059-2065, 2004.

Sala, O. E., Chapin, F. S.,3rd, Armesto, J. J., Berlow, E., Bloomfield, J., Dirzo, R., Huber-Sanwald, E., Huenneke, L. F., Jackson, R. B., Kinzig, A., Leemans, R., Lodge, D. M., Mooney, H. A., Oesterheld, M., Poff, N. L., Sykes, M. T., Walker, B. H., Walker, M. and Wall, D. H.: Global biodiversity scenarios for the year 2100, Science, 287, 1770-1774, 2000.

Shrestha, R. K., Strahm, B. D. and Sucre, E. B.: Greenhouse gas emissions in response to nitrogen fertilization in managed forest ecosystems, New Forests, 46, 167-193, 2015.

Smith, K., Dobbie, K., Ball, B., Bakken, L., Sitaula, B., Hansen, S., Brumme, R., Borken, W., Christensen, S. and Priemé, A.: Oxidation of atmospheric methane in Northern European soils, comparison with other ecosystems, and uncertainties in the global terrestrial sink, Global Change Biol., 6, 791-803, 2000.

Tilman, D., Fargione, J., Wolff, B., D'Antonio, C., Dobson, A., Howarth, R., Schindler, D., Schlesinger, W. H., Simberloff, D. and Swackhamer, D.: Forecasting agriculturally driven global environmental change, Science, 292, 281-284, 2001.

Tipping, E., Rowe, E., Evans, C. D., Mills, R. T., Emmett, B. A., Chaplow, J. and Hall, J. R.: N14C: A plant–soil nitrogen and carbon cycling model to simulate terrestrial ecosystem responses to atmospheric nitrogen deposition, Ecol. Model., 247, 11-26, 2012.

Treseder, K. K.: Nitrogen additions and microbial biomass: A meta-analysis of ecosystem studies, Ecol. Lett., 11, 1111-1120, 2008.

Tubiello, F. N. and Fischer, G.: Reducing climate change impacts on agriculture: Global and regional effects of mitigation, 2000–2080, Technological Forecasting and Social Change, 74, 1030-1056, 2007.

Wilkinson, M., Eaton, E., Broadmeadow, M. and Morison, J.: Inter-annual variation of carbon uptake by a plantation oak woodland in south-eastern England, Biogeosciences Discuss, 9, 9667-9710, 2012.

Yamulki, S., Anderson, R., Peace, A. and Morison, J.: Soil CO_2 CH_4 and N_2O fluxes from an afforested lowland raised peatbog in Scotland: implications for drainage and restoration, Biogeosciences, 10, 1051-1065, 2013.

Table 1: Fertiliser doses applied to soil within soil frames at the Deer Seat Site, Straits Inclosure

Level	Fertiliser	Ammonium nitrate fertiliser dose (kg N ha^{-1})	Equivalent amount per chamber area (0.134m^2) (g N ha^{-1})	Sample plot numbers receiving dose
FD1	N deposition measured at Straits	16	0.64	1,3,5
FD2	Forest fertiliser dose recommended by McIntosh (1983) in upland Britain	150	5.96	2,4,7
FD3	Extreme dose	400	15.88	6,8,9

Table 2: Summary of soil gas fluxes (mean of all plots) during 3 sampling days before fertiliser application at the Deer Seat Site, Straits Inclosure and mean soil gas fluxes measured over similar sampling period in 2013 from the Tower Site for comparison. SD= standard deviation. CV = % coefficient of variation

Gas	CO_2 (mg C m^{-2} d^{-1})	CH_4 (mg C m^{-2} d^{-1})	N_2O (µg N m^{-2} d^{-1})	NO (µg N m^{-2} d^{-1})	Number of chamber measurements
<u>Deer Seat Site (28 Sept -6 Oct 2014</u>)					
Average	2080.3	-1.76	144.4	8.41	27
SD	308.8	0.32	55.4	7.40	
CV (%)	14.8	13.1	38.4	88.0	
Minimum	1303.5	-2.53	18.6	0.00	
Maximum	2701.3	-1.24	262.7	27.60	
<u>Tower Site (20 Sept – 4 Oct 3013)</u>					
Average	2086.5	-1.23	102.4	4.10	12
SD	297.2	0.18	36.15	2.52	
CV (%)	14.2	14.6	35.3	61.5	
Minimum	1509.5	-1.54	26.00	0.09	
Maximum	2620.5	-1.02	144.00	6.87	

Table 3: Ratio of NO:N_2O fluxes measured at Deer Seat Site, Straits Inclosure, 28 September 2014 – 11 November 2014 for each fertiliser dose (FD)

Day	FD1 (%)	FD2 (%)	FD3 (%)
-6	2.97	6.05	6.58
-3	26.50	28.79	7.89
0	0.00	1.70	1.53
2	1.49	8.49	42.09
4	0.00	4.32	9.13
7	1.01	3.75	8.15
9	3.69	6.10	9.36
11	0.00	4.42	8.01
14	0.00	3.44	10.79
17	0.00	1.64	6.75
21	0.00	7.90	18.78
24	1.77	4.03	6.22
29	0.00	3.33	6.38
36	0.00	1.34	3.43
Average after day 0	0.72	4.43	11.73

Figure 1: Satellite image of the Straits Inclosure, Hampshire, UK showing Deer Seat Site (DS) and Tower Site (T) locations

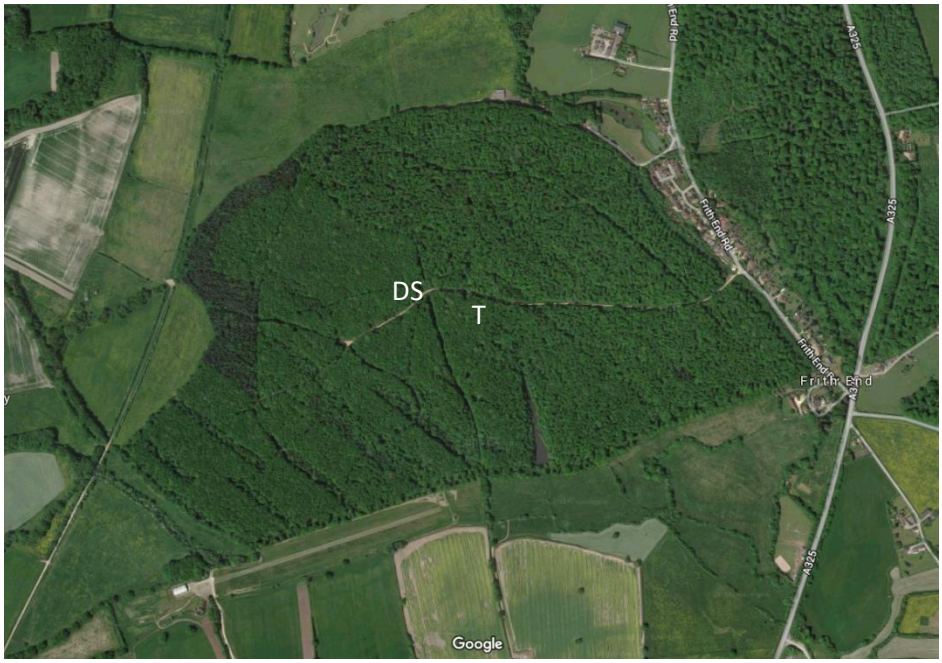

Figure 2: Fertiliser application using watering can extension within soil chamber frame

Figure 3: Climate data recorded at the Straits Inclosure for the study period (30 Sept – 24 Nov. 2014). Precipitation and maximum and minimum air temperatures (Tmax and Tmin, respectively) were recorded at the Tower Site. Soil surface temperature (T surface) was recorded at the Deer Seat Site during sampling days only. Day 0 = 6 October 2014.

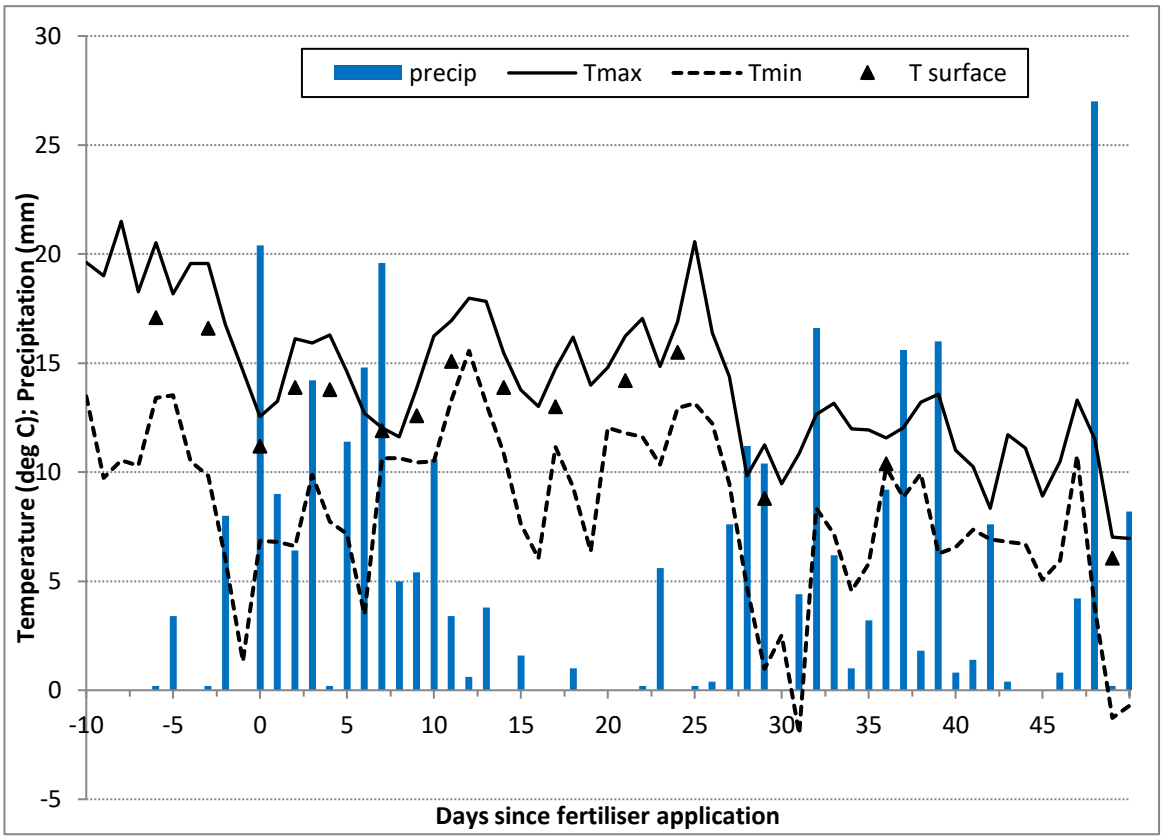

Figure 4: Soil gas fluxes measured at the Deer Seat Site, Straits Inclosure for a) N_2O, b) NO, c) $CO_2$and d) CH_4. Black arrow indicates fertiliser application day, 6 October 2014. Plot 2 (X) received FD2 but produced highest N_2O flux measurement on day 17.

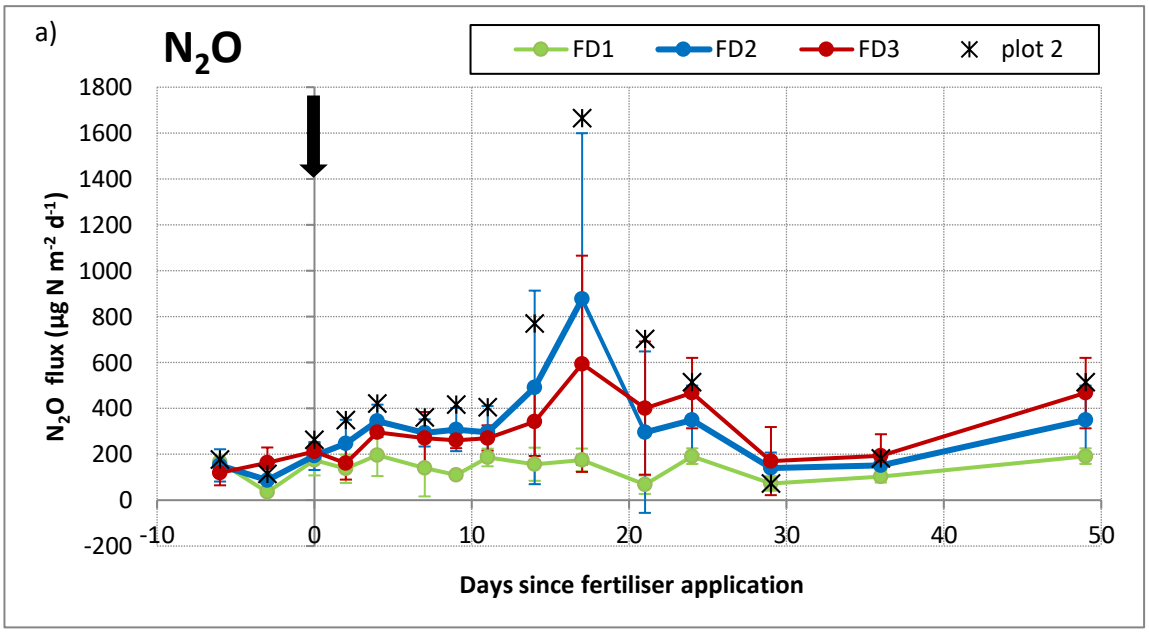

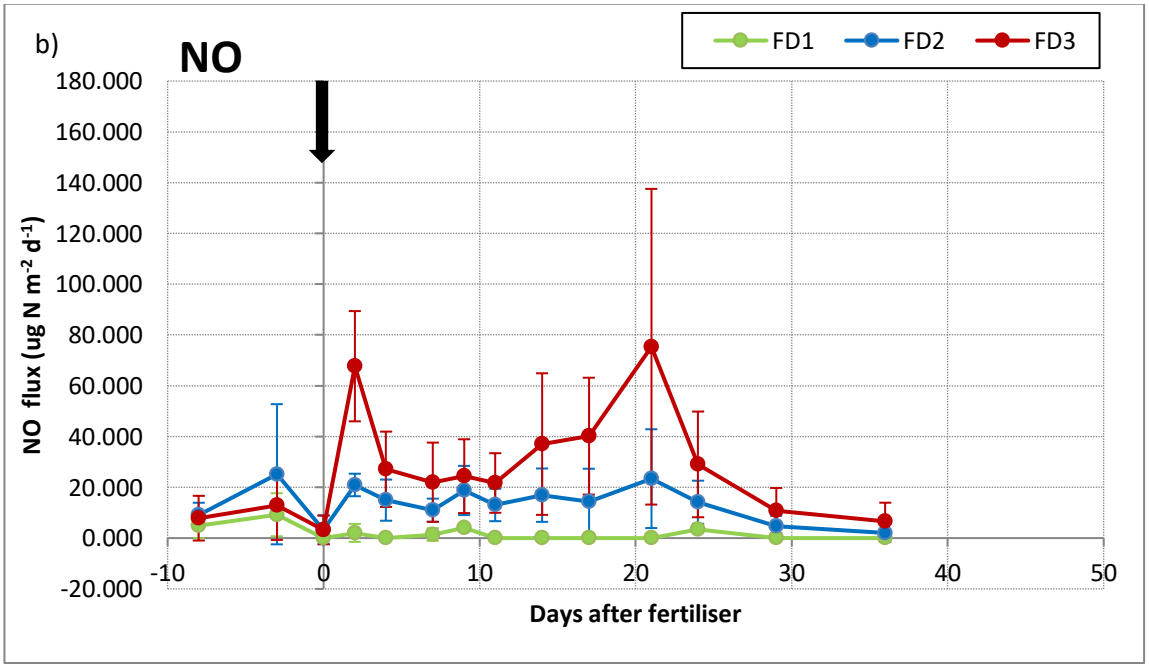

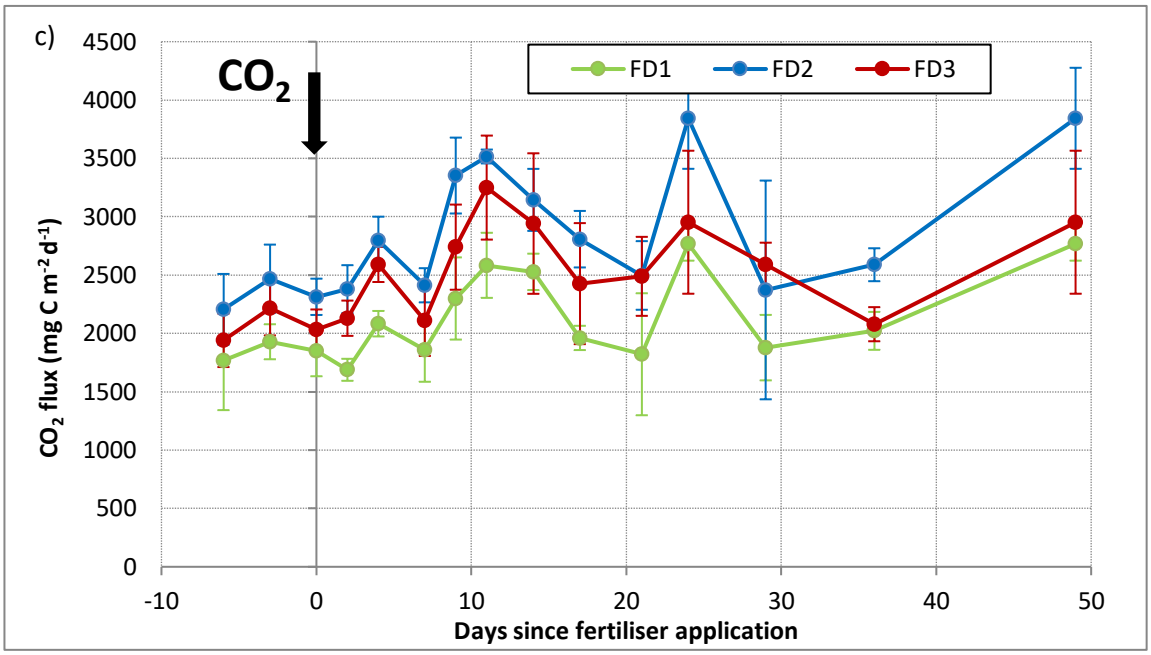
c)
CO2
FD1
FD2
FD3
4500
4000
3500
3000
2500
2000
1500
1000
500
0
CO2 flux (mg C m-2 d-1)
-10
0
10
20
30
40
50
Days since fertiliser application

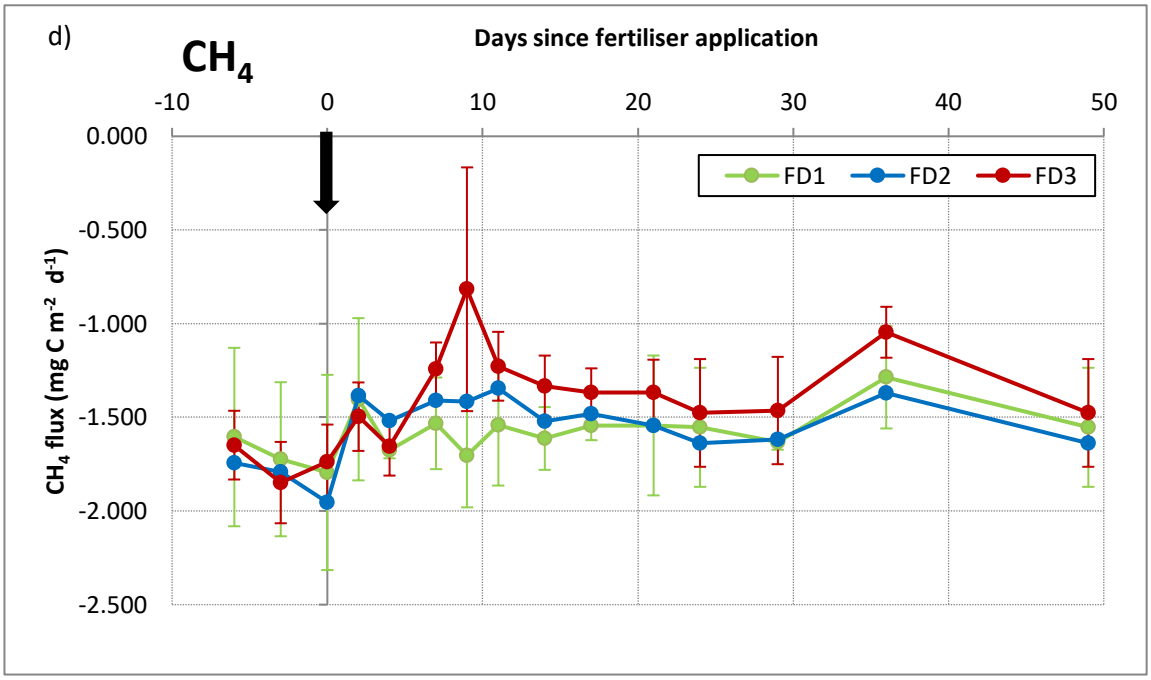
d)
CH4
Days since fertiliser application
-10
0
10
20
30
40
50
0.000
-0.500
-1.000
-1.500
-2.000
-2.500
FD1
FD2
FD3
CH4 flux (mg C m-2 d-1)

Figure 5: Average daily soil gas fluxes modelled by LandscapeDNDC before and after fertiliser application compared with measured data at the Deer Seat site, Straits Inclosure, Sept – Nov 2014; a) N_2O, b) NO, c) CO_2. All data normalised to average daily flux before day 0. Error bars represent 1 standard deviation. No negative NO fluxes were recorded.

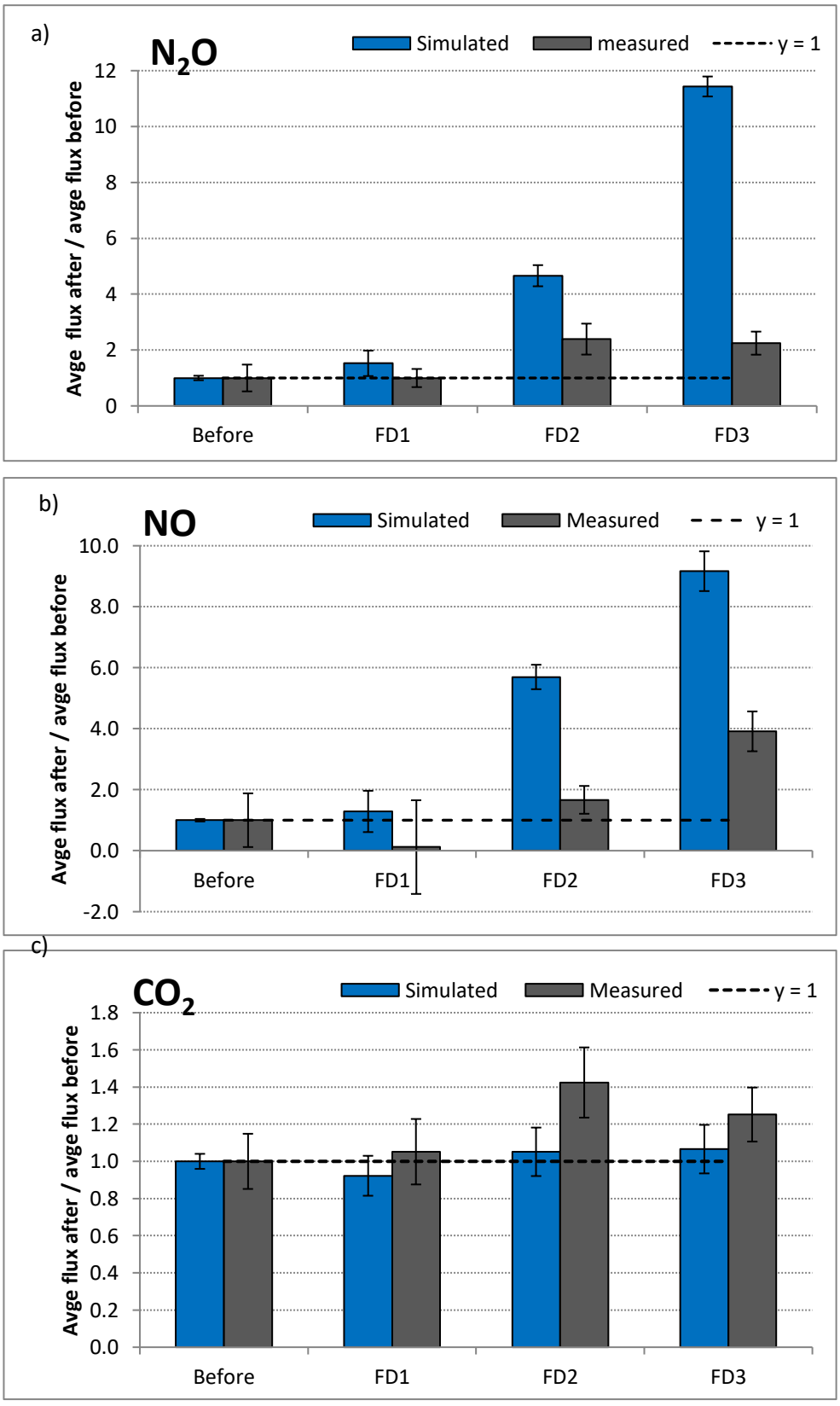

Chapter 6

Inter-Comparison of N_2O chambers using laser absorption spectrometry: quantification of systematic errors

J.F. Korhonen[1], M. Mäki[1,2], M. Korkiakoski[1], S. Bosco[3], C. Brümmer[4], S. Cade[5], M. S. Carter[6], E. Dařenová[7], J.-P. Delorme[4], T. Dementriades[8], J. Dušek[7], M. Galkowski[9], C.-M. Görres[10], E. Halmeenmäki[1], A. Herrmann[11], J. Hupp[8], M. Hurkuck[4], S. Jordan[12], R. Juszczak[13], M. Lee[14], C. Liu[15], A.M. Moffat[4], L. Merbold[16], N. Nickerson[17], J. Pumpanen[2], J. Smith[4], M. Strömgren[12], I. Volpi[3], M. Waniek[11], and M. Pihlatie[1]

Extended abstract submitted to Finnish National Centre of Excellence Annual Meeting October 2014

(Number of manuscript pages: 5)

My Contribution to this work:

- Carried out flux measurements on 2 soil chambers at the calibration facility
- Participated in workshop to review and discuss results following campaign

INTER-COMPARISON OF N_2O CHAMBERS USING LASER ABSORPTION SPECTROMETRY: QUANTIFICATION OF SYSTEMATIC ERRORS

J.f. Korhonen[1], M. Mäki[1,2], M. Korkiakoski[1], S. Bosco[3], C. Brümmer[4], S. Cade[5], M. S. Carter[6], E. Dařenová[7], J.-P. Delorme[4], T. Dementriades[8], J. Dušek[7], M. Galkowski[9], C.-M. Görres[10], E. Halmeenmäki[1], A. Herrmann[11], J. Hupp[8], M. Hurkuck[4], S. Jordan[12], R. Juszczak[13], M. Lee[14], C. Liu[15], A.M. Moffat[4], L. Merbold[16], N. Nickerson[17], J. Pumpanen[2], J. Smith[4], M. Strömgren[12], I. Volpi[3], M. Waniek[11], and M. Pihlatie[1]

1University of Helsinki, Dept. of Physics, Finland.
2University of Helsinki, Dept. of Forest Sciences, Finland.
3Institute of Life Sciences, Italy.
4Thünen Institute of Climate-Smart Agriculture, Germany.
5Royal Holloway, University of London, United Kingdom, and Forest Research, Alice Holt, United Kingdom.
6Technical University of Denmark, Denmark.
7CzechGlobe, Global Change Research Centre, Academy of Sciences, Czech Republic.
8LI-COR Biosciences, USA.
9AGH University of Science and Technology, Poland.
10University of Antwerp, Belgium.
11Humboldt-University, Albrecht-Daniel-Thaer Institute of Agricultural and Horticultural Sciences, Division of Soil Science, Germany.
12Swedish University of Agricultural Sciences, Sweden.
13Poznan University of Life Sciences, Poland.
14Scotland's Rural College, United Kingdom.
15Institute of Atmospheric Physics (IAP-CAS), Chinese Academy of Sciences, Beijing, China.
16Institute for Agricultural Sciences, ETH Zurich, Switzerland.
17Forerunner Research Inc., USA.

Keywords: chambers, fluxes, disturbance, nitrous oxide.

INTRODUCTION

Chamber method is the most commonly used method to measure greenhouse gas fluxes from soils. Nitrous oxide (N_2O) is a strong greenhouse gas and is emitted from soils. These emissions are characterized by high spatial and temporal variability, issues that can be addressed by a sufficient number of measurement locations and frequency in the measurements. Static chamber method has been associated with large systematic errors resulting from chamber disturbances, chamber design, flux calculation method, chamber operation, gas sampling, storage and analysis (Rochette and Eriksen-Hamel 2008; Christiansen *et al.,* 2011; Levy *et al.,* 2011; Pihlatie *et al.,* 2013). New techniques using laser absorption spectrometry open new possibilities to minimize some of these systematic errors by increasing the accuracy in the gas analysis and improving the resolution in the concentration measurements (Savage et al., 2014). Furthermore, the improved accuracy in gas analysis allows for shortening chamber closure times and hence decreasing chamber disturbances. When the laser absorption gas analyzers are used, the chambers are often operated as dynamic chambers (flow-through non-steady-state, FT-NS), commonly used in CO_2 flux measurements (Pumpanen *et al.,* 2004). Systematic errors related to the use of FT-NS chambers for N_2O emission measurements are currently poorly quantified. The

aim of this study was to quantify systematic errors related to FT-NS N_2O chambers, and to assess the effects of wind, chamber ventilation (vent-tube), collar insertion depth, and manual sampling on chamber fluxes measured by a variety of chamber designs.

METHODS

The chamber inter-comparison campaign was organized at Hyytiälä Forestry Field Station, Southern Finland during June-July 2014. The measurement system presented in Pumpanen et al. (2004) and Pihlatie et al. (2013) was modified for testing chambers used for measuring N_2O fluxes using laser absorption spectroscopy. The measurement system comprised of a large gas reservoir (stainless-steel tank, diameter 1.6 m, height 1.0 m, volume 2.6 m^3), covered with a perforated lid on top of which a layer of quartz sand with particle size of 0.2-0.6 mm was set to act as a porous media. Chamber measurements were conducted on top of the sand bed and these chamber fluxes were compared to simultaneously measured reference fluxes from the tank.

In total 22 chambers of different sizes, shapes and attributes (fan, vent-tube, sampling, seals) from different research groups were tested against the known reference fluxes. The measurements comprised of 'protocol measurements' and 'extra tests'. In the protocol measurements, each chamber measured fluxes repeatedly with and without external wind (1.5 m/s) from two different sand depths (0.2 m and 0.1 m). On average 6 replicate flux measurements per wind speed and sand depth were conducted. In the extra tests, the following tests were made in 3 replicates with selected chambers: vent-tube design and position, collar insertion depth, sealing material (rubber, water), manual sampling and headspace mixing. The fluxes measured from the tank ranged between 20 and 120 µg N m^{-2} h^{-1}.

At the start of the measurements, a high concentration of N_2O (1000 ppb) was injected into the tank, and the system was let to stabilize for 20 minutes to reach a steady-state condition. After the stabilization, chamber fluxes from the sand bed were measured together with measurements of the tank N_2O concentration, and the resulting reference fluxes. Chamber measurements were made in 3 replicates: each chamber closure being 10 minutes with a 20-min stabilization period between the chamber closures. N_2O concentrations in chamber headspace and in sand profile were measured with Quantum Cascade Lasers (QCL, Model CW-QC-TILDAS-76-CS, Aerodyne, Research Inc., Billerica, MA, USA) (vTI-1 and vTI2), and the concentration in the calibration tank was measured by an LGR N_2O/CO Analyzer (Model N_2O/CO-23d, Los Gatos Research, LGR, Mountain View, CA, USA). Leak rates of each chamber was measured by placing the chamber with collar into a water bath, injecting 1000 ppb N_2O in the chamber headspace, and following the N_2O concentration in chamber headspace over one hour.

Chamber fluxes were calculated by linear and non-linear fits to the concentration data as described in Pihlatie *et al.* (2013). Flux data was quality checked by goodness-of-fit analysis, and bad data was rejected based on normalized root-mean-square-error limit of 2%. References fluxes were calculated by a time-discrete exponential function as described in Pumpanen *et al.* (2004). All the fluxes were expressed as μg N_2O-N m^{-2} h^{-1}, and were calculated by Matlab-R2012a software (The MathWorks, Inc., Natick, MA, USA).

RESULTS

The tested flow-through non-steady-state (FT-NS) N_2O chambers tended to slightly underestimate the reference fluxes with linear flux calculation method (13%), whereas the chamber fluxes calculated by non-linear (exponential) flux calculation method did not differ from the reference fluxes (Table 1). The underestimations of the tested FT-NS chambers were smaller than those observed for non-flow-through non-steady-state (NF-NS) chambers tested in the campaigns for CO_2 and CH_4 (Pumpanen *et al.,* 2004; Pihlatie *et al.,* 2013). Wind outside the chamber as well as different depths of collar insertion did not influence the calculated chamber fluxes (Table 1).

Table 1: Mean ratio of chamber N_2O fluxes against reference fluxes calculated by linear and exponential fits, and their 95% confidence intervals from all the 22 chambers. Measurements conducted with sand depths of 20 cm and 10 cm, and mean of both sand depths.

	Linear	95% conf. int.	Exponential	95% conf. int.
Sand depth 20cm	0.89	± 0.07	0.98	± 0.09
Sand depth 10cm	0.86	± 0.05	0.94	± 0.10
All sand	0.87	± 0.05	0.96	± 0.07

The high-resolution N_2O data obtained from the chamber headspace, tank and soil profile by the QCL and LGR lasers provided unique and quantitative information of the short-term disturbances caused by the chambers. Our results strongly support the findings of Christiansen *et al.* (2011) that headspace air mixing improves the data quality, while poorly mixed headspace air created noise to the N_2O signal, leading to inaccurate estimation of the flux with exponential fitting. Also, the placement of a chamber disturbed both the headspace and soil concentration, and affected the resultant chamber fluxes. Those chambers which were directly pushed into the

soil without a collar, or chambers which had a water-seal between the collar and the chamber, disturbed the soil concentration the most (Figure 1). For example, placement of a chamber with water-seal led to an immediate drop in soil N_2O concentration underneath the chamber (Figure 1). This was interpreted to result from a pressure pulse temporarily pushing atmospheric N_2O into the soil and hence reducing N_2O gradient in the top of the sand. The decreased concentration gradient in the soil led to flux underestimation. The disturbances caused by chamber placement could be largely avoided when a chamber was equipped with a vent-tube and a rubber-seal between the collar and the chamber.

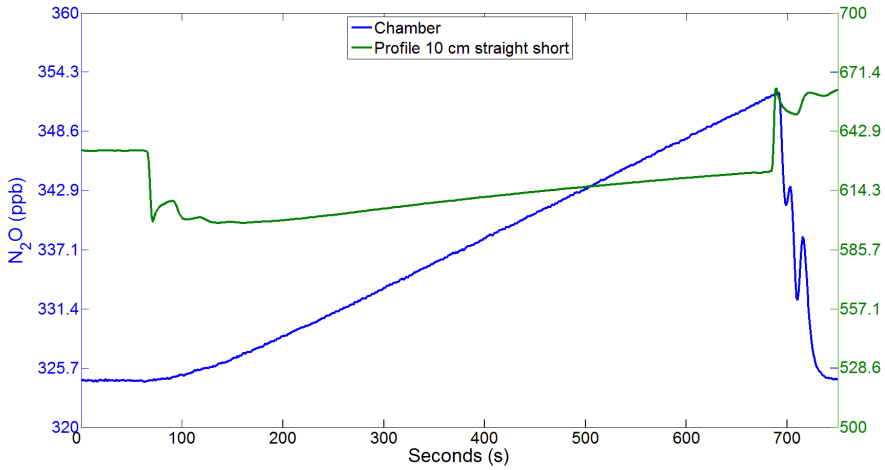

Figure 1: Example of chamber disturbance to the soil N_2O concentration and the following N_2O flux estimate of the chamber.

CONCLUSIONS

Systematic errors in N_2O chamber measurements can be quantified in laboratory measurements as shown in the campaign. Increased accuracy and measurement frequency due to the application of laser absorption spectrometry in N_2O chambers allows for minimizing some of the systematic errors, and hence leads to improved data quality. Soil N_2O profile data showed how sensitive the soil concentration gradient is to external disturbances caused by the placement of a chamber, if the pressure effect is not taken into account. This further underlines the importance of designing chambers so that the disturbance to the soil during a measurement is minimized.

ACKNOWLEDGEMENTS

This work was supported by InGOS TNA (Integrated non-CO_2 greenhouse gas observation system), ICOS-Finland, Academy of Finland Centre of Excellence (project 1118615) and Academy of Finland Research Fellow project (263858).

REFERENCES

Christiansen, J. R., Korhonen, J.F.J., Juszczak, R., Giebels, M., and Pihlatie, M. (2011). Assessing the effects of chamber placement, manual sampling and headspace mixing on CH4 fluxes in a laboratory experiment, Plant Soil, 343, 171-185, DOI 10.1007/s11104-010-0701-y.

Levy, P.E., Gray, A., Leeson, S.R., Gaiawyn, J., Kelly, M.P.C., Cooper, M.D.A., Dinsmore, K.J., Jones, S.K., Sheppard, L.J. (2011) Quantification of uncertainty in trace gas fluxes measured by the static chamber method. Eur. J. Soil Sci. 62, 811–821.

Pihlatie, M. K., Christiansen, J. R., Aaltonen, H., Korhonen, J. F. J., Nordbo, A., Rasilo, T., Benanti, G., Giebels, M., Helmy, M., Sheehy, J., Jones, S., Juszczak, R., Klefoth, R., Lobo-do-Vale, R., Rosa, A. P., Schreiber, P., Serca, D., Vicca, S., Wolf, B., and Pumpanen, J. (2013). Comparison of static chambers to measure CH4 emissions from soils, Agric. For. Met., 171, 124-136, DOI 10.1016/j.agrformet.2012.11.008.

Pumpanen, J., Kolari, P., Ilvesniemi, H., Minkkinen, K., Vesala, T., Niinisto, S., Lohila, A., Larmola, T., Morero, M., Pihlatie, M., Janssens, I., Yuste, J. C., Grunzweig, J. M., Reth, S., Subke, J. A., Savage, K., Kutsch, W., Ostreng, G., Ziegler, W., Anthoni, P., Lindroth, A., and Hari, P. (2004). Comparison of different chamber techniques for measuring soil CO2 efflux, Agric. For. Met., 123, 159-176, DOI 10.1016/j.agrformet.2003.12.001.

Rochette, P., Eriksen-Hamel, N.S., (2008). Chamber measurements of soil nitrous oxide flux: Are absolute values reliable? Soil Sci. Soc. Am. J. 72, 331–342.

Venterea, R.T., Spokas, K.A., Baker, J.M., (2009). Accuracy and precision analysis of chamber-based nitrous oxide gas flux estimates. Soil Sci. Soc. Am. J. 73, 1087–1093, http://dx.doi.org/10.2136/sssaj2008.0307.

Chapter 7 Critical Evaluation and Discussion

This study has investigated the model LandscapeDNDC and evaluated its use in the UK at an oak forest and a spruce forest and with added N in a forest soil. The purpose of any process-based model is to simplify, and reduce complex interacting processes to those key processes that are most important in determining the end result, in this case GHG fluxes. Measured data are required to calibrate, parameterise and test any process-based model and the more data available the better. The problem with measurements is that they are always subject to error, uncertainty and natural variation both spatially and temporally. This means that model evaluation is not straightforward. Therefore, this section starts by evaluating and discussing measurements made and used in this study and continues with discussing methods of evaluating the modelled results. This is followed by further analysis of results obtained in this study, suggestions for model software improvements and some contextual information and finishes with suggestions of future work. The sub-sections therefore are:

- Measurements –principally a discussion of uncertainties and measurement error
- Model evaluation – how to evaluate a model and possible problems
- Model outputs – critique of specific output generated
- Model software – some suggested improvements
- Context – setting LandscapeDNDC in the context of other models
- Future work – some suggestions for building on the work in this study.

7.1 Measurements

This study has used various forms of measured environmental data as model input and the simulation results have been compared with measured eddy covariance data and soil chamber data. The measurement methods are discussed below.

7.1.1 Eddy covariance measurements

Eddy covariance measurements (described in Section 2.4) are based on a technique which makes the following major assumptions (Burba and Anderson, 2012):

- Measurements are made inside the boundary layer of interest
- Measurements at a point can represent an upwind area
- Fetch, or 'flux footprint', is adequate, i.e. fluxes are only measured at the area of interest
- Flux is fully turbulent, i.e. most of the net vertical transfer is done by eddies

- Terrain is horizontal and uniform
- Instruments can detect very small changes at high frequency.

Thus, if any of these assumptions are not true, then errors will be present. For example, the terrain of the Griffin Forest is complex and not uniform throughout the flux footprint. Clement et al. (2012) have attempted to address this with a site-specific correction for advective flux loss which was applied over a whole day rather than the normal correction for night time only. This resulted in a change to the NEE of about 4 % (from 618 to 641 g C m^{-2} y^{-1}) in 1998 data (comparing results in Medlyn et al., 2005 with Clement et al., 2012). Although this is relatively small, it led to recalculations of the TER using an algorithm which included soil moisture as well as temperature and increased the TER by 26 % (from 1213 to 1530 g C m^{-2} y^{-1}) for the same year. These calculations clearly make a difference when comparing with modelled data. In contrast to the complex terrain of Griffin, the Straits Inclosure is in flat and uniform terrain but is only 90 ha in area, almost surrounded by farmed pasture land and at times the fetch may extend beyond the forested area and therefore may not be sampling exclusively from a forest source.

Baldocchi (2003) reviewed the eddy covariance technique at a time when there were slightly over 150 sites in the world and he was concerned that it was being used over increasingly longer timescales and over less than ideal surfaces. When the method is applied over complex terrain or during atmospheric conditions that vary, measurements of atmospheric storage, flux divergence and advection must also be included in the calculations. Summing the resulting NEE values for daily and annual figures can lead to random sampling errors and systematic bias, but these can be reduced by averaging over long periods. Gaps in data are inevitable in a system that is intended to be continuously recording. Gap-filling normally uses values from statistical or empirical models. Baldocchi (2003) suggests that empirical models are better as they are derived from a large statistical population and therefore are less likely to be subject to errors of bias. However, systematic bias errors are common at night when winds are light and intermittent and usually lead to underestimates in the measurement of ecosystem respiration, as was found at Griffin (Clement et al., 2012). Baldocchi (2003) concluded that estimates of NEE from eddy covariance were converging with estimates produced by measuring changes in biomass and soil carbon, provided they were multi-year studies and the eddy covariance measurements were compensated for systematic bias errors. Non-ideal sites can produce uncertainties in NEE of ± 100 - 200 g C m^{-2} y^{-1} but with appropriate corrections these could be reduced to values more common at ideal sites, of 50 g C m^{-2} y^{-1} (Baldocchi, 2003).

NEE from two eddy covariance towers set up 30 m apart in an extensive and homogeneous pine forest in Finland used values from a canopy exchange model to gap-fill and for inter-comparison

(Rannik et al., 2006). The conclusion from this study was that the main uncertainty of long term NEE could be related to day time measurements. The uncertainty on the annual NEE was estimated at ± 80 g C m^{-2} y^{-1}, mainly from day time observations. However, this is not a typical situation as data from the two sites were averaged to reduce random errors and although the forest was homogeneous the underlying terrain was complex. The annual average NEE at the site for 1997 - 2001 was 170 - 240 g C m^{-2} y^{-1}, which means the relative uncertainty was approximately 30 - 50 %. Hollinger et al. (2004) also compared results from 2 towers in the same spruce forest in USA but with different footprints (750 m apart). After 7 years of measurement, annual NEE values averaged 174 ± 46 g C m^{-2} y^{-1} (variation shown is inter-annual variation) with uptake differing between the two towers by 6 %. This indicates that local conditions are an important factor in any estimation of eddy covariance errors.

Spatial variability has been separated from uncertainty due to instrument and gap-filling errors in an experiment involving 7 eddy covariance towers at a pine forest in N Carolina (Oren at el., 2006). This involved 7 research groups measuring for one week in October 1997. They estimated that spatial variability contributed nearly half of the total variation in annual NEE even in a uniform pine plantation. They combined data from the 7 towers measured over one week with data from a single tower measured over several years, to estimate an inter-annual instrument error of 8 - 28 g C m^{-2} y^{-1} (3 - 5%), a gap-filling error of 62 - 110 g C m^{-2} y^{-1} and spatial standard deviation in annual NEE of 25 - 66 g C m^{-2} y^{-1}, giving a combined estimate of variability of 79 -127 g C m^{-2} y^{-1}.

The eddy covariance data used here from the Straits Inclosure and Griffin Forest were both processed with the same software (EdiRe, University of Edinburgh) and principles defined by Aubinet et al. (2000). Although no specific calculations have been made of the errors in these data, when comparing with simulated data, a figure of 15 % error was assumed. This was based on Goulden et al. (1996) whose measurements were on a deciduous forest and who have been cited as quoting an error of 15 % on annual NEE from eddy covariance data (e.g. Oren et al., 2006). In fact, they report combined effects of systematic errors, sampling uncertainty and estimation from calm nocturnal periods to be between -0.3 and + 8 t C ha^{-1} y^{-1}, which is a range of 15 – 38 % on the annual NEE of 2.1 t C ha^{-1} y^{-1}. Therefore, it seems reasonable to use a figure of 15 % error on eddy covariance data when comparing with simulations. At the Straits Inclosure, the mean annual NEE was 486 g C m^{-2} y^{-1}, which means that an error of 15 % would result in an absolute error of ± 73 g C m^{-2} y^{-1}. This is comparable to figures quoted above (e.g. Baldocchi, 2003 and Oren et al., 2006). At Griffin Forest, Clement et al. (2012) developed a site-specific correction for advection caused by the complex terrain and also developed an enhanced method

of respiration calculation that took into account soil moisture as well as temperature. This could result in a lower error on the annual results but in the absence of any specific information on the errors, the same assumption of 15 % error was made when comparing Griffin data with simulations. This results in an absolute error of 108 g C m^{-2} y^{-1} on an average annual NEE of 720 g C m^{-2} y^{-1}, which is not incompatible with figures quoted above.

In addition to errors in the measurement and processing of the net ecosystem exchange, it is important to note that further calculations are required to derive ecosystem respiration (TER) from these data. These calculations normally start with the night time flux values, when no photosynthesis takes place and CO_2 fluxes are assumed to be purely from respiration. As respiration rates increase with temperature, each day's respiration value is calculated from the relationship between night time and day time temperatures averaged over a 10-day period, using a Q10 function derived from the data (Lloyd and Taylor, 1994). This method was used by Wilkinson et al. (2012) at the Straits Inclosure and by Clement et al. (2012) at Griffin but the latter used an additional soil moisture dependence. The Sum of TER and (positive) NEE produces a figure for gross primary production (GPP). The TER and GPP values are therefore likely to have additional errors derived from this calculation of respiration. In statistical analysis for this study comparing these data with simulations all eddy covariance ecosystem values were assumed to have 15 % error, since no alternative estimates were available.

Luyssaert et al. (2007) created a global database of CO_2 balance data from forest ecosystems around the world and concluded that in all biomes there was a need for a substantial biome-specific closure term to close the CO_2 balance. This was taken as an indication that respiratory processes, advection and non-CO_2 carbon fluxes were not being adequately accounted for. This database was not exclusively from eddy covariance data but they did form a major part of it. The non-CO_2 carbon fluxes include CH_4 and volatile organic compounds (VOCs) which are not accounted for in LandscapeDNDC which also attempts to balance C and N cycling in the ecosystem. These would be useful additions, although this would add complexity to processes which are intentionally simplified.

7.1.2 Soil chamber measurements

The soil chamber or enclosure method (described in Section 2.1) of measuring trace gas fluxes from the soil is known to be subject to systematic and random errors in addition to errors associated with the large spatial variability of soil flux and low spatial coverage of measurements. Several studies have compared chambers and techniques by using a calibration tank as described in Section 2.4 for measuring the efflux of different gases. Pumpanen et al.

(2004) compared 20 different chambers for measuring soil CO_2 efflux and concluded that non-steady state non-flow-through chambers systematically underestimated CO_2 flux measurements on average by 4 - 14 % whereas no significant consistent differences were observed between flow-through chambers. The reliability of the chambers was not related to the measurement principle but to other factors such as collar design, mixing of headspace and size of sand particles used to mimic soil. Some chambers contained an internal fan for headspace mixing to ensure even distribution of CO_2 within the chamber. In some cases, this caused excessive turbulence and hence mass flow of CO_2 between the soil and the chamber. Some form of mixing is required when using non-flow-through chambers to ensure representative sampling. The chambers used for this study do not have fans in the headspace, and mixing is achieved by repeated filling and emptying of the syringe prior to sampling.

A similar experiment was later carried out to compare static chambers measuring CH_4 emissions from the same calibration tank (Pihlatie et al., 2013). In this case, there were 15 chambers and all were non-flow through non-steady state. These chambers underestimated the reference fluxes by an average 33% when using a linear flux calculation but there was no significant difference from the reference fluxes when using an exponential calculation ($p < 0.05$). The degree of difference from the reference flux was specific to each chamber and independent of the flux level. However, increasing the chamber height, area and volume ($h > 0.22$ m, $A > 0.1$ m^2 and $V > 0.015$ m^3) significantly reduced the flux underestimation, irrespective of calculation method. An alternative to increasing chamber height is decreasing closure time. The chambers used in this study are of the recommended size, having the dimensions: $h = 0.29$ m, $A = 0.152$ m^2, $V = 0.042$ m^3 (water sealed) and $h = 0.294$ m, $A = 0.134$ m^2, $V = 0.043$ m^3 (rubber sealed). Closure time needs to be short enough to ensure CO_2 concentration increases linearly but long enough to have a measurable change in CH_4 and N_2O concentrations. Analysis of results suggests that 1 hour is appropriate with the chambers used in this study.

The third chamber comparison experiment in this series took place in 2014 with a bigger version of the calibration tank, as described in Section 2.4, to compare N_2O chamber measurements. The two chambers used for this study were compared on the calibration tank at Hyytiala, Finland as part of the experiment, funded by Integrated non-CO_2 Greenhouse gas Observing System (InGOS). A comparison was made with other chambers and the different seals between chamber and frame (water seal for main Straits Inclosure measurements, WSC, and rubber seal for fertiliser experiments at Straits Inclosure, RSC). There was a total of 21 chambers compared. The extended abstract in Chapter 6 shows some of the preliminary results, and more are discussed below, but final results are not yet available. Each chamber was adapted to a flow-through

design to allow connection to a laser absorption spectrometry gas analyser to reduce the analysis errors.

Every chamber was subjected to a leak test in which the headspace was filled with 1000 ppb N_2O and the chamber was placed on its frame in a container filled to 4 cm with water and left for 1 hour. Both WSC and RSC repeated this experiment 3 times and the N_2O concentration reduced by 2.2 - 6.1 % during the hour. WSC performed better (average 3.0 % reduction) than RSC (average 4.6 %) but clips helped reduce the leakage in RSC (3.4 %). This represents an average level of leakage compared to other chambers studied (figures not available), i.e. there were approximately equal numbers of chambers better and worse.

Table 7.1 shows a comparison of fluxes calculated with laser absorption spectrometry gas analyser with fluxes from syringe gas sampling and GC analysis for WSC and RSC. This does not include reference flux data as it is still to be recalculated by the campaign organisers, following the discovery of an error in the original calculations. The gas sampling was as described in Section 2.1.1, involving 3 samples of 20ml taken at 0, 20, 40 and 60 minutes after closure and GC analysis was at the same laboratory in Alice Holt. However, unlike measurements at the Straits (Chap 3), the gas vials were not analysed until about 2 weeks after collection as they returned with the chambers overland. The results in Table 7.1 show measurements from these two chambers using syringe sampling were on average 13 % less than when using the laser analyser.

Figure 7.1 illustrates the range of chambers taking part in the comparison and Fig. 7.2 gives some preliminary results comparing flux measurements. This suggests that most chambers underestimated the N_2O flux and the exponential fit produced a larger flux than linear fit in all but two chambers. WSC and RSC perform well compared to other chambers and despite having a higher leak rate, RSC performs better than WSC. These results may, however, be subject to change when the reference flux has been recalculated. Preliminary conclusions suggest that the shape of the chamber, defined by the ratio of surface area to volume, is critical in determining the accuracy of flux measurements, as with CH_4 flux measurements (Pihlatie et al., 2013). The two chambers illustrated in the top left of Fig. 7.2 therefore have the worst results.

Although these are only preliminary results, they demonstrate that the chambers used in measurements at the Straits Inclosure are appropriate in size and shape and perform as well as most other chamber designs. They do, however underestimate the flux when using GC analysis and although this cannot yet be quantified, it seems to be at least 13 %.

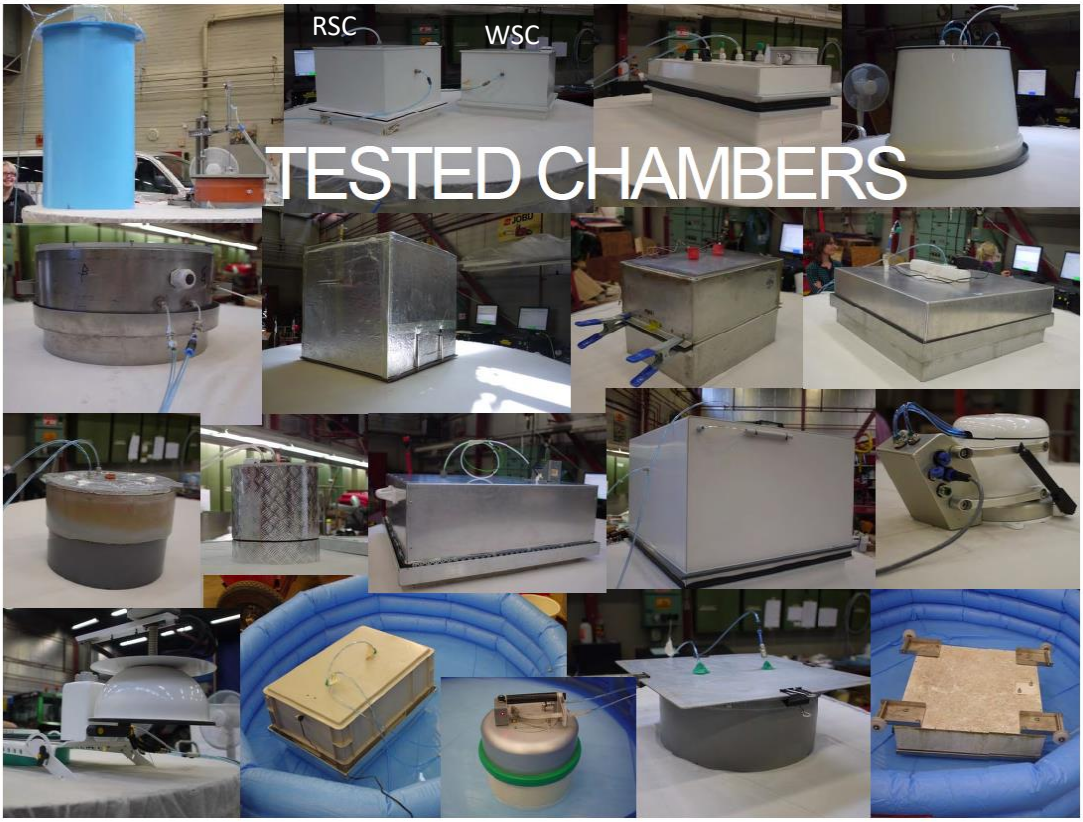

Figure 7.1: Chambers compared using calibration tank at Hyytiala, July 2014. WSC (water sealed chamber) and RSC (rubber sealed chamber) are marked at the top of the photo (Pihlatie et al., unpublished)

Table 7.1: N_2O fluxes calculated from two different chamber types on the calibration tank at Hyytiala. WSC = Water sealed chamber, RSC = rubber sealed chamber

Expt	Chamber	N_2O flux by GC	N_2O flux by laser analyser	Difference
		µg N_2O-N m^{-2} h^{-1}	µg N_2O-N m^{-2} h^{-1}	(%)
1	RSC with open vent	34.77	37.97	8.4
1	WSC with open vent	32.32	38.86	16.8
2	RSC no vent	29.51	33.37	11.5
2	WSC no vent	28.99	35.66	18.8
3	WSC no vent	28.56	31.80	10.2
3	Sand under chamber	Not available	Not available	-

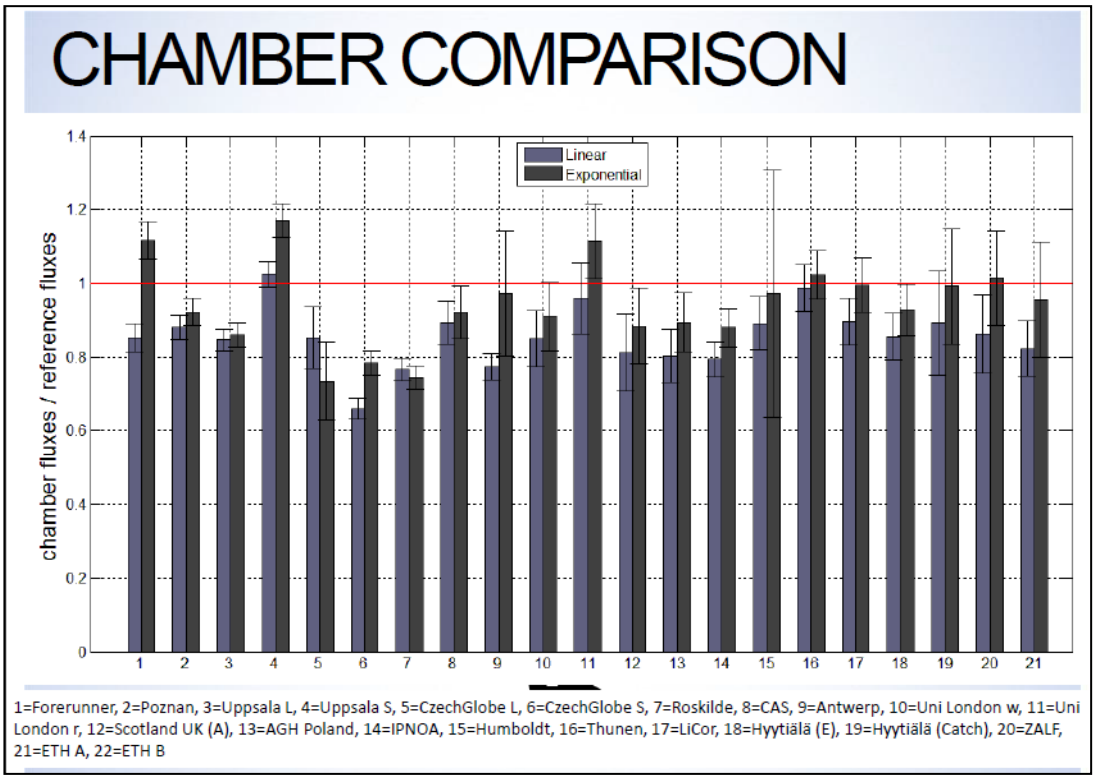

Figure 7.2: Preliminary results from comparison of 21 chambers at Hyytiala calibration facility. Chamber '10'= water sealed chamber (WSC) and chamber '11' = rubber sealed chamber (RSC) (Pihlatie et al., unpublished)

It is worth mentioning that the fluxes generated from this calibration facility when 1000 ppb N_2O in the tank diffuses through pure clean sand are far higher (fluxes from Table 7.1 average 740 - 850 µg N_2O-N m^{-2} d^{-1}) than have been measured at the clay-rich soils of the Straits Inclosure or Griffin Forest in normal circumstances. Only after adding the equivalent of 150 - 400 kg N ha^{-1} fertiliser did fluxes reach these levels (maximum flux without fertiliser = 255 µg N_2O-N m^{-1} d^{-1} (May 2014), maximum flux with fertiliser = 1664 µg N_2O-N m^{-1} d^{-1}). Only 2 measurements of > 800 µg N_2O-N m^{-1} d^{-1} were made during the fertiliser experiment. As a common cause for underestimation is the change in the diffusion gradient between soil and headspace following increase in concentration in the headspace (Hutchinson et al., 2000; Livingston et al., 2006; Kutzbach et al., 2007), lower fluxes are likely to require more time before this problem occurs.

Results from Chapter 6 show disturbance to the N_2O concentration in the sand under the chamber as a result of placement and removal. There is a proposal to investigate this effect and the gas build up within a chamber using a mathematical diffusion model (Creelman et al., 2013) to simulate different soil porosities and subsurface gas concentrations. The proposal originated in a workshop following the N_2O chamber comparison campaign at Hyytiala and it is hoped that it will put results from the calibration tank into context for real forest conditions.

Gas chromatography, the method used to analyse gas samples in this study for flux measurements, is known to be subject to errors. Since flux calculations require analysis of changes in concentration, rather than the absolute concentration of a gas, calibration to a known standard is less critical, but results from validation and repeatability tests shown in Table 2.1 indicate a limit of detection of 0.033 ppm for N_2O with ambient concentrations averaging 0.315 ppm. Samples from vials with a leaking seal were easily identified as the CO_2 concentration was low; in these cases, all measurements from such samples were rejected.

Calibration of the NO_x analyser was carried out at Royal Holloway laboratories. The fertiliser experiment served to test that the analyser could detect higher NO fluxes than it recorded throughout the main period of measurement at the Straits Inclosure.

In addition to errors of measurement, soil fluxes are subject to large natural spatial and temporal variation, and as measurements have shown in this study, the greatest variation is in N_2O and NO fluxes. Repeated measurements with increasing frequency are required to help account for this variation. Some research locations (e.g. Hyytiala, Finland and Hoeglwald, Germany) have permanent automated soil chambers in place. While this inevitably provides more data, the more frequent closure of chambers does affect the soil moisture and temperature conditions and therefore influences the resulting fluxes. Thus, it is collation of data from a series of measurement methods and error analyses, together with process-based models, that is the way forward.

7.1.3 Other measurements

Analyses were carried out on soil samples from the Straits Inclosure. Soil moisture data was used to assess the correlation with soil gas fluxes (data not shown) and with simulated soil moisture. Unfortunately, the nitrate and ammonium analyses did not give reliable results, since the de-ionised water used in the analyses was found to contain nitrates. Although the experiments were repeated, the samples had decomposed and it was shown that there was a correlation between time in the fridge and total N content, and particularly with NH_4 content, suggesting organic material had decomposed to NH_4 since sample collection. Therefore, this data was not included in the study.

Other environmental measurements, such as climate and soil temperature are also subject to errors, but these are not quantified here.

7.2 Model evaluation

The purpose of a process-based model may be:

- To help understand the processes being modelled (ideally confirm the understanding), or
- To predict the outcome of a scenario, involving a change; e.g. climate change or forest management practices.

As no measurements are possible in the future, a model's ability to predict the outcome of change relies on its ability to match measurements from the past and previous changes. To do this well, the processes modelled need to be well understood and appropriately simplified. Thus, models designed to predict the future (where there are no available measurements), are actually 'data hungry', requiring a large amount of data for validation. A problem may then occur when adjustments are made to parameters in the model to improve fit. This can result in bias, especially if the same data is used to 'validate' the model.

Three main problems of model validation have been identified (Medlyn et al., 2005) as follows:

- Equifinality – in which different models, or different parameterisations of the same model, can produce similar results, making it difficult to decide which is correct
- Insensitivity – results from the fact that the major source of variation in terrestrial ecosystems are annual and diurnal cycles, the scale of which can mask effects of other factors
- Uncertainty – present in parameters, model structure and data.

Chapter 3 compares results from two sub-modules of LandscapeDNDC (PnET and PSIM) but results are sufficiently different to rule out equifinality in this instance. There is a concern of insensitivity since PSIM in particular, does not show an inter-annual variation matching that found in eddy covariance data at the Straits Inclosure. Issues of uncertainty regarding measurements have been discussed in Section 7.1. Sensitivity analyses have been carried out to explore the effect of input values and key parameters on the results (Chapters 3 and 4). Most of the values tested were only varied by ± 10 %, due to time constraints. This should be extended to e.g. ± 20 % since many variables will have non-linear effects on the model results and there may be step changes, such as are found when pH < 5.

The term 'validation' previously used extensively in literature (e.g. Aber and Federer, 1992; Aber et al., 1996; Stange et al., 2000; Boyer et al., 2006) is now considered inappropriate because it implies that it shows the model to be correct. In fact, models, as with hypotheses, can only be

proved false, never correct (Medlyn et al., 2005). However, a study comparing 6 process-based forest growth models (Kramer et al., 2002) using eddy covariance data from 6 forest sites in Europe found they all produced accurate estimates of the EC data, despite differences at the process level. Therefore, accurate results do not necessarily come from correctly defined processes and reduces the reliability of the model's future predictions. Thus, the process carried out is 'evaluation', whereby the model's ability to match measured data is quantified.

When evaluating a model, there is a need to define what will be measured to perform the evaluation. Although data is available as daily values for eddy covariance and for model output, the frequency of soil chamber measurements is much sparser and subject to compounding errors of measurement, discussed above, when aggregating the data. Monthly and annual averaged or totalled data seemed to be the most appropriate. In the case of Straits Inclosure data, there were enough years of eddy covariance data to analyse results annually but this was not the case for Griffin Forest. The problem with comparing monthly data is that the seasonal variation dominates and there is a risk of insensitivity.

The r^2 correlation was not used to compare simulated with measured data on the advice of Medlyn et al. (2005) and Smith et al. (1997) because it fails to account for model bias, resulting from the use of measurements to calibrate the model. For example, temperature values input to LandscapeDNDC were also used to calculate 'measured' TER from eddy covariance data. Instead the ModEval software package from Smith et al. (1997) was used together with a calculation of modelling efficiency also defined in Medlyn et al. (2005) which estimates the proportion of variance explained by the 1:1 line (Mayer and Butler, 1993). Medlyn et al. (2005) recommends the statistic RMSE (present in ModEval) together with model efficiency as a means of assessing the goodness of fit of a model (equations given in Section 2.7).

Where data has been replicated, it is possible to assess the goodness of fit with the lack of fit statistic, present within ModEval, to determine whether the variation between simulated and measured data was greater than the variation within the measured data. This was not possible for the majority of the data because there were no replicates or replicated data were not available for this study. It could have been used for soil chamber measurements made between April 2013 and Aug 2014 at Straits Inclosure, however this was not carried out.

The complexity of the real world can often produce extra issues for models aimed at simplifying processes. The infestation of defoliating moth larvae at the Straits Inclosure (Pitman et al., 2010) was one such event that had a measurable effect on eddy covariance NEE data in 2009 and 2010.

If the infestation had not already been identified and analysed the reduced NEE in these years would have been difficult to understand.

7.3 Model output

Here some aspects of the output from LandscapeDNDC generated in this study is reviewed.

7.3.1 Bias in output

Residuals (the difference between measured and simulated data) have been used in Chap. 3 (Fig. 1c and Fig. 4) and Chap. 4 (Fig. 2b) to review differences over time and have shown variation in magnitude according to the season. Ideally, these residuals would be converted to a proportion of the measurement for a fairer analysis of the seasonal variation, but can be misleading when measurements are very small, e.g. GPP in winter. Residuals can also be used to test for bias by plotting against the simulated values (Medlyn et al, 2005) as shown in Fig.7.3 for data from the Straits Inclosure. This shows that ecosystem flux data simulated by PSIM was mostly unbiased, with no correlation apparent except a low negative correlation (R^2 = 0.10) between TER and the corresponding residuals. However, the same data simulated by PnET shows a stronger negative correlation for TER (R^2 = 0.44) in addition to a weak positive correlation for NEP (R^2 = 0.14). Thus, both models underestimated the higher values of TER and overestimated lower values, but by different amounts. This confirms the data illustrated in Chap. 3, Fig. 5(b) where TER is underestimated in winter and overestimated in late summer and autumn. The combination of the two errors results in a good annual average by the end of the year. Since NEP is derived from subtracting TER from GPP, the bias in TER simulations is carried forward to a bias in NEP simulations.

Daily air temperature is an important input to both models and temperature is a variable in many of the model processes. When daily average temperature data (used as input for the Straits Inclosure) was plotted against residuals, there was a weak correlation with simulated TER from both PnET (R^2 = 0.18) and PSIM (R^2 = 0.05) (Fig. 7.4). This suggests that a factor in the bias of respiration simulations is due to a poor temperature control in one or more of the respiration-related processes. There is a larger temperature-related bias in PnET than PSIM. The species parameter RESPQ10 is a Q10 function controlling the increase in leaf respiration with temperature in both PnET and PSIM. For these simulations, it has been set at 2.0, which is a commonly used value, but higher than the standard for PnET Q. robur (1.84). It could be further increased to improve the temperature control on respiration, but the result would be higher total annual TER and therefore adjustments would need to be made elsewhere, probably in

growth respiration parameters which are not linked to temperature, in order to maintain an appropriate annual TER.

The same residual analysis of PnET simulations has been carried out for Griffin data, illustrated in Figure 7.5. This shows strong bias from residuals in both GPP (R^2 = 0.53) and NEP (R^2 = 0.46) and in each case, residuals are correlated to daily average temperature data (Fig. 7.5 b and f). Unlike the Straits data, simulated TER does not show a bias. In this case, it appears the principal bias is with GPP, which is overestimated in warmer summer temperatures and underestimated in the winter (also shown in Chap. 4, Fig. 3a). Although temperature is part of the photosynthesis calculation (given in Appendix A.1), there is no parameter to control its effect. The bias here may be through a co-varying factor also correlated to temperature (e.g. photosynthetically active radiation), which needs further investigation. The principal way of reducing GPP in summer is through the parameter AMAXB and/or leaf area, but this would also have an effect in the winter, when GPP is underestimated. This shows, as with the Straits data, that well simulated annual data can be derived from compromises in sub-annual, seasonal data.

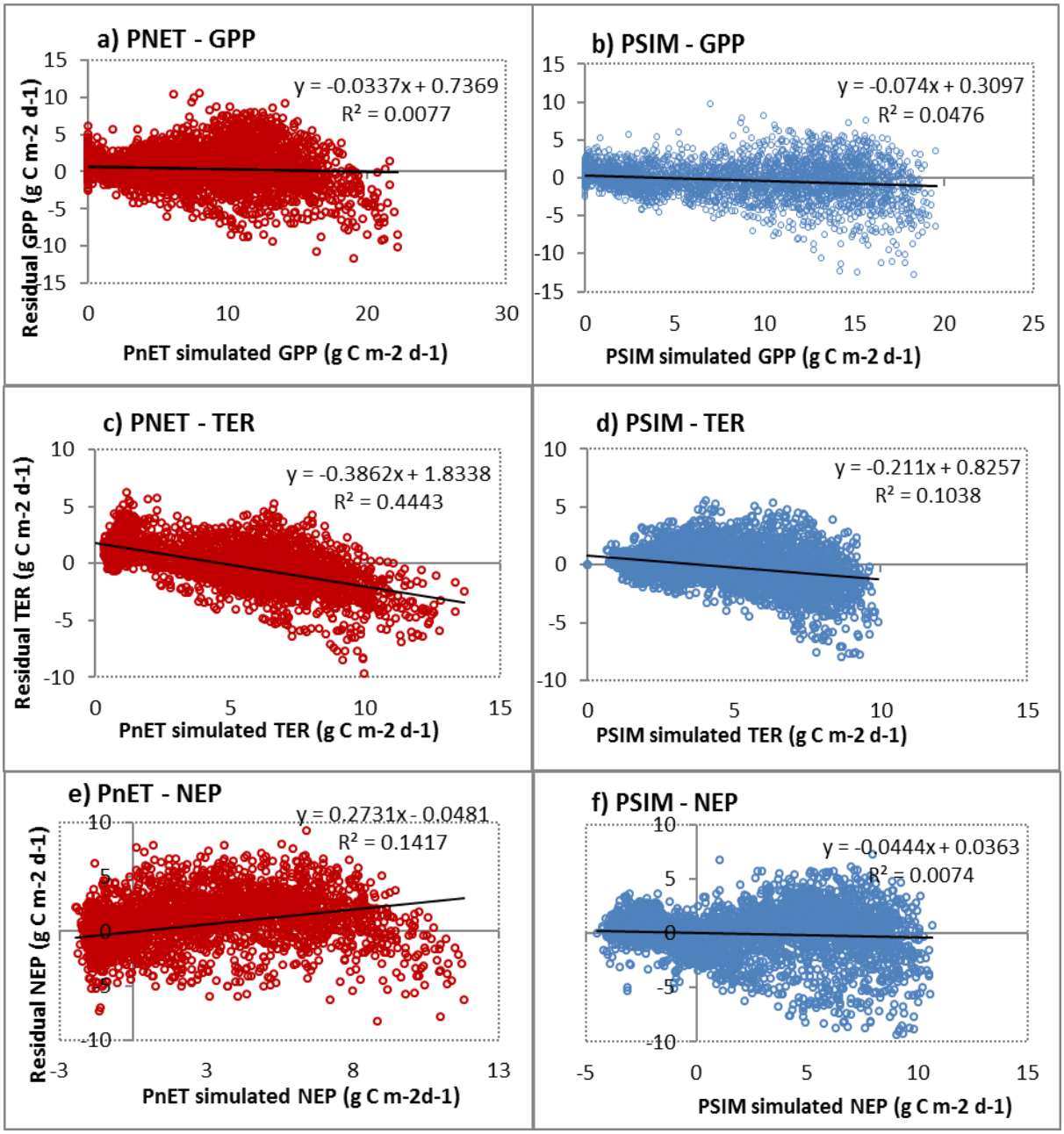

Figure 7.3 Residual analysis for the Straits Inclosure: Cross plots of daily residuals vs simulated ecosystem flux data for 1999 - 2014; a), c) and e) PnET results; b), d) and f) PSIM results.

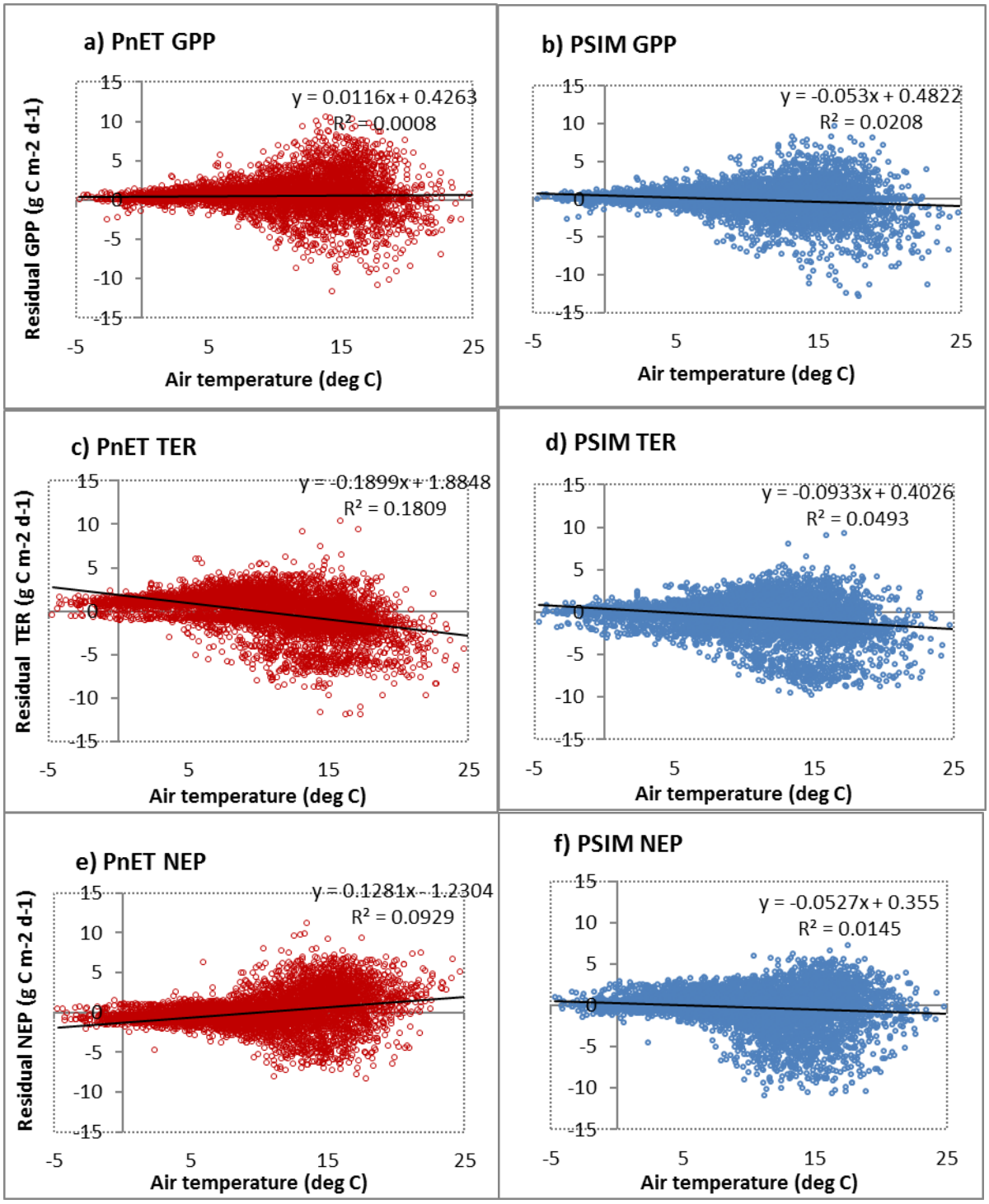

Figure 7.4: Residual analysis for the Straits Inclosure: Cross plots of daily residuals from ecosystem flux simulations vs daily air temperature for 1999-2014; a), c) and e) PnET results; b) d) and f) PSIM results.

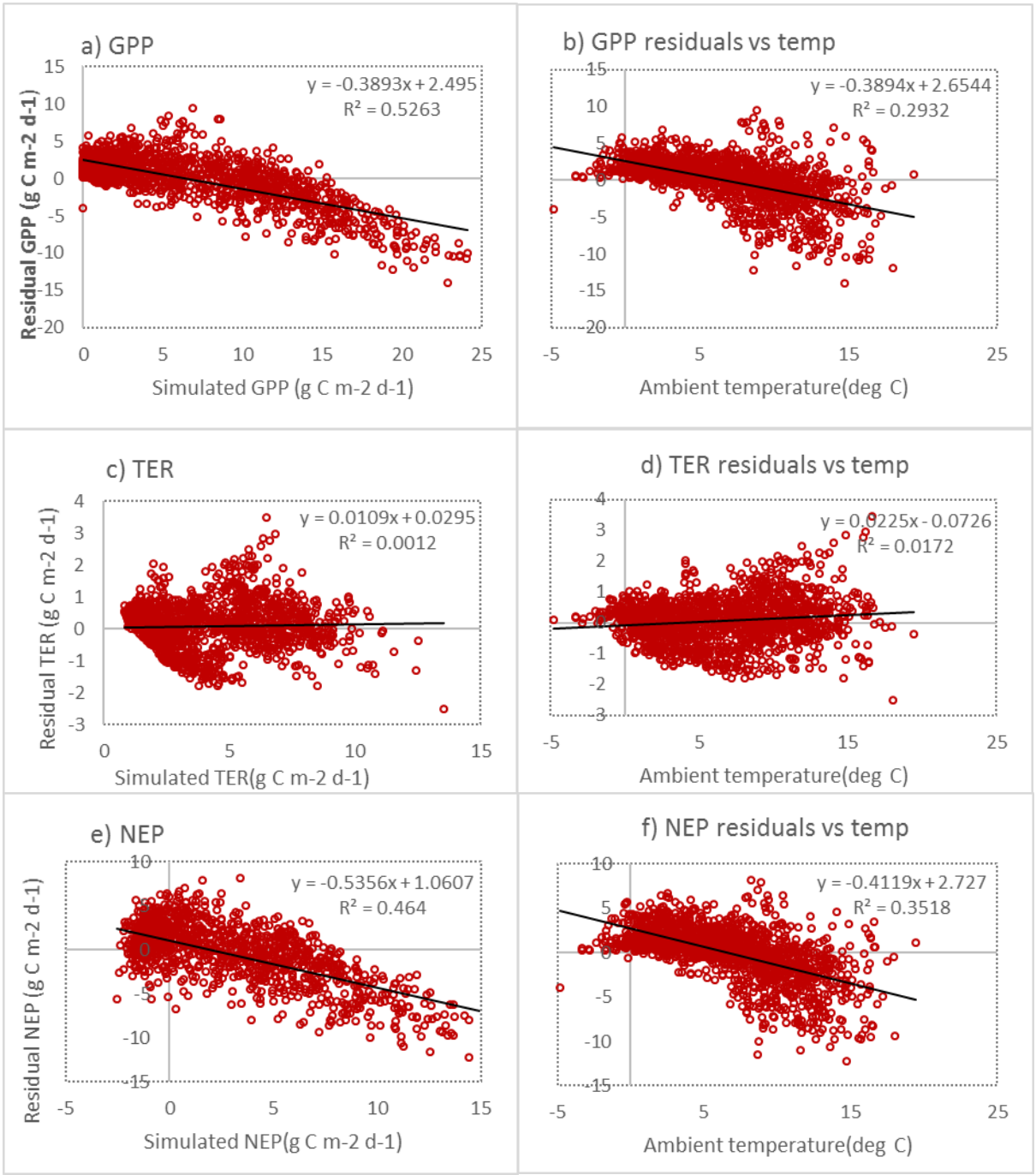

Figure 7.5: Residual analysis for Griffin Forest data from 1999-2000: a), c) and e) cross plots for daily residuals vs equivalent simulated ecosystem CO_2 flux data; b), d) and f) cross plots for daily residuals vs daily average air temperature.

7.3.2 Inter-annual variation

The fact that the model has been parameterised to match average annual data will have contributed to the bias mentioned above, aided by the model's simplification which does not allow photosynthesis in the winter in deciduous forests (and much reduced in evergreen forests). Thus, the winter GPP values will always be underestimated for single species deciduous forest models and these then need to be balanced by overestimating summer GPP values to produce an accurate annual total. The PSIM model has an advantage in modelling the understorey, with its earlier budburst, but must be missing some important control or process since it showed worse inter-annual variation at the Straits Inclosure than PnET which does not model an understorey. Further investigation of understorey parameters following measurements may lead to improvements in PSIM simulations for the Straits and potentially a third vegetation layer could be added to simulate the small amount of evergreen vegetation in the Straits Inclosure. It would also be interesting to model the Griffin Forest with PSIM and assess its ability to simulate inter-annual variation for a coniferous forest.

A review of 14 biosphere vegetation models (not including PnET and PSIM), with associated ecosystem CO_2 flux data from 2000-2006, concluded that most were unable to explain inter-annual variation in phenological transition dates sufficiently to match variations in GPP, and therefore better representation in vegetation phenology was required to predict climate change impacts (Richardson et al., 2012). Thus, the sub-modules PnET and PSIM are not alone in simulating inter-annual variation poorly, but it is a very important aspect of the models' purpose.

7.4 Model software

The LandscapeDNDC software has been developed at the Institute of Meteorology and Climate Research, Karlsruhe Institute of Technology, Germany by including process descriptions and structures from previously existing models (Haas et al. 2013). These previously existing models have been well documented in the literature from inception and in many cases, have undergone enhancements and modifications to processes, also documented in the literature. However, it is difficult to establish from documentation exactly which version of the processes are present in the current version of the LandscapeDNDC model. Communication with the developers is essential to understand the processes in use in the model.

LandscapeDNDC generates approximately 150 output variables, depending on the setup, for every day of a simulation run, in five different output files (also available aggregated into annual data). Respiration data is separated between the physiology (above ground) and soil chemistry

(below ground) output files, which use different units due to the different scales involved. There is therefore a need to generate customised code which automatically converts units, combines values and summarises the simulation results before they are reviewed. Details can be lost or not observed when automated processing takes place. It would be beneficial to have automated graphics integrated into the system for visual confirmation of processes, such as management events.

There is currently no up-to-date documentation and no structured explanation of the full set of parameters. When this project started in 2012, there was no access to change parameter values available to a normal user. This has subsequently changed but expert advice is required to understand all parameters, their normal ranges and the knock-on effects and consequences of changes. Documentation to explain or list changes made in new versions of the software would be helpful.

It has been suggested that process-based biogeochemical models, such as PnET-N-DNDC (the predecessor of LandscapeDNDC) are over-parameterised and that comparable results of N trace gas emissions could be obtained from empirical models (Kesik et al., 2005, de Bruijn et al., 2011). In theory, process-based models should work adequately without customising to local conditions, particularly because of the importance of meteorological conditions and soil properties which are given as input to such models, rather than parameters. However, this study shows that the LandscapeDNDC tree growth submodules need considerable customising of tree-related parameters to establish reasonable simulations at the ecosystem level.

There are two principal omissions in the capability of LandscapeDNDC software which are related to processes involving NO and CH_4. Although CH_4 emission has been modelled in a version of LandscapeDNDC used with rice crops (Kraus et al. 2015), it does not model CH_4 oxidation and the uptake that takes place in forest soils (Le Mer and Roger, 2001). As N_2O, CH_4 and CO_2 are the three most important GHGs and emissions of all three are increasing globally, any efforts at mitigation, including modelling, should address all three gases together (Tian et al., 2015). Since these gases are often measured together from soil chambers, as in this study, it would be advantageous to use the data together in process-based models. Similarly, the only NO uptake modelled in LandscapeDNDC is within the denitrification process, whereas NO can also be consumed as a result of oxidation processes (Medinets et al., 2015), causing a net NO uptake, which is not be simulated and therefore contributes to the over-estimation of NO emissions.

7.5 Context

The balance between photosynthesis and respiration in large forest ecosystems is key to the scale of carbon sequestration they can achieve and therefore how much mitigation of GHG emissions takes place. Ecosystem respiration was thought to be the more important factor for net ecosystem exchange and in forests, TER tends to be dominated by root and microbial soil respiration (Valentini et al., 2000). This was based on analyses of carbon exchange data from 15 European forests that showed carbon uptake increased with decreasing latitude, whereas GPP was largely independent of latitude and more related to stand age and levels of management. However, Lyssaert et al. (2007) in analysing a larger data set from around the world found that global patterns of GPP show clear relationships with mean annual temperature and annual precipitation. They concluded that NEP is mainly determined by non-climatic conditions such as stand age, management, site history and site disturbance, because these factors influence respiration. A better understanding of respiration should lead to a better understanding of carbon balance at the ecosystem level. Thus, studies such as this, considering stands of different ages and simulating the effects of thinning will help contribute to that understanding.

Carbon and nitrogen are closely linked in ecosystems. Many models have been developed to assess the carbon balance alone, e.g. soil organic matter models compared by Smith et al. (1997) and carbon and nitrogen together e.g. ECOSSE (Smith et al., 2010, Dondini et al., 2015), the simplified DecoNit (de Bruijn et al., 2010; de Bruijn et al., 2011), CENTURY (Parton et al., 1994), JULES (Krinner et al., 2009). This study is not a comparative study but one of evaluation and assessment of LandscapeDNDC and its ability to simulate greenhouse gas fluxes from forest soils in the UK. With some further work, recommended below, it is hoped that LandscapeDNDC can be used to model a greater variety of forests in the UK and its regional and land use change potential explored.

7.6 Future recommendations

The uncertainties of model predictions involving soil gas fluxes are large and future progress will be linked to advances in field measurements, spatial databases and model structures (Boyer et al., 2006). With this in mind, recommendations involve more measurements and improvements to the model.

7.6.1 More frequent soil flux measurements

Pulses of N_2O and NO can be emitted from soils when wet periods follow high rainfall events, resulting in very episodic emission patterns. An increased measurement frequency would reduce the uncertainties resulting from scaling up measurements made once or twice a month to produce an annual total. Automated, continuous measurements have their own problems resulting from changing the environmental conditions and therefore the soil gas fluxes. However, if high frequency, automated measurements were combined with less frequent manual measurements at the same site, the combined results should provide very useful information on the temporal variability of soil gas fluxes.

7.6.2 Improve soil analyses for N content at Straits Inclosure.

The soil N content is likely to be a major part of the control on N_2O and NO fluxes. It varies naturally with N content in the litter, which mainly accumulates in the autumn, but is also affected by natural and anthropogenic events such as the caterpillar infestation, storm damage and management thinning. Significant localised contributions come from macro-organisms and atmospheric N deposition, which mainly follows throughfall and is likely to be controlled by the tree canopy shape in summer and trunk in winter. Understanding any correlation between soil N content and fluxes of N_2O and NO and their spatial and temporal variation is beneficial to understanding the soil processes locally. Unfortunately soil analyses carried out for this study could not be used for this purpose.

7.6.3 Measure NO flux at Griffin Forest

NO has not yet been measured here and it would be interesting to know whether the simulations from Chap. 4 have overestimated NO fluxes as well as N_2O and CO_2. Meteorological data would need to be recorded at the same time, together with further measurements of N_2O and CO_2 to allow a fair simulation to take place concurrent with measurements. If the model can be refined to match these measurements, it could be applied in a predictive way to other UK spruce forests.

7.6.4 Measure soil gas fluxes from a UK forest with high N deposition

Thetford Forest in Norfolk is known to have a high N deposition rate as a result of intensive fertiliser use in surrounding East Anglian farmland. Measurements of soil N_2O and NO fluxes there, are expected to provide an end member for such fluxes from UK forest soils. This would have the benefit in helping define the relationship between N deposition and soil N fluxes for modelling purposes, but also to act as an incentive to minimise and control fertiliser use in the area.

7.6.5 Extend work on N addition to Straits inclosure

Although fertiliser is not used routinely in UK deciduous forests and is not now recommended for use in UK coniferous forests, it is still permitted on private land and is used extensively in other countries, such as USA. It has been used routinely in the UK in the past to establish coniferous plantations on marginal land, such as at Griffin Forest, and could be used privately on new afforested land. Experiments with addition of N fertiliser can also help understand the effects of increased N deposition. Chapter 5 has shown that the addition of N in sufficient quantities increases N_2O and NO effluxes and reduces CH_4 uptake. This experiment took place during a wet autumn and further experiments with a wider range of seasonal conditions together with a non-treatment control set would benefit our understanding of the processes.

7.6.6 Model Climate change scenarios with LandscapeDNDC.

This would use the model to make predictions on N_2O and NO emissions as well as C balance following different regional climate change scenarios projected for the UK climate by Murphy et al. (2009), for example.

7.6.7 Improvements to LandscapeDNDC software.

As discussed in Section 7.4, the software would benefit from the inclusion of processes for CH_4 oxidation and methanogenesis and oxidation of NO and N_2O, which allow uptake of the gases from the atmosphere. This is challenging from a modelling point of view as an atmospheric concentration would need to be defined and allowed to vary. Improved documentation for the model, particularly of parameters and process equations would also be helpful.

7.6.8 Diffusion modelling work for N_2O chamber comparison study

The N_2O chamber inter-comparison experiment involved sand as the porous medium in lieu of a soil and high concentrations of N_2O in the subsurface tank in order to increase fluxes to optimise throughput of measurements. The work proposed in Section 7.1.2 using a diffusion model developed by Creelman et al. (2013) would put this in the context of the real world of clay-rich soils and low subsurface concentrations.

Chapter 8 Conclusions

8.1 Simulation of soil gas fluxes from an oak plantation (Straits Inclosure)

LandscapeDNDC was evaluated with two alternative vegetation sub-modules, PnET and PSIM. Both required modifications to species parameters because oak had not been modelled before in the UK. PSIM produced a closer match to average annual eddy covariance data, but appears relatively insensitive to inter-annual variations. The ability of PSIM to model understorey trees separately from canopy trees is thought to explain this improved fit and is especially true when modelling thinning of the forest, where competition for light is an important factor. Annual soil fluxes simulated were of the same order of magnitude as those estimated from chamber measurements for all gases. PnET-simulated annual soil CO_2 fluxes were 30% lower than measured and the equivalent PSIM-simulated data were 24% higher than annual measurements. Both submodules slightly underestimated annual N_2O soil fluxes and overestimated NO soil fluxes compared to annual soil chamber measurements. Soil chambers have been shown to underestimate soil gas fluxes and estimating annual fluxes from monthly measurements can compound errors. As with ecosystem fluxes, inter-annual variation in soil gas fluxes was not well simulated by LandscapeDNDC.

8.2 Simulation of soil gas fluxes from a spruce plantation (Griffin Forest)

LandscapeDNDC was evaluated for use at Griffin spruce forest and produced a good match to annual and monthly eddy covariance data. However, soil CO_2 and N_2O fluxes were overestimated by a factor of about 2. Soil chamber data is probably underestimating both fluxes but the scale of the differences suggests there is a missing factor not accounted for in the model or the data.

8.3 Effect of fertiliser application on soil gas fluxes at an oak forest, measured and simulated

Adding N fertiliser to the Straits Inclosure soil produced increased fluxes of N_2O and NO, which were also simulated by LandscapeDNDC. However, the initial nutrient levels and microbial population, as demonstrated by the fluxes prior to N addition, are as important to the scale of

the subsequent flux as the amount of fertiliser N added. CH_4 uptake was reduced in plots with the highest fertiliser doses and CO_2 fluxes varied in relation to pre-treatment fluxes.

8.4 N_2O chamber comparison

Preliminary results suggest that N_2O soil chambers underestimate soil N_2O fluxes. The ratio of surface area to volume of the chamber is important, together with the length of time of closure, for the scale of systematic errors resulting from this method. Chamber placement may also affect the gas in the soil under the chamber.

References

Aubinet, M., Grelle, A., Ibrom, A., Rannik, Ü., Moncrieff, J., Foken, T., Kowalski, A., Martin, P., Berbigier, P. and Bernhofer, C.: Estimates of the annual net carbon and water exchange of forests: the EUROFLUX methodology., 2000.

Baldocchi, D. D.: Assessing the eddy covariance technique for evaluating carbon dioxide exchange rates of ecosystems: past, present and future, Global Change Biol., 9, 479-492, 2003.

Baldocchi, D. D., Hincks, B. B. and Meyers, T. P.: Measuring biosphere-atmosphere exchanges of biologically related gases with micrometeorological methods, Ecology, 1331-1340, 1988.

Ball, J. T., Woodrow, I. E. and Berry, J. A.: A model predicting stomatal conductance and its contribution to the control of photosynthesis under different environmental conditions, in: Progress in photosynthesis research, Springer, 221-224, 1987.

Baumgärtner, M. and Conrad, R.: Effects of soil variables and season on the production and consumption of nitric oxide in oxic soils, Biol. Fertility Soils, 14, 166-174, 1992.

Bhatti, J. S. and Bauer, I. E.: Comparing loss-on-ignition with dry combustion as a method for determining carbon content in upland and lowland forest ecosystems, Commun. Soil Sci. Plant Anal., 33, 3419-3430, 2002.

Bossel, H.: TREEDYN3 forest simulation model, Ecol. Model., 90, 187-227, 1996.

Boyer, E. W., Alexander, R. B., Parton, W. J., Li, C., Butterbach-Bahl, K., Donner, S. D., Skaggs, R. W. and Grosso, S. J. D.: Modeling denitrification in terrestrial and aquatic ecosystems at regional scales, Ecol. Appl., 16, 2123-2142, 2006.

Brown, J. R., Blankinship, J. C., Niboyet, A., van Groenigen, K. J., Dijkstra, P., Le Roux, X., Leadley, P. W. and Hungate, B. A.: Effects of multiple global change treatments on soil N2O fluxes, Biogeochemistry, 109, 85-100, 2012.

Burba, G. and Anderson, D.: A brief practical guide to eddy covariance flux measurements: principles and workflow examples for scientific and industrial applications, Li-Cor Biosciences, 2010.

Camargo, A., Marin, F., Sentelhas, P. and Picini, A.: Adjust of the Thornthwaite's method to estimate the potential evapotranspiration for arid and superhumid climates, based on daily temperature amplitude, Rev.Bras.Agrometeorol, 7, 251-257, 1999.

Chen, L., Driscoll, C. T., Gbondo-Tugbawa, S., Mitchell, M. J. and Murdoch, P. S.: The application of an integrated biogeochemical model(PnET-BGC) to five forested watersheds in the Adirondack and Catskill regions of New York, Hydrol. Process., 18, 2631-2650, 2004.

Clement, R. J., Jarvis, P. G. and Moncrieff, J. B.: Carbon dioxide exchange of a Sitka spruce plantation in Scotland over five years, Agric. For. Meteorol., 153, 106-123, 2012.

Creelman, C., Nickerson, N. and Risk, D.: Quantifying Lateral Diffusion Error in Soil Carbon Dioxide Respiration Estimates using Numerical Modeling, Soil Sci. Soc. Am. J., 77, 699-708, 2013.

De Bruijn, A. M. and Butterbach-Bahl, K.: Linking carbon and nitrogen mineralization with microbial responses to substrate availability—the DECONIT model, Plant Soil, 328, 271-290, 2010.

De Leenheer, L., Van Hove, J. and Van Ruymbeke, M.: Determination quantitative de la matiere organique du sol, Pedologie, 7, 324-347, 1957.

De Vos, B., Vandecasteele, B., Deckers, J. and Muys, B.: Capability of loss-on-ignition as a predictor of total organic carbon in non-calcareous forest soils, Commun. Soil Sci. Plant Anal., 36, 2899-2921, 2005.

Dondini, M., Jones, E. O., Richards, M., Pogson, M., Rowe, R. L., Keith, A. M., Perks, M. P., McNamara, N. P., Smith, J. U. and Smith, P.: Evaluation of the ECOSSE model for simulating soil carbon under short rotation forestry energy crops in Britain, GCB Bioenergy, 7, 527-540, 2015.

Farquhar, G., von Caemmerer, S. v. and Berry, J.: A biochemical model of photosynthetic CO_2 assimilation in leaves of C3 species, Planta, 149, 78-90, 1980.

Field, C. and Mooney, H.: Photosynthesis--nitrogen relationship in wild plants, in: On the Economy of Plant Form and Function: Proceedings of the Sixth Maria Moors Cabot Symposium, Evolutionary Constraints on Primary Productivity, Adaptive Patterns of Energy Capture in Plants, Harvard Forest, August 1983, 1986.

Finér, L., Ohashi, M., Noguchi, K. and Hirano, Y.: Factors causing variation in fine root biomass in forest ecosystems, For. Ecol. Manage., 261, 265-277, 2011.

Finér, L., Ohashi, M., Noguchi, K. and Hirano, Y.: Fine root production and turnover in forest ecosystems in relation to stand and environmental characteristics, For. Ecol. Manage., 262, 2008-2023, 2011.

Giltrap, D. L., Li, C. and Saggar, S.: DNDC: A process-based model of greenhouse gas fluxes from agricultural soils, Agric., Ecosyst. Environ., 136, 292-300, 2010.

Goulden, M. L., Munger, J. W., FAN, S., Daube, B. C. and Wofsy, S. C.: Measurements of carbon sequestration by long-term eddy covariance: Methods and a critical evaluation of accuracy, Global Change Biol., 2, 169-182, 1996.

Grote, R.: Integrating dynamic morphological properties into forest growth modelling: II Allocation and mortality, For. Ecol. Manage., 111, 193-210, 1998.

Grote, R.: Sensitivity of volatile monoterpene emission to changes in canopy structure: A model-based exercise with a process-based emission model, New Phytol., 173, 550-561, 2007.

Grote, R., Lavoir, A., Rambal, S., Staudt, M., Zimmer, I. and Schnitzler, J.: Modelling the drought impact on monoterpene fluxes from an evergreen Mediterranean forest canopy, Oecologia, 160, 213-223, 2009a.

Grote, R., Lehmann, E., Brümmer, C., Brüggemann, N., Szarzynski, J. and Kunstmann, H.: Modelling and observation of biosphere–atmosphere interactions in natural savannah in Burkina Faso, West Africa, Physics and Chemistry of the Earth, Parts A/B/C, 34, 251-260, 2009b.

Haas, E., Klatt, S., Fröhlich, A., Kraft, P., Werner, C., Kiese, R., Grote, R., Breuer, L. and Butterbach-Bahl, K.: LandscapeDNDC: a process model for simulation of biosphere–atmosphere–hydrosphere exchange processes at site and regional scale, Landscape Ecol., 28, 615-636, 2013.

Hollinger, D., Aber, J., Dail, B., Davidson, E., Goltz, S., Hughes, H., Leclerc, M., Lee, J., Richardson, A. and Rodrigues, C.: Spatial and temporal variability in forest–atmosphere CO_2 exchange, Global Change Biol., 10, 1689-1706, 2004.

Hutchinson, G., Livingston, G., Healy, R. and Striegl, R.: Chamber measurement of surface-atmosphere trace gas exchange: Numerical evaluation of dependence on soil, interfacial

layer, and source/sink properties, Journal of Geophysical Research: Atmospheres, 105, 8865-8875, 2000.

Hyvönen, R., Ågren, G. I., Linder, S., Persson, T., Cotrufo, M. F., Ekblad, A., Freeman, M., Grelle, A., Janssens, I. A. and Jarvis, P. G.: The likely impact of elevated [CO2], nitrogen deposition, increased temperature and management on carbon sequestration in temperate and boreal forest ecosystems: a literature review, New Phytol., 173, 463-480, 2007.

Ingwersen, J., Butterbach-Bahl, K., Gasche, R., Papen, H. and Richter, O.: Barometric process separation: new method for quantifying nitrification, denitrification, and nitrous oxide sources in soils, Soil Sci. Soc. Am. J., 63, 117-128, 1999.

IPCC: Climate Change 2013: The Physical Science Basis. Contribution of Working Group I to the Fifth Assessment Report of the Intergovernmental Panel on Climate Change [Stocker, T.F., D. Qin, G.-K. Plattner, M. Tignor, S.K. Allen, J. Boschung, A. Nauels, Y. Xia, V. Bex and P.M. Midgley (eds.)]. Cambridge University Press, Cambridge, United Kingdom and New York, NY, US, 2013.

Kempers, A. J. and Luft, A. G.: Re-examination of the determination of environmental nitrate as nitrite by reduction with hydrazine, Analyst, 113, 1117-1120, 1988.

Kesik, M., Ambus, P., Baritz, R., Brüggemann, N., Butterbach-Bahl, K., Damm, M., Duyzer, J., Horváth, L., Kiese, R. and Kitzler, B.: Inventories of N_2O and NO emissions from European forest soils, Biogeosciences, 2, 353-375, 2005.

Kiese, R., Li, C., Hilbert, D. W., Papen, H. and Butterbach-Bahl, K.: Regional application of PnET-N-DNDC for estimating the N2O source strength of tropical rainforests in the Wet Tropics of Australia, Global Change Biol., 11, 128-144, 2004.

Kramer, K., Leinonen, I., Bartelink, H., Berbigier, P., Borghetti, M., Bernhofer, C., Cienciala, E., Dolman, A., Froer, O. and Gracia, C.: Evaluation of six process-based forest growth models using eddy-covariance measurements of CO_2 and H_2O fluxes at six forest sites in Europe, Global Change Biol., 8, 213-230, 2002.

Kraus, D., Weller, S., Klatt, S., Haas, E., Wassmann, R., Kiese, R. and Butterbach-Bahl, K.: A new LandscapeDNDC biogeochemical module to predict CH_4 and N_2O emissions from lowland rice and upland cropping systems, Plant Soil, 386, 125-149, 2015.

Krinner, G., Viovy, N., de Noblet-Ducoudré, N., Ogée, J., Polcher, J., Friedlingstein, P., Ciais, P., Sitch, S. and Prentice, I. C.: A dynamic global vegetation model for studies of the coupled atmosphere-biosphere system, Global Biogeochem. Cycles, 19, 2005.

Kutzbach, L., Schneider, J., Sachs, T., Giebels, M., Nykänen, H., Shurpali, N., Martikainen, P., Alm, J. and Wilmking, M.: CO_2 flux determination by closed-chamber methods can be seriously biased by inappropriate application of linear regression, Biogeosciences, 4, 1005-1025, 2007.

Le Mer, J. and Roger, P.: Production, oxidation, emission and consumption of methane by soils: a review, Eur. J. Soil Biol., 37, 25-50, 2001.

Li, C., Frolking, S. and Frolking, T. A.: A model of nitrous oxide evolution from soil driven by rainfall events: 1. Model structure and sensitivity, J.Geophys.Res, 97, 9759-9776, 1992.

Li, C., Aber, J., Stange, F., Papen, H. and Butterbach-Bahl, K.: A process-oriented model of N_2O and NO emissions from forest soils: 1. Model development, JOURNAL OF GEOPHYSICAL RESEARCH-ATMOSPHERES, 105, 4369-4384, 2000-02-27.

Livingston, G. P., Hutchinson, G. L. and Spartalian, K.: Trace Gas Emission in Chambers: A Non-Steady-State Diffusion Model, Soil Sci. Soc. Am. J., 70, 1459-1469, 2006.

Lloyd, J. and Taylor, J.: On the temperature dependence of soil respiration, Funct. Ecol., 315-323, 1994.

Luyssaert, S., Inglima, I., Jung, M., Richardson, A., Reichstein, M., Papale, D., Piao, S., SCHULZE, E., Wingate, L. and Matteucci, G.: CO2 balance of boreal, temperate, and tropical forests derived from a global database, Global Change Biol., 13, 2509-2537, 2007.

Makela, A., Hari, P., Berninger, F., Hanninen, H. and Nikinmaa, E.: Acclimation of photosynthetic capacity in Scots pine to the annual cycle of temperature, Tree Physiol., 24, 369-376, 2004.

Mayer, D. and Butler, D.: Statistical validation, Ecol. Model., 68, 21-32, 1993.

McMaster, G. S. and Wilhelm, W.: Growing degree-days: one equation, two interpretations, Agric. For. Meteorol., 87, 291-300, 1997.

Medinets, S., Skiba, U., Rennenberg, H. and Butterbach-Bahl, K.: A review of soil NO transformation: associated processes and possible physiological significance on organisms, Soil Biol. Biochem., 80, 92-117, 2015.

Medlyn, B., Barton, C., Broadmeadow, M., Ceulemans, R., De Angelis, P., Forstreuter, M., Freeman, M., Jackson, S., Kellomäki, S. and Laitat, E.: Stomatal conductance of forest species after long-term exposure to elevated CO2 concentration: A synthesis, New Phytol., 149, 247-264, 2001.

Medlyn, B. E., Berbigier, P., Clement, R., Grelle, A., Loustau, D., Linder, S., Wingate, L., Jarvis, P. G., Sigurdsson, B. D. and McMurtrie, R. E.: Carbon balance of coniferous forests growing in contrasting climates: model-based analysis, Agric. For. Meteorol., 131, 97-124, 2005.

Medlyn, B. E., Robinson, A. P., Clement, R. and McMurtrie, R. E.: On the validation of models of forest CO2 exchange using eddy covariance data: some perils and pitfalls, Tree Physiol., 25, 839-857, 2005.

Molina-Herrera, S., Grote, R., Santabárbara-Ruiz, I., Kraus, D., Klatt, S., Haas, E., Kiese, R. and Butterbach-Bahl, K.: Simulation of CO_2 Fluxes in European Forest Ecosystems with the Coupled Soil-Vegetation Process Model "LandscapeDNDC", Forests, 6, 1779-1809, 2015.

Murphy, J. M., Sexton, D., Jenkins, G., Booth, B., Brown, C., Clark, R., Collins, M., Harris, G., Kendon, E. and Betts, R.: UK climate projections science report: climate change projections, 2009.

Oren, R., HSIEH, C., Stoy, P., Albertson, J., Mccarthy, H. R., Harrell, P. and Katul, G. G.: Estimating the uncertainty in annual net ecosystem carbon exchange: Spatial variation in turbulent fluxes and sampling errors in eddy-covariance measurements, Global Change Biol., 12, 883-896, 2006.

Pereira, A. R. and Pruitt, W. O.: Adaptation of the Thornthwaite scheme for estimating daily reference evapotranspiration, Agric. Water Manage., 66, 251-257, 2004.

Pihlatie, M. K., Christiansen, J. R., Aaltonen, H., Korhonen, J. F., Nordbo, A., Rasilo, T., Benanti, G., Giebels, M., Helmy, M. and Sheehy, J.: Comparison of static chambers to measure CH 4 emissions from soils, Agric. For. Meteorol., 171, 124-136, 2013.

Pilegaard, K., Hummelshøj, P. and Jensen, N.: Nitric oxide emission from a Norway spruce forest floor, Journal of Geophysical Research: Atmospheres, 104, 3433-3445, 1999.

Pilegaard, K., Skiba, U., Ambus, P., Beier, C., Brüggemann, N., Butterbach-Bahl, K., Dick, J., Dorsey, J., Duyzer, J. and Gallagher, M.: Factors controlling regional differences in forest soil emission of nitrogen oxides (NO and N_2O), Biogeosciences, 3, 651-661, 2006.

Pitman, R., Vanguelova, E. and Benham, S.: The effects of phytophagous insects on water and soil nutrient concentrations and fluxes through forest stands of the Level II monitoring network in the UK, Sci. Total Environ., 409, 169-181, 2010.

Pumpanen, J., Kolari, P., Ilvesniemi, H., Minkkinen, K., Vesala, T., Niinistö, S., Lohila, A., Larmola, T., Morero, M. and Pihlatie, M.: Comparison of different chamber techniques for measuring soil CO_2 efflux, Agric. For. Meteorol., 123, 159-176, 2004.

Rannik, Ü., Kolari, P., Vesala, T. and Hari, P.: Uncertainties in measurement and modelling of net ecosystem exchange of a forest, Agric. For. Meteorol., 138, 244-257, 2006.

Read, D. J., Freer-Smith, P., Morison, J., Hanley, N., West, C. and Snowdon, P.: Combating climate change: a role for UK forests. An assessment of the potential of the UK's trees and woodlands to mitigate and adapt to climate change., The Stationery Office Limited, 2009.

Reich, P., Walters, M., Kloeppel, B. and Ellsworth, D.: Different photosynthesis-nitrogen relations in deciduous hardwood and evergreen coniferous tree species, Oecologia, 104, 24-30, 1995.

Richardson, A. D., Anderson, R. S., Arain, M. A., Barr, A. G., Bohrer, G., Chen, G., Chen, J. M., Ciais, P., Davis, K. J. and Desai, A. R.: Terrestrial biosphere models need better representation of vegetation phenology: results from the North American Carbon Program Site Synthesis, Global Change Biol., 18, 566-584, 2012.

Rowell, D. L.: Soil Science: Methods and Applications, Prentice Hall - Pearson Education Ltd, Harlow, England, 1994.

Ryden, J. and Rolston, D.: The measurement of denitrification, in: Gaseous loss of nitrogen from plant-soil systems, Springer, 91-132, 1983.

Saggar, S., Andrew, R., Tate, K., Hedley, C., Rodda, N. and Townsend, J.: Modelling nitrous oxide emissions from dairy-grazed pastures, Nutr. Cycling Agroecosyst., 68, 243-255, 2004.

Searle, P. L.: The Berthelot or indophenol reaction and its use in the analytical chemistry of nitrogen. A review, Analyst, 109, 549-568, 1984.

Seebach, L., Strobl, P., San Miguel-Ayanz, J., Gallego, J. and and Bastrup-Birk, A.: Comparative analysis of harmonised forest area estimates for European countries, Forestry, 0, 1-15, 2011.

Smith, J., Gottschalk, P., Bellarby, J., Chapman, S., Lilly, A., Towers, W., Bell, J., Coleman, K., Nayak, D. and Richards, M.: Estimating changes in Scottish soil carbon stocks using ECOSSE. I. Model description and uncertainties, Climate Research, 45, 179-192, 2010.

Smith, P., Smith, J., Powlson, D., McGill, W., Arah, J., Chertov, O., Coleman, K., Franko, U., Frolking, S. and Jenkinson, D.: A comparison of the performance of nine soil organic matter models using datasets from seven long-term experiments, Geoderma, 81, 153-225, 1997.

Stange, F., Butterbach-Bahl, K., Papen, H., Zechmeister-Boltenstern, S., Li, C. and Aber, J.: A process-oriented model of N_2O and NO emissions from forest soils: 2. Sensitivity analysis and validation, Journal of Geophysical Research: Atmospheres, 105, 4385-4398, 2000.

Swanson, R. V. and Flanagan, L. B.: Environmental regulation of carbon dioxide exchange at the forest floor in a boreal black spruce ecosystem, Agric. For. Meteorol., 108, 165-181, 2001.

Tian, H., Chen, G., Lu, C., Xu, X., Ren, W., Zhang, B., Banger, K., Tao, B., Pan, S. and Liu, M.: Global methane and nitrous oxide emissions from terrestrial ecosystems due to multiple environmental changes, Ecosystem Health and Sustainability, 1, 1-20, 2015.

Thornthwaite, C. W. and Mather, J. R.: Instructions and tables for computing potential evapotranspiration and the water balance, 1957.

Valentini, R., Matteucci, G., Dolman, A., Schulze, E., Rebmann, C., Moors, E., Granier, A., Gross, P., Jensen, N. and Pilegaard, K.: Respiration as the main determinant of carbon balance in European forests, Nature, 404, 861-865, 2000.

Wilkinson, M., Eaton, E., Broadmeadow, M. and Morison, J.: Inter-annual variation of carbon uptake by a plantation oak woodland in south-eastern England, Biogeosciences Discuss, 9, 9667-9710, 2012.

Yamulki, S., Anderson, R., Peace, A. and Morison, J.: Soil CO_2 CH_4 and N_2O fluxes from an afforested lowland raised peatbog in Scotland: implications for drainage and restoration, Biogeosciences, 10, 1051-1065, 2013.

Yamulki, S., Harrison, R. M., Goulding, K. and Webster, C.: N_2O, NO and NO_2 fluxes from a grassland: Effect of soil pH, Soil Biol. Biochem., 29, 1199-1208, 1997.

Yuan, Z. and Chen, H. Y.: Fine root biomass, production, turnover rates, and nutrient contents in boreal forest ecosystems in relation to species, climate, fertility, and stand age: literature review and meta-analyses, Crit. Rev. Plant Sci., 29, 204-221, 2010.

Zhang, Y., Li, C., Trettin, C. C., Li, H. and Sun, G.: An integrated model of soil, hydrology, and vegetation for carbon dynamics in wetland ecosystems, Global Biogeochem. Cycles, 16, 9-1-9-17, 2002.

Appendices

Appendix A: PnET vegetation sub-module

(modified from Molina-Herrera et al. (2015) supplementary information)

A.1: Photosynthesis

The daily amount of C fixed by photosynthesis is controlled by daily meteorological conditions (solar radiation and temperature), light use efficiency, leaf area and leaf N concentration. Climate conditions and leaf area are calculated for each canopy layer, determined by tree height (mature forests contain canopy layers 0.5 m deep). The amount of foliage varies between pre-defined minimum and maximum values. Foliage growth (budburst) starts each year when a threshold of accumulated daily average temperature (growing degree days) is exceeded and ends when a second threshold of growing degree days is exceeded. Leaf fall starts on any day when net C gain turns negative after a predefined autumn day, SENESCSTART.

Daily gross photosynthesis, or assimilation, $GrossA_{max}$ is calculated from maximum photosynthetic rate A_{max} according to (Aber and Federer, 1992). It depends on N concentration and is modified by vapour pressure deficitD_{vpd}, temperature D_{tem}, and daylight duration D_{ayL} (Equation (A1)). An additional conversion factor (*cf*) is needed to gain C assimilation in units kg C m^{-2}.

$$GrossA_{max} = A_{max} \times (AMAXF + BASEFOLRESPFRAC) \times D_{vpd} \times D_{tem} \times D_{ayL} \times cf \quad \text{(A1)}$$

$$A_{max} = AMAXA + AMAXB \times FolNCon \quad \text{(A2)}$$

Code	Description	Units
AMAXF	fraction of instantaneous early-morning maximum photosynthesis	(0-1)
BASEFOLRESPFRAC	Respiration as a fraction of maximum photosynthesis	(0-1)
AMAXA	Intercept of relation between maximum photosynthetic rate and foliar N	nmol CO_2 $g^{-1} \cdot s^{-1}$
AMAXB	Maximal net photosynthetic rate	nmol CO_2 $g^{-1} \cdot s^{-1}$/% N
FolNCon	Foliar N concentration	% N

Temperature modification for photosynthesis is based on an optimum function with minimum and maximum daily temperature ($PSNTMAX$, $PSNTMIN$) as parameters (Equation (A3)). The

limitation of photosynthesis at low air humidity D_{vpd} is determined by water vapour pressure deficit with a saturation curve according to Equation (A4).

$$D_{tem} = \max(0, \frac{\left(PSNTMAX - T_{day}\right) \times \left(T_{day} - PSNTMIN\right)}{\left(\frac{PSNTMAX - PSNTMIN}{2}\right)^2}) \quad \text{(A3)}$$

$$D_{vpd} = 1 - (DPV1 \times pow\,(vpd, DVP2)) \quad \text{(A4)}$$

DPV1 and DPV2 represent empirical coefficients.

Maximum gross photosynthesis is used to calculate photosynthesis on leaf and canopy scale by reducing $GrossA_{max}$ depending on light, water availability and leaf biomass per canopy layer.

$$PHS_{gross\ canopy} = \sum_{layers} GrossA_{max} \cdot \mathrm{Light_{eff}} \cdot \mathrm{W_{ava}} \cdot DW_{fol,lay} \quad \text{(A5)}$$

With *lay* being the canopy layer index.

Parameter	Description	Units
$\mathrm{Light_{eff}}$	light use efficiency	(0–1)
$\mathrm{W_{ava}}$	relative available soil water content	%
$\mathrm{DW_{fol}}$	dry weight of the foliage	

The light use efficiency $\mathrm{Light_{eff}}$ factor depends on photosynthetically active radiation in the specific canopy layer and is derived from radiation in the canopy layer above and foliage distribution as follows:

$$\mathrm{Light_{eff}} = 1 - \mathrm{e}^{-((\mathrm{Ilay} \times \log(2))/\mathrm{HALFSAT})} \quad \text{(A6)}$$

$$Ilay = PAR \times e^{(-EXT \times LAIlay)} \quad \text{(A7)}$$

Parameter	Description	Units
I	radiation intensity	umol $m^{-2} \cdot s^{-1}$
$\mathrm{LAI_{lay}}$	leaf area index	$m^2 \cdot m^{-2}$
EXT	light extinction (attenuation) coefficient	(0–1)

PAR	photosynthetically active radiation	umol $m^{-2}{\cdot}s^{-1}$
HALFSAT	half saturation light intensity	umol $m^{-2}{\cdot}s^{-1}$

The relative water availability factor W_{ava} is determined from soil water content relative to total soil water holding capacity aggregated over all soil layers and weighted by fine root distribution (Grote et al., 2009).

$$W_{ava} = \min(1, \sum_{layers} \frac{WClay - WCmin}{(WCmax - WCmin) \times H2OREF} \times \frac{Mfrtlay}{Mfrt}) \quad \text{(A8)}$$

Parameter	Description	Units
wc_{lay}	Water content in each soil layer	%
WCmax	Maximum water content	$mm{\cdot}m^{-3}$
WCmin	Minimum water content	$mm{\cdot}m^{-3}$
H2OREF	relative available soil water content at which stomata conductance is affected (0–1)	(0–1)
Mfrtlay	Species-specific fine root biomass per soil layer	kg $DW{\cdot}m^{-2}$
Mfrt	Species-specific fine root biomass	kg $DW{\cdot}m^{-2}$

Photosynthetic activity depends on foliar N concentration which is calculated from uptake and foliage demand. N uptake is assumed to be the minimum between demand and availability. The latter is calculated separately in each soil layer from N content of soil solutes, differentiated into NO_3 and NH_4 using species-specific exploitation parameters, EXP_NO3 and EXP_NH4 . These exploitation parameters reflect the degree to which the roots are able to deplete the soil available inorganic N.

$$N_{avai} = (EXP\_NO3 * NO3_{avai-Soil}) + (EXP\_NH4 * NH4_{avai-Soil}) \quad (9)$$

Parameter	Description	Units

EXP_NO3	Species-specific relative exploitation rate of NO_3 from roots	(0–1)
EXP_NH4	Species-specific relative exploitation rate of NH_4 from roots	(0–1)
$NO3_{avai\text{-}soil}$	nitrate in the soil solution	kg N·m^{-2}
$NH4_{avai\text{-}soil}$	ammonium in the soil solution	kg N·m^{-2}

N taken up from the roots is distributed into the various tree compartments according to their relative demand, using an optimum N concentration as target value (Grote, 1998). The optimum foliar N concentration within a specific canopy layer is defined by a fixed optimum concentration which is decreased proportionally to the increase in specific leaf area from top to bottom. Specific leaf area is linearly increased in relation to canopy height (Grote et al., 2011).

$$NCFOLOPTlay = NCFOLOPT \times \left(\frac{SLAMIN}{sla}\right) \quad \text{(A10)}$$

$$sla = SLAMAX - (SLAMAX - SLAMIN) \times \left(\frac{hflFolCum}{hflFol}\right) \quad \text{(A11)}$$

Parameter	Description	Units
SLAMAX	specific leaf area in the shade	m^2·kg^{-1}
SLAMIN	specific leaf area under full light	m^2·kg^{-1}
NCFOLOPT	optimum nitrogen concentration of foliage	(kg N·kg^{-1} DW)
NCFOLOPTlay	optimum nitrogen concentration per foliage layer	(kg N·kg^{-1} DW)
hflFolCum	cumulative height of foliage layers	m
hflFol	height of a foliage layer	m

A.2: Respiration

Ecosystem respiration is separately calculated for autotrophic $AUT_{org,resp}$ and heterotrophic $HET_{org,resp}$ organisms. Autotrophic organisms (here: trees) spend energy on growth respiration $rGro$ and maintenance (= 'residual' respiration) $rRes$. The latter is separated by compartments: foliage, fine roots, living wood, and buds. While foliage respiration is defined by the photosynthesis calculation (Equation (A12)), other residual respiration rates are calculated relative to biomass and temperature with empirically defined parameters:

$$rFol = \left(PHS_{gross\ canopy} - PHS_{net\ canopy}\right) \quad \text{(A12)}$$

$$rFrt = \frac{RootAllocC \times ROOTMRESPFRAC}{(1 + ROOTMRESPFRAC + GRESPFRAC)} \quad \text{(A13)}$$

$$rSap = PHS_{gross\ canopy} \times WOODMRESPA \quad \text{(A14)}$$

The carbon allocation into root growth (RootAllocC) was originally defined solely dependent on two empirical parameters (Aber et al., 1992). This has been modified to respond to average annual temperature in order to get a more general relationship (Chen et al., 2004; Finer et al., 2011; Yuan et al., 2010).

$$RootAllocC = TMult \times FRTLOSS\_SCALE \times RootC \quad \text{(A15)}$$

$$TMult = exp\left(0.1 \times (Tave - 7.1\ )\right) \times 0.68 \quad \text{(A16)}$$

Code	Description	Units
$RootAllocC$	daily root C allocation	g C·m^{-2}
$ROOTMRESPFRAC$	ratio of fine root maintenance respiration to biomass production	(0–1)
$GRESPFRAC$	growth respiration, fraction of allocation	(0–1)
$TMult$	temperature factor	(0–1)
$RootC$	fine root carbon	g C·m^{-2}
$Tave$	annual average temperature	°C
$FRTLOSS\_SCALE$	scaling factor for fine root loss	(0–1)
$PHS_{net\ canopy}$	net canopy photosynthesis	nmol CO_2·g^{-1}·s^{-1}

$WOODRESPA$	wood maintenance respiration as a fraction of gross photosynthesis	(0–1)

Similarly, C is lost during species specific growth. Foliage $FolGResp$, roots $RootGResp$, and wood $WoodGResp$ respirations depend on daily biomass and a common species specific parameter.

$$FolGResp = FolProdC \times GRESPFRAC \quad \text{(A17)}$$

$$WoodGResp = WoodProdC \times GRESPFRAC \quad \text{(A18)}$$

$$RootGResp = RootProdC \times GRESPFRAC \quad \text{(A19)}$$

Parameter	Description	Units
$FolProdC$	foliage carbon production over the integration timestep	g DW·m^{-2}
$WoodProdC$	Wood carbon production over the integration timestep	g DW·m^{-2}
$RootProdC$	root carbon production over the integration timestep	g DW·m^{-2}
$GRESPFRAC$	growth respiration, fraction of allocation	(0-1)

Finally, net photosynthesis is calculated from gross photosynthesis and foliage respiration as a fraction of *Amax* (Equation (A19)). Foliage respiration is differentiated into the light period $light_{resp}$ and the night $dark_{resp}$ which both are characterized by their different temperatures.

$$PHS_{net.canopy} = PHS_{gross\ canopy} - \left(light_{resp} + dark_{resp}\right) * DW_{ffoliage} \quad \text{(A20)}$$

$$Light_{resp} = BASEFOLRESPFRAC \times A_{max} \times \mathrm{RESPQ10}^{\left(\frac{T_{day} - \mathrm{PSNOPT}}{10}\right)} \times D_{ayLength} \times cf \quad \text{(A21)}$$

$$dark_{resp} = BASEFOLRESPFRAC \times A_{max} \times \mathrm{RESPQ10}^{\left(\frac{T_{night} - \mathrm{PSNOPT}}{10}\right)} \times N_{ightLength} \times cf \quad \text{(A22)}$$

Name	Description	Units
$BASEFOLRESPFRAC$	Respiration as a fraction of maximum photosynthesis	(0–1)
$\mathrm{RESPQ10}$	Q10 for leaf respiration	Unitless
T_{night}	Average temperature during the night	°C

T_{day}	Average temperature during daylight hours	°C
PSNOPT	optimum daytime temperature for photosynthesis	°C
$D_{ayLength}$	daylight duration	Hours
$N_{ight\ Length}$	night time duration	Hours

Likewise, heterotrophic organisms spend energy during soil organic matter decomposition processes that are calculated by the DNDC model. The model considers the activity of microbes which decompose litter from three pools and reutilize C from death of microbial biomass. In the current study, soil processes are assumed to be valid at any site and are not subject of parameter changes here. For further descriptions see Li *et al.* (2000) and Stange et al., 2000.

A.3: Evapotranspiration

Evapotranspiration is the sum of evaporation from leaves (transpiration) and from the soil surface. It is limited by water availability and potential evaporation. Water availability for canopy evaporation is limited by water stored at the leaf surface, which is a function of precipitation, ground coverage, leaf area, and species-specific leaf storage capacity. To account for some water interception of deciduous trees during the leafless period, an additional minimum interception has been defined dependent on wood biomass.

$$intcept = min\ (ri \times densf, interceptmax - leaf_{water}) \quad \text{(A23)}$$

$$densf = (fDens \times (1 - FGAP) \quad \text{(A24)}$$

$$intceptmax = (Woodmass \times 1\ e^{10} + LAI \times MWFM) \quad \text{(A25)}$$

$$leaf_{water} = WC_{canopy} \quad \text{(A26)}$$

Name	Description	Units
$intcept$	Actual interception	m·h^{-1}
ri	actual rainfall per timestep	m·ts^{-1}
$densf$	density factor	0–1
$fDens$	fraction of ground coverage	0–1

$FGAP$	throughfall fraction for a closed canopy	0–1
$Woodmass$	Woody biomass	kg DW
LAI	Species-specific leaf area index	$m^2 \cdot m^{-2}$
$MWFM$	specific interception capacity of foliage	($m \cdot m^{-2}$ LAI)
WC_{canopy}	amount of water in canopy layers	$mm \cdot m^{-2}$

Precipitation not intercepted is considered as input to the soil surface. Soil water availability is given by the water stored within 0.3 m or rooting depth for soil evaporation and transpiration, respectively. Water runoff and movement between soil layers depends on water input, soil layer water content, and soil layer specific properties such as field capacity, wilting point, saturated water flow, and clay content. For further description see Kiese *et al.* (2011).

Daily potential evaporation is calculated with a modified Thornthwaite approach [Pereira et al., 2004; Camargo et al., 1999; Thornthwaite et al., 1957) using daily and mean monthly temperatures as independent variables.

$$EP = 16\times \left(10 \cdot \frac{T_{eff}}{thorni}\right)^{A} \quad \text{(A27)}$$

$$T_{eff} = 0.72 \cdot (T_{avg} + T_{max} - T_{min}) \quad \text{(A28)}$$

$$thorni = (0.2\times T_{month})^{1.514} \quad \text{(A29)}$$

$$A = 0.49239 + 0.0179 \cdot thorni - 7.71 \cdot 10^{-5} \cdot \sqrt{thorni} + 6.75 \cdot 10^{-7} \cdot thorni^3 \quad \text{(A30)}$$

Name	Description	Units
T_{eff}	effective temperature for evaporation	°C
T_{month}	estimated average monthly temperature	°C
A	Thornthwaite exponent A	-
$thorni$	summation of monthly heat index	-

Potential evaporation is diminished by surface evaporation and the remaining demand is used as an upper boundary for transpiration. Actual transpiration demand or daily potential transpiration $PTra_{day}$ is calculated according to the water use efficiency $Wuec$ concept

(Equation (A28)), which depends on species-specific water use efficiency constants, water availability, and vapor pressure deficit.

$$Wuec = \left(WUECMAX - (WUECMAX - WUECMIN) \times min\left(1, \left(\frac{\mathrm{wc_{soil}} - \mathrm{wc_{min}}}{\mathrm{wc_{max}} - \mathrm{wc_{min}}}\right)\right)\right) \times \frac{Soil_{height}}{Soil_{cum\ depth}} \quad \text{(A31)}$$

$$PTra_{day} = \frac{PHS_{gross,canopy} \times 10^{-6}}{Wuec} * VPD \quad \text{(A32)}$$

Name	Description	Units
$WUECMAX$	maximum water use efficiency constant	mg CO_2·g H_2O^{-1}
$WUECMIN$	minimum water use efficiency constant	mg CO_2·g H_2O^{-1}
$\mathrm{WC_{soil}}$	soil water content of a soil layer	m·m^3
$Soil_{height}$	height of the soil layer	cm
WC_{min}	minimum water content per soil pore space	m·m^{-3}
$\mathrm{WC_{max}}$	maximum water content per soil pore space	m·m^{-3}
$Soil_{cum\ depth}$	cumulative soil depth	m

Appendix B Mineralisation sub-module

Nernst Equation (as explained in Li, 2007)

The Nernst equation is a basic thermodynamic formula defining soil Eh based on concentrations of the dominant oxidants and reductants existing in the soil liquid phase (Stumm and Morgan 1981):

$Eh = Eo + RT/nF \cdot \ln([O]/[W])$

Where: Eh is redox potential (V)

Eo = standard redox potential (V)

R = gas constant

T = temperature in Kelvin

N = number of electrons transferred in redox reaction

F = Faraday constant

[O] = the concentration of the oxidant (mol L^{-1})

[W] = the concentration of the reductant (mol L^{-1})

Michaelis-Menton equation

In biochemistry, the Michaelis–Menten equation describes the rate of enzyme reactions by relating the reaction rate, V, to the concentration of the substrate, [S]. V_{max} is the maximum rate achievable by the system at maximum substrate concentration. The constant, K_m, is the substrate concentration at which the reaction rate is half V_{max}.

$V = V_{max} [S] / (K_m + [S])$

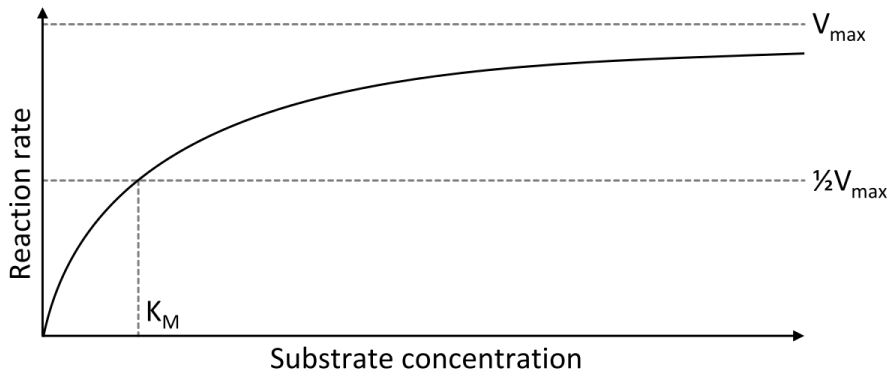

This equation is also widely applied in describing the kinetics of microbial growth with dual nutrients (Paul and Clark 1989; Li et al 2007):

$$R = Rmax \cdot DOC/ (Ka + DOC) * [O]/(Kb + [O])$$

Where:

R is reaction rate,

Rmax = maximum reaction rate,

DOC = concentration of dissolved organic C,

[O] = concentrations of oxidant, and

Ka = a half saturation constant for DOC and oxidant

Kb = a half saturation constant for oxidant

Paul EA, Clark FE 1989. Dynamics of residue decomposition and soil organic matter turnover. *In* Soil Microbiology and Biochemistry, 2nd edn, Ed. EA Paul and FE Clark., pp. 157–166, Academic Press, San Diego

Stumm W, Morgan JJ 1981. Oxidation and Reduction. *In* Aquatic Chemistry: An Introduction Emphasizing Chemical Equilibria in Natural Waters, 2nd edn, Ed. W Stumm and JJ Morgan, pp. 418–503, John Wiley & Sons, New York.

Appendix C Denitrification sub-module

Functions and Parameters for Denitrification (from Li et al, 2000)

Eqn no	Description	Equation
1	Relative growth rate of NOx denitrifiers	$\mu_{NOx} = \mu_{NOx(max)}$ [DOC]/ (K_c + [DOC]) [NO_x] / (K_n +[NO_x])
2	Relative growth of total denitrifiers	$\mu_g = F_t (\mu_{NO3} F_{pH1} + \mu_{NO2} F_{pH2} + \mu_{NO} F_{pH2} + \mu_{N2O} F_{pH3})$
		$F_t = 2^{((T-22.5)/10)}$
		$F_{pH1} = 1 - 1 / (1 + e^{(pH-4.25/0.5)})$
		$F_{pH2} = 1 - 1 / (1 + e^{(pH-5.25/1.0)})$
		$F_{pH3} = 1 - 1 / (1 + e^{(pH-6.25/1.5)})$
3	Denitrifier growth rate	$R_g = \mu_g B_d$
	Death rate	$R_d = M_c Y_c B_d$
	Rate of consumption of soluble carbon	$R_c = (\mu_g / Y_c + M_c) B_d$
4	Consumption rate of N oxides	$R_{NOx} = (\mu_{NOx} / Y_{NOx} + M_{NOx} [NO_x] /[N]) B_d$
5	Nitrogen assimilation rate	$q_N = R_g / CN$
6	Gas diffusion factor	$V = D_{max}$ afps (1 – anvf) F_{clay} $2^{T/20}$
		$F_{clay} = 0.13 - 0.079$ clay

afps = air-filled pore space

anvf = volumetric fraction of anaerobic microsites

B_d = Denitrifier biomass (kg Cm^{-2})

Clay = Clay fraction in the soil

CN = C/N ratio in denitrifiers (3.45 [VanVerseveld and Stouthamer 1978)

D_c = Consumption rate of soluble carbon by denitrifiers (kg C m^{-3} h^{-1})

D_{max} = Maximum diffusion rate in air (m^2 h^{-1})

DNO_x = Consumption rate of N oxides by denitrifiers (kg N m^3 h^{-1})

[DOC] = Soluble C concentration (kgm^{-3})

F_{clay} = Clay factor

F_t = Temperature factor

F_{pH1} = pH factors for NO_3^- denitrifiers

F_{pH2} = pH factors for NO_2^- and NO denitrifiers

F_{pH3} = pH factors for N_2O denitrifiers

K_c = Half saturation value of soluble carbon (0.017 kg Cm^{-3})[Shan & Coulman, 1978]

K_n = Half saturation value of N oxides (0.083 kg Nm^{-3}) [Shan & Coulman, 1978]

M_c = Maintenance coefficient of C (0.0076 **kg N** kg^{-1} h^{-1}) [Van Verseld et al, 1977]

M_{NOx} = Maintenance coefficient of N oxides (0.09, 0.035 and 0.079 **kg N** kg^{-1} h^{-1} for $NO3^-$, NO_2^-, (+NO*) and N_2O, respectively based on Van Verseld et al [1977]

[N] = Concentration of all NO_x (kg Nm^{-3})

$[NO_x]$ = Concentration of NO_3^-, NO_2^- , NO and N_2O (kg N m^{-3})

pH = Soil pH

q_n = nitrogen assimilation rate (kg N ha^{-1} h^{-1})

R_d = Denitrifier death rate

R_g = Denitrifier growth rate

T = Soil temperature (°C)

v = Gas diffusion factor (%)

Y_c= Maximum growth rate of denitrifiers on soluble carbon (0.503 kg C /kg C) [Van Verseld et al 1977]

Y_{NOx} = Maximum growth rate of denitrifiers on N oxides (0.401, 0.428 and 0.151 kg C / kg N for NO_3^-, NO_2^-, (+NO*) and N_2O, respectively based on Van Verseld et al [1977]

μ_g = relative growth rate of total denitrifiers (1/h)

μ_{NO3} = }

μ_{NO2} = } Relative growth rate of NO_3^-, NO_2^-, NO and N_2O denitrifiers

μ_{NO} = }

μ_{N2O} = }

μ_{NOx} = Relative growth rate of NOx denitrifiers (1/h)

$\mu_{NOx(max)}$ = Maximum growth rates (0.67 1/h for NO_3^-, NO_2^- denitrifiers and 0.34 1/h for NO and N_2O denitrifiers, based on Hartel and Alexander [1987]. The parameters are shared by NO and N_2O due to lack of data for NO.

Appendix D Nitrification sub-module

(from Li et al, 2000)

D.1: Functions and Parameters for Nitrification

Eqn no	Description	Equation
1	Relative growth rate of nitrifiers	$\mu_g = \mu_{max}\,([DOC]/(1+[DOC]) + F_m/(1+F_m))$
2	Relative death rate of nitrifiers	$\boldsymbol{\mu_d = a_{max}\, B_n / \frac{(5+[DOC])}{(1+F_m)}}$
3	Net increase in nitrifiers' biomass	$\mu_b = (\mu_g - \mu_d)\, B_n\, F_t\, F_m$
4	Nitrification rate	$R_n = R_{max}\, [NH_4]\, B_n\, pH$
5	Temperature factor	$F_t = ((60 - T)/ 25.78)^{3.503}\ e^{(3.503\,(T-34.22/25.78)}$
6	Moisture factor	If wfps > 0.05, $F_m = 1.01 - 0.21$ wfps If wfps <= 0.05, $F_m = 0$
7	NO production from nitrification	$NO = 0.0025\, R_n\, F_t$
8	N_2O production from nitrification	$N_2O = 0.0006\, R_n\, F_t$ wfps

a_{max} = maximum death rate for nitrifiers (1.44 1/d, from Blagodatsky & Richter, 1998)

B_n = Biomass of nitrifiers (kg C ha^{-1})

[DOC] = Concentration of dissolved organic carbon (kg C ha^{-1})

F_m = Moisture factor

F_t = Temperature factor

$[NH_4]$= concentration of ammonium (kg N ha^{-1})

NO = NO production from nitrification

N_2O = N_2O production from nitrification (Ingwersen et al 1999)

pH = soil pH

R_n = Nitrification rate

R_{max} = Maximum nitrification rate (1/h)

T = soil temperature (°C)

Wfps = water filled pore space

μ_{max} = maximum growth rate for nitrifiers (4.87 1/d, from Blagodatsky et al, 1998)

(* incorrect ref in Li paper)

μ_b = net increase in nitrifier biomass

μ_d = relative death rate of nitrifiers

μ_g = relative growth rate of nitrifiers

D.2: Functions and Parameters for Chemo-denitrification

Eqn no	Description	Equation
1	Production rate of NO from chemodenitrification kg N ha^{-1} d^{-1}	$R_{chem} = a\ R_n\ F_t\ F_{pH}$
	Temperature function	$F_t = 0.03\ nT + 0.2$
	pH factor	$F_{pH} = 2236\ e^{[-2.5*pH]}$

F_t = Temperature factor (based on Yamulki et al. (1997)

F_{pH} = pH factor (based on Blackmer and Cerrato (1986))

R_n = nitrification rate

T = soil temperature

pH = soil pH

a = constant co-efficient